

HORIZONTAL TUBE-SIDE CONDENSATION OF STEAM IN  
THE PRESENCE OF A NON-CONDENSABLE GAS. 4

THIS THESIS HAS BEEN ACCEPTED FOR  
THE DEGREE OF MSC (1990)  
AND A COPY MAY BE PLACED IN THE  
UNIVERSITY LIBRARY.

ALFRED OSWAGO | ONG'IRO

A thesis submitted in partial fulfillment for the  
degree of Master of Science in Mechanical  
Engineering of the University of Nairobi

Department of Mechanical Engineering

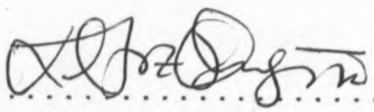
1990

UNIVERSITY OF NAIROBI LIBRARY



0101658 3

This thesis is my own original work and  
has not been presented for a degree  
in any other University.

Signature.....  
( Alfred Oswago Ong'iro)

This thesis has been submitted for examination  
with my approval as University Supervisor.

Signature.....  
(Dr. J. F. Kanyua)

CONTENTS

	PAGE
CONTENTS	i
ACKNOWLEDGEMENT	vi
ABSTRACT	vii
NOMENCLATURE	ix
CHAPTER 1 INTRODUCTION	
1.1 GENERAL	1
1.2 DIRECT CONTACT CONDENSER	2
1.2.1 BAROMETRIC CONDENSER	2
1.2.2 LOW LEVEL-JET CONDENSER	5
1.3 SURFACE CONDENSER	5
1.3.1 SHELL AND COIL CONDENSER	6
1.3.2 TUBE IN TUBE CONDENSER	6
1.3.3 SHELL AND TUBE CONDENSER	6
1.4 NON-CONDENSABLE GAS	7
1.4.1 NON CONDENSABLE GAS (NCG) GENERAL	11
1.4.2 EFFECT OF NCG ON CONDENSER AND TURBINE PERFORMANCE	12
1.4.3 GAS EXTRACTION SYSTEMS	12
CHAPTER 2 LITERATURE REVIEW	
2.1 INTRODUCTION	14
2.2 EXISTING HEAT TRANSFER CORRELATIONS	14

2.3	PRESSURE DROP IN HORIZONTAL TUBE	34
CHAPTER 3 THEORY		
3.1	INTRODUCTION	35
3.2	HEAT TRANSFER	35
3.3	MASS TRANSFER	37
3.4	BASIC ASPECTS OF TWO PHASE FLOW AND HEAT TRANSFER IN HORIZONTAL TUBES	42
3.5	PROPERTIES OF MIXTURES	46
3.6	DEVELOPMENT OF AN EQUATION FOR HEAT TRANSFER	51
3.7	DEVELOPMENT OF FORMULAE USED IN EVALUATING RESULTS FROM EXPERIMENTAL DATA	55
3.8	COMPARISON OF PREDICTED AND EXPERIMENTAL HEAT TRANSFER COEFFICIENTS	58
CHAPTER 4 PREDICTING PRESSURE DROP ACROSS THE TEST SECTION		
4.1	GENERAL	59
4.2	HOMOGENEOUS FLOW PROPERTIES	59
4.3	CALCULATION METHOD	61
CHAPTER 5 EXPERIMENTAL WORK		
5.1	GENERAL	64
5.2	DESCRIPTION OF EXPERIMENTAL RIG	64

5.2.1	STEAM GENERATOR	66
5.2.2	STEAM-AIR MIXER	66
5.2.3	AIR HEATER	67
5.2.4	TEST SECTION	67
5.2.5	AIR SYSTEM	68
5.2.6	COOLING WATER SYSTEM	69
5.2.7	PROTECTION AGAINST HEAT LOSSES	69
5.3	EXPERIMENTAL PROCEDURE	70
CHAPTER 6	ANALYSIS OF DATA	
6.1	INTRODUCTION	74
6.2	REDUCTION OF EXPERIMENTAL DATA	74
6.3	COMPARISON OF EXPERIMENTAL AND PREDICTED CONDENSATION HEAT TRANSFER COEFFICIENT	77
6.4	COMPARISON OF EXPERIMENTAL AND PREDICTED TEMPERATURE PROFILES	78
6.5	LOCAL AXIAL CONDENSATION HEAT TRANSFER COEFFICIENT	80
6.6	COMPARISON BETWEEN PREDICTED AND EXPERIMENTAL PRESSURE DROP	82
6.7	ERROR ANALYSIS	84
6.7.1	INTRODUCTION	84
6.7.2	ACCURACY OF EXPERIMENTAL CONDENSATION HEAT TRANSFER COEFFICIENT VALUES	87

6.7.3	ACCURACY OF EXPERIMENTAL VALUES OF PRESSURE LOSS ACROSS TEST SECTION	88
-------	---	----

## CHAPTER 7 DISCUSSION

7.1	INTRODUCTION	91
7.2	EFFECT OF NCG MASS CONCENTRATION	91
7.3	EFFECT OF TUBE DIAMETER	95
7.4	EFFECT OF FLUID INLET TEMPERATURE	99
7.5	COMPARISON BETWEEN THEORETICAL AND EXPERIMENTAL TEMPERATURE PROFILES	106
7.6	COMPARISON OF EXPERIMENTAL AND PREDICTED HEAT TRANSFER COEFFICIENT	113
7.7	COMPARISON OF PREDICTED AND EXPERIMENTAL PRESSURE DROPS	118

## CHAPTER 8 CONCLUSIONS AND RECOMMENDATIONS

8.1	CONCLUSIONS	120
8.2	RECOMMENDATIONS	122

## APPENDIX 1 SIZING OF THE EXPERIMENTAL RIG COMPONENTS

1.1	GENERAL	124
1.2	STEAM GENERATOR	124
1.3	STEAM SUPERHEATER	124
1.4	AIR HEATER	129

1.5	AIR-STEAM MIXER	130
1.6	TEST SECTION	136

APPENDIX 2 PROPERTIES OF WORKING FLUIDS

2.1	PROPERTIES OF DRY AIR	139
2.2	PROPERTIES OF STEAM AND WATER	140
2.2.1	SATURATED WATER	140
2.2.2	SATURATED STEAM	141
2.2.3	SUPERHEATED STEAM	143
2.3.1	RECOGNITION OF A PERFECT GAS MIXTURE	144

APPENDIX 3	CALIBRATION CHARTS	150
------------	--------------------	-----

APPENDIX 4	COMPUTER PROGRAMS	153
------------	-------------------	-----

APPENDIX 5	TYPES OF GAS EXTRACTORS	176
------------	-------------------------	-----

APPENDIX 6	TABULATED READINGS	185
------------	--------------------	-----

APPENDIX 7	GRAPHS	221
------------	--------	-----

REFERENCES		250
------------	--	-----

### ACKNOWLEDGEMENT

I am thankful and express my gratitude to my project supervisor Dr. J. F. Kanyua and the rest of academic and technical staff in the Department of Mechanical Engineering of the University of Nairobi, for the cooperation they extended to me during the course of this work.



ABSTRACT

An apparatus was constructed for experimental work on condensation of steam-air mixtures in a horizontal tube. The effects of inlet fluid temperature, air mass concentration and tube diameter on the rate of condensation were investigated. It was found that condensation heat transfer coefficient drops by approximately 50% within an air mass of 3% and there after the drop in the heat transfer coefficient became gradual. For fixed air mass concentration and inlet fluid temperature, the heat transfer coefficient increased with a decrease in tube diameter. For fixed tube diameter and air mass concentration, the mean heat transfer coefficient decreased with increasing inlet fluid temperature.

From measurement of pressure drop across the test section, it was found that the theoretical model based on a two phase pressure drop equation, integrated piece wise along the test section and making use of global parameters for every section gave values comparable to those determined from the experiment.

From the theoretical model based on condensation heat transfer coefficient in the presence of non condensable gases correlation, it was found that the model predicted temperature profiles accurately in the range of saturated steam but was subject to errors in the superheat region.

The comparison between the experimental values of condensation heat transfer coefficient at zero concentration of air and those predicted by Shah(1979) and Akers et al(1958) showed that the former correlation consistently predicted much higher values at all conditions while the latter predicted values closer to experimental values especially at saturation and small degrees of superheat.

NOMENCLATURE

a	Area of cross section [ $m^2$ ]
A	Surface area [ $m^2$ ]
c	Concentration of a constituent [ $kg\ mol/m^3$ ]
$c_p$	Specific heat capacity at constant pressure [ $kJ/kg\ K$ ]
d	Diameter of the tube [ m ]
D	Mass diffusivity [ $m^2/s$ ]
$d_r$	Deviation from the mean value
e	Error in a quantity
f	Frictional factor
g.	Gravitational constant [ $N/kg$ ]
G	Mass flux [ $kg/m^2$ ]
$h_m$	Heat transfer coefficient by all correlation except Nusselt's [ $W/m^2K$ ]
$h_{nu}$	Heat transfer coefficient by Nusselt's correlation [ $W/m^2K$ ]
$h_{fg}$	Latent heat of vaporization [ $kJ/kg$ ]
k	Thermal conductivity [ $W/m\ K$ ]
$K_G$	Mass diffusion coefficient
l	Length [ m ]
$\dot{m}$	Mass flow rate [ $kg/s$ ]
m	Mass [ kg ]
M	Molecular mass [ $kg\text{-mole}$ ]
N	Number of moles
P	Pressure [ $N/m^2$ ]

$P_r$	Reduced pressure
$Q$	Quantity of heat [ kJ ]
$q$	Heat flux [ $W/m^2$ ]
$R$	Thermal resistance [ $m^2 K/W$ ]
$t$	Temperature [ $^{\circ}C$ ]
$th$	Thickness [ m ]
$U$	Overall heat transfer coefficient [ $W/m^2 K$ ]
$u$	Velocity [ m/s ]
$V$	Volume [ $m^3$ ]
$W$	Mass fraction
$x$	Dryness fraction
$Y$	Mole fraction
$z$	Any quantity referred to in the error analysis
$\Delta$	Difference in quantities
$\lambda$	Flowing volume hold up
$\mu$	Viscosity [ kg/m s ]
$\rho$	Density [ $kg/m^3$ ]
$\phi$	Any quantity used in the error analysis.

### Subscripts

a	Air
c	Condensate -gas interface or condensate
cu	Copper
g	Vapour (steam)
i	Any of the constituents used in the summation
l	Liquid phase
m	Wall condition
ns	Non-slip quantities
sat	Saturated condition
t	Total of liquid and gaseous phase
v	Gaseous phase
f	Cooling water
1	Inlet conditions
2	Outlet conditions

## CHAPTER ONE.

### INTRODUCTION.

#### 1.1 GENERAL.

In the recent years growth of computer based design methods has led to the need for accurate heat transfer data rather than the empirical relationships derived from experience. The need for this type of information arose from three sources:-

1. Need by designers for detailed information so that they may optimize their designs to produce products which are effective and competitive in the todays market.
2. For operators of plant who need to decide on the optimum operating conditions or in less fortunate situations require to diagnose faults which have already occurred owing to the departure from design conditions.
3. For the safety of plant operation ,it is necessary to know the maximum safe operating limit with precision in order that adequate safety margins may be allowed.

It was the purpose of this project to set up a suitable experiment to generate the heat transfer data that may be used to develop the necessary accurate design equations

which may partially meet the above three mentioned needs for geothermal plant heat exchangers and for other heat exchangers which handle vapours mixed with non condensable gases(NCG).The main sources of NCG are air leakages into the exchangers,the dissolution of dissolved gases and the geothermal type NCG which come mixed with geo-fluid from the well.

This work deals with the effect of the NCG on the rate of condensation, so to aid better understanding of the work, the rest of the chapter discusses the types of condensers, the effects of NCG on their working etc.

## 1.2 DIRECT CONTACT CONDENSERS

These involve mixing of the vapour with a cooling liquid [Figure 1.1] so that the vapour can reject its latent heat and may be sensible heat to the cooling liquid with a consequent increase in the temperature of the cooling liquid .They are either of the barometric or the low level-jet types.

### 1.2.1 THE BAROMETRIC CONDENSERS

The vapour enters the condenser shell at the lower end and travels upwards towards the top of the shell(Figure 1.2). Circulating cooling water entering at the upper part

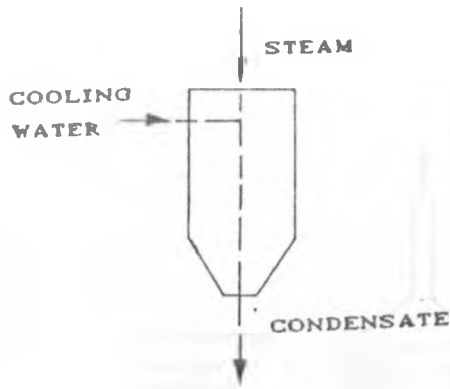


FIGURE 1.1: DIRECT CONTACT CONDENSER

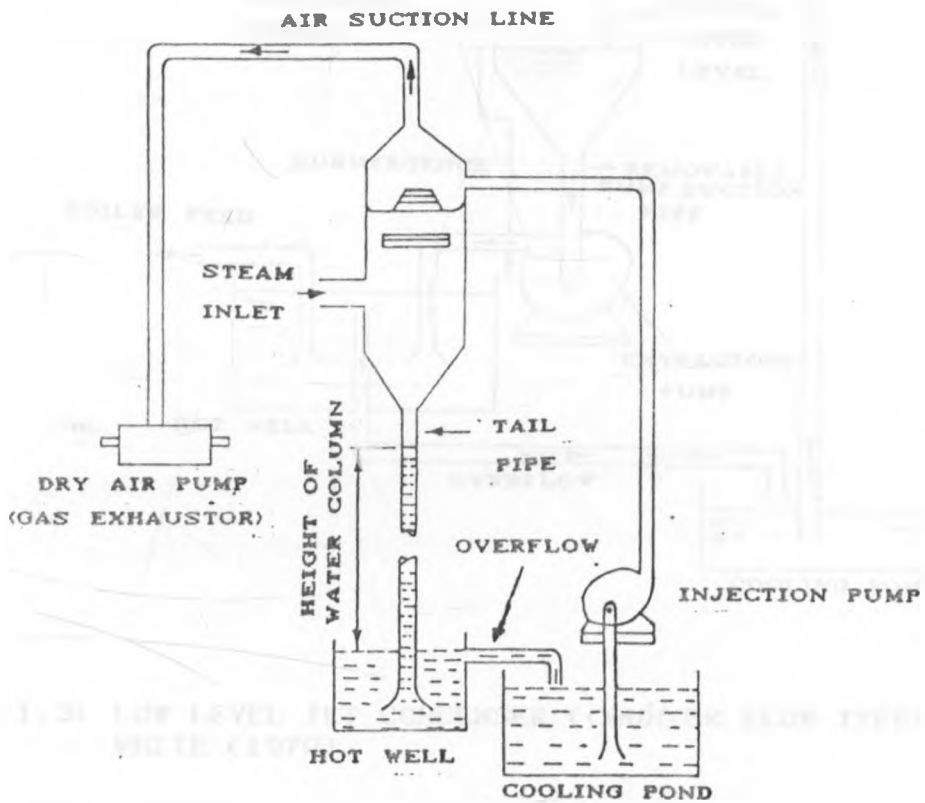


FIGURE 1.2: HIGH LEVEL DIRECT CONTACT CONDENSER (BAROMETRIC CONDENSER)  
WHITE (1979)



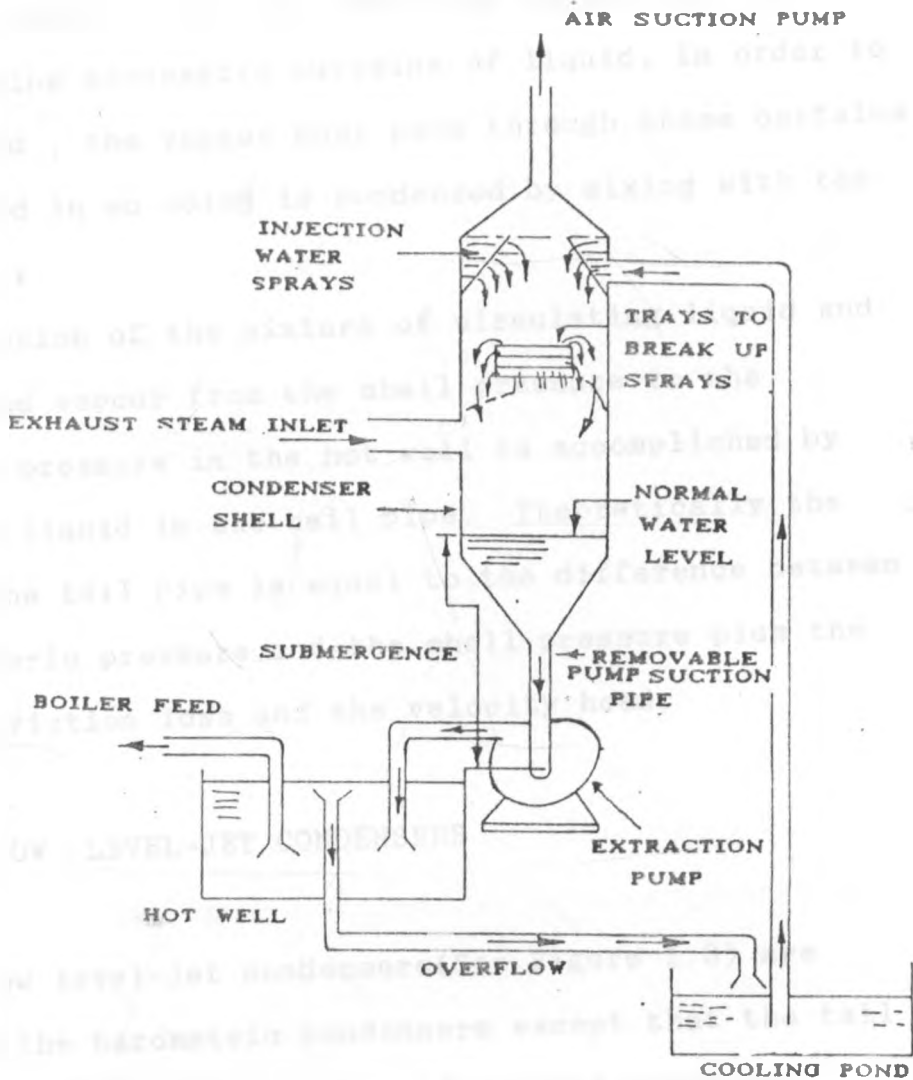


FIGURE 1.3: LOW LEVEL JET CONDENSER (COUNTER FLOW TYPE)  
WHITE (1979)

of the shell impinges on the top baffle and cascades downward by gravity over the remaining baffles and baffle rings , forming successive curtains of liquid. In order to travel upward , the vapour must pass through these curtains of liquid and in so doing is condensed by mixing with the cooling water.

Compression of the mixture of circulating liquid and the condensed vapour from the shell pressure to the atmospheric pressure in the hot well is accomplished by a column of liquid in the tail pipe. Theoretically the height of the tail pipe is equal to the difference between the atmospheric pressure and the shell pressure plus the tail pipe friction loss and the velocity head.

### 1.2.2 THE LOW LEVEL-JET CONDENSERS

The low level-jet condensers(See Figure 1.3) are similar to the barometric condensers except that the tail pipe is eliminated. The mixture of cooling water and condensate is compressed from the condenser pressure to essentially atmospheric pressure either by a pump or by use of the kinetic energy of the water jet. Elimination of the tail pipe reduces the head room required by the condenser.

### 1.3 THE SURFACE CONDENSERS

In the surface condensers(See Figure 1.4), the vapour condenses as it comes into contact with the cooler surface of tubes through or outside of which the cooling medium flows.The cooling medium does not contaminate the condensate formed and vice versa and hence surface condensers are widely used in the thermal power plants where water treatment is expensive.

The design and construction of surface condensers vary in the arrangement, the number of tubes,the number of water passes,the number of vapour passes, the way the cooling medium is distributed inside the condensers and the method of air removal etc. There are three main types: .the shell and tube;the shell and coil and the tube in tube. In all the cases ,varying degrees of counter flow is attempted.

#### 1.3.1 SHELL AND COIL CONDENSERS

Shell and coil condensers(See Figure 1.5) have cooling tube in one or more continuous or assembled coils contained within a shell. The vapour condenses on the outside or the inside of the tubes while the cooling water flows on the other side.

### 1.3.2 TUBE-IN-TUBE CONDENSERS

Tube in tube condensers (See Figure 1.6) consist of assemblies of two tubes, one within the other in which the vapour is condensed in either the annular space or the inner tube. Condensation heat transfer coefficients are more difficult to predict especially when condensation occurs within the tube or annulus because the mechanism differs considerably from condensation on the outside of an isolated horizontal tube.

### 1.3.3 SHELL AND TUBE CONDENSERS

Shell and tube condensers (See Figures 1.7 to 1.10), the vapour condenses on the outside of the tubes and circulating or cooling liquid circulates through tubes in a single or a multi-pass circuit or vice versa. The proximity of the vapour inlet and the cooling liquid outlet may adversely affect the condenser performance and therefore baffles are added at the inlet and/or the outlet connection to diminish this effect.

To further increase heat transfer coefficient enhanced heat transfer surfaces e.g spiral grooves and ridges , internal fins and other devices to promote turbulence and to augment heat transfer are provided.

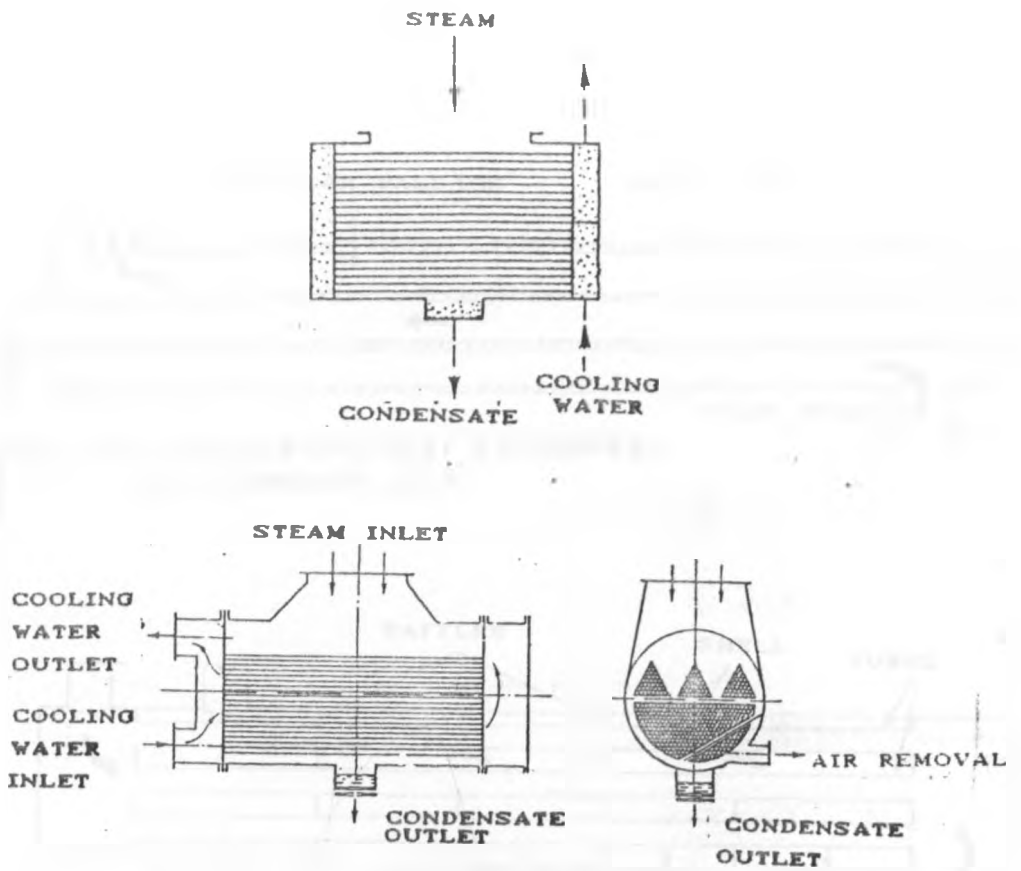


FIGURE 1.4: SURFACE CONDENSERS BUTTERWORTH (1977)

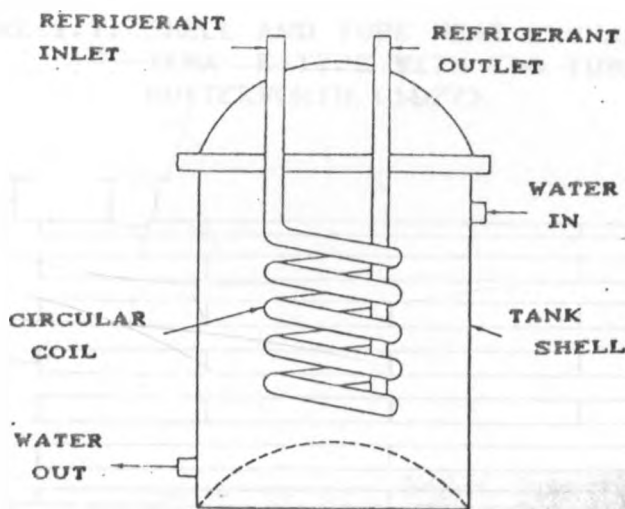


FIGURE 1.5: SHELL AND COIL CONDENSERS BUTTERWORTH (1977)

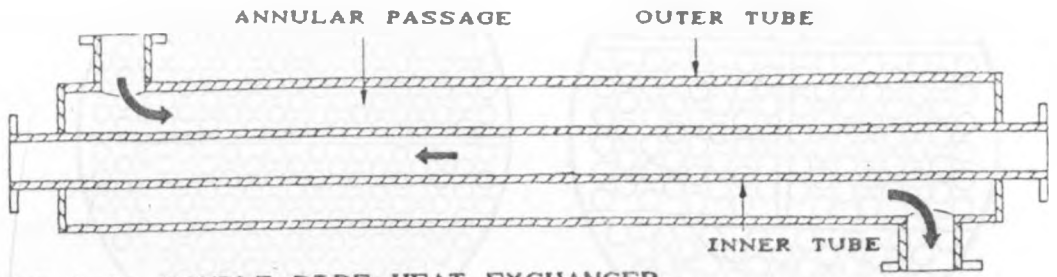


FIGURE 1.6: DOUBLE-PIPE HEAT EXCHANGER BUTTERWORTH (1977)

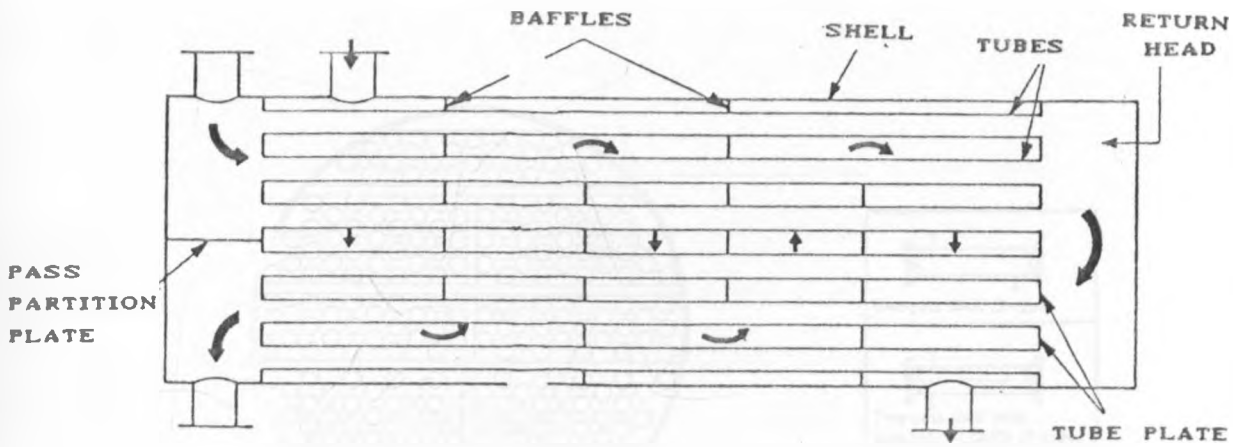


FIGURE 1.7: SHELL AND TUBE HEAT EXCHANGER TEMA E-TYPE WITH TWO TUBE-SIDE PASSES BUTTERWORTH (1977)

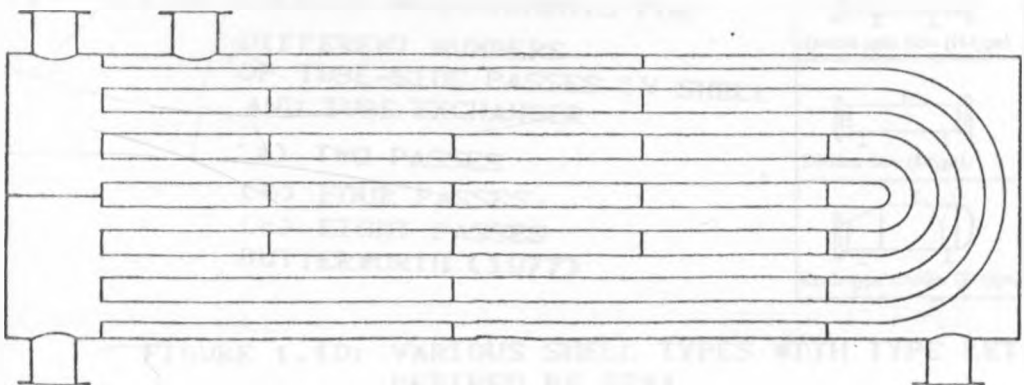
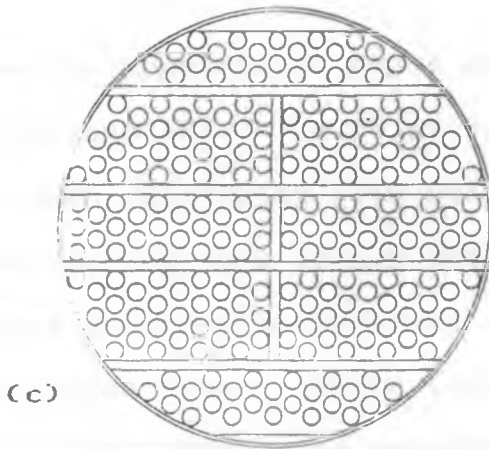
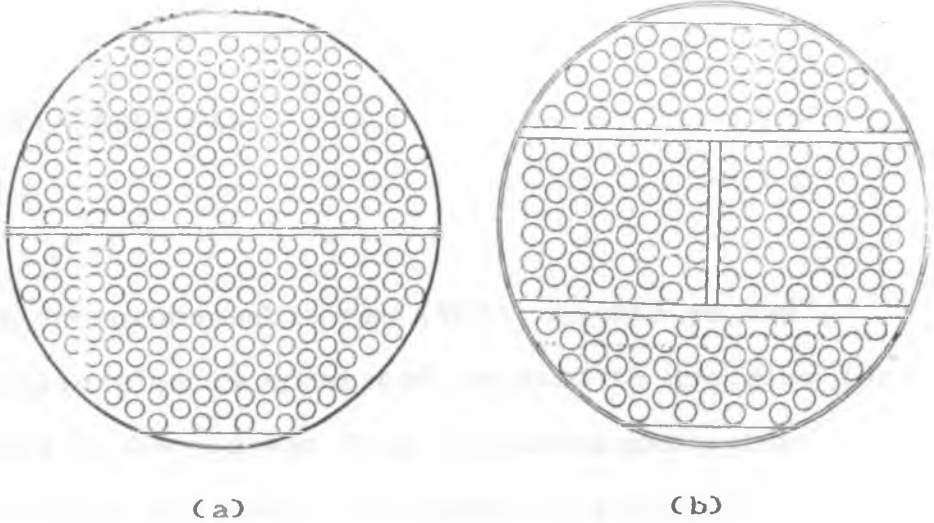
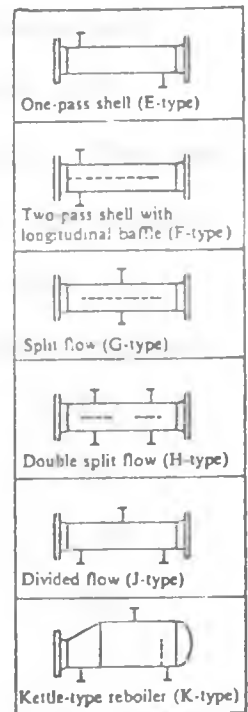


FIGURE 1.8: SHELL AND TUBE HEAT EXCHANGER TEMA U-TYPE WITH TWO TUBE-SIDE PASSES BUTTERWORTH (1977)



(c)

**FIGURE 1.9: VARIOUS ARRANGEMENTS FOR DIFFERENT NUMBERS OF TUBE-SIDE PASSES IN SHELL AND TUBE EXCHANGER**  
 (a) TWO PASSES  
 (b) FOUR PASSES  
 (c) EIGHT PASSES  
 BUTTERWORTH (1977)



**FIGURE 1.10: VARIOUS SHELL TYPES WITH TYPE LETTERS DEFINED BY TEMA**  
 BUTTERWORTH (1977)

#### 1.4 NON-CONDENSABLE GAS.

##### 1.4.1 GENERAL.

The term non-condensable gas (NCG), as far as the geothermal application is concerned is used to describe the gases that have to be removed from the turbo-generator condensers or other equipment in order to maintain relatively low condenser pressure and high turbine power output.

The NCG usually consists of gases originating from the geothermal fluid and air. The relative proportions and quantities of each gas varies from field to field and sometimes from well to well within the same field. The gas content in steam is usually expressed in percent by weight in primary separated steam. White (1979) gives the following total NCG contents by weight for various fields:-

Larderello (Italy)	10%
Geysers (USA)	1%
Wairakei (New Zealand)	0.2%
Olkaria (Kenya)	0.2%

The composition of NCG also varies from well to well for example:

Wairakei (New Zealand)- 97.3% CO<sub>2</sub>, 2.3% H<sub>2</sub>S, 0.1% CH<sub>4</sub>,  
0.3% N<sub>2</sub>.

Olkaria (Kenya)- 1-12% H<sub>2</sub>S, 99-88% CO<sub>2</sub>.



#### 1.4.2 EFFECT OF NCG ON CONDENSER PERFORMANCE AND TURBINE PERFORMANCE.

It has been shown by Sparrow and Lin (1964) that the presence of very small amounts of NCG in the bulk of vapour causes considerable reduction in the condensation heat transfer rates and thus condenser capacity due to build up of gas at the liquid vapour interface and the blanketing effect of the stratum of gas left as the vapour condenses.

When NCG is present in a steam power plant, it will accumulate in the condenser leading to an increase in the turbine outlet pressure. This effect will lead to a reduction in the turbine output power and the overall efficiency of the plant. Detailed studies on the effect of NCG on power output are given by Khalifa and Michaelides (1978) and the other authors.

#### 1.4.3 GAS EXTRACTION SYSTEMS

Because of the effect of NCG on the heat transfer rates and the turbine power output, a gas extraction system is normally installed to remove the NCG from turbo-generator condensers.

The main types of gas exhaustion systems are: Reciprocating vacuum pump, steam jet ejector, liquid ring pump, radial blower and centrifugal compressors. These are

illustrated in Appendix 5 as Figures A5.1 to A5.5

In general the gas extraction systems are inefficient and therefore the power consumption of such systems is high. Whether this is of any real consequence is dependent on the monetary value placed on the steam. The steam consumption by these systems is of real importance if it is considered in terms of the power that could be generated if that steam were utilized in a turbo-generator. This means a balance has to be struck between the level of NCG to be tolerated in various plant components and the power to be foregone to operate the gas exhaustion system. Therefore accurate data on the effect of NCG on the heat exchanger performance is necessary to pin point the optimum point of operation.

CHAPTER TWO  
LITERATURE REVIEW.

2.1 INTRODUCTION.

Condensation heat transfer has been studied widely for many years and several different techniques and apparatus for obtaining experimental data have evolved. In the present study, interest will be confined to the film condensation of vapours on the inside of horizontal tubes of various diameters in the presence of non-condensable gas (NCG).

2.2 EXISTING HEAT TRANSFER CORRELATIONS

Nusselt (1916) combined heat and mass balances to derive Equation 2.1 for heat transfer coefficient for a pure vapour film condensing on the outside of a horizontal tube:

$$h_{Nu} = 0.725 \left[ \frac{k^3 \rho^2 h_{fg} g}{\mu d \Delta t} \right]^{1/4} \quad (2.1)$$

Chato (1962) by modifying Equation 2.1 suggested the following expression for heat transfer coefficient for a

pure vapour film condensing on the inside of a horizontal tube:

$$h_{Nu} = 0.555 \left[ \frac{g \rho \left( \rho - \rho_v \right) k^3 h'_{fg}}{\mu d \Delta t} \right]^{1/4} \quad (2.2a)$$

where

$$h'_{fg} = h_{fg} + \frac{3}{8} c_{p,l} (t_g - t_m) \quad (2.2b)$$

Equation 2.2 has been shown to apply for refrigerants at low vapour Reynolds number such that

$$Re_v = \frac{\rho_v u_v d}{\mu_v} < 35,000 \quad (2.2c)$$

where  $Re_v$  is evaluated at inlet conditions.

In a comprehensive review of the work in this field and after additional experimental investigations, Akers et al (1958) reported that for condensing vapours in either horizontal or vertical tubes, the following relations correlated the practical data to within  $\pm 20\%$  .:

$$Nu_d = 5.03 Re_d^{1/3} Pr^{1/3} \quad Re_d < 5 \times 10^4 \quad (2.3a)$$

$$Nu_d = 0.0265 Re_d^{0.8} Pr^{1/3} \quad Re_d > 5 \times 10^4 \quad (2.3b)$$

where  $Re_o = Re_L + Re_v (\rho_L / \rho_v)^{1/2}$  (2.3c)

and  $Re_L$  and  $Re_v$  are based on mass fluxes defined by assuming the whole flow is composed of either the liquid or the vapour respectively i.e superficial mass fluxes.

Shah (1979) derived a dimensionless correlation for predicting the heat transfer coefficient during film condensation on the inside of a horizontal tube. Shah (1979) verified his correlation by using a wide variety of data from experiments using fluids such as water, R-11, R-22, Methanol and Ethanol condensing on the inside of a horizontal, inclined and vertical tubes of diameters ranging from 7mm to 40mm and for reduced pressure ( $P/P_c$ ) range of 0.002 to 0.44, saturated temperature from 21°C to 310°C, vapour qualities from 0 to 100% and Prandtl number from 1 to 13. The correlation was given as:

$$h_{TP} = h_L \left[ (1-x)^{0.8} + 3.8x^{0.76} \left( \frac{(1-x)^{0.04}}{P_R^{0.38}} \right) \right] \quad (2.4a)$$

$$Nu = \frac{h_L d}{k_L} = 0.023 Re_L^{0.8} Pr_L^{0.4} \quad (2.4b)$$

where  $x$  refers to vapour quality along the tubes.

Defining the mean heat transfer coefficient as  $h_{TPM}$  then:

$$h_{TPM} = \frac{1}{L} \int_0^L h_{TP} dL \quad (2.4c)$$

By assuming a linear variation of vapour quality and expanding the second term in Equation (2.4a) by binomial theorem and neglecting the small terms,  $h_{TFM}$  becomes:

$$h_{TF} = \frac{h_L}{x_2 - x_1} \left[ \frac{-(1-x)^{1.8}}{1.8} + \frac{3.8}{p_R^{0.98}} \left( \frac{x^{1.76}}{1.76} - \frac{0.04x^{2.76}}{2.76} \right) \right]_{x_1}^{x_2} \quad (2.4d)$$

This worker presented results from the correlation he derived together with those of other workers in graphical form as shown on Figures 2.1 to 2.5. The mean deviation of the data of the other workers from the Equation 2.4 a was reported to be  $\pm 15.4\%$ .

Analysis of condensation in the presence of NCG is complex because concentration and temperature gradients are set up in vapour-gas mixture and consequently buoyancy forces owing to both concentration and temperature differences are created. Another physical mechanism of potential importance is the so called inter facial resistance which results from the fact that the net condensation of vapour at an interface is actually the differences between the simultaneous processes of evaporation and condensation. The kinetic theory of gases show that the imbalance between these two processes must be

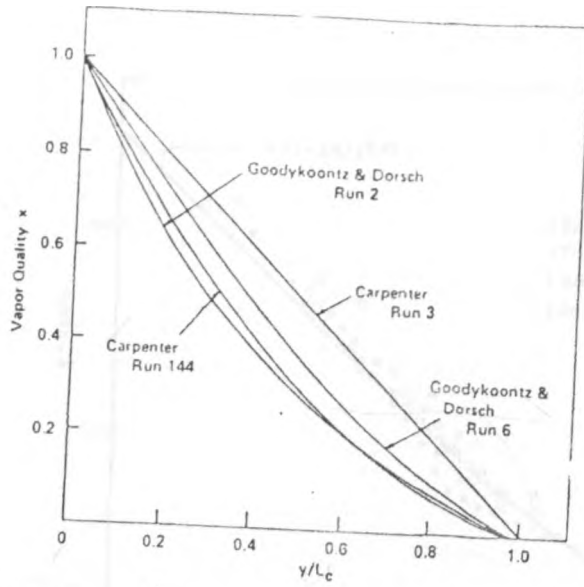


FIGURE 2.1: VARIATION OF VAPOUR QUALITY WITH DIMENSIONLESS CONDENSING LENGTH SHAH (1979)

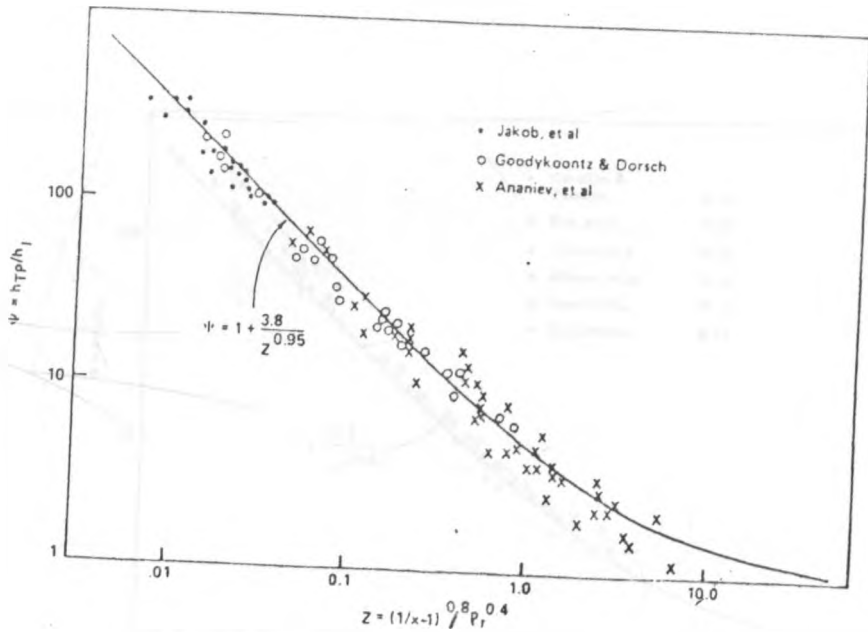


FIGURE 2.2: COMPARISON OF SOME CONDENSING WATER DATA WITH EQUATION 2.4 SHAH (1979)

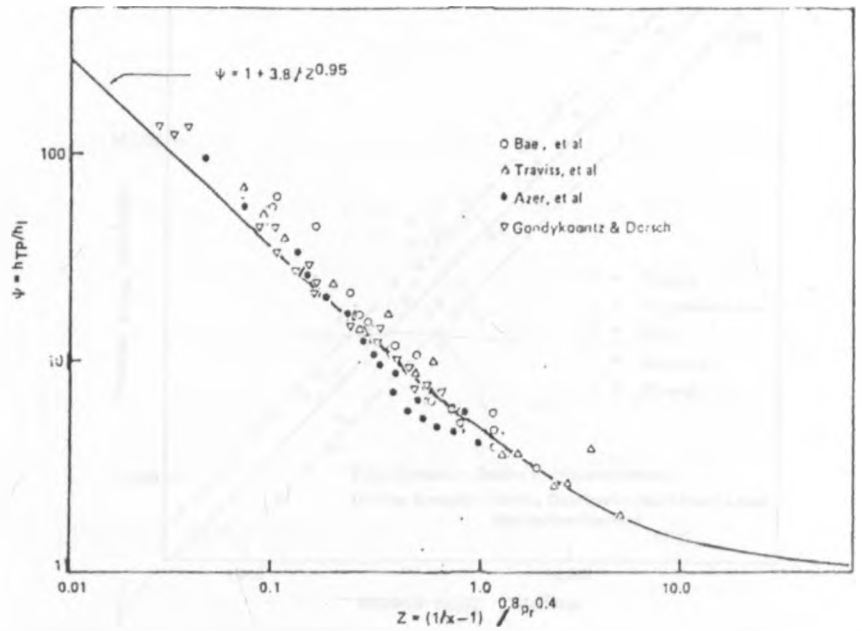


FIGURE 2.3: COMPARISON OF EQUATION 2.4 WITH SOME DATA OF R-12 AND R-113 SHAH (1979)

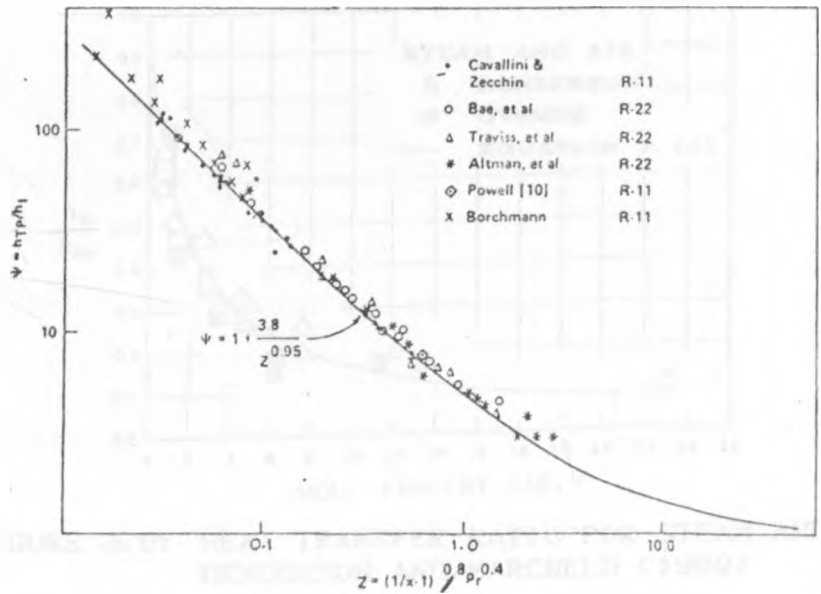


FIGURE 2.4: COMPARISON OF EQUATION 2.4 WITH SOME DATA OF R-11 AND R-22 SHAH (1979)



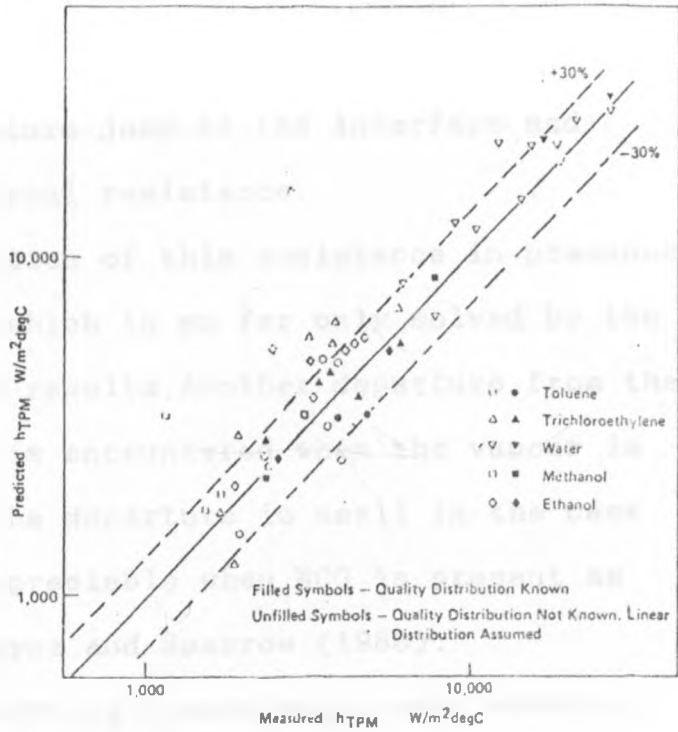


FIGURE 2.5: COMPARISON OF MEAN HEAT TRANSFER COEFFICIENTS REPORTED BY CARPENTER WITH PREDICTIONS OF EQUATION 2.4 SHAH (1979)

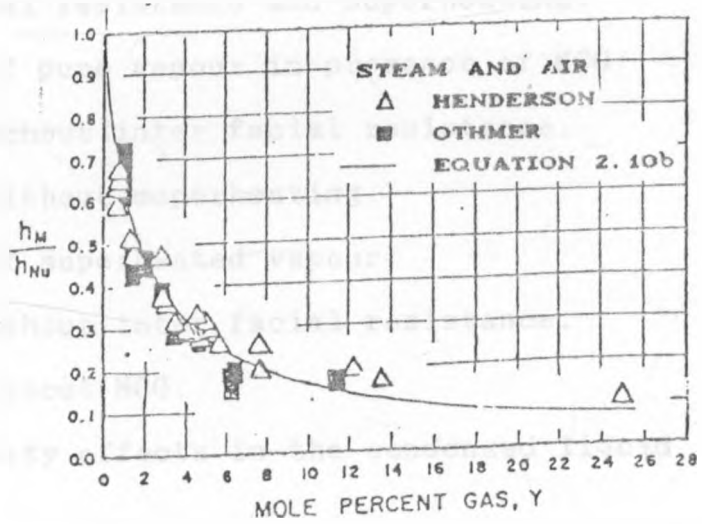


FIGURE 2.6: HEAT TRANSFER RATIO FOR STEAM AND AIR HENDERSON AND MARCHELO (1969)

accompanied by a temperature jump at the interface and hence the additional thermal resistance.

The analytical solution of this resistance in presence of the NCG is a problem which is so far only solved by the partial use of empirical results. Another departure from the classical Nusselt model is encountered when the vapour is superheated. Although the departure is small in the case of pure vapour, it is appreciable when NCG is present as has been shown by Minkowycz and Sparrow (1966).

In view of their technical importance, most workers have selected steam as the vapour and air as the NCG. The main lines of past and present research can be categorized along the following lines:

1. Condensation of pure vapour:

-Inter facial resistance and superheating.

2 Condensation of pure vapour in presence of NCG:

-With or without inter facial resistance.

-With or without superheating.

3 Condensation of superheated vapour:

-With or without inter facial resistance.

-With or without NCG.

4 Variable property effects in the condensed liquid layers.

A quantitative approach for the case where NCG is present was given by Othmer(1929) where measured quantities of air were introduced into steam and condensation

proceeded at various temperature drops and different steam temperatures. A complex empirical equation relating the heat transfer coefficient of the condensing steam to the temperature drop, steam temperature and NCG concentration was presented as:

$$\text{Log}_{10} h_M = [1.213 - 0.00242t_g] \log_{10} \Delta t + \left[ \frac{\log_{10} \Delta t}{3.439} - 1 \right] \times \left[ \log_{10} (Y + 0.505) - 1.551 - 0.009t_g \right] \quad (2.5)$$

in which  $h_M$  is in Btu/hr-sq.ft.-°F,  $t$  in °F and  $Y$  is percent molar concentration of air in the mixture.

Other than Othmer (1929) few investigators considering the condensation on the inside of horizontal tubes have attempted to correlate the heat transfer coefficient with the concentration of NCG.

For condensation of steam on the inside of vertical tubes, Meisenburg et al (1936) found that the ratio of observed heat transfer coefficient  $h_m$  to Nusselt's (1916) predicted value  $h_{Nu}$  was given by:

$$\left[ \frac{h_m}{h_{Nu}} \right] = 1.17 / (100W)^{0.11} \quad (2.6)$$

$W$  = mass percent of air in the mixture where  $W$  varied from 0.002 to 0.04. Hampson (1951) found the heat transfer coefficient ratio to vary as:

$$h_m/h_{Nu} = 1.2-20W \quad (2.7)$$

Henderson and Marchello(1969) also performed experiments using a steam - air system and toluene - Nitrogen system condensing inside horizontal tubes. These workers defined a ratio H where:

$$H = h_m/h_{Nu} \quad (2.8)$$

where  $h_m$  and  $h_{Nu}$  were evaluated under same conditions.

Making use of Antoine Equation [Chapman (1939) for the vapour pressure- temperature relation of the condensable and the equation for binary-mixture with one gas constant to relate the concentration and the temperature at the vapour-liquid interface to those of wall and bulk values. The treatment resulted in a series expansion for H in terms of mole concentration of NCG (Y), the general expression is:

$$H = 1/(1+C_1Y+C_2Y^2+C_3Y^3+\dots) \quad (2.9)$$

and for the first two and one terms respectively

$$H = 1/(1+C_1Y+C_2Y^2) \quad (2.10a)$$

$$H = 1/(1+C_1Y) \quad (2.10b)$$

where Y is the mole fraction of NCG in the mixture and

$C_1, C_2, C_3, \dots$  are constants. To evaluate constants

$C_1, C_2, C_3, \dots$  use was made of the least squares method to

fit the data. The final equations of ratio H from

Henderson and Marchello (1969) are shown graphically on

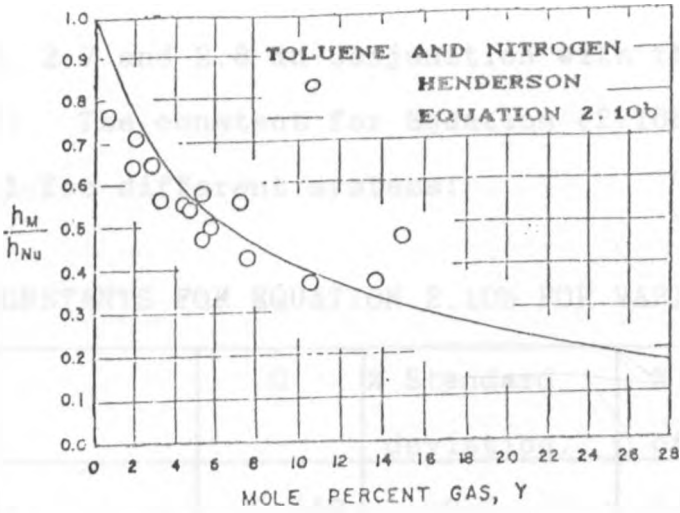


FIGURE 2.7: HEAT TRANSFER RATIO FOR TOLUENE AND NITROGEN HENDERSON AND MARCHELO (1969)

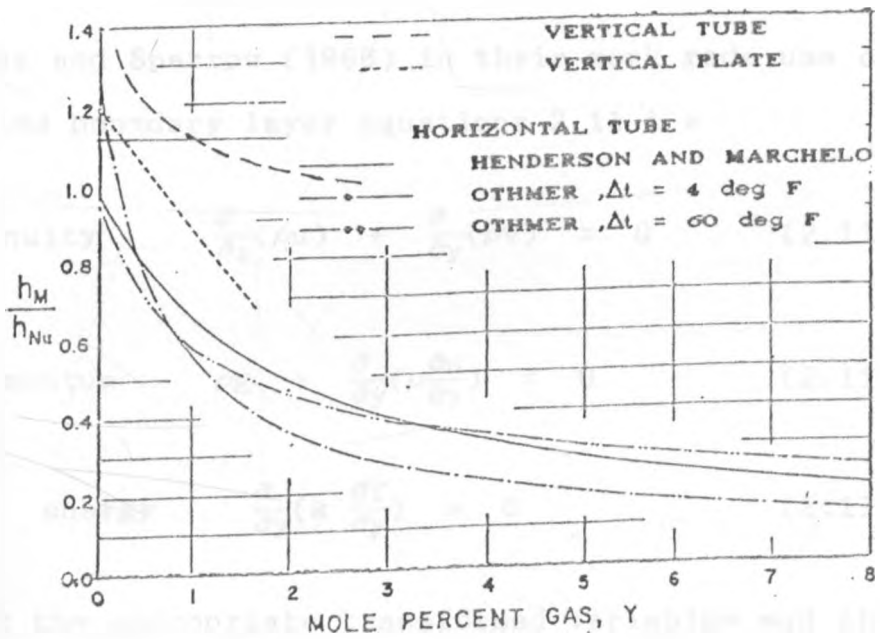


FIGURE 2.8: HEAT TRANSFER RATIO CORRELATION FOR STEAM AND AIR SYSTEM HENDERSON AND MARCHELO (1969)

Figures 2.6, 2.7 and 2.8 in conjunction with those of Othmer(1929). The constant for Equation (2.10b) is given on Table 2.1 for different systems:

TABLE 2.1:CONSTANTS FOR EQUATION 2.10b FOR VARIOUS SYSTEMS

System	C	% Standard deviation.	% Mole ratio of NCG range.
Steam-Air	0.510	9.2	0.64 - 25.1
Toluene-Nitrogen	0.149	8.7	0.71 - 59.1
Benzene-Nitrogen	0.076	14.3	7.10 - 20.3

Minkowycz and Sparrow (1966) in their work made use of the simplified boundary layer equations 2.11 i.e

$$\text{continuity} \quad \frac{\partial}{\partial z}(\rho u) + \frac{\partial}{\partial y}(\rho v) = 0 \quad (2.11a)$$

$$\text{momentum} \quad \rho g + \frac{\partial}{\partial y}(\mu \frac{\partial u}{\partial y}) = 0 \quad (2.11b)$$

$$\text{energy} \quad \frac{\partial}{\partial y}(k \frac{\partial T}{\partial y}) = 0 \quad (2.11c)$$

and by using the appropriate transformed variables and the theory of binary mixtures numerically solved these governing equations.

These workers decided to compare their result i.e heat transfer in presence of NCG with that of standard Nusselt's

model. In Nusselt's model they considered the thermal driving force to be  $[t_{SAT,g} - t_m]$  and derived the appropriate reference temperature, numerical solution of the governing equations for liquid layer were carried out for prescribed values of  $t_{SAT}$  ranging from  $26.7^\circ\text{C}$  to  $100^\circ\text{C}$  for pressure levels of 0.5 bar to 1 bar and the temperature difference  $[t_{SAT,g} - t_m]$  varying from  $1^\circ\text{C}$  to  $25^\circ\text{C}$ . The variable heat transfer coefficient results thus obtained were compared to Nusselt's model. It was found that virtual coincidence between the two sets of results could be obtained by evaluating properties appearing in Nusselt's model at a reference temperature  $t^*$  defined as:

$$t^* = t_m + 0.31(t_{SAT,g} - t_m) \quad (2.12)$$

Minkowycz and Sparrow(1966) presented the heat transfer results in the form of ratio of heat fluxes from their model ( $q$ ) to those from Nusselt's ( $q_{Nu}$ ), i.e ( $q/q_{Nu}$ ) for the case of the effect of NCG on the local wall heat flux for the cases where the bulk was saturated and superheated as shown in Figures 2.9 to 2.14.

In a later work Sparrow and Minkowycz (1969) did further computations of  $q/q_{Nu}$  for steam - air systems where mass fraction of air ( $W$ ) was assigned values of 0.005, 0.02, 0.05, 0.10 and, in addition at each fixed mass fraction of air, temperature difference was varied from  $2^\circ\text{F}$

(-16.7°C) to 40°F (4.4°C) for bulk temperatures of 80°F (26.2°C) and 212°F (100°C).

The results were presented graphically as shown in the Figures 2.15 to 2.19.

Sparrow and Minkowycz (1969) in their conclusion observed that the reduction in the heat transfer rate due to NCG was accentuated at low operating pressures. Also in general the condensation in forced convection flow was much less sensitive to the presence of NCG than in gravity flow and the interfacial resistance was negligible in forced convection flow. In Figures 2.15 to 2.19 depicting the work of Sparrow and Minkowycz (1969), the departure of  $q/q_{Nu}$  from unity is a direct measure of the effect of the NCG on the condensation heat transfer rate. It is also seen that the ratio of  $(q/q_{Nu})$  increases with  $(t_{\infty} - t_v)$  for small values i.e. about 2-7°C to a maximum and then decreases gradually with an increase in  $(t_{\infty} - t_v)$  in forced convection flow.



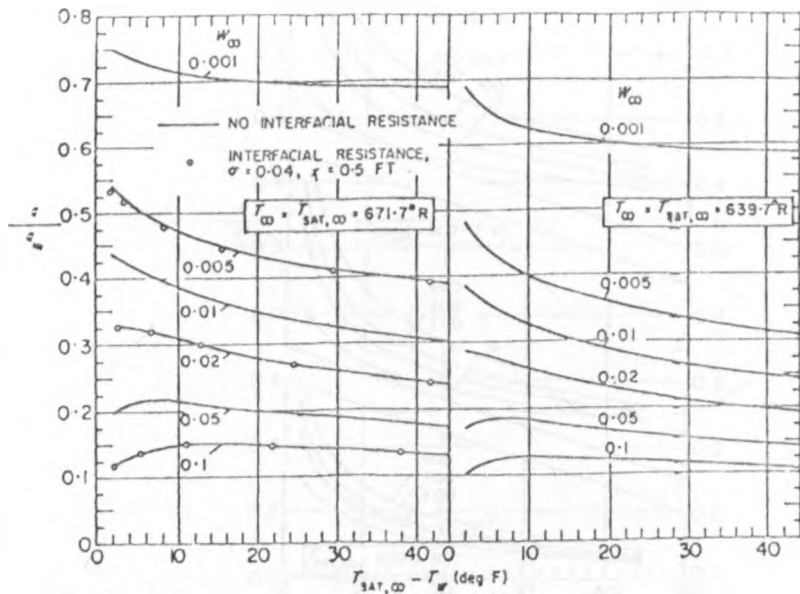


FIGURE 2.9: CONDENSATION HEAT TRANSFER IN THE PRESENCE OF NCG, SATURATED BULK TEMPERATURE  $T_{SAT, \infty} = 671.7 R$  AND  $639.7 R$  SPARROW AND MINKOWYCZ (1966)

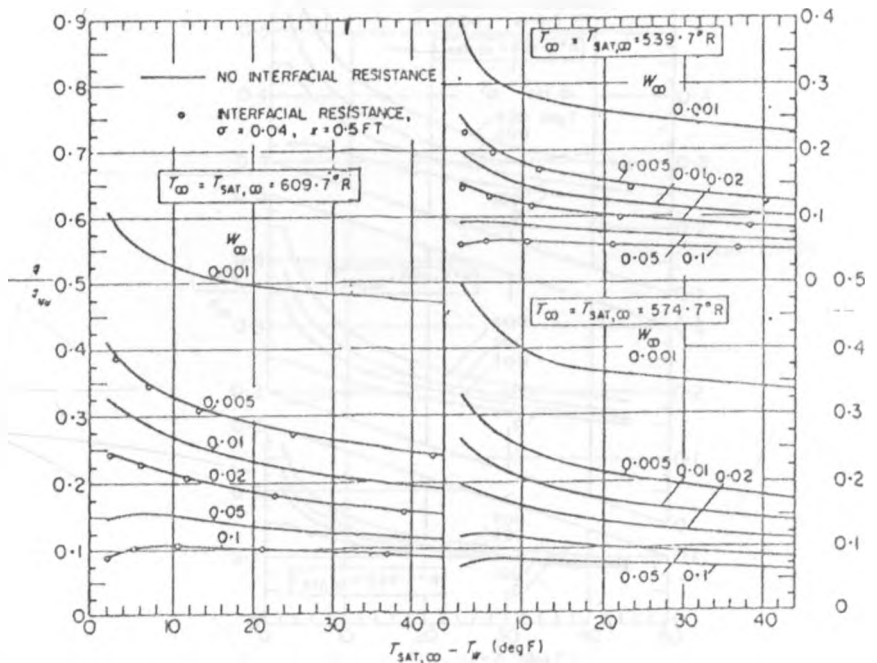


FIGURE 2.10: CONDENSATION HEAT TRANSFER IN THE PRESENCE OF NCG, SATURATED BULK TEMPERATURE  $T_{SAT, \infty} = 609.7 R$ ,  $574.7 R$  AND  $539.7 R$  SPARROW AND MINKOWYCZ (1966)

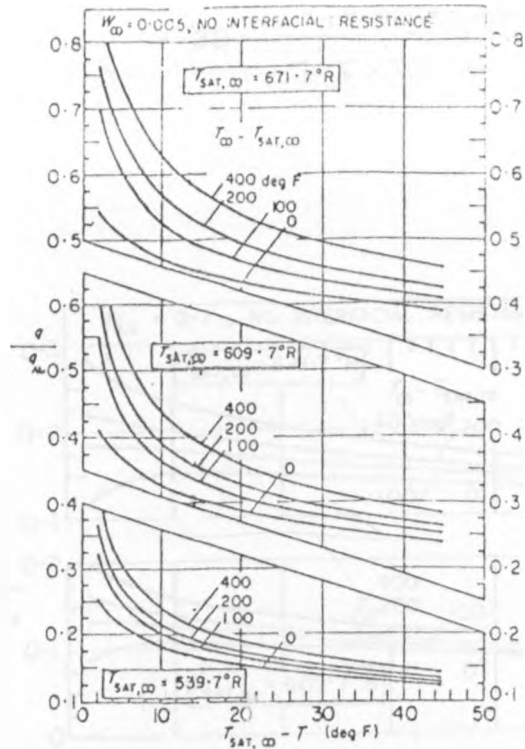


FIGURE 2.11: CONDENSATION HEAT TRANSFER IN THE PRESENCE OF NCG, SUPERHEATED BULK,  $W_{\infty} = 0.005$  SPARROW AND MINKOWYCZ (1966)

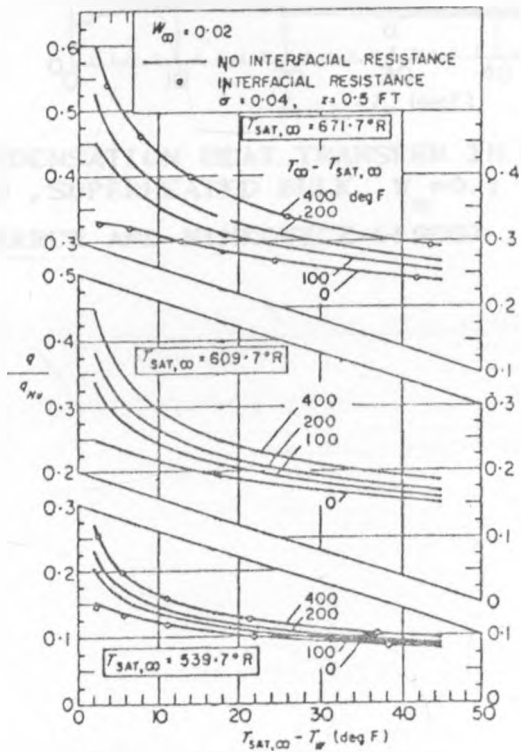


FIGURE 2.12: CONDENSATION HEAT TRANSFER IN THE PRESENCE OF NCG, SUPERHEATED BULK,  $W_{\infty} = 0.02$  SPARROW AND MINKOWYCZ (1966)

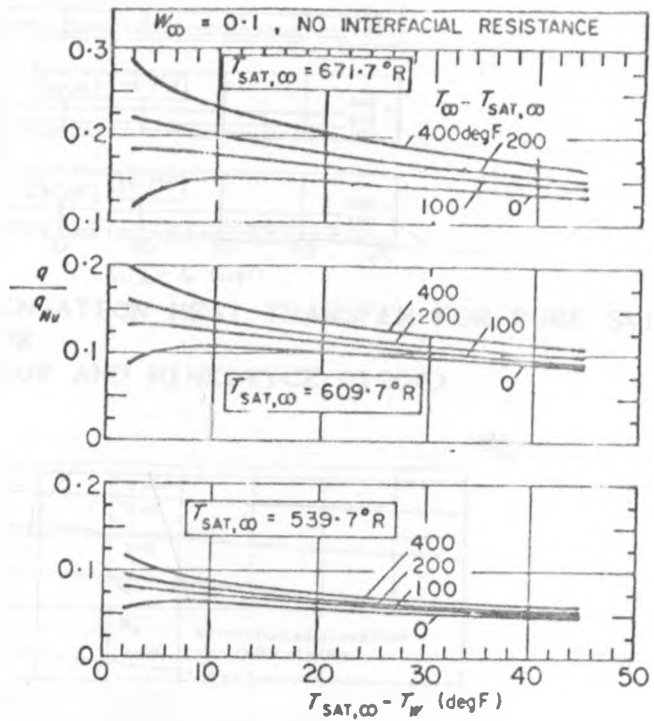


FIGURE 2.13: CONDENSATION HEAT TRANSFER IN THE PRESENCE OF NCG, SUPERHEATED BULK,  $W_{\infty} = 0.1$   
SPARROW AND MINKOWYCZ (1966)

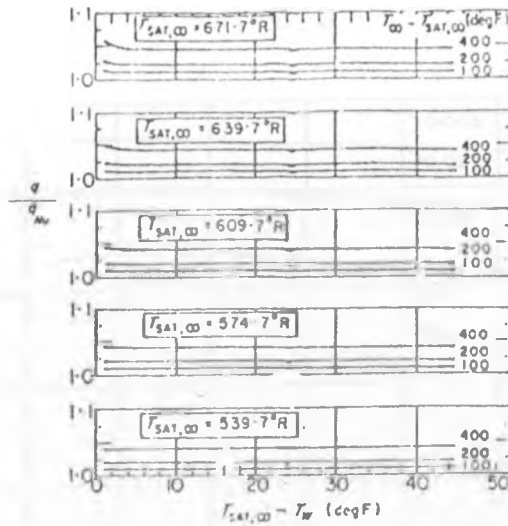


FIGURE 2.14: CONDENSATION HEAT TRANSFER FOR PURE SUPERHEATED VAPOUR  
SPARROW AND MINKOWYCZ (1966)

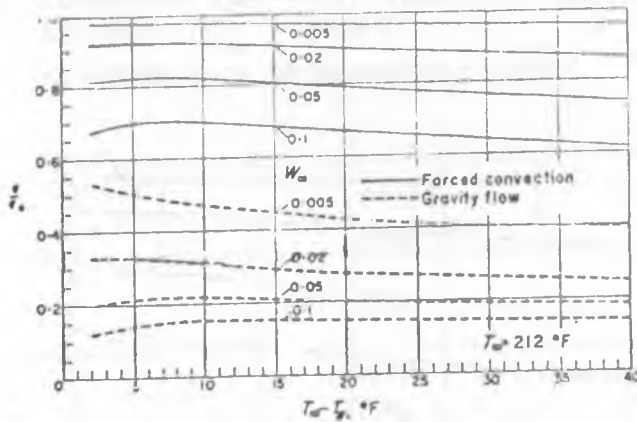


FIGURE 2.15: CONDENSATION HEAT TRANSFER FOR PURE STEAM-AIR SYSTEM  $T_{\infty} = 671$  R  
SPARROW AND MINKOWYCZ (1969)

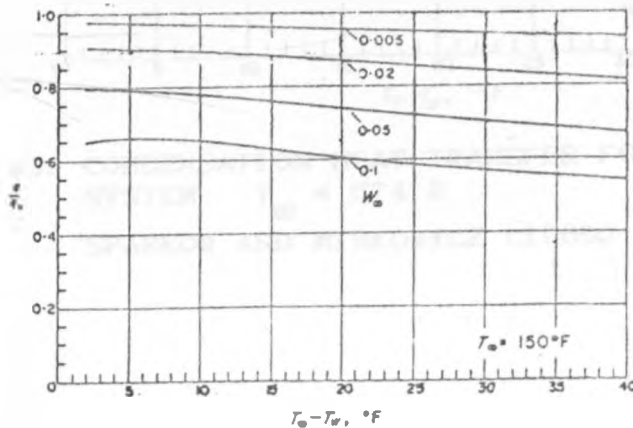


FIGURE 2.16: CONDENSATION HEAT TRANSFER FOR PURE STEAM-AIR SYSTEM  $T_{\infty} = 609$  R  
SPARROW AND MINKOWYCZ (1969)

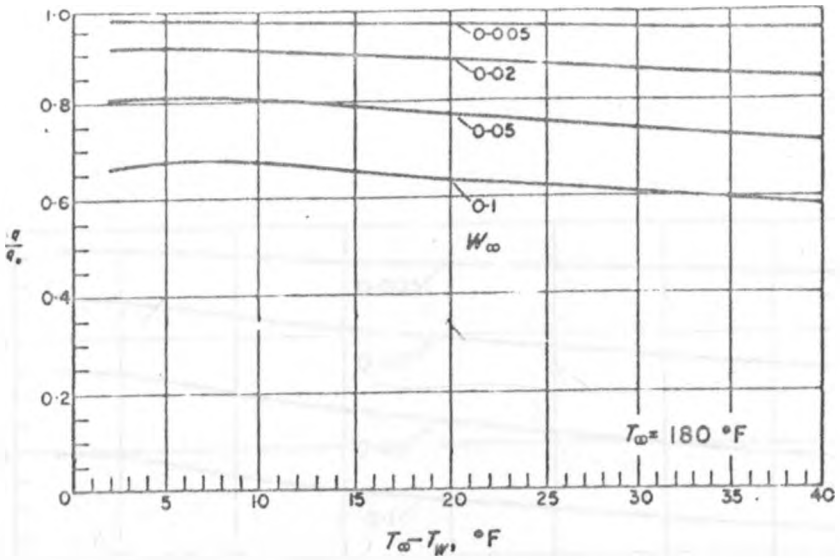


FIGURE 2.17: CONDENSATION HEAT TRANSFER FOR PURE STEAM-AIR SYSTEM  $T_\infty = 629\text{ R}$  SPARROW AND MINKOWYCZ (1969)

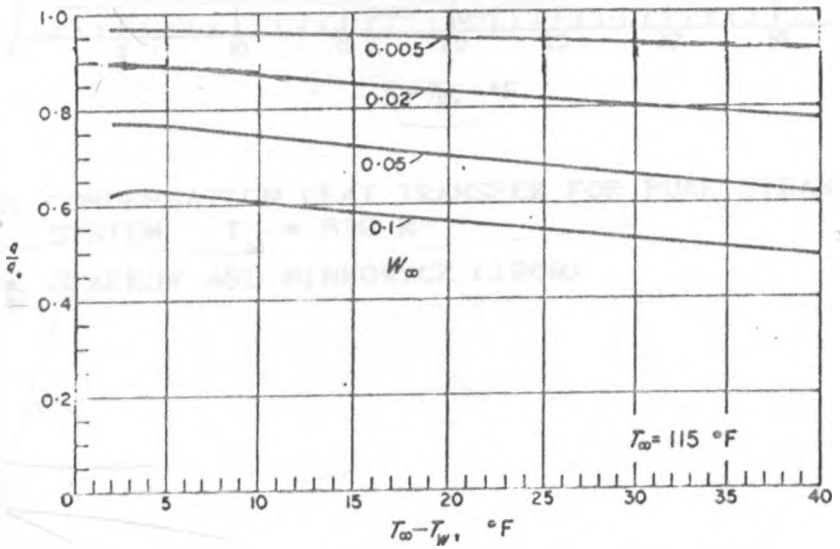


FIGURE 2.18: CONDENSATION HEAT TRANSFER FOR PURE STEAM-AIR SYSTEM  $T_\infty = 574\text{ R}$  SPARROW AND MINKOWYCZ (1969)

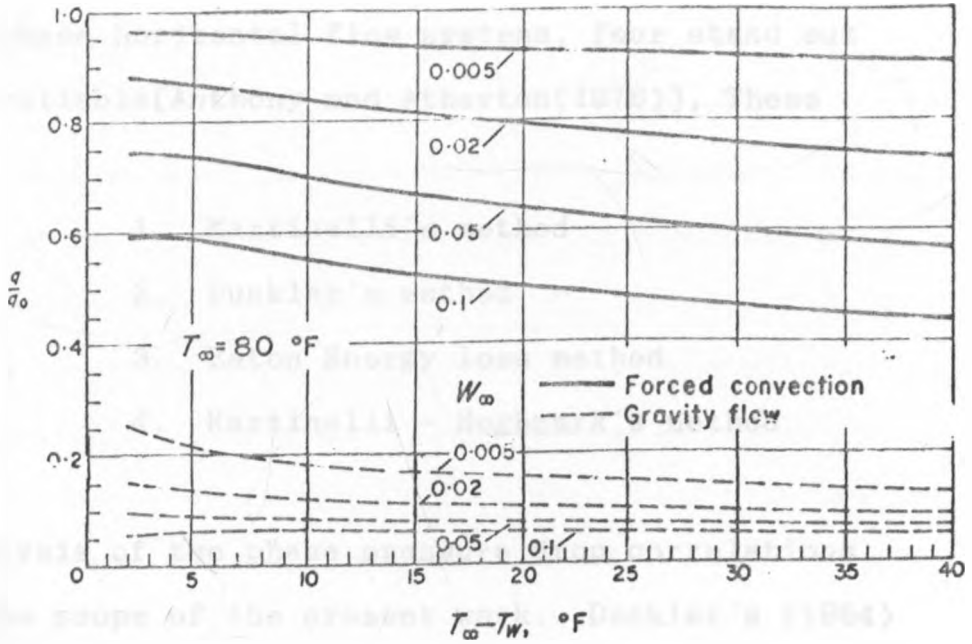


FIGURE 2.19: CONDENSATION HEAT TRANSFER FOR PURE STEAM-AIR SYSTEM  $T_\infty = 539\text{ R}$  SPARROW AND MINKOWYCZ (1969)

### 2.3 PRESSURE DROP IN HORIZONTAL TUBE.

Among the many correlations for estimating pressure drop in two phase horizontal flow systems, four stand out as the most reliable[Anthony and Atherton(1976)], These are:-

1. Martinelli's method
2. Duckler's method
3. Eaton Energy loss method
4. Martinelli - Hughmark's method

The analysis of two phase pressure drop correlations is outside the scope of the present work. Duckler's (1964) method will be used through out the present work. The other pressure drop predictions methods are given in the work by Anthony and Atherton (1976).

## CHAPTER THREE

### THEORY

#### 3.1 INTRODUCTION.

The procedure used in the theoretical modeling for what occurred in the test section which was essentially a tube in tube condenser is based mostly on the work due to Colburn and Hougen (1934) The application of the method requires knowledge of heat and mass transfer, properties of mixtures and theory of two phase flow with heat transfer in a horizontal tube. The analysis will be limited to only two components since the test section only handled steam-air mixture. As shown in the Appendix 2, the range of steam-air mixtures covered in this work satisfied the conditions to be treated as a perfect mixture and this considerably simplified the analysis.

#### 3.2 HEAT TRANSFER.

The prediction of the rates at which heat is convected away from a solid surface by an ambient fluid involves a thorough understanding of the principles of heat conduction, fluid dynamics and boundary layer theory. All the complexities involved in such an analytical approach may be lumped together in terms of a single parameter by introduction of Newton law of cooling:



$$Q/A = h(t_g - t_m) \quad (3.1)$$

The quantity  $h$  in this equation is variously known as heat transfer coefficient film coefficient, or unit thermal conductance. The unit conductance is not a material property but a complex function of the composition of the fluid, the geometry of the solid surface and the hydrodynamics of the fluid motion past the surface.

In the heat transfer analysis of heat exchangers, various thermal resistances in the path of heat flow from the hot to the cold fluid are combined into a suitable overall heat transfer coefficient  $U$ . Considering that the total thermal resistance  $R$  to the heat flow across a tube between the inside and the outside flow, is composed of the following thermal resistances:

$$R = \left( \begin{array}{l} \text{Thermal resistance} \\ \text{of the inside flow} \end{array} \right) + \left( \begin{array}{l} \text{Thermal resistance} \\ \text{of tube material} \end{array} \right) + \left( \begin{array}{l} \text{Thermal resistance} \\ \text{of the outside flow} \end{array} \right) \quad (3.2)$$

In this particular case the thermal resistance of the inside flow will be split further into resistance from steam - air in the bulk of the flow and in the condensate surface, resistance through condensate film, resistance through dirt or fouling.

The Colburn and Hougen (1934) method consider simultaneous heat and mass transfer processes. It is therefore appropriate that the next section deals with mass transfer.

### 3.3 MASS TRANSFER.

The mechanism of mass transfer by convection is analogous to heat transfer by convection. In convective mass transfer the bulk velocities are significant, i.e both the components in a binary mixture are moving with an appreciable velocity.

It is advantageous, to express the heat transfer factor  $J_H$  for a liquid flowing inside a tube by the dimensionless form [Kern(1950)]:

$$j_H = \left[ \frac{hd}{k} \right] \left[ \frac{\mu c_p}{k} \right]^{-1/3} = \left[ \frac{h}{c_p G} \right] \left[ \frac{\mu c_p}{k} \right]^{2/3} \left[ \frac{Gd}{\mu} \right] \quad (3.3a)$$

$$j_H = Nu Pr^{-1/3} = (h/c_p G) Pr^{2/3} Re \quad (3.3b)$$

$$G = \dot{m}_l / \pi d_l^2 \quad (3.3c)$$

where

$hd/k$ ) = Nu Nusselt number

$\mu c_p/k$ ) = Pr Prandtl number

$Gd/\mu$ ) = Re Reynolds number

G = mass flux of the liquid

$\dot{m}_l$  = mass flow rate of the liquid

Because Pr is nearly constant over a temperature range of 20-200 °C and since from heat balance in an exchanger for cooling water:

$$Q = \dot{m}_v c_{pv} (t_2 - t_1) = h\pi dL(\Delta t) \quad (3.4)$$

Substituting for G and h using equations 3.3c and 3.4 respectively equation 3.3a as becomes;

$$\frac{j_H}{(dG/\mu)} = \left[ \frac{t_2 - t_1}{\Delta t} \right] \left[ \frac{d}{4L} \right] \left[ \frac{\mu c_p}{k} \right]^{2/3} \quad (3.5)$$

The value of  $j_H$  can be read from the graph presented as Figure 3.1.

When a vapour is absorbed from a vapour gas mixture, which is not saturated with molecules of the solvent, diffusion may occur in two directions: molecules of vapour may pass into the absorbent, and molecules of absorbent may pass into the gas. In the passage of vapour from gas body into a condensate film consisting of liquid alone the transfer of matter is in one direction and molecules of matter transferred from gas to liquid is given in differential form by Kern (1950)

$$d(N_d) = d \left[ \frac{G a P_v}{M_m P_t} \right] = K_G (\Delta P) (dA) \quad (3.6)$$

Where A = diffusion surface area ( $\pi d(dL)$ )

a = flow area of gas and vapour ( $\pi d^2/4$ )

G = Mass velocity

$K_G$  = Mass diffusion coefficient

$M_m$  = Mean molecular weight of vapour and NCG mixture

$P_v$  = Partial pressure of vapour in gas body

$P_c$  = Partial pressure of vapour at condensate film

$P_t$  = Total pressure on the system

$\Delta P$  = Instantaneous driving potential ( $P_v - P_c$ )

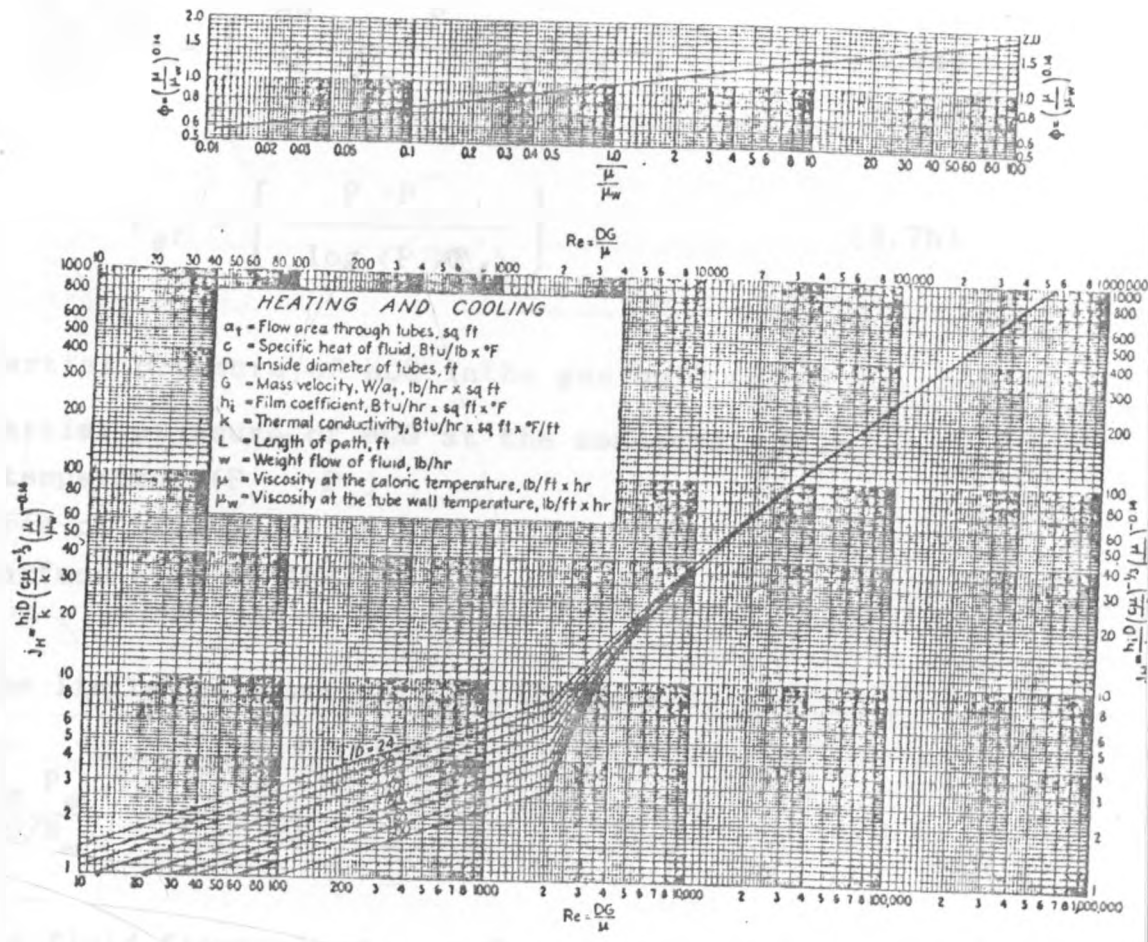


FIGURE 3.1: TUBE-SIDE HEAT TRANSFER CURVE  
 SIEDER AND TATE (1936)

The coefficient  $K_g$  is simply the dimensional rate which makes  $dN_d$  equal to the right hand side of Equation 3.6. Regrouping variables and integrating, Equation 3.6 becomes;

$$\frac{K_g P_{gf}}{G/M_m} = \left[ \frac{dP_v}{\Delta P} \right] \left[ \frac{P_{gf}}{P_t} \right] \left[ \frac{a}{dA} \right] \quad (3.7a)$$

$$P_{gf} = \left[ \frac{P_g - P'_g}{\log (P_g/P'_g)} \right] \quad (3.7b)$$

where  $P_g$  = Partial pressure of NCG in the gas bulk ( $P_t - P_v$ )

$P'_g$  = Partial pressure of NCG at the condensate film temperature ( $P_t - P_c$ )

$a$  = area of cross section

$A$  = surface area of the tube

Putting the limits in equation 3.7a, it becomes;

$$\frac{K_g P_{gf}}{G/M_m} = \left[ \frac{P_1 - P_2}{\Delta P} \right] \left[ \frac{P_{gf}}{P_t} \right] \left[ \frac{a}{A} \right] \quad (3.8)$$

When a fluid flows along a surfaces, the particles within the fluid exchange momentum with the stationary film at the surface, causing a pressure drop in the fluid in the direction of flow. It is entirely conceivable that a similar condition occurs when a vapour traveling along a surface condenses against the condensate film which it enters by moving at right angles to the direction of flow and giving up the momentum. For a given quantity of fluid

flowing in a tube and a total diffusion or heat transfer surface, the amount of skin friction will be greater if the path consists of a long small bore tube than for a short tube of large diameter. The index of these is the ration  $A/a$  or when used in a diffusion factor, its reciprocal  $a/A$ . The properties associated with skin friction are combined in Schmidt number because the difference between the bulk temperature and that of condensate film is small,  $P_{gf}$  is approximately equal to  $P_c$ , and for low NCG concentration  $P_g$  is approximately equal to  $P_t$ , then the ratio  $P_{gf}/P_t$  is approximately equal to 1. Kern(1950) has shown that by designating the diffusion factor as  $j_d$  and arbitrary using two-thirds power of Schmidt number then:

$$j_d = (P_1 - P_2) / \Delta P (a/A) (\mu/\rho D)^{2/3} \quad (3.9)$$

Equations 3.5 and 3.9 are of similar form. From an extension of the Reynolds analogy to distillation, where the analogy between mass and heat transfer is very close, there is a good reason to believe that  $j_H$  and  $j_d$  are the same function of Reynolds number and are equal [Kern(1950)]. Relationship between diffusion and heat transfer is then obtained by equating equations 3.5 and 3.9 and solving for  $K_d$

$$K_d = \frac{h(\mu c_p/k)^{2/3}}{c_p P_{gf} M_m (\mu/\rho D)^{2/3}} \quad (3.10)$$

The principal deduction from equation 3.10 is that the rates of diffusion and heat transfer do not occur independently and ratio  $P_{gr}/P_g$  is not always unity but should be calculated for incremental changes in the surface.

The overall coefficient of heat transfer varies greatly during condensation of a vapour from a NCG because the potential for diffusion varies greatly as the vapour is removed from the gas body leaving a higher percentage of inert gas. This implies that it is not simply a case of finding true temperature difference but heat transfer coefficient also varies as  $dQ$  or distance from inlet varies. The surface area of heat exchange can only be defined by the fundamental equation.

$$A = \int \frac{dQ}{U(\Delta t)} \quad (3.11)$$

The best method of evaluating the integral is by numerical integration for small but finite  $dQ$ .

### 3.4 BASIC ASPECTS OF TWO PHASE FLOW AND HEAT TRANSFER IN HORIZONTAL TUBES.

The main characterizing feature of two phase gas-liquid flow is the fact that an interface exists between the two phases and this interface takes a wide variety of forms. There is an almost infinite range of

possibilities, but, in general, the surface tension effects tend to create curved interfaces leading to spherical shapes (e.g droplets or bubbles).

The description of two phase flow can be simplified by classifying types of inter facial distributions and calling these flow regimes or flow patterns. It is stressed at the outset that these classifications of the types of flow though extremely useful, are still highly qualitative and often very subjective. For a horizontal flow, the main complicating feature is that gravitational forces act on the liquid phase causing it to be displaced towards the bottom of the channel. Flow regimes in horizontal flow are illustrated in figure 3.2. The regimes are defined as follows:-

1. Bubble flow:- Here bubbles tend to flow at the top of the tubes.
2. Plug flow:- The characteristic bullet shaped bubbles occur, but they tend to move in a position closer to top of tube smaller bubbles may also exist.
3. Stratified flow:- Here, gravitational separation is complete, liquid flowing along the bottom of tube and gas along the top part.
4. Wavy flow:- As gas velocity is increased in stratified flow, waves are formed on the gas-liquid interface giving the 'Wavy-flow' regime.



5. Slug flow:- When the waves in wavy flow grow big enough to touch the upper surface of tube, then slug flow regime is entered, with large frothy slugs of liquid interspersed with regions where there is a wavy stratified layer at bottom of the tube.
6. Annular Flow:- In horizontal tubes annular flow occurs at high gas flow rates. There is usually entrapment of liquid phase droplets in the gas core, and a further complication in horizontal flows is that the film at the bottom of the tube is often very much thicker than the film at the top owing to gravitational effects giving drainage around the periphery.

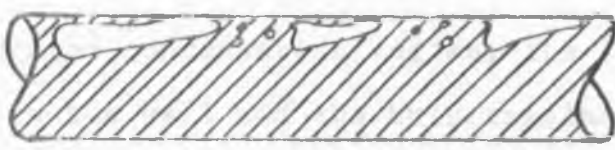
Figure 3.3 depicts various flow and heat transfer regimes in a forced convection of vapour inside a horizontal tube subjected to loss of uniform heat flux by Özisik(1985).

In the liquid deficient regimes of condensation heat transfer, vapour quality continuously decreases and temperature difference between the wall and the bulk increases with a corresponding increase in the heat transfer coefficient.

FLOW DIRECTION →



BUBBLE FLOW



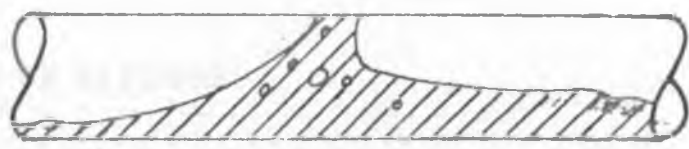
PLUG FLOW



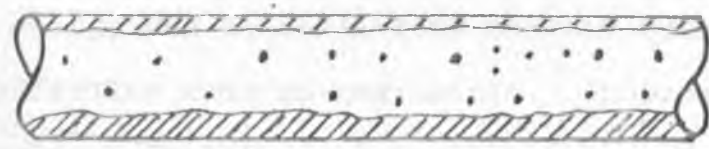
STRATIFIED FLOW



WAVY FLOW



SLUG FLOW



ANNULAR FLOW

FIGURE 3.2: FLOW PATTERNS IN HORIZONTAL FLOW BUTTERWORTH (1979)

In the two phase forced convection regime the temperature difference decreases with the distance along the tube because of increase in the thickness of liquid film as the vapour velocity decreases.

In the saturated condensation regime, the temperature difference between the wall and the bulk remains fairly constant and therefore heat transfer coefficient remains constant. Clearly the analysis of heat transfer in two phase flow is a very complicated matter because it involves numerous heat transfer regimes and transitions between them, any further details on the subject is beyond the scope of this work and the reader is referred to other publications in this subject.

### 3.5 PROPERTIES OF MIXTURES.

If a mixture is a perfect gas mixture, the contribution to the potential energy due to collisions between both the like and unlike molecules must be negligible. In order to show that mixtures used in this work could be treated as perfect, the mixture state least likely to be perfect i.e with 30% NCG by mass is shown in Appendix 2 to be a perfect mixture and for the rest of this work, laws of perfect mixtures will be used to calculate the values of properties used.

CONVECTIVE HEAT TRANSFER FROM VAPOUR	LIQUID DEFICIENT REGION	TWO PHASE FORCED CONVECTIVE HEAT TRANSFER THROUGH LIQUID FILM	SATURATED CONDENSATION	SUB- COOLING	CONVECTIVE HEAT TRANSFER TO LIQUID	
SINGLE PHASE VAPOUR	MIST FLOW	ANNULAR FLOW WITH ENTRAINMENT	ANNULAR FLOW	SLUG FLOW	BUBBLE FLOW	SINGLE PHASE LIQUID

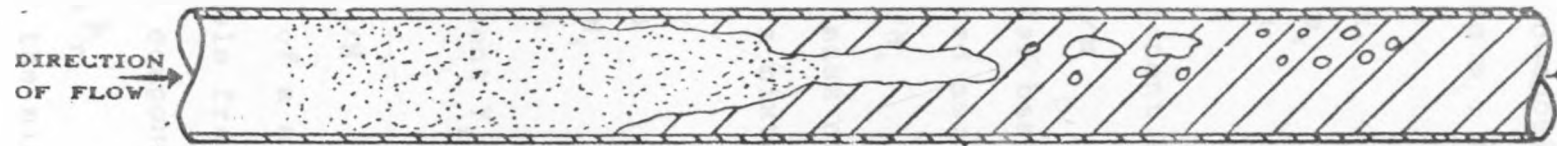


FIGURE 3.3: TWO PHASE FLOW IN A HORIZONTAL TUBE WITH  
UNIFORM REMOVAL OF HEAT  
ÖZİŞİK (1985)

In a mixture of a given composition produced by mixing  $k$  components of desired masses  $m_i$ , the total mass of mixture  $m$  is defined as:

$$m = \sum_{i=1}^{i=k} m_i \quad (3.12)$$

The mass fraction  $W$  of a component is given by:

$$W_i = m_i/m \quad (3.13)$$

to specify a mixture on a molar basis, the number of moles  $N_i$  for any component is defined as:

$$N_i = m_i/M_i \quad (3.14)$$

where  $M_i$  = molecular mass of the component.

The total number of moles in a mixture of  $k$  constituents  $N$  is given by:

$$N = \sum_{i=1}^{i=k} N_i \quad (3.15)$$

The mole fraction of a component  $Y_i$  of a component is given by:

$$Y_i = N_i/N \quad (3.16)$$

The effective molecular mass of a mixture of  $k$  constituents is defined in terms of its mole fractions is:

The partial pressure  $P_i$  of a component is given by:

$$P_i = Y_i P_T \quad (3.18)$$

where  $P_T$  = Total pressure of the mixture.

The present work is limited to a mixture of two components i.e steam and air and therefore only two subscripts will be used in the rest of the expressions.

The properties of air are given in the Appendix 2.1 and those of steam in the Appendix 2.2.2 and Appendix 2 2.3

In this section only the equations used for evaluating the mixture properties are given. Subscripts ' g ' will be used for steam and

' a ' for air.

The following expressions are for the relevant mixture properties of steam and air:-

Density ( $\rho$ ) [ $\text{kg}/\text{m}^3$ ]

$$\rho = \frac{m_a + m_g}{\left( \frac{m_a}{\rho_a} \right) + \left( \frac{m_g}{\rho_g} \right)} \quad (3.19)$$

Specific heat capacity at constant pressure ( $c_p$ ) [ $\text{kJ}/\text{kg}\cdot\text{K}$ ]:

$$c_p = \frac{Y_g c_{p,g} M_g + Y_a c_{p,a} M_a}{Y_g M_g + Y_a M_a} \quad (3.20)$$

Viscosity ( $\mu$ ) Experimental viscosities of several gases as reported by Kestin and Leiden (1959) show that its variation with pressure is only significant at very high reduced temperatures and low reduced pressures. The range of air-steam mixture used in this work does not fall in any of these extremes, therefore in this only temperature variation of viscosity is considered.

Using the Chapman-Enskog (1939)

expression for a binary mixture, then  $\mu$  [kg/ms] is given by:

$$\mu = \frac{Y_g \mu_g}{Y_g + Y_a \zeta_{g,a}} + \frac{Y_a \mu_a}{Y_a + Y_g \zeta_{a,g}} \quad (3.21)$$

$$\zeta_{g,a} = \frac{\left[ (1 + \mu_g/\mu_a)^{0.5} (M_g/M_a)^{0.25} \right]^2}{\left[ 8(1 + M_g/M_a) \right]^{0.5}} \quad (3.22a)$$

$$\zeta_{a,g} = \zeta_{g,a} (\mu_a/\mu_g)(M_g/M_a) \quad (3.22b)$$

Thermal conductivity(k)- Using Wassiljewa(1904) equation for thermal conductivity of a binary mixture then for steam and air k is given by Equations similar to 3.21,3.22a and 3.22b but with k replacing  $\mu$ .

Diffusivity(D)- The diffusivity D of air and steam is given by Vargaftik(1975) as:

$$D = D_o \left[ \frac{(t+273)}{273} \right]^n \quad (3.23)$$

where  $D_o = 0.216 \times 10^{-4} \text{ m}^2/\text{s}$  and  $n = 1.8$ .

### 3.6 DEVELOPMENT OF AN EQUATION FOR HEAT TRANSFER.

Colburn and Hougen (1934) demonstrated that the results of their analogy culminating into equation 3.24 holds on the higher side for a flow inside a tube, a flow across a single tube and a flow along a plane surface. In each case an appropriate value of  $h$  is substituted in equation for condensation of vapour in the presence of NCG.

To establish an equation which may be solved from point to point for  $U$  and  $\Delta t$  as in Equation 3.24, it should only be necessary to sum up all the resistances in series at an average cross section for each increment  $dQ$ . In the condensation of a vapour from an NCG, the quantity of heat which leaves the gas film must equal the quantity picked up by the cooling water. The total heat flow across the gas film is the sum of the latent heat carried by vapour diffusion into the condensate film plus the sensible heat removed from the gas because of the temperature difference  $(t_g - t_c)$ . The heat load expressed in terms of the tube side, the annular side and the overall potential per unit area when a mixture of gas and vapour flows in a tube is:

$$h_s(t_g - t_c) + K_a M_g h_{fg}(P_v - P_c) = h_o(t_c - t_w) = U(t_g - t_w) \quad (3.24a)$$

$$\frac{1}{h_a} = \frac{1}{h_v} + \frac{1}{h_{d,i}} + \frac{1}{h_{d,o}} + \frac{1}{h_m} \quad (3.24b)$$

$$\frac{1}{h_o} = \frac{1}{h_a} + \frac{1}{h_c} \quad (3.24c)$$



where all the resistances are based on the internal diameter of the tube.

$t_g$  = The temperature of vapour-gas core.

$t_c$  = The temperature of condensate.

$t_w$  = The cooling water temperature.

$P_v$  = The partial pressure of vapour in the gas body.

$P_c$  = The partial pressure of vapour at condensate film.

$M_g$  = The molecular weight of vapour.

$h_{fg}$  = The latent heat of vaporization of vapour.

$h_s$  = The gas film conductance.

$h_a$  = The combined cooling water, the metal wall and the scale conductances.

$h_c$  = The condensate conductance.

$h_m$  = The tube wall conductance.

$h_{d,i}$  = The scale conductance on the inside of the tube.

$h_{d,o}$  = The scale conductance on the outside of the tube.

$h_w$  = The cooling water film conductance.

$h_o$  = The combined conductances other than gas film conductance

The possibility of sub cooling the condensate which in this work is water, has been omitted from heat balance, since it is not significant compared to the larger latent effects [Kern (1950)].

In the application of Equations 3.24a, 3.24b and 3.24c to the solution of an actual heat exchanger it is assumed that there is a single value of  $t_g$  and  $t_c$  at any cross section and hence of  $P_v$  and  $P_c$ .

To explain the sequence of calculation done by computer program in Appendix 4.1, the method and order of applying Equations 3.24 is given below. Equations 3.7b, 3.10, 3.11 and 3.24 are repeated here for ease of reference:

$$P_{gf} = (P_a - P'_a) / (\log_e P_a / P'_a) \quad (3.7b)$$

where  $P_a = P_T - P_g$  and  $P'_a = P_T - P'_g$

$$K_G = \frac{h_c (\mu c_p / k)^{2/3}}{c_p P_{gf} M (\mu / \rho D)^{2/3}} \quad (3.10)$$

$$A = \int \frac{dQ}{U \Delta t} \quad (3.11)$$

The terms LHS and RHS will refer to first and second terms respectively in the Equation 3.24 i.e

$$\text{LHS} = h_a (t_g - t_c) + K_G M_g h_{fg} (P_v - P_c) \quad \text{and} \quad \text{RHS} = h_o (t_c - t_v)$$

The steps used in the solution of Equation 3.24a are numbered in sequence of application.

1. A complete exchanger must be assumed to fix annular side and tube side flow areas. The surface area is obtained by integration on assumption of true counter flow.
2.  $h_a$  and  $h_o$  are computed from Equation 3.3a and 3.24c respectively. Use of average values of

$h_a, h_c, h_m, h_{di}, h_{do}$  and  $h_v$  is acceptable but not for  $h_g$  which has to be evaluated at every section as mass velocity of gas phase changes from point to point.

3. From the value of  $h_g$ , value of  $(K_a \cdot P_{gf})$  is obtained from Equation 3.10.
4. The first interval of calculation is fixed by fixing  $t_g$ , which also fixes  $dQ$  for the interval.
5. A starting value of  $t_c$  is assumed and its value is continuously adjusted until LHS and RHS terms of Equation 3.24 balance. For each assumed value of  $t_c$  it is necessary to compute a new value of  $P_{gf}$ , since the pressure of vapour at the condensate film is the saturation pressure corresponding to  $t_c$ .
6. When LHS and RHS of Equation 3.24 balance the total heat load transferred per unit area is the same as the load which must have been transferred overall i.e.  $U(t_g - t_w)$ . To minimize the error introduced by the trial and error method into subsequent calculations,  $U(t_g - t_w)$  is equated to the mean value of LHS and RHS terms of Equation 3.24 i.e.

$$U(t_g - t_w) = (LHS + RHS) / 2 \quad (3.25)$$

7. From  $dQ$  obtained in (4) and  $U(t_g - t_w)$  value,  $dA$  for the interval is obtained i.e.

$$dA = dQ / U(t_g - t_w) \quad (3.26)$$

8. Then proceed to next interval by assuming a lower value of  $t_g$  and starting from step 4. This is done

repeatedly until value of  $t_g$  equals the exit temperature from the heat exchanger of the gas vapour mixture.

A computer program incorporating the above outlined procedures to calculate the temperature of steam - air at any axial position from the inlet to test section is given in Appendix 4.2. The same computer program was used to size the test section by inputting numerical values of inlet conditions of steam-air mixture and desired exit conditions.

### 3.7 DEVELOPMENT OF FORMULAE USED IN EVALUATING RESULTS FROM EXPERIMENTAL DATA.

The computer program in Appendix 4.1 was used to calculate the condensation heat transfer coefficient ( $h$ ) from experimental data. The steps used in writing of the program are as follows and for more clarity [See Figure 5.1] of the test rig.

1. The mean wall temperature was calculated from temperature readings from the various wall thermocouples:

$$t_m = \sum_{i=1}^{i=p} t_{m,i} / p \quad (3.26)$$

2. The mean steam-air temperature was calculated from the steam-air temperature readings at the various points:

$$t_g = \sum_{i=1}^{i=r} t_{g,i} / r \quad (3.27)$$

3. The mass flow rate of steam ( $\dot{m}_g$ ) was calculated from mass of condensate collected in a given time when the cooling water flow rate was adjusted such that all the steam was condensed . i.e apparatus was set for total condensation.

4. The mass flow rate of air ( $\dot{m}_a$ ) was calculated from volume flow rate measurements and ambient conditions.

5. The thermocouple temperature readings were corrected by use of calibration curve in Appendix 3 as Figure 3.1.

6. The mass concentration of air in the mixture (W) was calculated from :

$$W = M_a / (M_a + M_g) \quad (3.28)$$

7. The total amount of heat  $Q_{TOT}$  taken up by cooling water was calculated as:

$$Q_{TOT} = \dot{m}_v c_{p,v} \Delta t_v \quad (3.29)$$

Where

$\dot{m}_v$  = The mass flow rate of cooling water

$c_{p,w}$  = The specific heat capacity of water at constant pressure

$\Delta t_v$  = The cooling water (outlet temperature-inlet temperature)

8. Because the thermocouples measured outer tube wall temperature a correction was made to get the actual value of inside wall temperature from heat balance

$$Q_{TOT} = k_{Cu} A(\Delta t_{corr}/th) \quad (3.30)$$

Where

th = tube thickness

$\Delta t_{corr}$  = temperature drop across tube wall

$k_{Cu}$  = thermal conducting of copper tube

A = Surface area.

9. The actual temperature drop between the steam-air core and the inner tube wall temperature is then given by:

$$\Delta t = t_g - t_m - \Delta t_{corr} \quad (3.31)$$

$t_m$ ,  $t_g$  and  $\Delta t_{corr}$  are evaluated from Equations 3.26, 3.27 and 3.30b respectively.

10. From heat balance, and by definition of heat transfer coefficient (h):

$$h = Q_{TOT}/A\Delta t \quad (3.32)$$

11. Tables were then prepared using the computer program in Appendix 4.1 and are presented in Appendix 6.

### 3.8 COMPARISON OF PREDICTED AND EXPERIMENTAL HEAT TRANSFER COEFFICIENTS.

The experimental heat transfer coefficient for both liquid film and gas resistances combined may be represented as:

$$Q = h_{exp} A(t_g - t_m) \quad (3.33)$$

where  $t_m$  = The inner tube wall temperature

$t_g$  = The gas bulk temperature

Using a similar method to that proposed by Henderson and Marchello (1969) i.e

$$H = h_{exp} / h_m \quad (2.8)$$

where  $h_{exp}$  and  $h_m$  are experimental and predicted heat transfer coefficient respectively with the values of  $h_m$  calculated by use of Equations 2.3a, 2.3b, 2.4a and 2.4b with property values evaluated at similar conditions to these in the experiment. Because two correlations were used in the comparison, the two different values of H are differentiated by further defining the following:

$h_{m,sh}$  = The value of  $h_m$  when Equation (2.4) was used.

$h_{m,ac}$  = The value of  $h_m$  when Equation (2.3) was used.

$H_{sh}$  = The value of H when  $h_m = h_{m,sh}$  in the Equation(2.8).

$H_{ac}$  = The value of H when  $h_m = h_{m,ac}$  in the Equation(2.8).

The comparison is shown on the Tables presented in the Appendix 6.3 and the graphs presented in the Appendix 7 as Figures A7.19 to A7.30.

## CHAPTER FOUR

### PREDICTING LOSS OF PRESSURE ACROSS THE TEST SECTION.

#### 4.1 GENERAL

In general pressure loss receives contribution from three effects: friction, acceleration and elevation thus:

$$\frac{\partial P}{\partial z} = \frac{\partial P}{\partial z} \Big|_{\text{Friction}} + \frac{\partial P}{\partial z} \Big|_{\text{Acceleration}} + \frac{\partial P}{\partial z} \Big|_{\text{Elevation}} \quad (4.1)$$

For a horizontal flow which is the relevant case in this work, the last term, is of course, zero.

In this model it was assumed that the condensate flowed as an annular ring with steam-air as the core to reduce the problem complexity and numerical computation. The core was considered to be a perfect mixture of steam and air whose thermodynamic and transport properties could be predicted by methods of section 3.5. The acceleration term was estimated by the homogeneous flow model of Andeen and Griffith (1968):

$$\frac{\partial P}{\partial z} \Big|_{\text{Acceleration}} = G_t (u_{ns,2} - u_{ns,1}) \pi d^2 / 4 \quad (4.2)$$

The variables  $G_t$ ,  $u_{ns,1}$ , are defined below in the next paragraph.



Among the many correlations for estimating the frictional pressure drop in two phase horizontal flow system, Duckler's method(1964) is accurate and simple to use as it requires just little more manipulation than that for a single phase pressure drop calculation and also it does not require consideration of flow regimes. In a homogeneous flow, a two phase fluid is considered as a single phase fluid whose properties are volumetric average of the properties of the two phases. Defining flowing volume hold up ( $\lambda$ ) as the ratio of liquid volumetric flow rate to the total volumetric flow or equivalently as the ratio of liquid superficial velocity to the total superficial velocity i.e

$$\lambda = V_l / (V_l + V_g) = u_{sl} / (u_{sl} + u_{sg}) \quad (4.3)$$

The properties of the pseudo -single phase fluid are determined from the following equations:

$$\text{Velocity } (u_{ns}) = u_{sl} + u_{sg} \quad (4.4a)$$

$$\text{Mass velocity } (G_t) = 4\dot{m}_t / \pi d^2 \quad (4.4b)$$

$$\text{Viscosity } (\mu_{ns}) = \lambda \mu_l + (1-\lambda) \mu_g \quad (4.5)$$

$$\text{Density } (\rho_{ns}) = \lambda \rho_l + (1-\lambda) \rho_g \quad (4.6)$$

$$\text{Reynolds number } (Re_{ns}) = dG_t / \mu_{ns} \quad (4.7)$$

$$\frac{\partial p}{\partial z} \Big|_{\text{friction}} = \frac{f_{ns} G_t^2}{2\rho_{ns} d} \quad (4.8)$$

$f_{ns}$  is evaluated from the smooth tube friction factor equation by Duckler(1964)

$$f_{ns} = \left[ 2 \log_{10} \left[ \frac{Re_{ns}}{4.5223 \log_{10}(Re_{ns}) - 3.8215} \right] \right]^{-2} \quad (4.9)$$

Because of the errors introduced by the assumptions of having a perfect mixture of steam and air at the core and of annular flow profile, no attempt was been made to introduce a correction for the pipe roughness as this would only increase complexity while giving no significant accuracy improvement in the results.

#### 4.3 CALCULATION METHOD

To minimize the errors that would arise because of the drastic changes in the composition of core and annulus along the test section, the test section was subdivided into several intervals as shown in Figure 4.1

The temperature, composition and mass flow rate of gas core (steam-air) and of liquid annulus (condensate) are known from analysis in section 3.6 at several axial positions along the test section from the inlet to the exit.

Considering the  $(k-1)^{th}$  and  $k^{th}$  interval mean bulk temperature i.e:

$$t_{g,k} = (t_{g,k} + t_{g,k-1})/2 \quad (4.10)$$

$$\text{The mean mole fraction of air } Y_{a,k} = (Y_{a,k} + Y_{a,k-1})/2 \quad (4.11)$$

$$\text{The mean mole fraction of steam } Y_{g,k} = (1 - Y_{a,k}) \quad (4.12)$$

The mean properties of the core are then calculated using the equation in section 3.5.

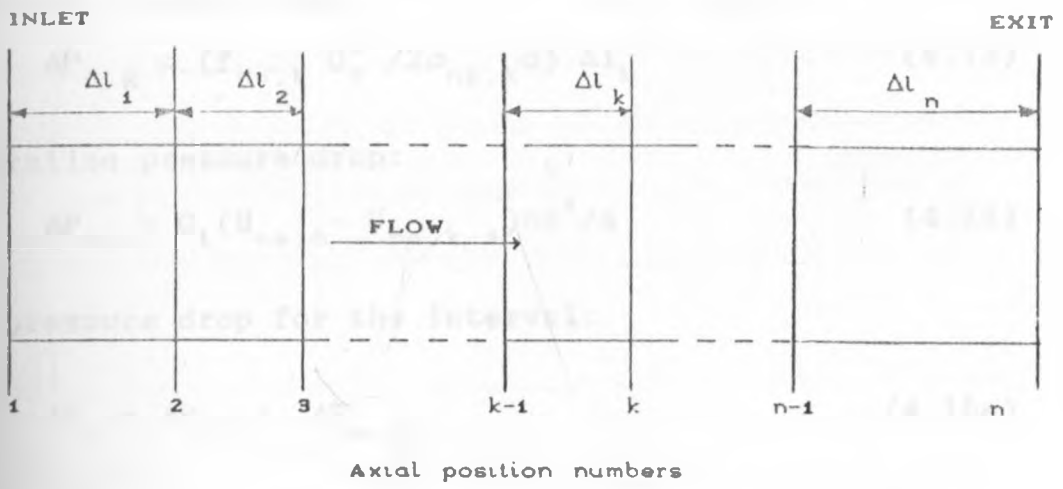


FIGURE 4.1:- SUB-DIVISION OF THE TEST SECTION.

To calculate the value of properties to be used in the homogeneous flow model, the flowing volume hold up ( $\lambda$ ) was calculated by assuming that the core mass flow rate was the sum of flow rates of air and steam and had a uniform mixture thermodynamic and transport properties, then:

Frictional pressure drop:

$$\Delta P_{f,k} = (f_{ns,k} G_t^2 / 2\rho_{ns,k} d) \Delta l_k \quad (4.13)$$

Acceleration pressure drop:

$$\Delta P_{a,k} = G_t (U_{ns,k} - U_{ns,k-1}) \pi d^2 / 4 \quad (4.14)$$

Total pressure drop for the interval:

$$\Delta P_k = \Delta P_{f,k} + \Delta P_{a,k} \quad (4.15a)$$

The total pressure drop over the whole test section  $\Delta P$  was a summation of the drops across each interval i.e

$$\Delta P = \sum_{k=1}^{k=n} \Delta P_k \quad (4.15b)$$

Substituting for  $\Delta P_{f,k}$  and  $\Delta P_{a,k}$  using Equation 4.3 and 4.14 then Equation 4.15b becomes:

$$\Delta P = \sum_{k=1}^{k=n} \left[ \left( f_{ns,k} G_t^2 \Delta l_k / 2\rho_{ns,k} d \right) + \left( \pi d^2 G_t (U_{ns,k} - U_{ns,k-1}) / 4 \right) \right] \quad (4.15c)$$

A computer program was used to do the actual calculation and this is presented in Appendix 4.3.

## CHAPTER 5

### EXPERIMENTAL WORK

#### 5.1 GENERAL

Experimental data were obtained for steam-air mixtures condensing inside horizontal pipes of different diameters. The two pipe diameters i.e 25.4mm and 38.1mm were used. The test section was kept at atmospheric pressure during all the tests.

The mass concentration of air in the steam-air mixture was varied from 0% up to 30%. The temperature of the steam-air mixture fed into the test section varied from 95°C to 220°C. The effect of the mass flow rate of mixture on the pressure loss in the condenser was also considered.

#### 5.2 DESCRIPTION OF EXPERIMENTAL RIG

The structural design and design drawings of the experimental rig are given in the Appendix 1. The schematic drawing of the experimental rig is as shown in Figure 5.1.

## CHAPTER 5

### EXPERIMENTAL WORK

#### 5.1 GENERAL

Experimental data were obtained for steam-air mixtures condensing inside horizontal pipes of different diameters. The two pipe diameters i.e 25.4mm and 38.1mm were used, The test section was kept at atmospheric pressure during all the tests.

The mass concentration of air in the steam-air mixture was varied from 0% up to 30%. The temperature of the steam-air mixture fed into the test section varied from 95°C to 220°C. The effect of the mass flow rate of mixture on the pressure loss in the condenser was also considered.

#### 5.2 DESCRIPTION OF EXPERIMENTAL RIG

The structural design and design drawings of the experimental rig are given in the Appendix 1 The schematic drawing of the experimental rig is as shown in Figure 5.1.

### 5.2.1 STEAM GENERATOR

The steam generator was speedylec type 236 from BASTIAN and ALLEN LTD, England. This was an electrode boiler with a maximum rating of  $0.01 \text{ Kgs}^{-1}$  and 10 bar. The output from the generator was varied by a load selector switch from 0% to 100% of full load, so that any desired output pressure and flow rate could be set. The steam leaving the generator was saturated but because of heat losses from the pipe work before the test section, a little super heating was desirable so as to deliver the mixture as dry steam at the inlet to the test section. A superheater using a cartilage heater was incorporated immediately after the steam generator.

### 5.2.2 STEAM-AIR MIXER

The steam-air mixer mixed the slightly superheated steam and the air to give a homogeneous mixture which was then fed into the test section. The mixing was aided by the fast moving steam entraining a jet of preheated and metered amount of air fed in through a nozzle. To avoid unnecessary turbulence in the test section, a 1m length calming section was included between the mixer and test section.

### 5.2.3 AIR HEATER

The air was preheated to the same temperature as steam so as to eliminate temperature differential within the air-steam mixer. The air was heated by a series of cartilage heaters whose total output power was controlled by use of a power transformer.

### 5.2.4 TEST SECTION

The test section consisted of a horizontal tube in tube condenser with the steam air mixture flowing inside the inner copper tube and cooling water flowed counter current to this in the annulus. Two test diameters were used one of inside diameter of 25.4mm (1") and the other of inside diameter 38.1mm(1.5"). In both cases the tubes were enclosed in a steel pipe of inside diameter of 76.2mm(3"). The total length of tube exposed to cooling water was 4000mm.

On the outer wall of the copper tube were fixed type J thermocouples to record wall temperature. Three of these thermocouples were fixed at each of the 10 equally spaced position along the tube. The readings recorded by these thermocouples were used to determine the mean wall temperature as well as the temperature profile along the tube.



At each of the above mentioned 10 positions one further thermocouple of type K in this case was placed inside the copper tube to record the fluid core temperature as well as the axial temperature profile. The lead wires from the thermocouples were placed on the cooling water side and then to a digital temperature read-out. One thermocouple was placed just outside the test section to determine the temperature of steam-air mixture at the inlet to the test section. A water manometer was connected across the test section to determine the pressure drop across the test section.

#### 5.2.5 AIR SYSTEM

The air was drawn via a regulating valve from a compressed air line installed in the laboratory. The valve regulated both the flow rate and delivery pressure. The air flow rate was measured using one of the following two methods.

1. For the flow rates of 0-15 l/min an air rotameter manufactured by Madishield was used.
2. For higher flow rates, a thermal anemometer TA 400 of AIR FLOW INSTRUMENTS was used. The velocity profile inside a 50.8mm (2") diameter perspex tube was plotted from which the volumetric flow rate of air was calculated. The pressure of air after the regulator was either recorded by a water manometer or on a 0-1 bar Bourdon gauge.

The air was led into a strainer to remove oil and dust particles, then heated in the air heater to the same temperature as steam. The heated air was then fed into the mixer through a non return valve to prevent back flow of steam into the air line.

#### 5.2.6 COOLING WATER SYSTEM

A constant level tank installed one floor(4m) above the apparatus supplied the cooling water through a 25.4mm (1") internal diameter flexible hose to a flow regulating valve and then to a TECQUIPMENT water rotameter calibrated in litres/minute. The cooling water was then led past a thermometer in a pocket to the test section.

From the condenser a similar thermometer in pocket gave the outlet temperature of the cooling water. At the outlet the cooling water was then drained to an underground tank where it was cooled and then recycled by a pump back to the constant head tank.

#### 5.2.7 PROTECTION AGAINST HEAT LOSSES

The steam generator, the superheater, the air heater, the air supply line, the steam-air mixer and the test section were insulated using a 10mm thick fibre glass clad with aluminium foil. This virtually eliminated heat losses from the rig and also served aesthetic purposes.

### 5.3 EXPERIMENTAL PROCEDURE.

The aim of the experiment was to give condensation heat transfer data when the following were varied:

- i) Air mass concentration in the steam-air mixture.
- ii) Steam-air mixture temperature at the inlet to the test section
- iii) Tube inside diameter.

The steps given below (1-7) were such that in any one test only one of the above mentioned parameters was varied while the other two were kept constant.

The test section was assembled using the 25.4mm(1") inside diameter copper tube. The following were then carried out:

1. The steam generator was set to the desired output pressure and approximate mass flow rate by making use of the load selector switch on the steam generator. The accurate value of steam mass flow rate was calculated from the time it took to accumulate 10kg of condensate when the test section was set for total condensation i.e cooling water flow rate was such that all the steam was condensed. This was carried out at least three times to check for consistency.

2. The cooling water mass flow rate was then adjusted to the initial value to be used in the test and steam-air inlet temperature to test section was also set to the desired value.
3. The equipment was operated under this test condition for sometime to ensure that a steady state existed.
4. The following readings were then recorded in the order they are listed to give one set of readings for a run.

- i) Steam thermocouple readings
- ii) Tube wall thermocouple readings
- iii) Cooling water mass flow rate, inlet and outlet temperatures
- iv) Pressure loss across the test section
- v) Air volume flow rate, temperature and pressure
- vi) Ambient temperature and pressure

To reduce error in the readings which could arise from unsteady state, meter malfunction etc, these readings were taken after every 15 minutes until two successive sets coincided.

5. A known amount of air preheated to the same temperature as steam was introduced into the steam to give the initial desired air mass concentration in the mixture. The readings of step 4 were then recorded. This was repeatedly done with at least 5 different values of air flow rates to give readings for the effect of mass concentration of air.

6. The air input to steam-air mixer was stopped, and then the steam inlet temperature to the test section was changed to a new value by regulating the heat input to the superheater. Steps 3-5 were then again carried out. Other values of steam-air inlet temperature to test section were similarly set, at least four different values were used to give data on the effect of fluid inlet temperature to the test section.
7. After sufficient data had been taken using 25.4mm(1") inside diameter tube, the test section was dismantled and the 25.4mm(1") was replaced with a 38.1mm(1.5") inside diameter tube. Steps 1-6 were then followed once more with the 38.1mm(1.5") copper tube.
8. The type J and K thermocouples were then calibrated by use of an oil bath and an accurate mercury in glass thermometer.

The accuracy of the experimental results depended

on:-

1. Careful regulation of steam and air flow rates, pressures and temperatures.
2. Accuracy in the measurement of flow rate of steam, air and cooling water.
3. Accuracy in the measurement of tube wall, steam, air and cooling water temperatures.

In all the cases accurate instruments were employed and sufficient time was given for the experimental runs to ensure readings were taken under steady state conditions.

## CHAPTER SIX

### ANALYSIS OF DATA

#### 6.1 INTRODUCTION

The reduction of data to more basic units of flow and temperature and to calculate the desired quantities such as mean temperature, experimental heat transfer coefficient, Reynolds number and so forth was done using the computer program in Appendix 4.1.

In this section only the relevant flow chart is used to explain the sequence and the tabulated values from the computer print out presented as Tables in the Appendix 6 and the graphs presented as Figures in the Appendix 7

The formulas used to calculate the various quantities are presented in chapter 3 which covered the theoretical introduction. Theoretical modeling was done for both the steam-air core temperature profiles and the pressure drop across test section using programs presented in Appendix 4, only the relevant flow charts are presented here.

#### 6.2 REDUCTION OF EXPERIMENTAL DATA TO GET LOCAL CONDENSATION HEAT TRANSFER COEFFICIENTS

The flow chart of the required steps is presented as Figure 6.1. The following parameters were calculated from the result sheet for any run(experimental data):-

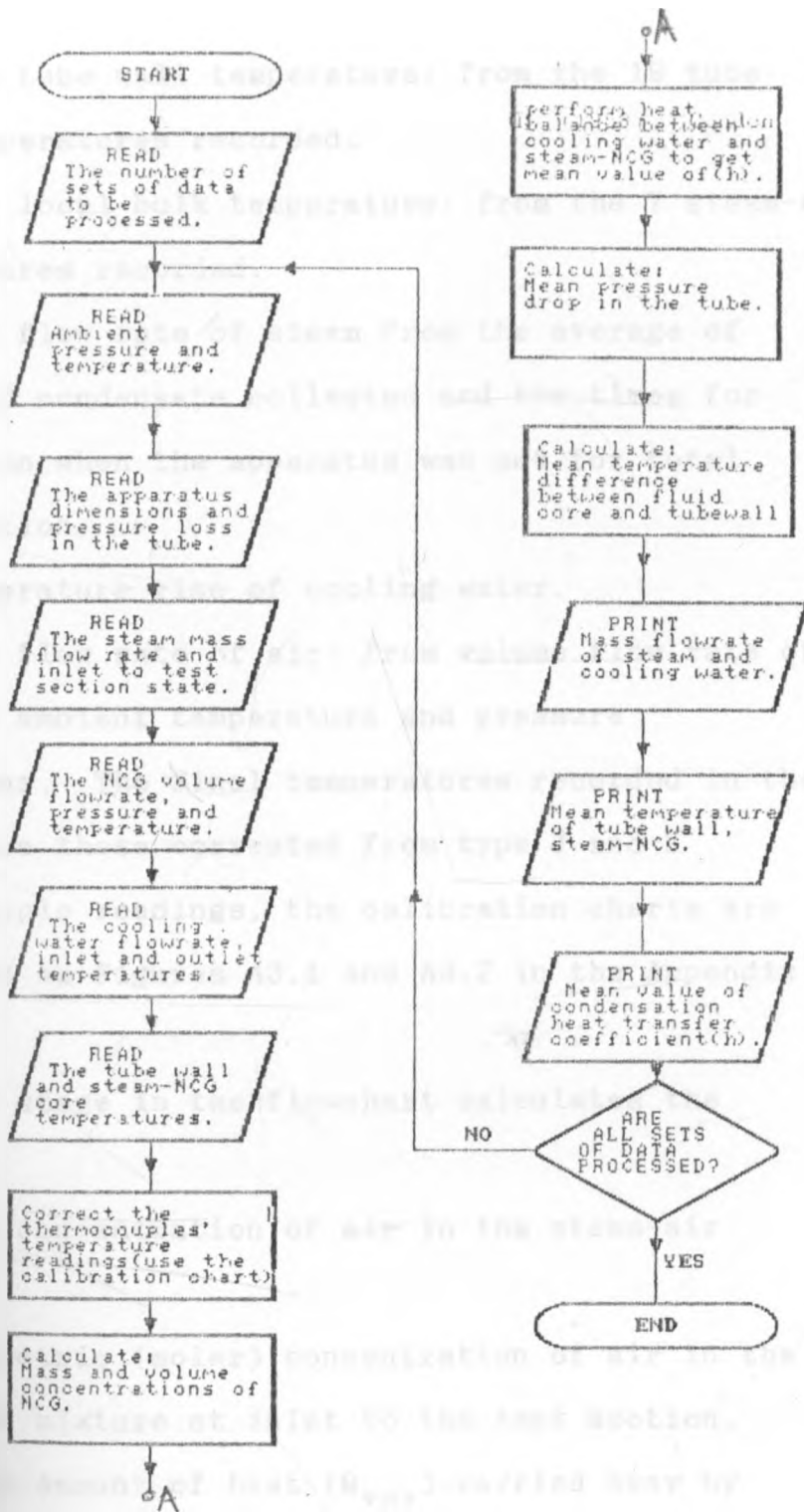


FIGURE 6.1: THE FLOWCHART OF THE COMPUTER PROGRAM USED FOR PROCESSING EXPERIMENTAL DATA



1. The mean tube wall temperature: from the 19 tube wall temperatures recorded.
2. The mean local bulk temperature: from the 7 steam-air temperatures recorded.
3. The mass flow rate of steam from the average of masses of condensate collected and the times for collection when the apparatus was set for total condensation.
4. The temperature rise of cooling water.
5. The mass flow rate of air: from volume flow rate of air, the ambient temperature and pressure conditions. The final temperatures recorded in the tables are those corrected from type J and K thermocouple readings, the calibration charts are presented as Figures A3.1 and A3.2 in the Appendix 3.

The next stage in the flowchart calculates the following:-

1. The mass concentration of air in the steam-air mixture.
2. The volumetric (molar) concentration of air in the steam-air mixture at inlet to the test section.
3. The total amount of heat ( $Q_{TOT}$ ) carried away by cooling water.
4. The temperature difference between the steam-air core and the tube wall and the correction for the temperature across the copper tube wall.

- 5 Setting up a heat balance between heat flux through the wall and heat carried away by cooling water and evaluating the value of  $h$  from the Equation 6.1

$$Q_{TOT} = hA\Delta t \quad (6.1)$$

6. The mean pressure drop across the test section

The calculated results are presented as Tables in the Appendix 6 as Tables A6.1 to A6.12 and the graphical representation as Figures in Appendix 7 (Figures A7.1 to A7.12.)

### 6.3 COMPARISON OF EXPERIMENTAL CONDENSATION HEAT TRANSFER COEFFICIENT TO THE CORRELATIONS.

The ratio of experimental to predicted heat transfer coefficient defined in section 3.8 i.e

$$H = h_{exp}/h_m \quad (6.2)$$

Where  $h_{exp}$  = the experimental value of heat transfer coefficient

$h_m$  = Heat transfer coefficient based on equation 2.3 and 2.4, and is calculated for the two tube diameters used i.e 25.4mm and 38.1mm.

To further differentiate between the values obtained from Equations 2.3 and 2.4, the following variables used in the analysis are defined as:

$h_{m,Ac}$  = Heat transfer coefficient when the correlation of Equation 2.3 due to Ackers et al (1958) is used.

$h_{m,sh}$  = Heat transfer coefficient when the correlation of Equation 2.4 due to Shah (1979) is used.

$H_{Ac}$  - denotes when  $h_m$  in Equation 6.2 is set as equal to  $h_{m,Ac}$ .

$H_{Sh}$  - denotes when  $h_m$  in Equation 6.2 is set as equal to  $h_{m,sh}$ .

These values are tabulated in Appendix 6 (Tables A6.13 to A6.14) The graphical presentation of these data is given in Appendix 7 (Figures A7.13 to A7.23).

#### 6.4 COMPARISON OF EXPERIMENTAL AND THEORETICAL STEAM-AIR AXIAL TEMPERATURE PROFILES.

Colburn and Hougen (1934) in their treatment showed that at any particular axial point in the test section the quantity of heat flowing per unit time per unit surface area through the resistances of the condensate layer, the metal wall, the scales and the cooling water film could be equated to heat flow through the gas film. The heat flow through the gas film is made up of sensible heat lost by mixture and the latent heat transferred as the vapour diffuses through the gas film and condenses in the condensate film. The total heat flow is represented by an overall coefficient  $U$ , multiplied by the overall temperature drop between the steam-air mixture and the cooling water. i.e the heat flow to the condensate surface is equal to the heat flow from the condensate surface and

these are equated to  $U\Delta t$  as in Equation 3.24a rewritten for sake of clarity.

$$h_s(t_g - t_c) + K_o M_v h_{fg}(p_v - p_c) = h_o(t_c - t_v) = U\Delta t. \quad (3.24a)$$

At any value of  $t_g$  in the test section, all the variables in Equation 3.24a are known and the value of  $U\Delta t$  is obtained by trial and error substitution of several values of  $t_c$  until the desired equality is obtained. By choosing six or more different values of  $t_g$  by subdividing the temperature interval between the inlet and the outlet temperature of steam-air mixture to the test section into six or more intervals.

For every interval by trial and error method the values of  $U\Delta t$  are evaluated. Performing graphical integration of Equation (3.11):

$$A = \sum_{i=1}^{i=n} \frac{dQ_i}{(U\Delta t)_i} \quad (6.3)$$

where  $n$  = the number of intervals considered. The total surface area of the test section could be evaluated. For any the intervals, the required surface area for heat transfer  $A_i$  could be evaluated from

$$A_i = \frac{dQ_i}{(U\Delta t)_i} = \pi d(\Delta l)_i \quad (6.4)$$

Where  $(\Delta l)_i$  = length of tube in the interval. By calculating the value of  $(\Delta l)_i$  then the axial position along the test length at which the relevant value of  $t_g$

occurred could be found. The values of  $t_g$  and their respective axial positions are given in Appendix 6 (Tables A6.24 to A6.29) and used to plot graphs for comparison of predicted and experimental steam-air core temperature profiles are presented as Figures 7.10 and 7.14.

The whole of the procedure was done by a computer program, presented in Appendix 4.2 and only the flow chart of the procedure is presented in this chapter as Figure 6.2.

#### 6.5 LOCAL CONDENSATION HEAT TRANSFER COEFFICIENT AXIAL PROFILES.

When a vapour is at a temperature above the saturation temperature corresponding to the vapour partial pressure, no condensation occurs. The vapour simply cools down, becoming less superheated until the saturation temperature is attained. Therefore in such cases the test section was likely to have two regions, a de-superheating section and a condensing section. An attempt was made to map the test section to show roughly how far each of the above regions extended by estimating the local values of heat transfer coefficient along the test length by making an assumption of linear temperature profile for the cooling water. This was not such an absurd assumption as the temperature rise of cooling water was small, the maximum recorded being  $13^{\circ}\text{C}$ .

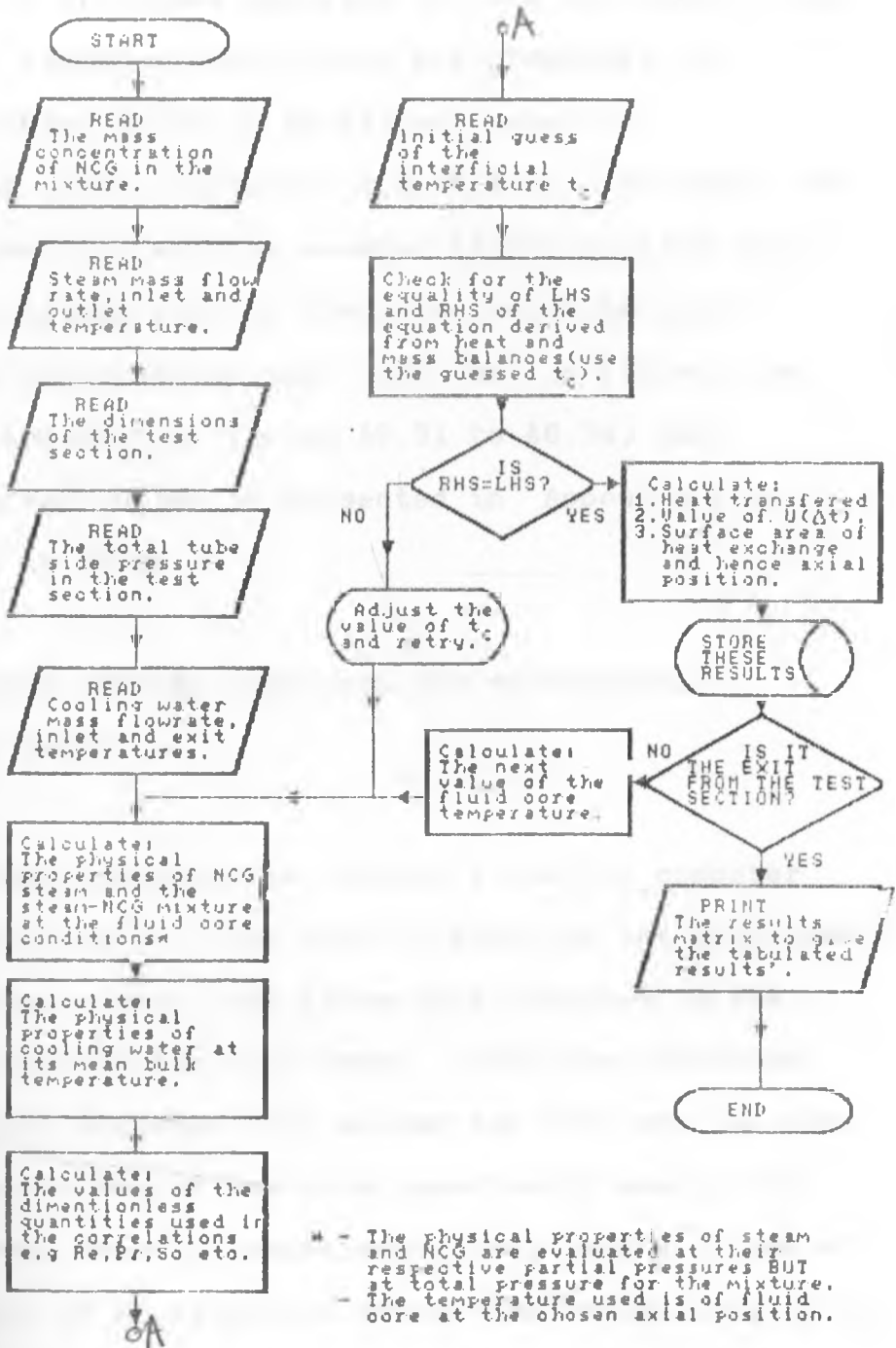


FIGURE 6.2: THE FLOWCHART OF THE COMPUTER PROGRAM USED TO PREDICT FLUID CORE TEMPERATURE PROFILE AND IN SIZING THE TEST SECTION

Tables for the cases analysed showing estimated values of local heat transfer coefficient are presented in Appendix 6 (Tables A6.35 to A6.40) and graphical representation given in Figures 7.6 to 7.9. The fluid core temperature profiles and the assumed linear cooling water temperature profiles used in the calculation of local values of the condensation heat transfer coefficient are presented in Appendix 6 (Tables A6.31 to A6.34) and graphical representation is presented in Appendix 7 as Figures A7.24 to A7.28.

#### 6.6 COMPARISON BETWEEN PREDICTED AND EXPERIMENTAL PRESSURE DROP.

The methods presented in chapter 4 and the computer program in Appendix 4.3 were used to generate the predicted values of pressure drop, and these were compared to the values obtained from the experiment. Both the predicted and experimental pressure drop across the test section when the tube diameter was 38.1mm were numerically small, the maximum achieved from the experiment being  $117\text{N/m}^2$  (12mm of water). Because of experimental errors the reliability of experimental pressure drops for comparison to predicted values was questionable and hence are not presented. The data presented are those obtained with tube diameter of 25.4mm. These are presented in Appendix 6 (Table A6.41) and graphical representation presented as Figure 7.15.

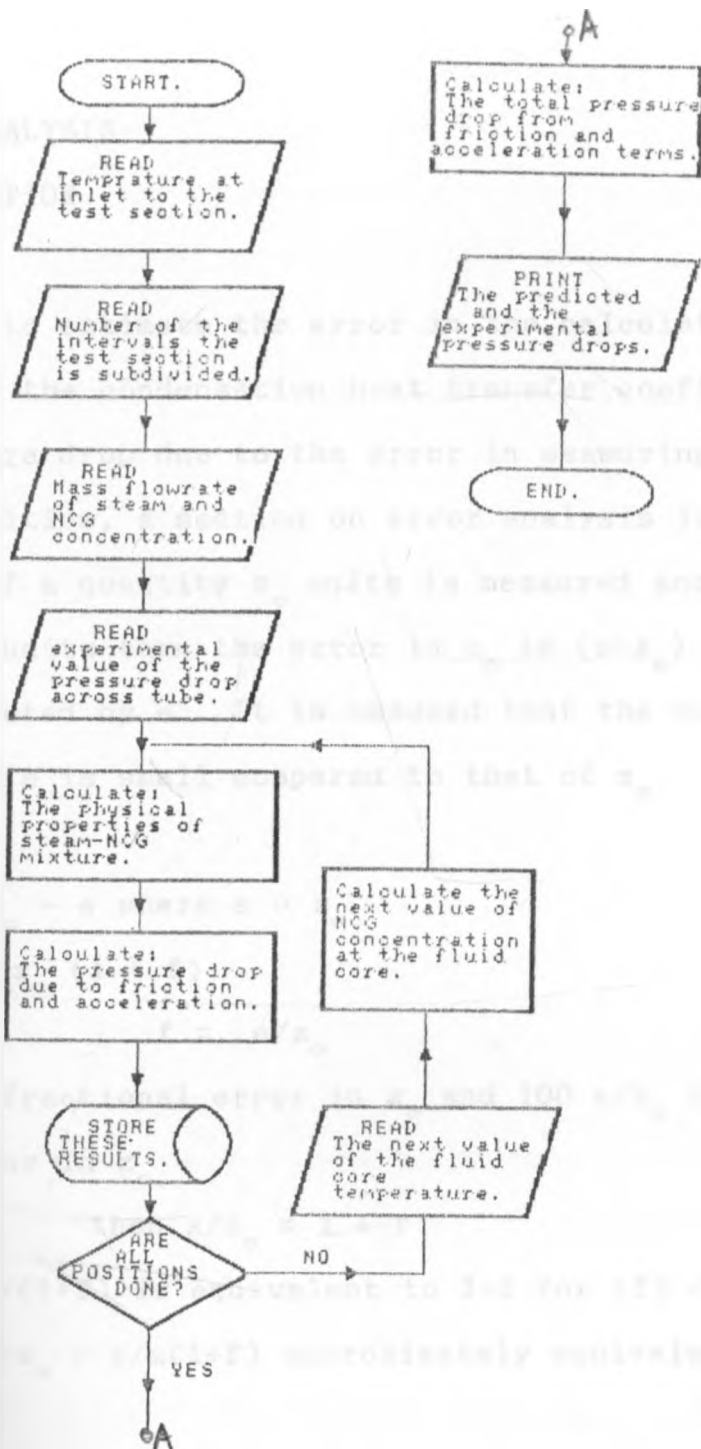


FIGURE C.3: THE FLOWCHART OF THE COMPUTER PROGRAM USED TO CALCULATE THE PREDICTED PRESSURE DROP ACROSS THE TEST SECTION(TUBE-SIDE)



## 6.7 ERROR ANALYSIS

### 6.7.1 INTRODUCTION

In order to estimate the error in the calculated results i.e in the condensation heat transfer coefficient and the pressure drop due to the error in measuring the relevant quantities, a section on error analysis is introduced. If a quantity  $z_0$  units is measured and recorded as  $z$  units then the error in  $z_0$  is  $(z-z_0)$  henceforth denoted by  $e$ . It is assumed that the numerical value of error  $e$  is small compared to that of  $z_0$ .

$$z = z_0 + e \text{ where } e \ll z_0 \tag{6.5a}$$

$$z = z_0 (1 + f) \tag{6.5b}$$

$$f = e/z_0 \tag{6.5c}$$

$f$  is known as fractional error in  $z_0$  and  $100 e/z_0$  is percentage error in  $z_0$ .

$$\text{then } z/z_0 = 1 + f \tag{6.6}$$

and  $z_0/z = 1/(1+f)$  is equivalent to  $1-f$  for  $(f) \ll 1$   
 $e/z_0 = e/z \cdot z/z_0 = e/z(1+f)$  approximately equivalent to  $e/z$ .

If a quantity  $z_0$  units is measured  $n$  times and recorded as  $z_1, z_2, \dots, z_n$  units then for any of the measurement  $r$ ;  $z_r = z_0 + e_r$  and the arithmetic mean  $\bar{z}$  of the  $r^{\text{th}}$  measurements is:

$$\bar{z} = (z_1+z_2+ \dots + z_n)/n \tag{6.7a}$$

$$\bar{z} = z_o+(e_1+e_2 + \dots + e_n)/n \tag{6.7b}$$

Since the errors  $e_1, e_2, \dots, e_n$  may have opposite signs, thus  $E$ , the largest numerical error in any of the measurements is such that:

$$(e_1+ e_2+ \dots + e_n)/n \leq E. \tag{6.7c}$$

and consequently  $\bar{z} - z_o \leq E$ .

It is not possible to find  $e_1, e_2, \dots, e_n$  or  $E$  since  $z_o$  is not known. It is usual therefore to examine the scatter or dispersion of measurement not about  $z_o$  but about  $\bar{z}$  then for any reading say the  $r^{th}$  reading  $z_r$

$$z_r = z + d_r \tag{6.8a}$$

where  $d_r$  = deviation of  $z_r$  from  $\bar{z}$  or the residual of  $z_r$ .

$$z_r = z_o + e_r = \bar{z} + d_r. \tag{6.8b}$$

$$\text{and } (e_1+ e_2+ \dots + e_n) = n(\bar{z} - z_o). \tag{6.8c}$$

$$\text{and } (d_1+ d_2+ \dots + d_n) = 0. \tag{6.8d}$$

Accuracy refers to the closeness of measurement to the "actual" or the "real" value of the physical quantity whereas precision is used to indicate the closeness with which the measurements agree with one another quite independently of any systematic error involved, thus measurements  $z_1, z_2, \dots, z_n$  are of high precision if the residuals  $d_r$  are small whatever the value of  $(\bar{z} - z_o)$ , whereas accuracy of measurements is high if errors  $e_r$  are small in which case  $(\bar{z} - z_o)$  is also small.

Accuracy therefore includes precision but the converse is not necessarily true. In most cases more is known on precision of an instrument than on its accuracy.

Calculus can be used in the estimation of errors. For supposing  $z$  is a measured quantity and  $\phi$  is a quantity from the formula:

$$\phi = f(z) \tag{6.9}$$

If  $\delta z$  is the error in  $z$ , the corresponding error in  $\phi$  is  $\delta\phi$  where:

$$\lim_{\delta z \rightarrow 0} \frac{\delta\phi}{\delta z} = \frac{d\phi}{dz} \tag{6.10a}$$

therefore 
$$\frac{\delta\phi}{\delta z} = \frac{d\phi}{dz} \tag{6.10b}$$

if  $\delta z$  is small enough

and the error in  $\phi$  is approximately given by:

$$\delta\phi = \frac{d\phi}{dz} \delta z. \tag{6.11}$$

When the quantity  $\phi$  is a function of more than one quantity then partial differentiation is applied .

For  $\phi = f( z_1 , z_2 , \dots , z_n )$ :

$$\delta\phi = \frac{\partial\phi}{\partial z_1} \delta z_1 + \frac{\partial\phi}{\partial z_2} \delta z_2 + \dots + \frac{\partial\phi}{\partial z_n} \delta z_n. \tag{6.12}$$

Further details on error analysis is beyond the scope of the present work and the reader is referred to texts such as Topping (1962) and Holman (1985).

### 6.7.2 ACCURACY OF THE EXPERIMENTAL VALUE CONDENSATION HEAT TRANSFER COEFFICIENT(h)

From Equation 6.1,

$$h = \dot{m}_v c_{pv} \Delta t_v / \pi(dl)\Delta t_m \quad (6.13)$$

Using Equation 6.12, and rearranging the fractional error in the heat transfer coefficient h,  $\delta h$ , is

$$\frac{\delta h}{h} = \frac{\delta \dot{m}_v}{\dot{m}_v} + \frac{\delta c_{pv}}{c_{pv}} + \frac{\delta(\Delta t_v)}{\Delta t_v} - \frac{\delta d}{d} - \frac{\delta l}{l} - \frac{\delta(\Delta t_m)}{\Delta t_m} \quad (6.14)$$

The maximum possible error due to the limitation of measuring instruments are as below.

$$\delta \dot{m}_v = \pm 8.33 \times 10^{-3} \text{ kgs}^{-1}$$

$$\delta d = \pm 0.001 \text{ m}$$

$$\delta l = \pm 0.001 \text{ m}$$

$$\delta(\Delta t_v) = \pm 1^\circ \text{C}$$

$$\delta(\Delta t_m) = \pm 0.5^\circ \text{C}$$

The error in the mean value of  $c_{pv}$  due to the variation of cooling water temperature in the test section is

$$\delta c_{pv} = \pm 0.003 \text{ kJ/kg K.}$$

The measured values in the experiment are as below;

where there was a variation in the value of a variable, the minimum measured value was used when applying Equation 6.14.

$$\dot{m}_v = 0.502 \text{ kg/s}$$

$$c_{p,v} = 4.181 \text{ kJ/kg K}$$

$$\Delta t_v = 8 \text{ }^\circ\text{C}$$

$$\Delta t_m = 9 \text{ }^\circ\text{C}$$

$$d = 25.4\text{mm}$$

$$L = 4000\text{mm}$$

Substituting the numerical values into Equation 6.14:

$$\begin{aligned} \frac{\delta h}{h} &= \frac{0.00833}{0.502} + \frac{0.003}{4.181} + \frac{1}{8} - \frac{1}{25.4} - \frac{1}{400} - \frac{0.5}{9} \\ &= 0.047 \\ &= 5\% \end{aligned}$$

The maximum error in the values of condensation heat transfer coefficient (h) is then  $\pm 5\%$ .

### 6.7.3 ACCURACY OF EXPERIMENTAL PRESSURE LOSS ACROSS THE TEST SECTION

In the evaluation of the experimental pressure drop across the test section, a manometer with water as the working fluid was used. The pressure drop  $\Delta P$  is calculated from the formula:

$$\Delta P = (\rho_m - \rho)gh \quad (8.15)$$

where

$\rho_m$  = density of the manometric fluid

$\rho$  = density of the fluid in the conduit

h = manometer head reading

Using Equation 6.15 then:

$$\frac{\delta(\Delta P)}{\Delta P} = \left[ \frac{\partial(\Delta P)}{\partial(\rho_m - \rho)} \delta(\rho_m - \rho) + \frac{\partial(\Delta P)}{\partial h} \delta h \right] \frac{1}{\Delta P} \quad (6.15a)$$

$$\frac{\delta(\Delta P)}{\Delta P} = \frac{\delta(\rho_m - \rho)}{(\rho_m - \rho)} + \frac{\delta h}{h} \quad (6.15b)$$

The errors in the density of water ( $\rho_m$ ) and of the fluid in the conduit ( $\rho$ ) are as a result of temperature fluctuations. The range of the temperature variation for the steam-air mixture in the pressure tapping pipes were practically the same as those of water in the manometer due to the long uninsulated lengths of the pressure tapping pipes. That temperature range was between 25 °C and 30 °C.

The steam-air mixture in the pressure tapping pipes was considered to have properties similar to those of air saturated with water vapour at same temperature as the mixture. The numerical values of the parameters of Equation 6.15b are as below:

Density of saturated air at 30 °C ,0.811 bar	= 0.895 kg/m <sup>3</sup>
Density of saturated air at 25 °C ,0.811 bar	= 0.872 kg/m <sup>3</sup>
Density of water at 30 °C	= 958 kg/m <sup>3</sup>
Density of water at 25 °C	= 997 kg/m <sup>3</sup>

$\delta(\rho_m - \rho)$  = maximum value of  $(\rho_m - \rho)$  - minimum value of  $(\rho_m - \rho)$

$$\delta(\rho_m - \rho) = (997 - 0.872) - (958 - 0.895) = 39.0 = \pm 19.5 \text{ kg/m}^3$$

The error in the measurement of the manometric head because of oscillation of the manometric fluid was taken as  $\pm 2.5$  mm of water. Substituting the numerical values into Equation 6.15b and using the maximum head in the manometer of 69 mm of water, then:

$$\frac{\delta(\Delta P)}{\Delta P} = \frac{1}{996.45} \times 19.5 + \frac{2.5}{69} = \pm 6\%$$

The maximum error in the calculated values of the pressure drop across the test section is  $\pm 6\%$ .



## CHAPTER SEVEN

### DISCUSSION

#### 7.1 INTRODUCTION

In the present work, the aim was to find the effects of NCG on condensation heat transfer coefficient ( $h$ ) of steam on the inside of a horizontal tube when the following parameters were varied:-

- i) The percent mass concentration of NCG in the steam.
- ii) The inside tube diameter.
- iii) The initial temperature of steam-air.

#### 7.2 EFFECT OF NCG MASS CONCENTRATION

The effect of initial air mass concentration on the mean condensation heat transfer coefficient ( $h$ ) is shown in Appendix 7 as Figures A7.1 to A7.12. The value of  $h$  is seen to decrease very rapidly with small increases in air mass concentration.

The value of  $h$  then decreases slowly until it becomes virtually constant at high gas concentration. The reduction of  $h$  is explained by the fact that when steam is mixed with NCG and it condenses, the NCG will be left between new steam and its condensate, so that after

condensation has commenced the cold surface will be blanketed by a stratum of air and the new steam will either have to displace or pass through this layer of NCG before it in turn can be condensed. Also NCG being denser than steam, steam is displaced upwards in the tube cross section, this further reduces the "actual" surface area of heat transfer between the steam and the cooler surface of the tube resulting in a further reduction in the value of  $h$ . This effect becomes greater towards the exit end of the test section as the proportion of NCG in the steam NCG mixture increases and also in cases of high initial NCG concentration.

In order to explain the large reduction in the value of  $h$  by presence of even very small amounts of NCG in the vapour, Sparrow and Lin (1964) suggested that even a very small amount of NCG in the bulk of vapour causes a large build up of NCG at liquid-vapour interface. A consequence of this build up is that the partial pressure of vapour at the interface is reduced, this in turn lowers the temperature at which the vapour condenses and thus diminishes the effective thermal driving force.

At relatively high NCG concentrations, the mixture heat transfer characteristics are strongly dependent on the heat transfer properties of NCG and therefore the value of  $h$  does not vary with NCG concentration. This is seen in Figures A7.1 to A7.12.

### 7.3 EFFECT OF TUBE DIAMETER

The effect of tube diameter on the mean condensation heat transfer coefficient ( $h$ ) is shown on Figures 7.1 to 7.3. For a fixed inlet temperature and NCG concentration, the smaller tube 25.4mm (1") gave a higher value of  $h$  than the tube of diameter 38.1mm(1.5").

This difference is very significant at low NCG concentrations. The difference in the value of  $h$  became smaller at higher NCG concentrations. The reasons for this trend are thought to be:-

- i) For similar mass flow rates, NCG concentrations and inlet temperature, the Reynolds number for the smaller tube was higher and therefore the value of  $h$ , which is a function of Reynolds number, was higher than that of the larger tube.
- ii) The higher Reynolds numbers caused more rippling and turbulence at the liquid-vapour interface and hence promoted higher heat transfer rates in the smaller tube for same mass flow rate [Othmer(1929)].
- iii) The existence of an annular-mist type of flow in the smaller tube, as opposed to the stratified flow regime in the larger tube, promoted intimate contact between the phases and hence higher heat transfer rates.
- iv) The higher velocities of vapour in the smaller

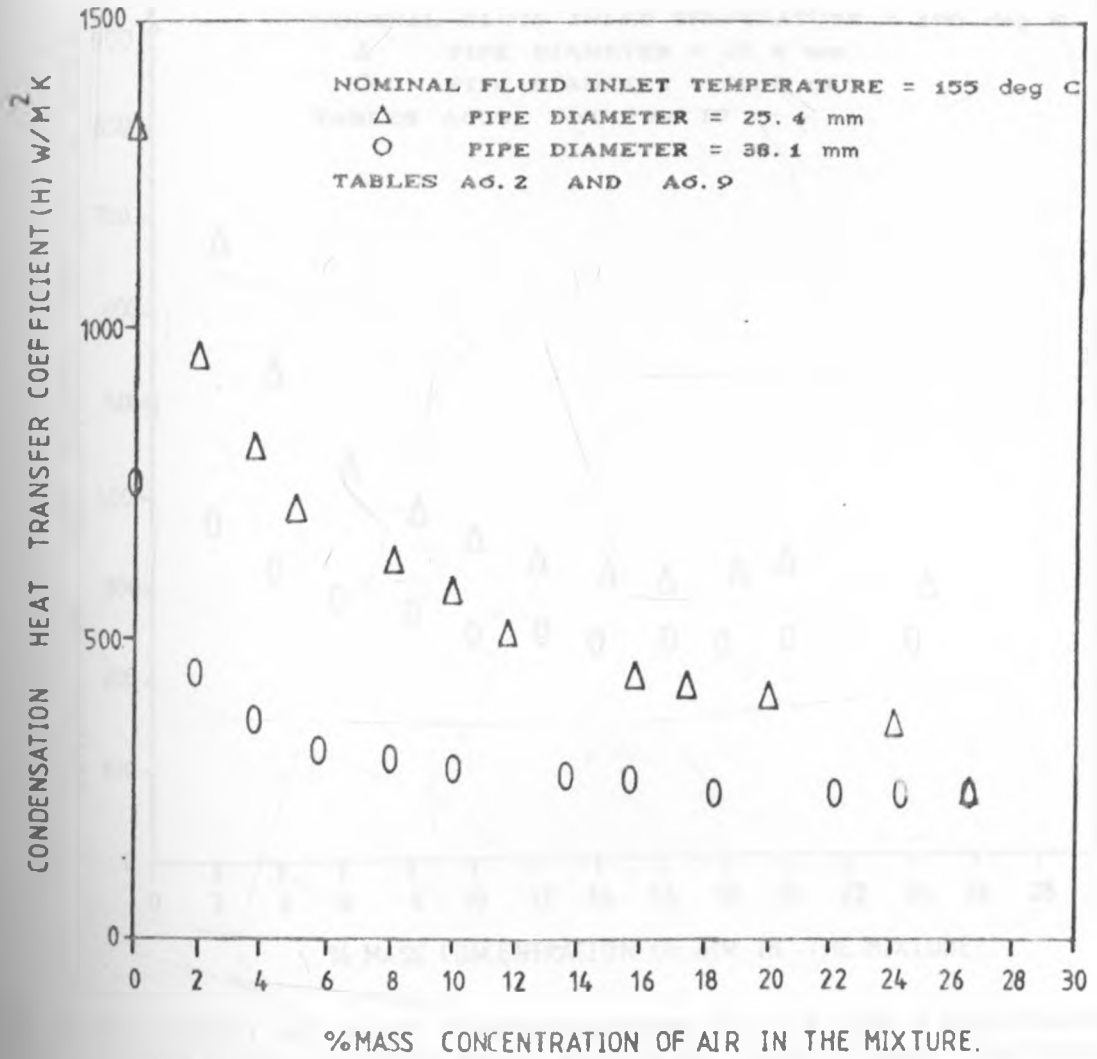


FIGURE 7.1: EFFECT OF MASS CONCENTRATION OF AIR AND PIPE DIAMETER ON CONDENSATION HEAT TRANSFER COEFFICIENT FOR FIXED INLET TEMPERATURE

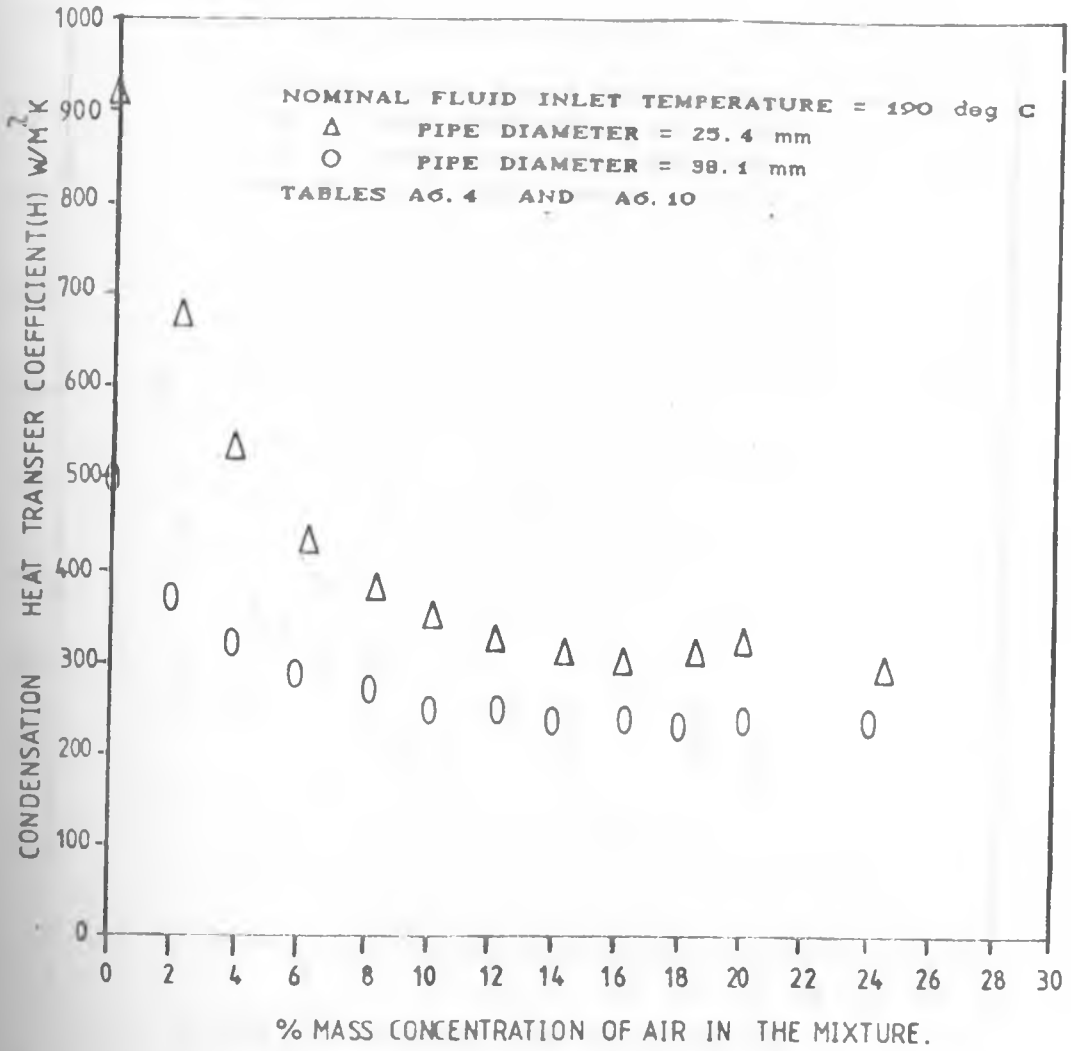


FIGURE 7.2: EFFECT OF MASS CONCENTRATION OF AIR AND PIPE DIAMETER ON CONDENSATION HEAT TRANSFER COEFFICIENT FOR FIXED INLET TEMPERATURE

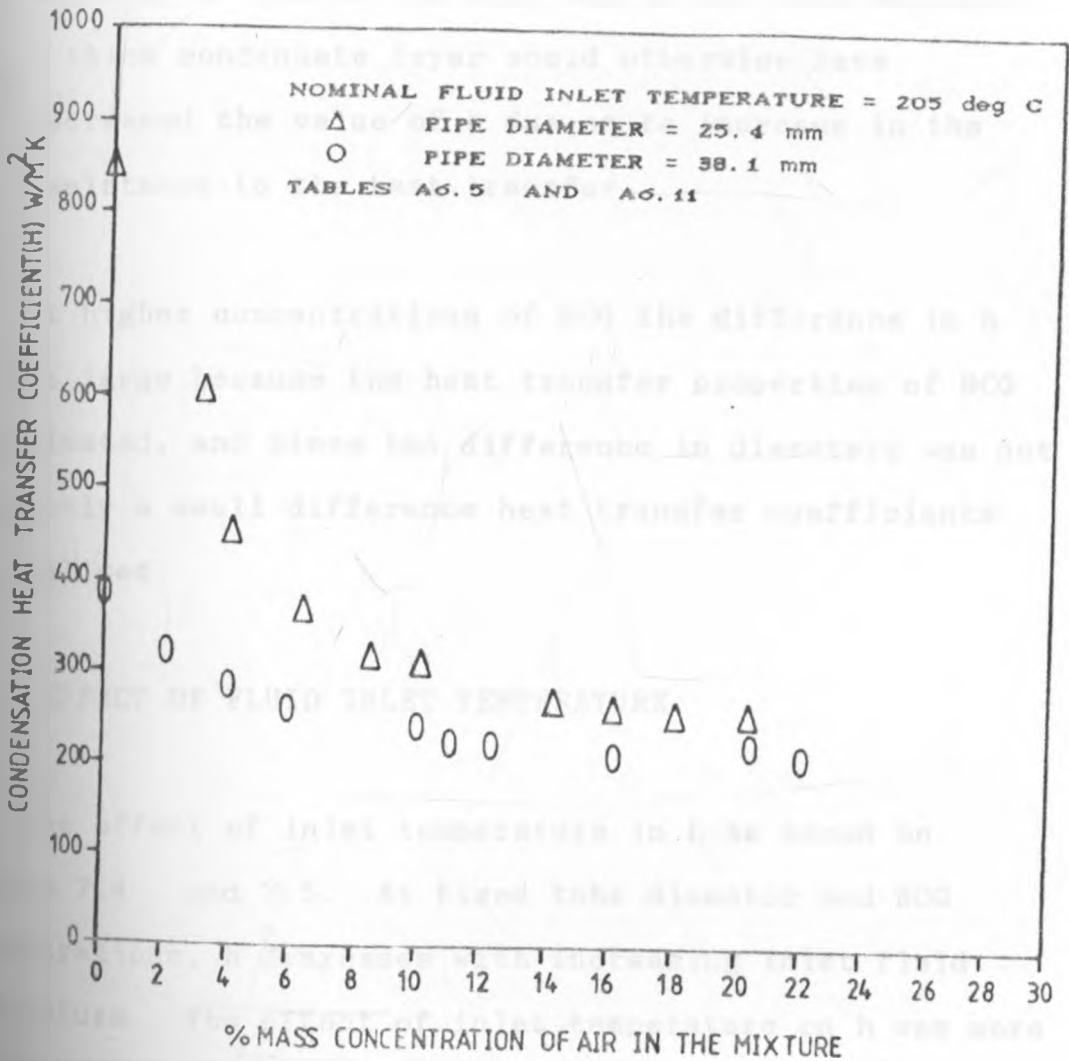


FIGURE 7.3: EFFECT OF MASS CONCENTRATION OF AIR AND PIPE DIAMETER ON CONDENSATION HEAT TRANSFER COEFFICIENT FOR FIXED INLET TEMPERATURE

tube helped in driving off the condensate and prevented the formation of a thick condensate film especially towards the exit end of the test section. A thick condensate layer would otherwise have decreased the value of  $h$  due an to increase in the resistance to the heat transfer.

At higher concentrations of NCG the difference in  $h$  was not large because the heat transfer properties of NCG predominated, and since the difference in diameters was not large only a small difference heat transfer coefficients was realised.

#### 7.4 EFFECT OF FLUID INLET TEMPERATURE

The effect of inlet temperature in  $h$  is shown on Figures 7.4 and 7.5. At fixed tube diameter and NCG concentrations,  $h$  decreases with increasing inlet fluid temperature. The effect of inlet temperature on  $h$  was more pronounced at relatively low NCG concentrations. The theory suggests that the value of  $h$  should increase with an increase in the inlet fluid temperature because of a bigger temperature difference between steam-air core temperature and tube wall i.e a bigger thermal driving force. This difference was due to the fact that, for a steam-NCG mixture at atmospheric pressure and at a temperature higher



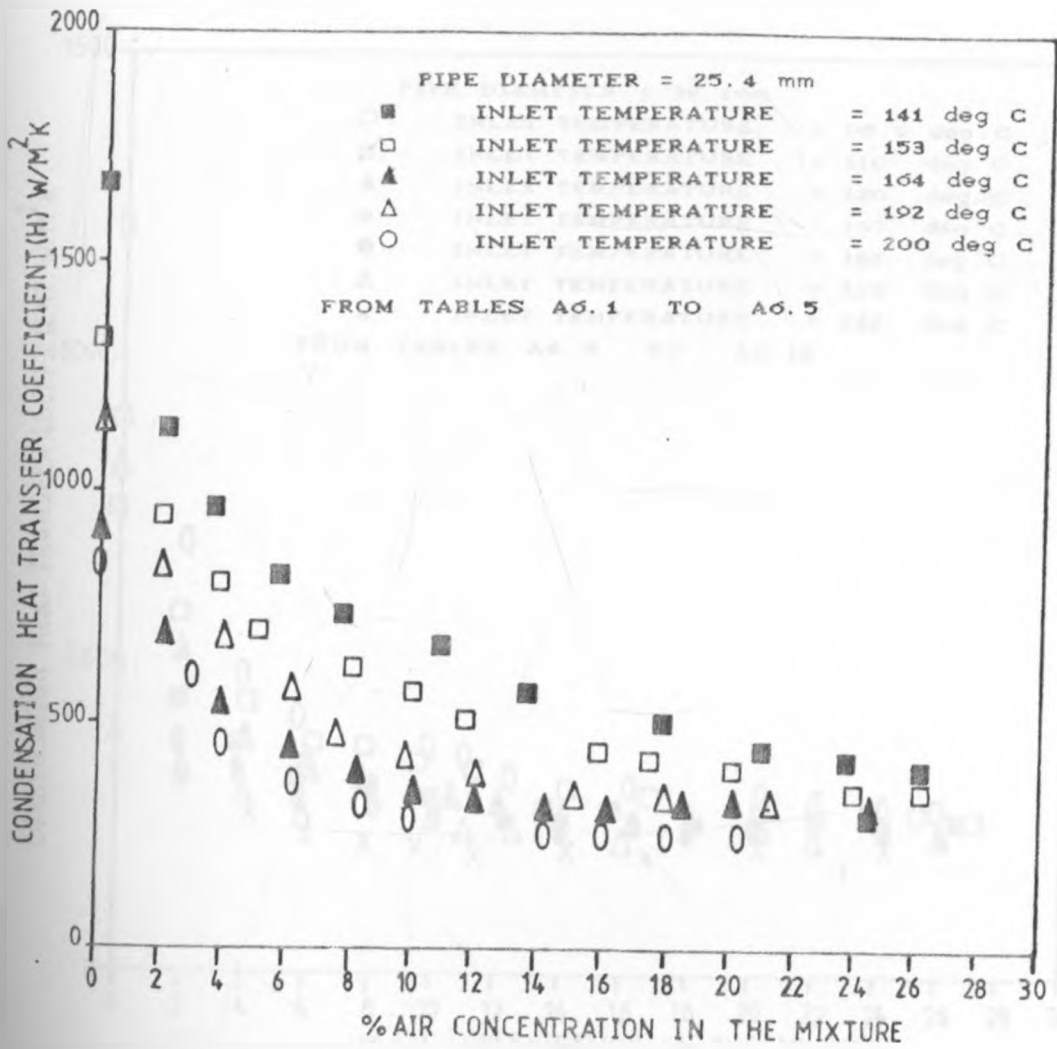


FIGURE 7.4: EFFECT OF MASS CONCENTRATION OF AIR AND INLET TEMPERATURE ON CONDENSATION HEAT TRANSFER COEFFICIENT FOR FIXED PIPE DIAMETER

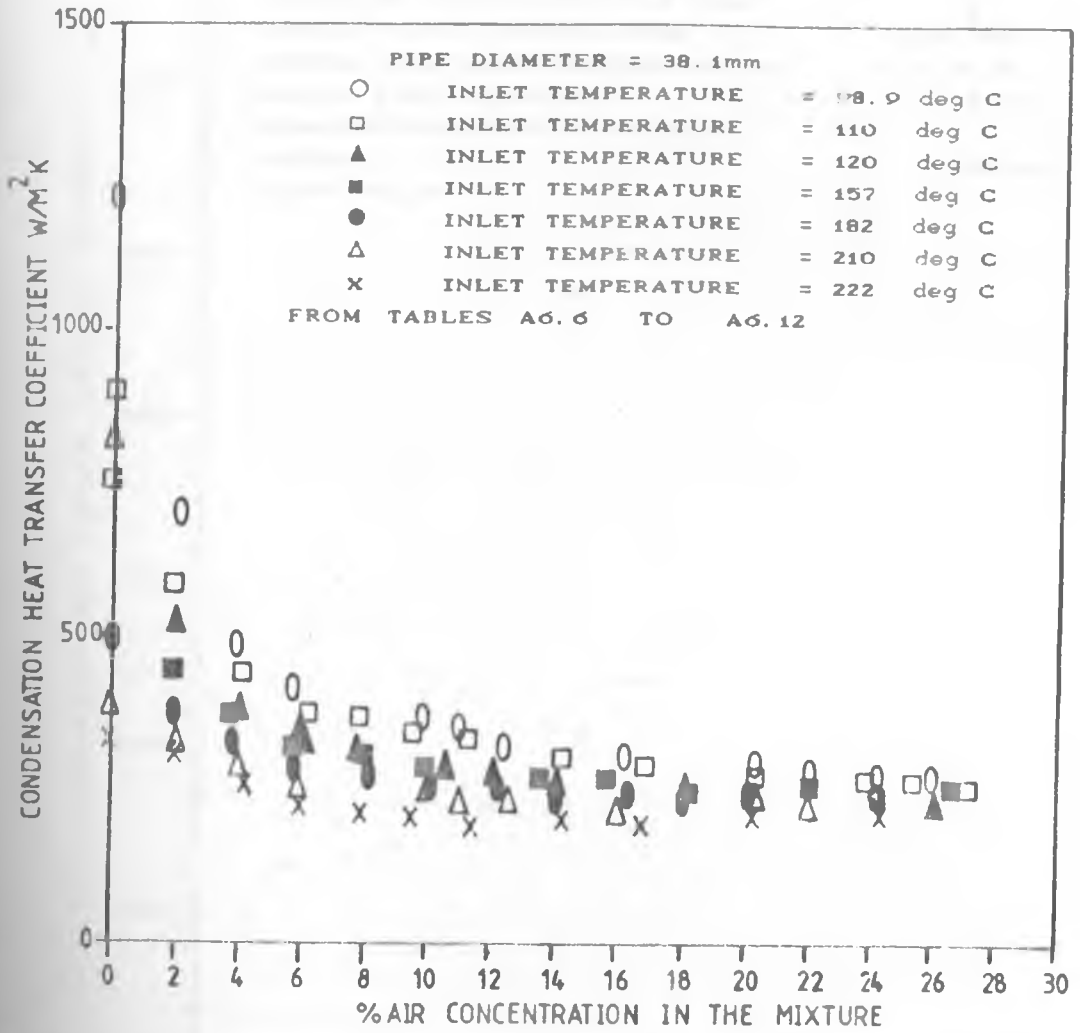


FIGURE 7.5: EFFECT OF MASS CONCENTRATION OF AIR AND INLET TEMPERATURE ON CONDENSATION HEAT TRANSFER COEFFICIENT FOR FIXED PIPE DIAMETER

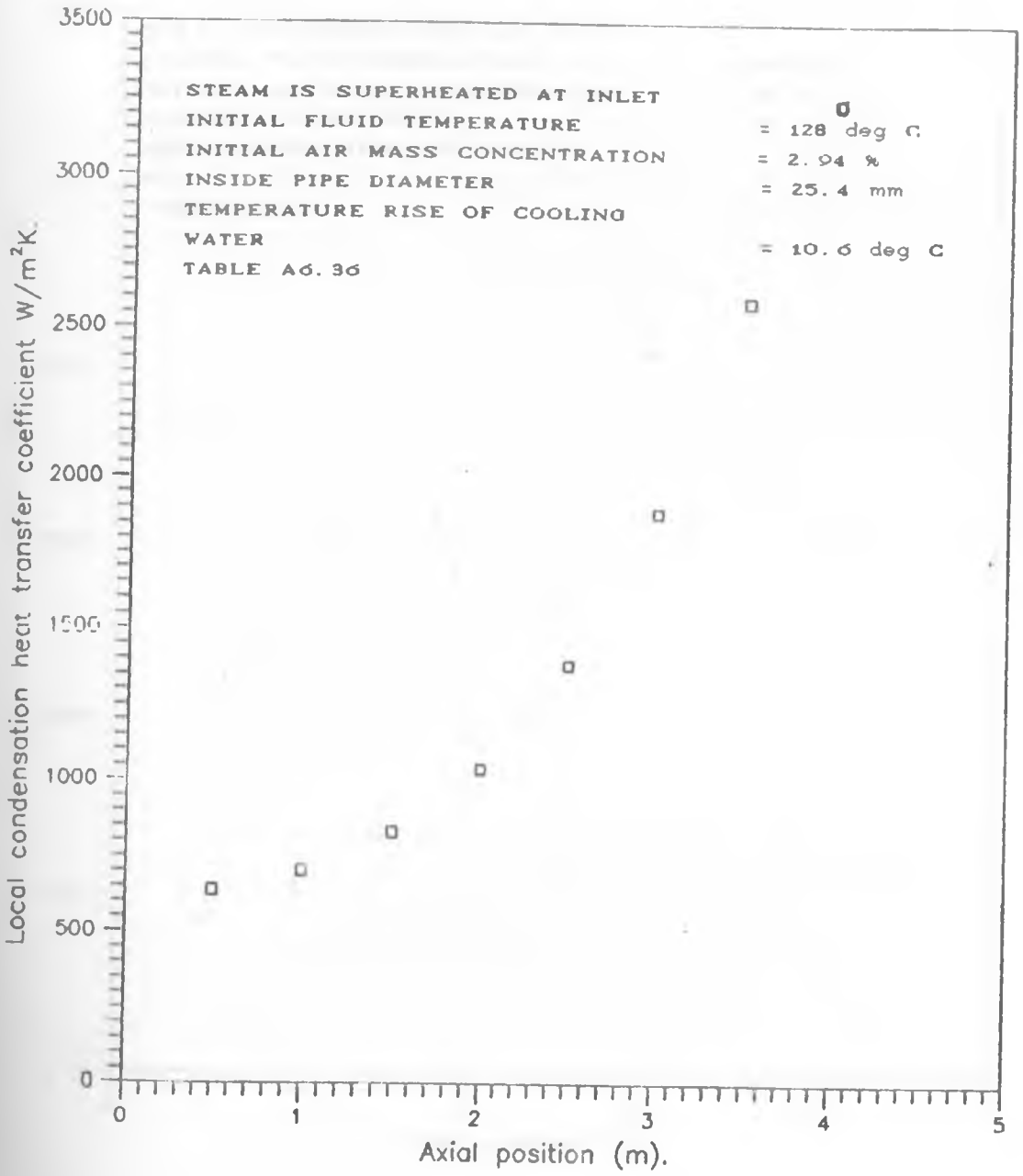


FIGURE 7.6: LOCAL CONDENSATION HEAT TRANSFER COEFFICIENT PROFILE ALONG THE TEST SECTION

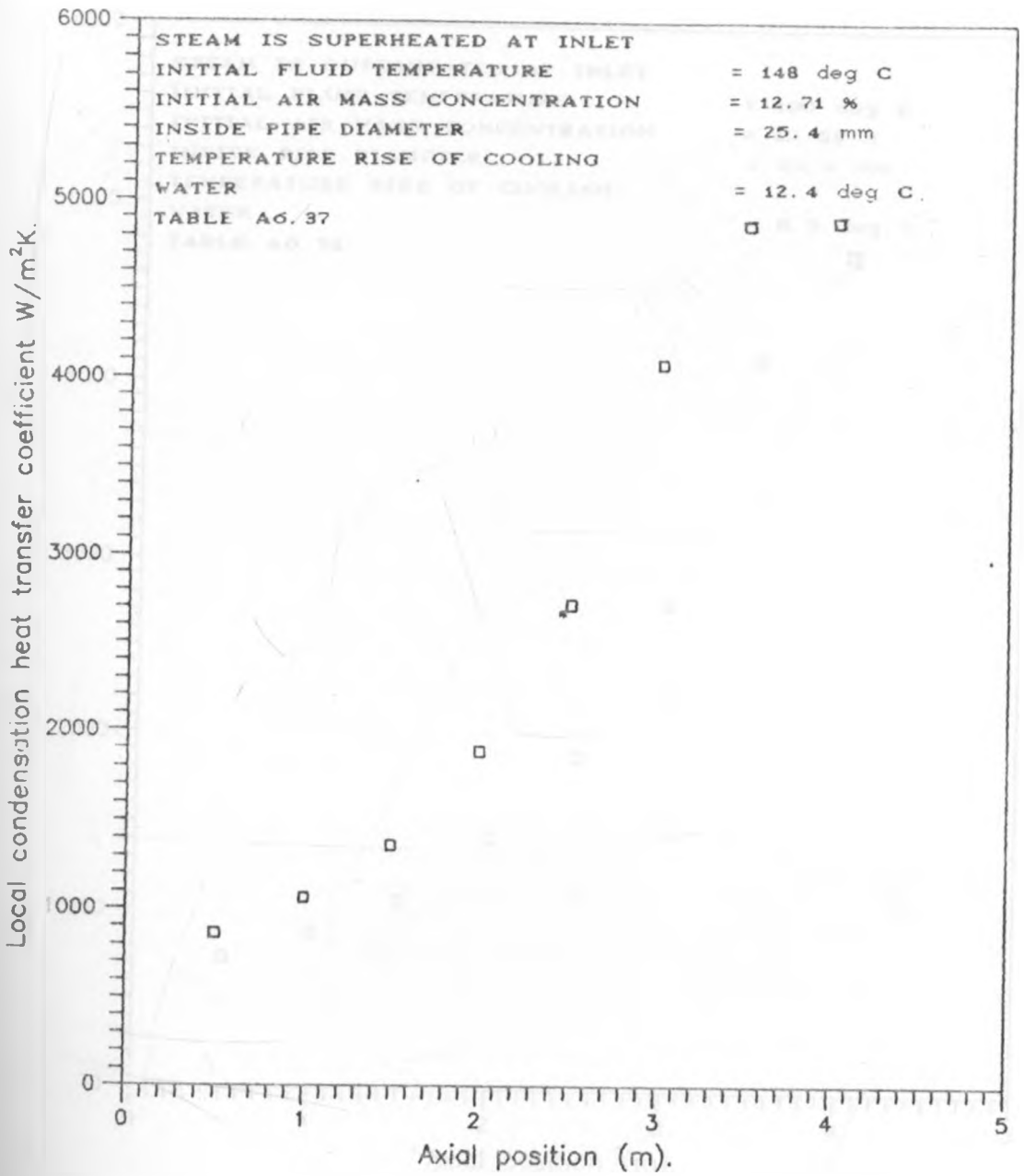


FIGURE 7.7: LOCAL CONDENSATION HEAT TRANSFER COEFFICIENT PROFILE ALONG THE TEST SECTION

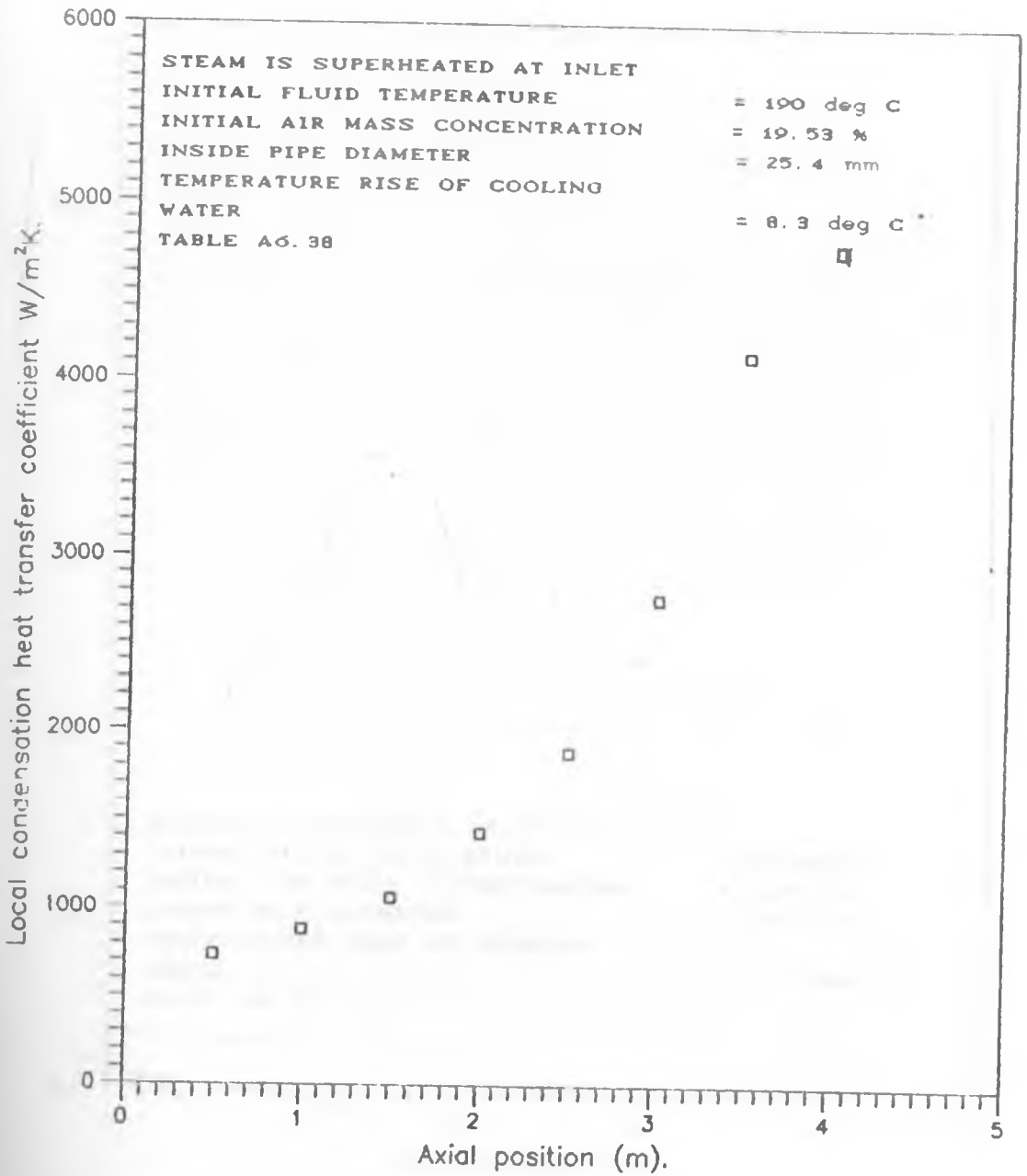


FIGURE 7.8: LOCAL CONDENSATION HEAT TRANSFER COEFFICIENT PROFILE ALONG THE TEST SECTION

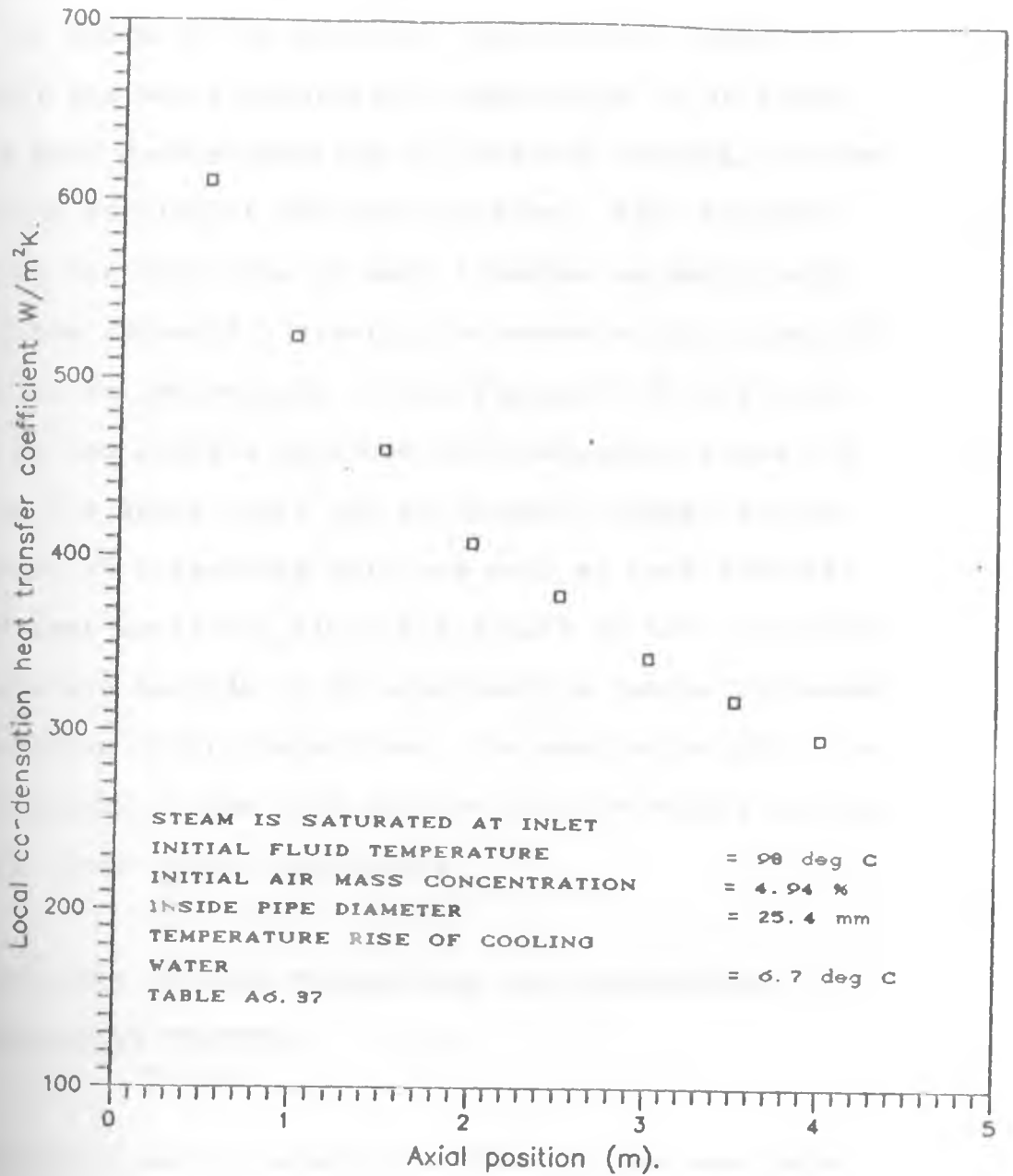


FIGURE 7.9: LOCAL CONDENSATION HEAT TRANSFER COEFFICIENT PROFILE ALONG THE TEST SECTION

than saturation temperature corresponding to the partial pressure of steam in the mixture, condensation would not occur until the above saturation temperature is attained. Therefore only de-superheating or sensible cooling occurred in the first portion of the test section. Heat transfer coefficient for this type of heat transfer is relatively low. But the value of  $h$  greatly increased at the onset of condensation as can be seen in the Figures 7.6 to 7.8, as compared to the profile obtained with saturated steam, in the Figure 7.9 where there was no dramatic change in the local values of  $h$  implying only one mode of heat transfer along the test section. Since the length of tube occupied by the sensible cooling or de-superheating regime increased with increasing inlet temperature, the mean value of  $h$  over the whole length of the test section thus decreased with an increasing fluid inlet temperature.

#### 7.5 COMPARISON BETWEEN THEORETICAL AND EXPERIMENTAL TEMPERATURE PROFILES.

The method used in sizing the test section was based on that of Colburn and Hougen (1934). Even for saturated steam at the inlet to the test section this method has very little experimental evidence in the literature to support it. In this work a comparison was made between experimental temperature profile and those predicted by the model to gauge on how close they agree.

For the cases considered the results are presented in Figures 7.10 and 7.14.

The agreement is close once the steam-air mixture has reached saturation state but the theoretical model predicted higher temperatures in the superheat region. This shows that a better procedure should still be sought for sizing of integral cooler-condensers if the steam-NCG mixture is superheated at the inlets to the cooler-condensers.

#### 7.6 COMPARISON OF EXPERIMENTAL AND PREDICTED HEAT TRANSFER COEFFICIENTS.

The predicted values of condensation heat transfer coefficient ( $h_m$ ) were calculated using Equation 2.3 and 2.4. These are presented in Appendix 7 as Figures A7.13 to A7.23. For ease of reference the following figures are reproduced; Figures A7.17 and A7.18 for cases of near saturation, A7.14 for the case of mild degree of superheat and A7.23 for the case of high degree of superheat. The difference of ratios  $H_{Ac}$  and  $H_{Sh}$  from unity (when NCG concentration is zero) indicated the departure of experimental condensation heat transfer coefficient ( $h_{exp}$ ) from those predicted by the above two correlations. The



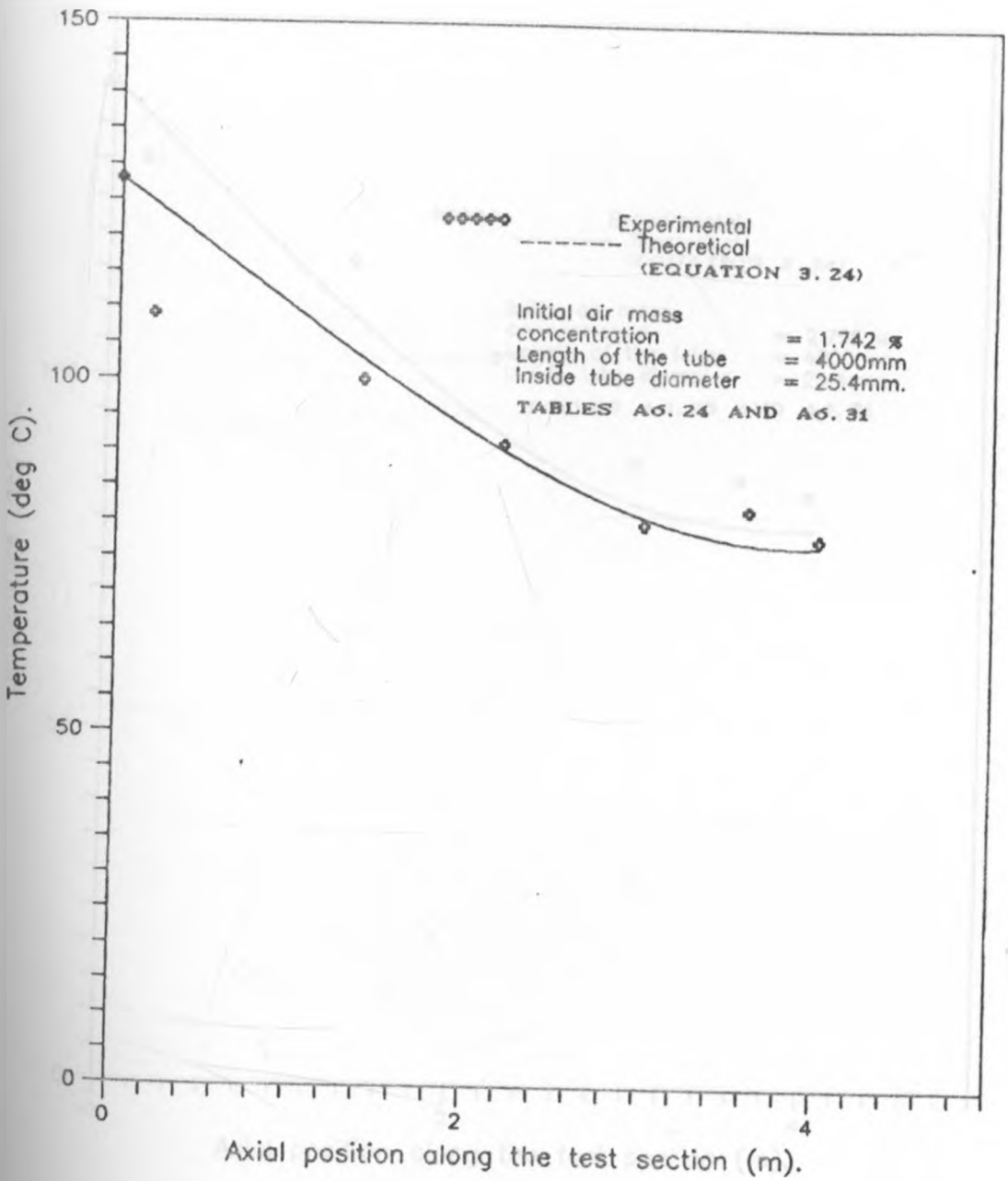


FIGURE 7.10: COMPARISON BETWEEN THEORETICAL AND EXPERIMENTAL TEMPERATURE PROFILES

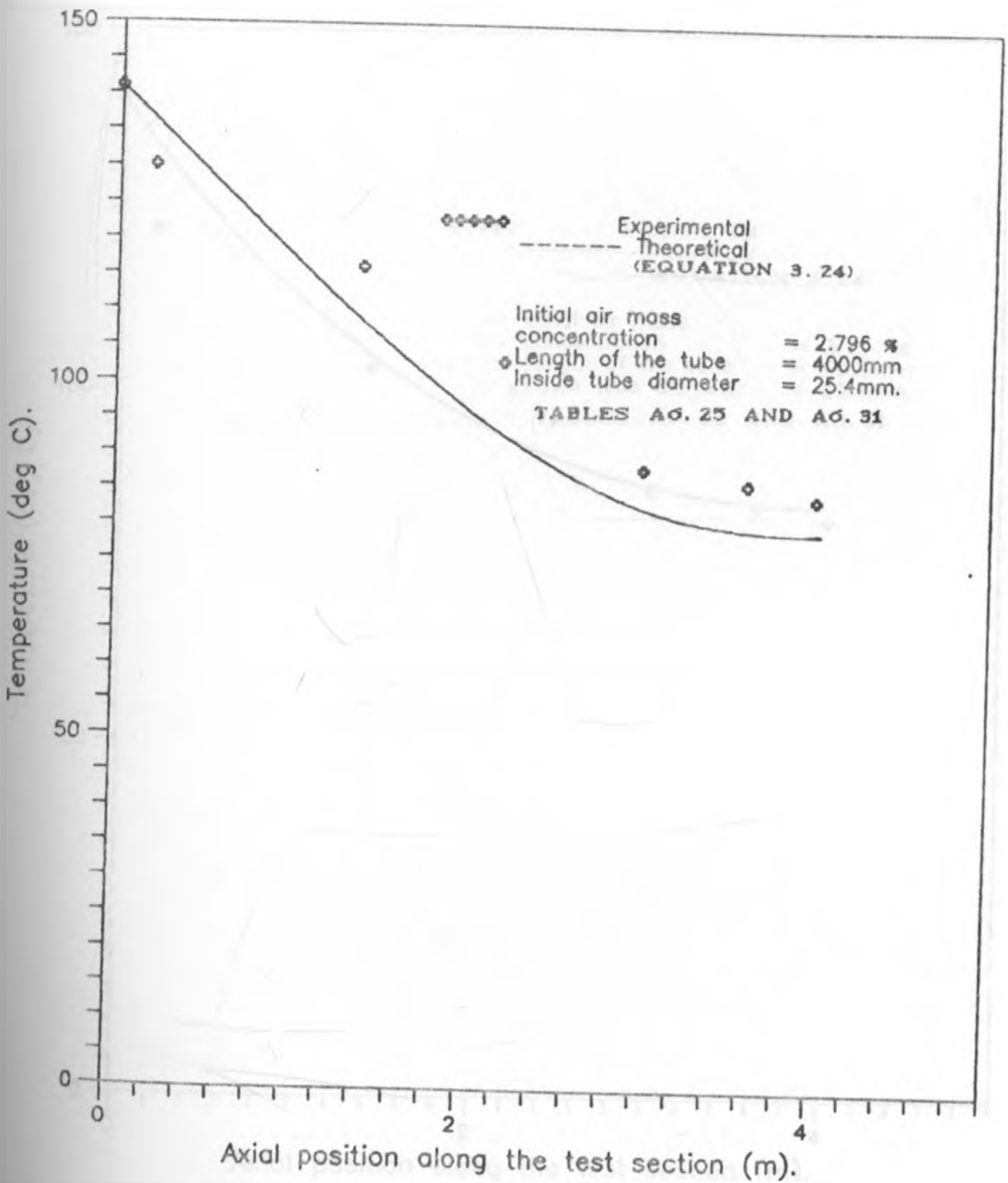


FIGURE 7.11: COMPARISON BETWEEN THEORETICAL AND EXPERIMENTAL TEMPERATURE PROFILES

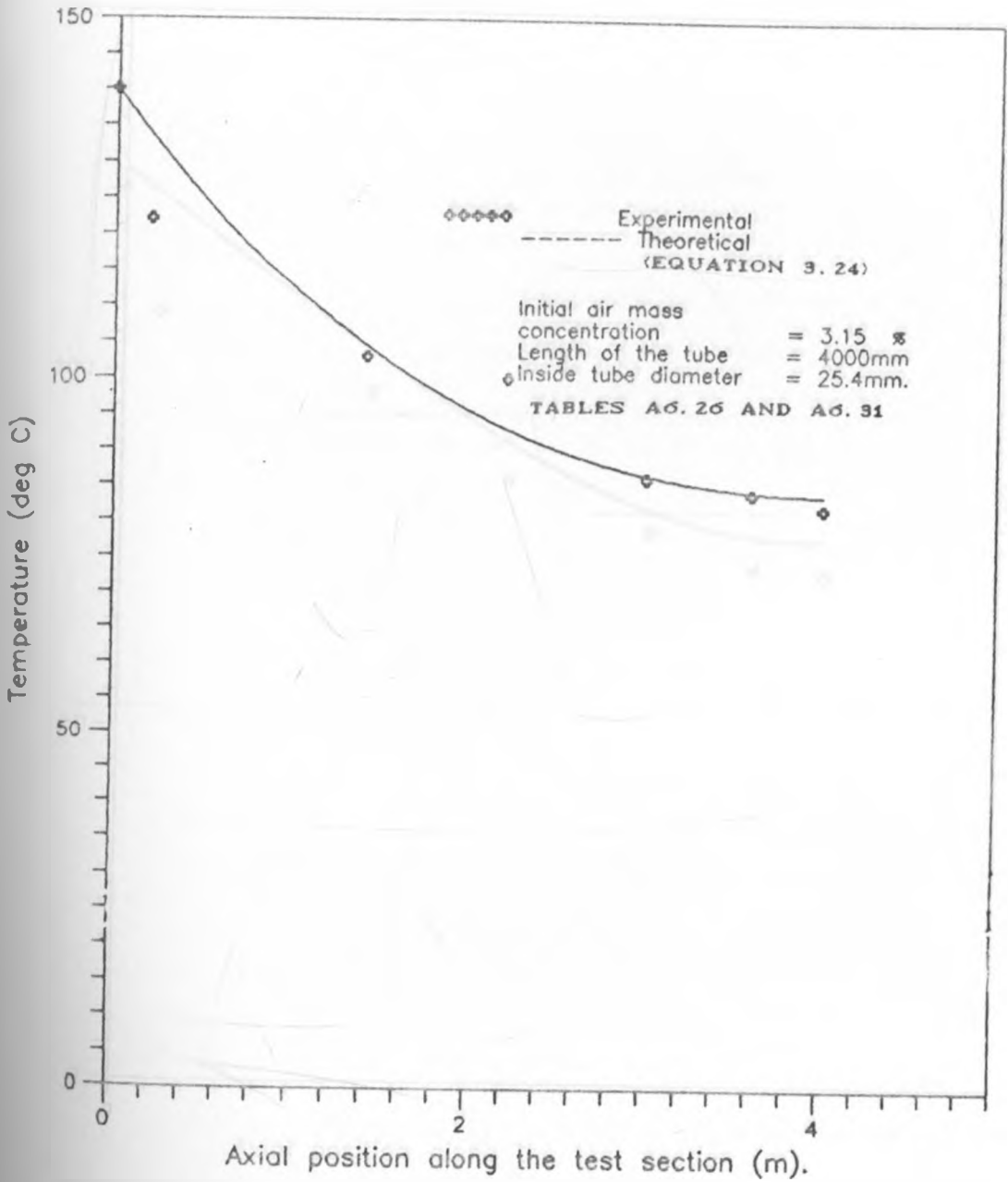


FIGURE 7.12: COMPARISON BETWEEN THEORETICAL AND EXPERIMENTAL TEMPERATURE PROFILES

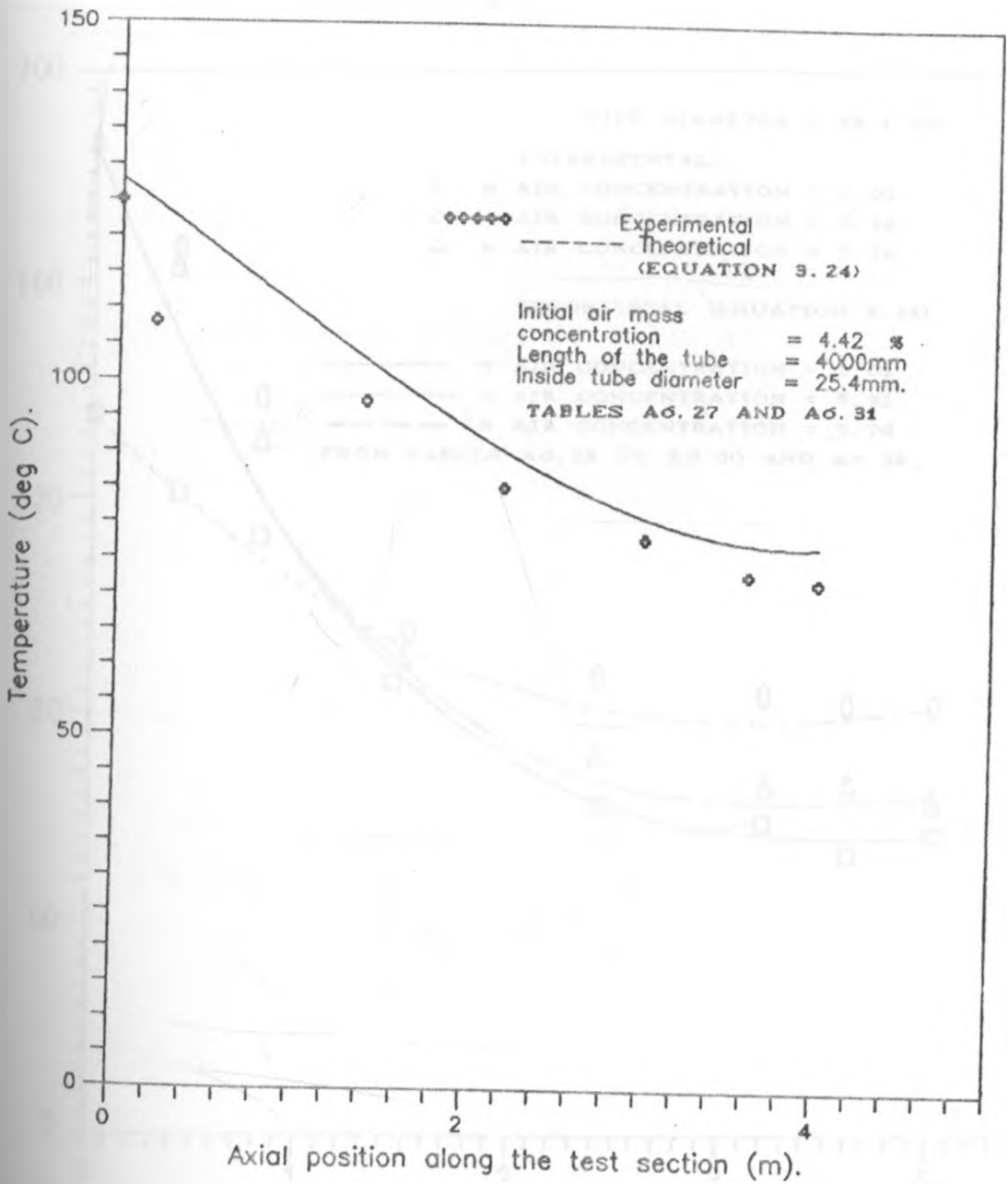


FIGURE 7.13: COMPARISON BETWEEN THEORETICAL AND EXPERIMENTAL TEMPERATURE PROFILES

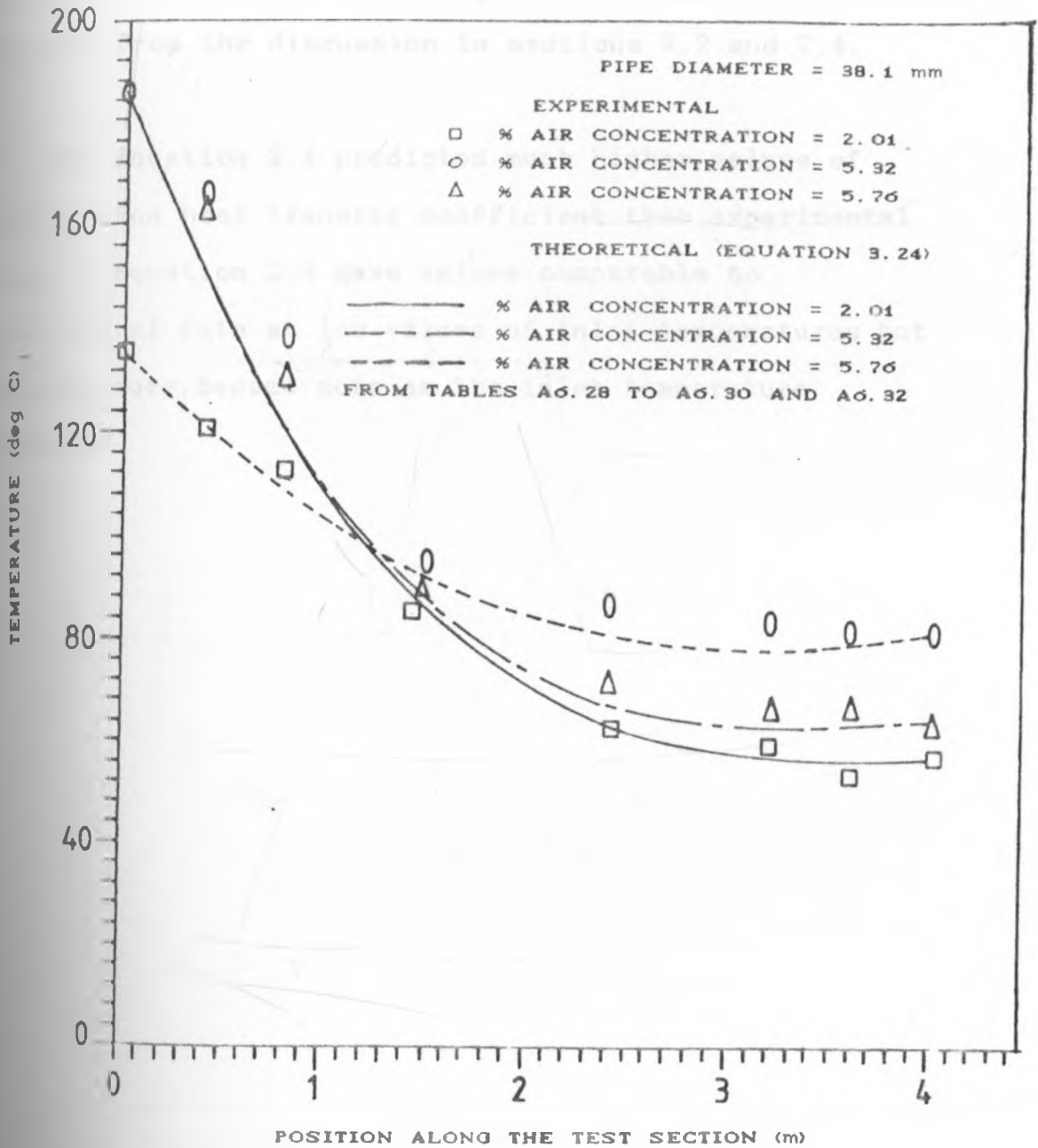


FIGURE 7.14: COMPARISON BETWEEN THEORETICAL AND EXPERIMENTAL TEMPERATURE PROFILES

departures were greater as both the inlet temperature of steam air and the NCG concentration increased, which was as expected from the discussion in sections 7.2 and 7.4.

The Equation 2.4 predicted much higher values of condensation heat transfer coefficient than experimental values. Equation 2.3 gave values comparable to experimental data at low values of inlet temperatures but the departure became more as the inlet temperature increased.

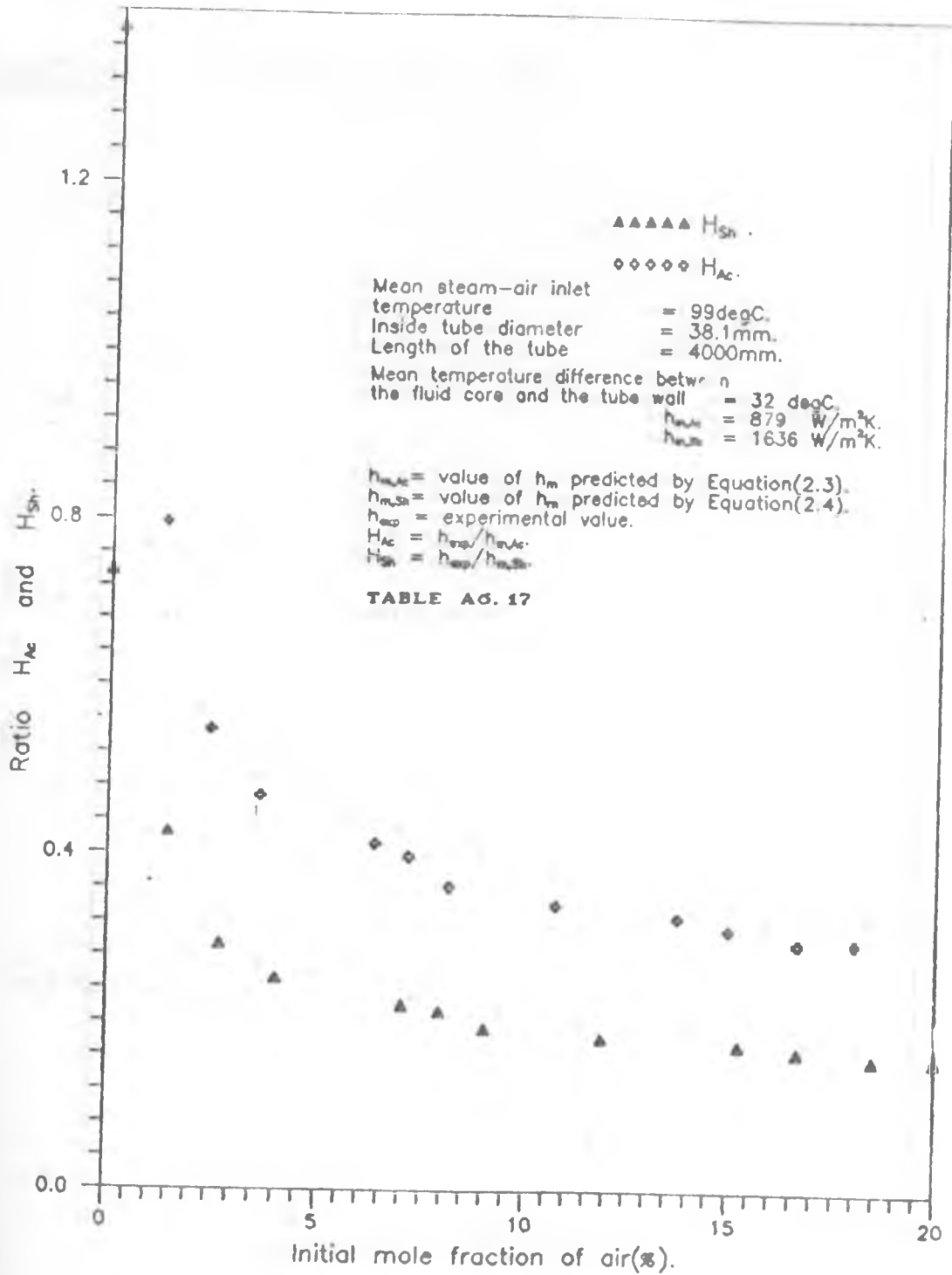


FIGURE A7.17: RATIOS OF EXPERIMENTAL TO PREDICTED CONDENSATION HEAT TRANSFER COEFFICIENT v INITIAL MOLE FRACTION OF AIR IN THE MIXTURE

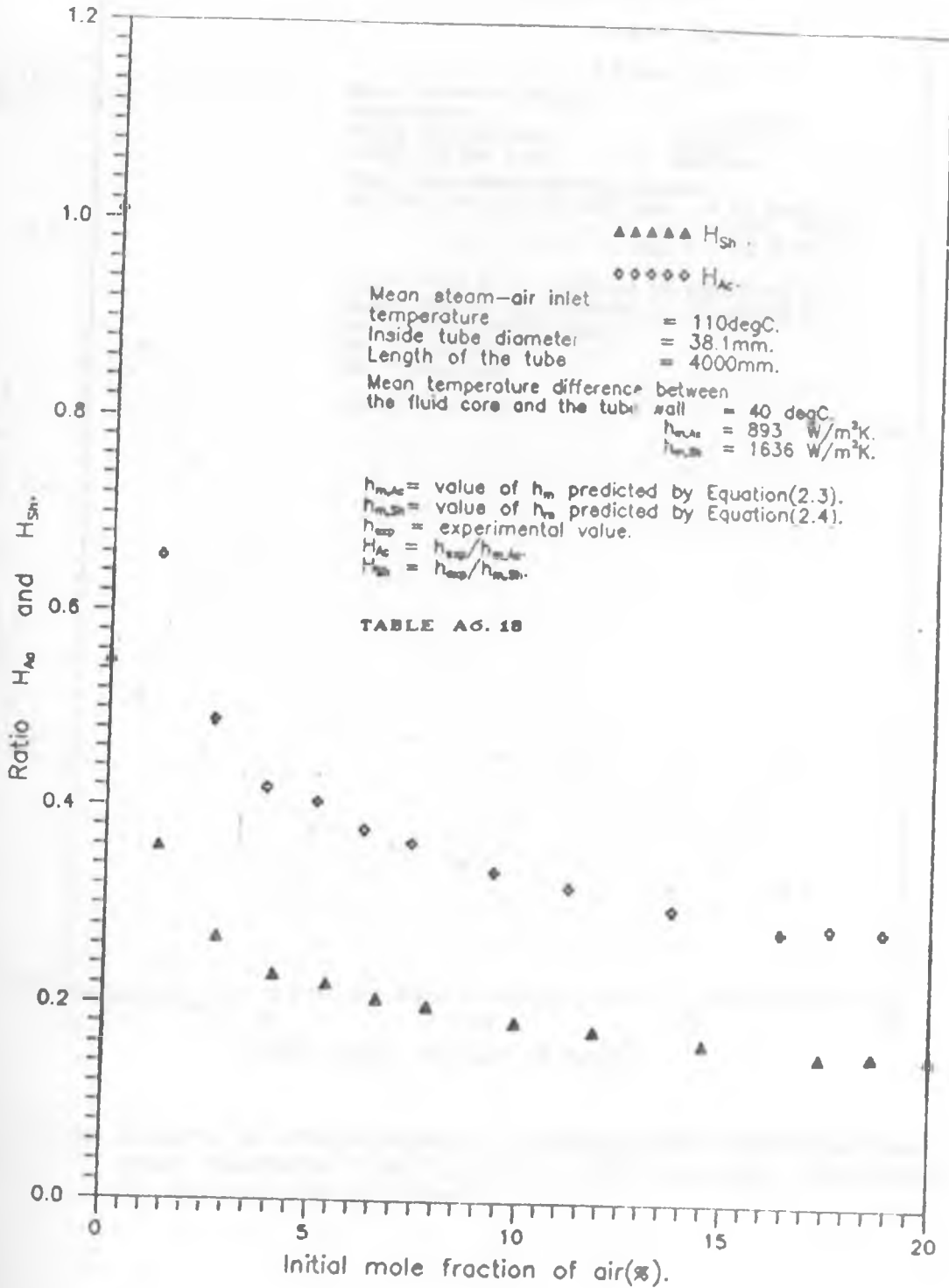
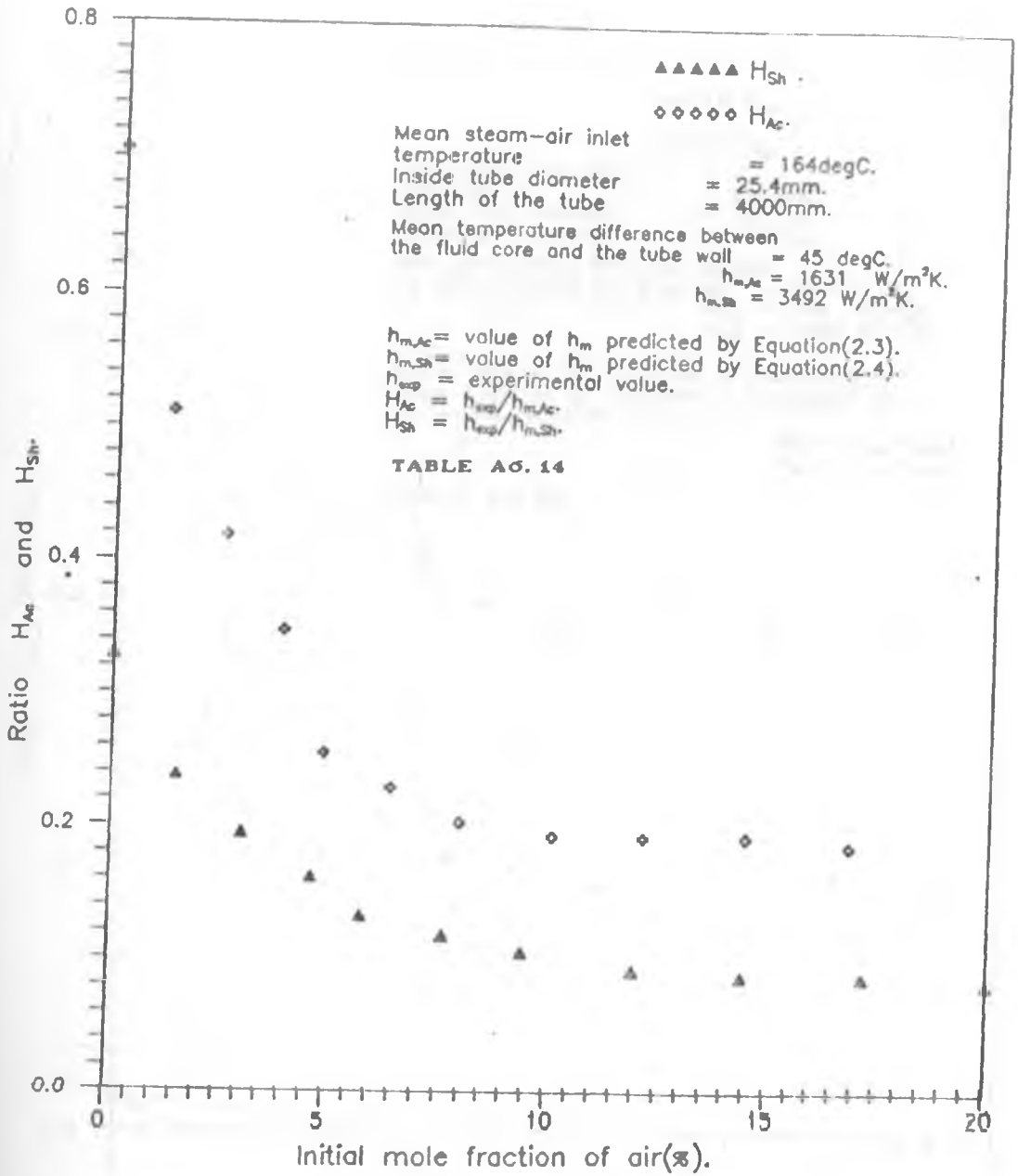


FIGURE A7.18: RATIOS OF EXPERIMENTAL TO PREDICTED CONDENSATION HEAT TRANSFER COEFFICIENT v INITIAL MOLE FRACTION OF AIR IN THE MIXTURE





**FIGURE A7.14: RATIOS OF EXPERIMENTAL TO PREDICTED CONDENSATION HEAT TRANSFER COEFFICIENT  $\nu$  INITIAL MOLE FRACTION OF AIR IN THE MIXTURE**

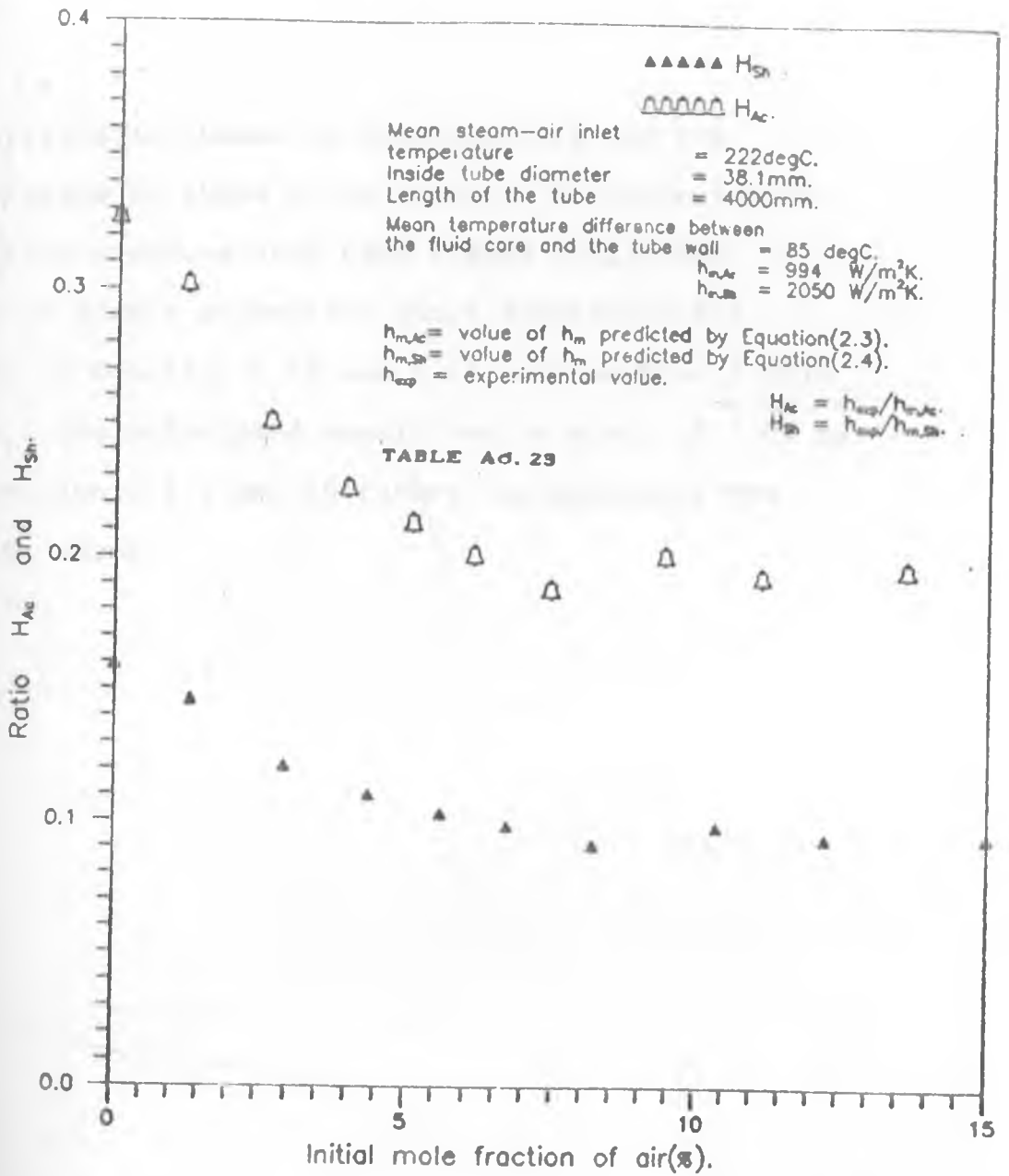


FIGURE A7.23: RATIOS OF EXPERIMENTAL TO PREDICTED CONDENSATION HEAT TRANSFER COEFFICIENT  $\nu$  INITIAL MOLE FRACTION OF AIR IN THE MIXTURE

## 7.7 COMPARISON OF PREDICTED AND EXPERIMENTAL PRESSURE DROPS.

The correlation based on Equation 4.16 and the computer program is shown to be suitable for calculating two phase flow pressure drop (See Figure 7.15) The assumption of global parameters which simplified the application of Equation 4.13 and 4.14 is therefore a fair assumption. The calculated result had an error of  $\pm 6\%$  as shown in section 6.7.2 and therefore the agreement was deemed to be close.

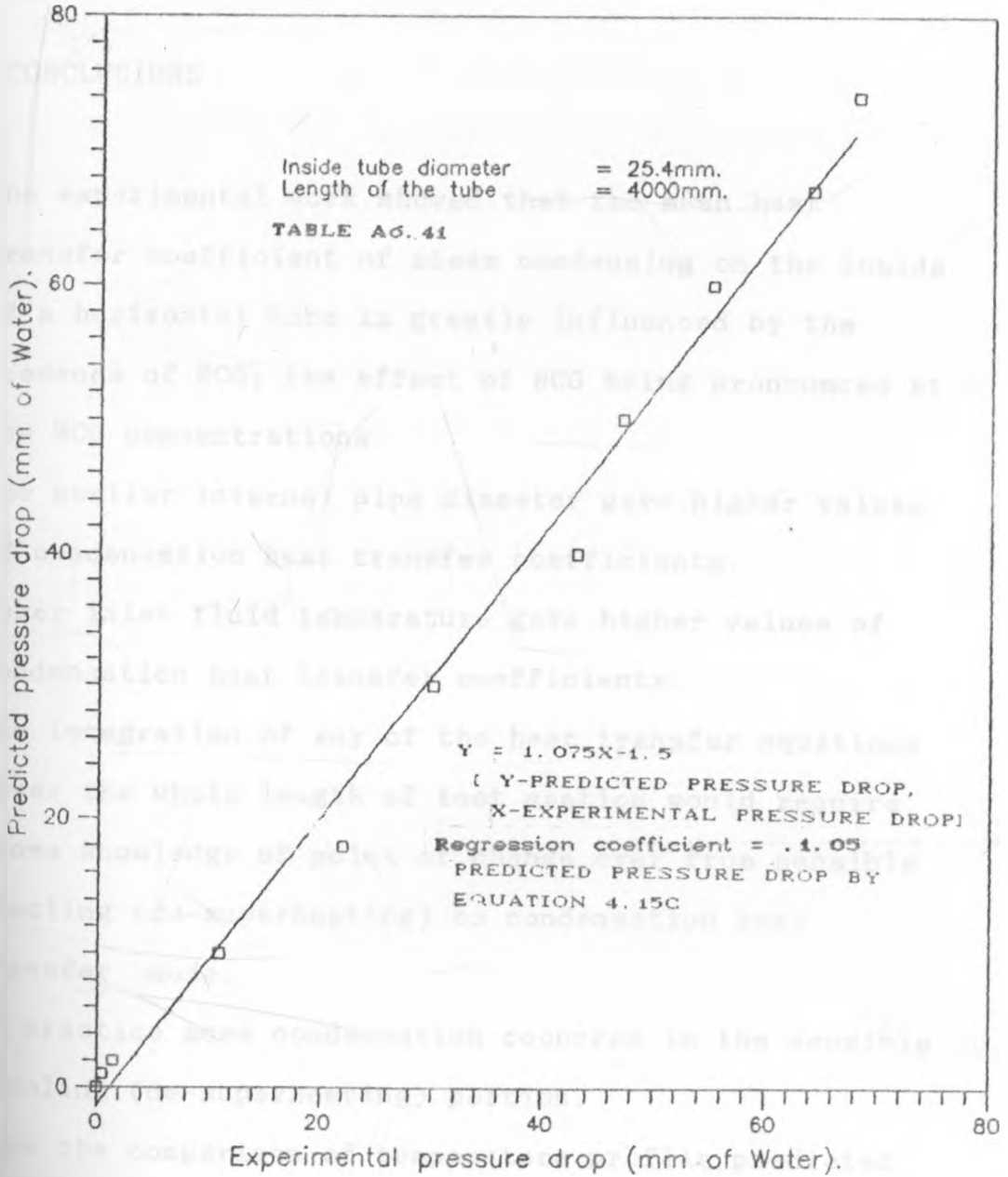


FIGURE A7.15: RATIOS OF EXPERIMENTAL TO PREDICTED CONDENSATION HEAT TRANSFER COEFFICIENT v INITIAL MOLE FRACTION OF AIR IN THE MIXTURE

## CHAPTER EIGHT

### CONCLUSIONS AND RECOMMENDATIONS

#### 8.1 CONCLUSIONS

1. The experimental work showed that the mean heat transfer coefficient of steam condensing on the inside of a horizontal tube is greatly influenced by the presence of NCG, the effect of NCG being pronounced at low NCG concentrations.
2. The smaller internal pipe diameter gave higher values of condensation heat transfer coefficients.
3. Lower inlet fluid temperature gave higher values of condensation heat transfer coefficients.
4. The integration of any of the heat transfer equations over the whole length of test section would require some knowledge of point of change over from sensible cooling (de-superheating) to condensation heat transfer mode.
5. In practice some condensation occurred in the sensible cooling (de-superheating) portion.
6. From the comparison of temperature profile predicted by Colburn and Hougen (1934) and experimental temperature profiles from the present work, is seen that the Colburn and Hougen (1934) method is satisfactory for initially saturated conditions but not for initially superheated conditions.

7. The pressure loss as predicted by methods of section 6.6 gave values that closely agreed with the experimental values. This shows that any more refinement in the model which would require more numerical work is not necessary. The assumption of global parameters used in the analysis was a fair compromise.
8. The error analysis gave the maximum error in the measurement of heat transfer as  $\pm 5\%$  and that of pressure drop in test section as  $\pm 8\%$ . To reduce these error ranges any further would require more accurate instrumentation and better control in the generation of steam, compressed air etc.

## 8.2 RECOMMENDATIONS

1. The work by Othmer (1929) showed that the condensation heat transfer coefficient decreased with an increase in temperature difference between the steam-NCG core and the tube wall. In this work no attempt was made to investigate this any further and any future work should investigate quantitatively the effect of this temperature difference as one of the variable.
2. Other workers investigating condensation of vapours inside enclosed conduits have shown quantitatively that factors like rippling and turbulence on the liquid vapour interface, the two phase flow patterns and tube inclination influence the rate of condensation. Further work should be done to determine the effect of these parameters quantitatively on condensation in the presence of NCG.
3. It is also necessary to formulate a model that would cater for superheated steam condensing in the presence of NCG as the Colburn and Hougen(1934) does not predict accurate results.

APPENDICES



## APPENDIX ONE

### SIZING OF THE EXPERIMENTAL RIG COMPONENTS

#### 1.1 GENERAL

The experimental rig consisted of the boiler, steam superheater, air heater, steam-air mixture and the test section. The isometric drawing of the rig lay out is presented as drawing number 1.

#### 1.2 STEAM GENERATOR

An existing steam generator was used. It was Speedylec type 236 from BASTIAN and ALLEN LTD, ENGLAND. It was an electrode boiler with a maximum rating of 0.01 kg/s and 10 bar. The output could be varied by means of a load selector switch from 0% to 100% of the full load.

#### 1.3 STEAM SUPERHEATER.

The steam used in the tests was required to be superheated or saturated at the inlet to the test section. a superheater with a variable heating capacity was used for this purpose. the set up used is as shown in Figure A1.3

Air was preheated by an electric heating element and then passed into the superheater consisting of a single shell and three tube passes. The steam flowed inside the tube while hot air flowed on the outside of the tube.

### Specification

Maximum steam mass flow rate	= 0.01 kg/s
Temperature of steam at the inlet to the superheater	= 95 °C.
Maximum temperature of steam required at the exit from the superheater	= 230 °C.
Maximum air mass flow rate	= 0.02 kg/s
Tube diameter	= 25.4 mm.
Tube material is copper.	

To ensure that the hot air heated up the whole steam tube, the air temperature at the exit should be at least 50 °C higher than that of incoming steam. Therefore the air temperature at the exit from the superheater should be 145 °C i.e. (95 + 50) °C.

Heat balance for the superheater:

$$\dot{m}_a c_{p,a} (t_{hi} - t_{ho}) = \dot{m}_g c_{p,g} (t_{co} - t_{ci}) \quad (A1.1)$$

Substituting the numerical values and solving for

$t_{hi}$ ;

$$0.02 \times 1.075 (t_{hi} - 145) = 0.01 \times 4.46 (230 - 95)$$

$$t_{hi} = 425 \text{ °C.}$$

Approximate air temperature at inlet to air heater is 20°C.

Power required by the air heater:

$$\begin{aligned}\dot{m}_a c_{p,a} \Delta t_a &= 0.02 \times 1.075 \times (425 - 20) \text{ kW} \\ &= 8.7 \text{ kW. (Say 9 kW)}\end{aligned}$$

The steam tubes were staggered at 250mm pitch centres to limit the height and width of the shell to 300mm by 300mm as Figure A1.2..

For staggered arrangement the correlations used to calculate the heat transfer coefficient are given by Özişik(1985) as:

$$Re_d = (dG_{max})/\mu \quad (A1.2a)$$

$$G_{max} = \rho u_{max} \quad (A1.2b)$$

$$u_{max} = \frac{(s_T/d)}{(s_T/d)-1} u_\infty \quad (A1.2c)$$

and  $u_\infty$  is the velocity at a point in the heat exchanger before the fluid enters the tube bank. Air was let into the tube bank through a pipe having an internal diameter of 25.4mm (1").

Mean bulk air temperature =  $(425+145)/2$  °C. = 285°C.

At this temperature and atmospheric pressure the properties of dry air are as below:

$$\rho = 0.616 \text{ kg/m}^3.$$

$$k = 4.357 \times 10^{-2} \text{ W/m-K.}$$

$$\mu = 2.849 \times 10^{-5} \text{ kg/ms.}$$

$$\text{Pr} = 0.680.$$

$$u_{\infty} = \frac{4 \dot{m}_a}{\rho \pi d^2} \quad (\text{A1.3})$$

substituting in the known numerical values and solving for

$u_{\infty}$ :

$$\begin{aligned} u_{\infty} &= (4 \times 0.02) / (0.616 \times \pi \times (0.0254)^2) \text{ m/s.} \\ &= 63.9 \text{ m/s.} \end{aligned}$$

From Equation A1.2c for  $u_{\text{max}}$ :

$$\begin{aligned} u_{\text{max}} &= 63.9 \times \left[ \frac{0.25/25.4 \times 10^{-3}}{(0.25/25.4 \times 10^{-3}) - 1} \right] \text{ m/s} \\ &= 71.2 \text{ m/s.} \end{aligned}$$

From Equation A1.2b, for  $G_{\text{max}}$ :

$$\begin{aligned} G_{\text{max}} &= (71.2 \times 0.616) \text{ kg/m}^2 \\ &= 43.8 \text{ kg/m}^2 \end{aligned}$$

From Equation A1.2a:

$$\text{Re}_d = (43.8 \times 25.4 \times 10^{-3}) / (2.849 \times 10^{-5}) = 39.08 \times 10^3.$$

$$\text{Nu}_d = h_m d / k = C_2 \text{Re}_d^m \text{Pr}^{0.36} \quad (\text{A1.4})$$

where  $C_2 = 0.35 s_T / s_D = 0.35 \times (0.25 / 0.25) = 0.35$ , making

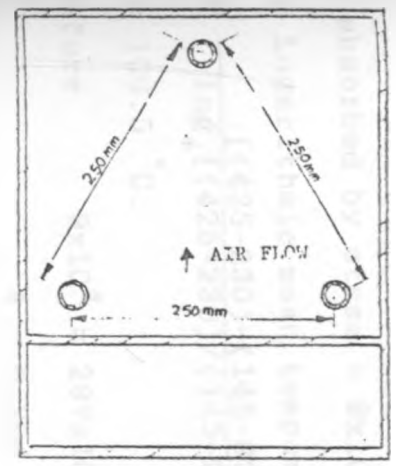
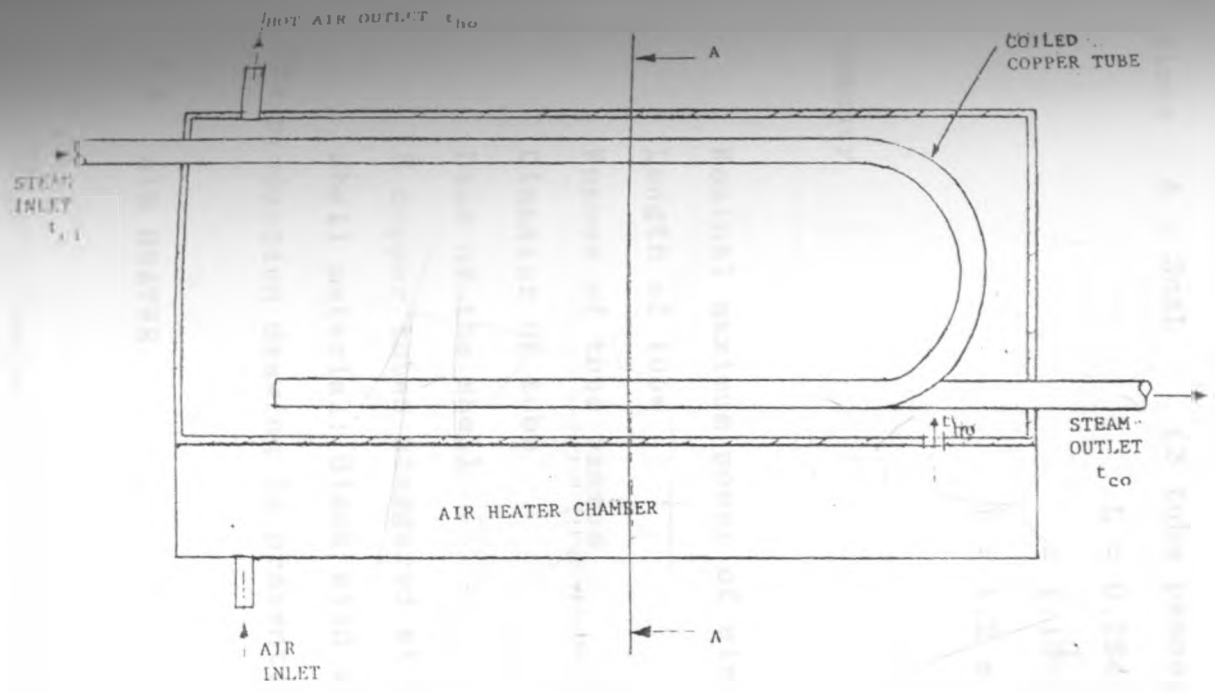
$$n = 0.6.$$

From Equation A1.4  $h_m$  becomes:

$$h_m = 0.35 \times (39.08 \times 10^3)^{0.6} \times 0.68^{0.36} \times 4.357 \times 10^{-2} / 25.4 \times 10^{-3}$$

$$= 297.4 \text{ W/m}^2\text{K.}$$

To estimate the total length of the tube L a heat balance is done:



SECTION A - A.

$$S_T = S_D = 250\text{mm}$$

FIGURE A1.1: SUPERHEATER

$$\text{Heat absorbed by steam} = 9 \times 10^3 = h_m A (\Delta t_m).$$

$\Delta t_m$  = Logarithmic mean temperature difference.

$$= \frac{[(425-230)-(145-95)]}{\log_e [(425-230)/(145-95)]} \text{ } ^\circ\text{C}.$$

$$= 106.5 \text{ } ^\circ\text{C}.$$

Therefore  $9 \times 10^3 = 297 \times 106.5 A.$

$$A = 0.284 \text{ m}^2.$$

Since  $A = 3\pi dL$  (3 tube passes).

$$L = 0.284 / (3 \times 25.4 \times 10^{-3} \times \pi) \text{ m}^2.$$

$$= 1.19 \text{ m}$$

$$L = 1.2 \text{ m}.$$

### Summary

Nominal maximum power of air heater = 9 kW.

Length of tube = 1200mm.

Number of tube passes = 3.

Diameter of tube = 25.4 mm.

Size of the shell = 1500mm x 300mm x 300mm.

3 copper tubes staggered at 250 mm pitch centres.

Shell material: Black mild steel.

The production drawing is presented as drawing number 2.

### 1.4 AIR HEATER.

The air heater is included to preheat the air to be mixed with steam to ensure that the steam dryness does not change significantly during the mixing process. The input

to electric element used was controlled by a variac transformer to give the desired heating range.

### Specifications

Maximum mass concentration of air in the mixture = 30%

Maximum flow rate of steam = 0.01kg/s.

Maximum temperature of air at the heater exit = 230°C.

Air temperature at the inlet to the heater = 20°C.

Maximum flow rate of air =  $0.01 \times [0.3 / (1 - 0.3)]$

= 0.0043 kg/s.

At maximum operating conditions, the mean bulk temperature of air is : 125°C i.e  $(230 + 20) / 2$ . The dry air properties at this temperature and atmospheric pressure are as below:

$$c_{p,a} = 1.0135 \text{ kJ/kg.}$$

The power of the element required =  $\dot{m}_a c_{p,a} (t_{out} - t_{in})$ .

$$= 0.0043 \times 1.0135 \times (230 - 20) \text{ kW.}$$

$$= 0.92 \text{ kW.}$$

A 1 kW. heating element is sufficient. The production drawing is presented as drawing number 3.

### 1.5 AIR- STEAM MIXER.

The objective of mixing is homogenization , manifesting itself in a reduction of concentration and temperature gradient within the chamber.

Mixing is therefore undertaken in order to attain an intimate mutual distribution of constituent materials.

The simplest and the cheapest way of mixing gases is in a pipe. If the gas mixture flows at sufficiently high speed, the effect of molecular diffusion is enhanced by turbulent diffusion. The mixer sized for this work was of type whereby preheated air was introduced through a nozzle into a flowing stream of steam.

#### Specifications

The lowest temperature used in the work was 99°C; the sizing was done for this condition as this is when rate of molecular diffusion is least.

Maximum mass flow rate of steam	=0.01 kg/s
Maximum mass flow rate of air	=0.0043 kg/s
Diameter of the air nozzle	=3 mm

The average value of mass transfer coefficient  $K_c$  in the nozzle mixer, according to Perry and Chilton (1973), is given by;

$$\frac{dK_c}{D} = 0.03 \left( \frac{\mu_a \rho_g d}{\mu_g} \right)^{0.88} Sc_g^{0.5} \quad (A1.6)$$



where  $d$  = Diameter of nozzle (m).

$D$  = Diffusivity ( $m^2/s$ ).

$u_a$  = Velocity of air at exit from the nozzle (m/s).

$\rho_g$  = Density of steam ( $kg/m^3$ ).

$\mu_g$  = Viscosity of steam ( $kg/ms$ ).

$Sc_g$  = Schimidt number of steam.

Properties of air at  $99^\circ C$  and at one atmosphere.

Density  $\rho_a = 0.8824 kg/m^3$ .

Properties of steam at  $99^\circ C$ . and at one atmosphere.

$\rho_g = 0.590 kg/m^3$ .

$\mu_g = 12 \times 10^{-6} kg/ms$

$k_g = 24.8 \times 10^{-3} W/m^2K$ .

$$D = D_o \left[ \frac{(t+273)}{273} \right]^n \quad (A1.7)$$

where  $D_o = 0.216 \times 10^{-4} m^2/s$  and  $n = 1.8$ .

substituting in the numerical values;

$$D = 0.216 \times 10^{-4} \times [(99+273)/273]^{1.8} m^2/s.$$

$$= 3.77 \times 10^{-5} m^2/s.$$

$$u_a = \frac{4 \dot{m}_a}{\pi d^2 \rho_a} \quad (A1.8)$$

substituting in the numerical values;

$$u_a = 4 \times 0.0043 / [(0.8824 \pi \times (3 \times 10^{-3})^2)] = 172 m/s.$$

Mass transfer coefficient  $K$  from Equation (A1.7) is given by:

$$K_c = 0.03 \left( \frac{172 \times 0.59 \times 3 \times 10^{-9}}{12 \times 10^{-6}} \right)^{0.88} \times \left( \frac{12 \times 10^{-6}}{0.59 \times 3.77 \times 10^{-5}} \right)^{0.5} \\ \times \left( \frac{3.77 \times 10^{-5}}{3 \times 10^{-9}} \right)$$

$$= 7.059 \text{ m/s.}$$

To accommodate the nozzle and to ease its installation, a tube diameter of 50.8mm(2") was chosen.

$$\text{Mole flow rate of steam} = 0.01/18.02 = 5.55 \times 10^{-4} \text{ kgmol/s.}$$

$$\text{Mole flow rate of air} = 0.0043/28.96 \\ = 1.485 \times 10^{-4} \text{ kgmol/s.}$$

$$\text{Mole fraction of air} = 0.21.$$

To estimate the mixing length required, it was assumed that at nozzle inlet the difference in concentration of steam at center line and wall equals the mass concentration of air in the mixture and after the mixing length,  $l$ , this difference dropped to zero. The surface area of mixing was based on the diameter of the perforated tube.

$$\text{density of mixture } \rho = \frac{1}{(0.3/0.8824) + (0.7/0.59)} \\ = 0.865 \text{ kg/m}^3.$$

In every 1 kg of steam-air mixture there is 0.3 kg of air and 0.7 kg of steam.

Concentration of air per  $m^3$  of mixture

$$\begin{aligned} &= \frac{0.3}{1/0.865} \text{ kg/m}^3 \text{ of mixture.} \\ &= 0.259 \text{ kg/m}^3 \text{ of mixture.} \end{aligned}$$

Setting mass balance of air over length  $l$ :

$$\dot{m}_a = K_c A (\Delta C_1 - \Delta C_2). \quad (\text{A1.9})$$

$$A = \pi d l \quad (\text{A1.10})$$

$$\Delta C_1 = 0.259 \text{ kg/m}^3.$$

$$\Delta C_2 = 0 \text{ kg/m}^3.$$

$$d_o = 12.5 \text{ mm.}$$

$$K_c = 7.059 \text{ m/s.}$$

$$\dot{m}_a = 0.0043 \text{ kg/s.}$$

Substituting and solving for  $l$ :

$$l = 0.0043 / (7.059\pi \times 12.5 \times 10^{-3} \times 0.259) = 131.7 \times 10^{-3} \text{ m.}$$

Length of 150mm is sufficient.

#### Summary

Diameter of the tube = 50.8mm.

Diameter of the nozzle = 3mm.

Diameter of the perforated tube = 12.5 mm.

Length of the perforated tube = 150mm.

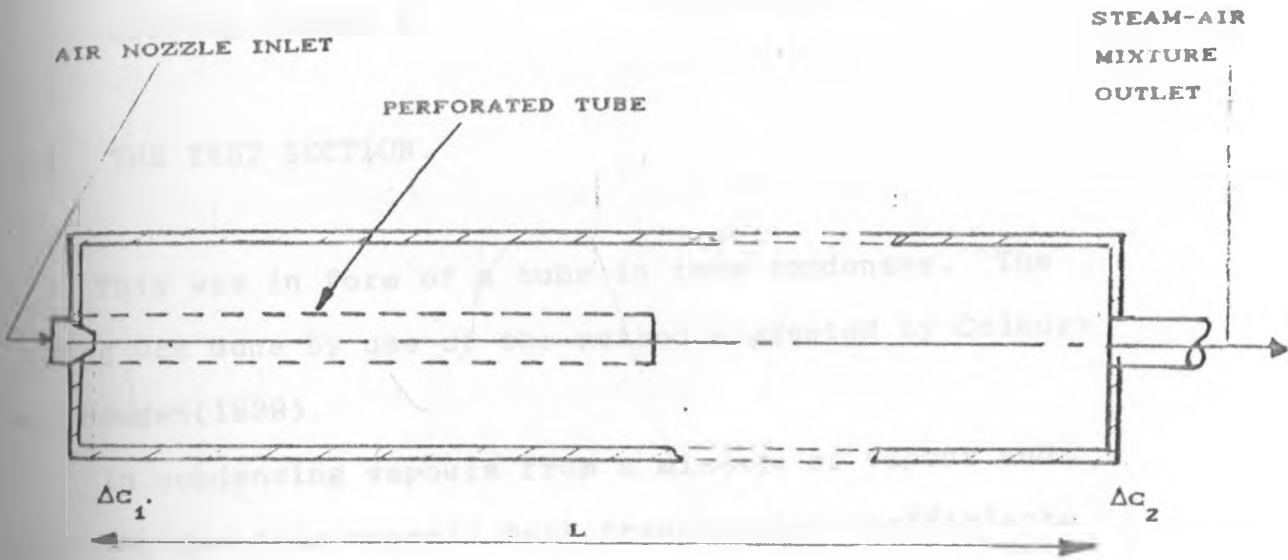


FIGURE A1.2: STEAM-AIR MIXER

Including a calming section of length 300mm, the total length of the air-steam mixture becomes equal to 450mm.

The production drawing of the mixture is presented as drawing number 4.

#### 1.6 THE TEST SECTION.

This was in form of a tube in tube condenser. The sizing was done by use of the method suggested by Colburn and Hougen(1939).

In condensing vapours from a mixture of vapour and NCG, the gas film overall heat transmission coefficients varied widely from point to point in the apparatus, and also the change in heat content of the gaseous mixture was proportional to the change in the temperature along the axial length. For these reasons no simple relationship expressing the mean temperature difference between the gas-vapour and cooling water stream could be used.

The method used for computing the surface area of the condenser was one in which values of  $(1/U\Delta t)$  were determined at sufficient number of points along the path of gas flow to permit calculation of a correct average value of  $(U\Delta t)$  by graphical integration. The average value of  $(U\Delta t)$  at any point in the test section was obtained through trial and error, by equating the heat transferred through

the condensate, the tube wall and the cooling water to the sum of the heat transferred by sensible cooling of the uncondensed gas the latent heat equivalent of the vapour transferred by diffusion and condensed. The necessary surface area was obtained by multiplying the heat transferred per unit time by integrated average value of  $(1/U\Delta t)$ .

The necessary heat transfer coefficients i.e of vapour, condensate film, fouling and cooling water were estimated by the methods of section 3.4. The computer program used for generating the temperature profiles of steam-air core along the axial length of the test section was used to size the test section by changing the program inputs from those of section 3.4 to the following:

1. The maximum and minimum mass flow rates of steam and air to be used,
2. The maximum and minimum mass flow rate of cooling water to be used, and then by varying the lengths and diameters of tube and shell, the flow rate of cooling water and its permissible temperature rise, the resulting temperature profiles were studied until reasonable compromise between the temperature profile, cooling water flow rate and corresponding temperature rises (i.e the temperature rise should not exceed  $60^{\circ}\text{C}$  where bubbling would interfere with the results) was

achieved.

### Specifications

Maximum cooling water mass flow rate = 0.5 kg/s.  
cooling water inlet temperature = 25°C.  
Maximum mass flow rate of steam = 0.01 kg/s.  
Maximum mass flow rate of air = 0.0043kg/s.  
(to give maximum air mass concentration of 30%).  
Maximum inlet temperature of the steam-air mixture.  
=230°C.

with these conditions as inputs to the computer program the best combination realized is as listed under summary:

### Summary

Tube length = 4000mm.  
Tube diameters = 25.4mm(1") and 38.1mm(1.5").  
Shell diameter = 76.2mm(3").  
The production drawing is presented as drawing number 5.

APPENDIX TWO.

PROPERTIES OF THE WORKING FLUIDS

2.1 THERMODYNAMIC AND TRANSPORT PROPERTIES OF DRY AIR.

Because of the use of computer programs to evaluate the data, it was necessary to fit the properties of dry air extracted from the tables by Rogers and Mayhew(1987) by polynomial regression of order 3. The resulting equations are as presented below, covering the temperature range 0-300 °C

Specific heat capacity at constant pressure(  $c_p$  ).

$$c_p = \sum_{i=0}^{i=3} A_i t^i. \quad (A2.1)$$

$c_p$  [kJ/kg] and  $t$  [°C] .

$$A_0 = 1.0039, A_1 = 0.22895 \times 10^{-4}, A_2 = 0.45159 \times 10^{-6},$$

$$A_3 = -0.24151 \times 10^{-9}.$$

Viscosity ( $\mu$ ).

$$\mu = \sum_{i=0}^{i=3} B_i t^i \times 10^{-5} \quad (A2.2)$$

$\mu$  [ kg/ms ] and  $t$  [ °C ].

$$B_0 = 1.716, B_1 = 0.49347 \times 10^{-2}, B_2 = -0.38290 \times 10^{-5},$$

$$B_3 = 0.2789 \times 10^{-8}$$



Thermal conductivity (k).

$$k = \sum_{i=0}^{i=3} C_i t^i \times 10^{-5} \quad (\text{A2.3})$$

k [ kW/m-K ] and t [ °C ].

$$C_0 = 2.413, C_1 = 0.78584 \times 10^{-2}, C_2 = -0.37978 \times 10^{-5},$$

$$C_3 = 0.1487 \times 10^{-8}.$$

Density ( $\rho$ ):- Use is made of perfect gas equation.

$$\rho = p/RT \quad (\text{A2.4})$$

$\rho$ [kg/m<sup>3</sup>], p[N/m<sup>2</sup>], T[K] and R = 287.1 [J/kg-K].

## 2.2 THERMODYNAMIC AND TRANSPORT PROPERTIES OF SATURATED WATER, SATURATED STEAM AND SUPERHEATED STEAM AT STANDARD ATMOSPHERIC PRESSURE.

The regression equations presented are based on tables by Rogers and Mayhew (1987). The temperature range is 0-300°C.

### 2.2.1 SATURATED WATER.

Specific heat capacity at constant pressure ( $c_{pf}$ ).

$$c_{pf} = \sum_{i=0}^{i=3} A_i t^i \quad (\text{A2.5})$$

$c_{pf}$  [J/kg-K] and t [ °C ].

$$A_0 = 1855.9, A_1 = 1.01299, A_2 = -0.01147,$$

$$A_3 = 0.162415 \times 10^{-3}.$$

Viscosity ( $\mu_f$ )

$$\mu_f = \left[ \sum_{i=0}^{i=2} B_i t^i \right]^{-1} \times 10^{-6} \quad (\text{A2.6})$$

$\mu_f$  [ kg/m s ] and  $t$  [ °C ].

$$B_0 = 0.435509 \times 10^{-9}, \quad B_1 = 0.282519 \times 10^{-4},$$

$$B_2 = 0.34405 \times 10^{-7}$$

Thermal conductivity ( $k_f$ ).

$$k_f = \sum_{i=0}^{i=3} C_i t^i. \quad (\text{A2.7})$$

$k_f$  [ W/m<sup>2</sup> ] and  $t$  [ °C ].

$$C_0 = 0.56903, \quad C_1 = 1.865 \times 10^{-9}, \quad C_2 = -0.7998 \times 10^{-5},$$

$$C_3 = 0.5256 \times 10^{-8}$$

Density ( $\rho_f$ ).

$$\rho_f = \left[ \sum D_i t^i \right]^{-1}. \quad (\text{A2.8})$$

$\rho_f$  [ kg/m<sup>3</sup> ] and  $t$  [ °C ].

$$D_0 = 1 \times 10^{-9}, \quad D_1 = 0.000, \quad D_2 = 3.87 \times 10^{-9}.$$

### 2.2.2 SATURATED STEAM.

Saturation pressure ( $p_s$ ).

$$p_s = \sum_{i=0}^{i=3} A_i t^i + \frac{A_4}{t+273}. \quad (\text{A2.9})$$

$p_s$  [ bar ] and  $t$  [ °C ].

$$A_0 = 0.17372, \quad A_1 = 6.2861 \times 10^{-5}, \quad A_2 = 36.7147 \times 10^{-8},$$

$$A_3 = 61.568 \times 10^{-11}, \quad A_4 = 48.764.$$

Specific heat capacity at constant pressure ( $c_{pg}$ ),

$$c_{pg} = \sum_{i=0}^{i=3} B_i t^i \quad (A2.10)$$

$$c_{pg} \text{ [J/kgK]} \quad \text{and} \quad t \text{ [}^\circ\text{C]}.$$

$$B_0 = 1845.7, \quad B_1 = 4.7559, \quad B_2 = -0.1230,$$

$$B_3 = 1.3507 \times 10^{-3}.$$

Viscosity ( $\mu_g$ ),

$$\mu_g = \sum_{i=0}^{i=3} C_i t^i \quad (A2.11)$$

$$\mu_g \text{ [} \times 10^6 \text{ kg/ms]} \quad \text{and} \quad t \text{ [}^\circ\text{C]}.$$

$$C_0 = 8.5038, \quad C_1 = 0.0323, \quad C_2 = 0.4196 \times 10^{-4},$$

$$C_3 = -0.1212 \times 10^{-6}.$$

Thermal conductivity ( $k_g$ ),

$$k_g = \sum_{i=0}^{i=3} D_i t^i \quad (A2.12)$$

$$k_g \text{ [W/m-K]} \quad \text{and} \quad t \text{ [}^\circ\text{C]}.$$

$$D_0 = 0.01617, \quad D_1 = 0.09407 \times 10^{-3}, \quad D_2 = -0.2434 \times 10^{-6},$$

$$D_3 = 0.1542 \times 10^{-7}.$$

Density ( $\rho_g$ )

$$\rho_g = \left[ \sum_{i=0}^{i=3} E_i t^i \times (100p)^{-1} \right]^{-1} \quad (A2.13)$$

$\rho_g$  [ kg/m<sup>3</sup> ] , p [bar] and t [ °C ].

$$E_c = 126 , E_1 = 0.433 , E_2 = 441 \times 10^{-6} , E_3 = -3.9 \times 10^{-6} .$$

Latent heat of vapourisation (  $h_{fg}$  ).

$$h_{fg} = \sum_{i=0}^{i=3} F_i t^i . \quad (A2.14)$$

$h_{fg}$  [J/kg] and t [ °C ].

$$F_0 = 2501500 , F_1 = -2433.5 , F_2 = 1.8339 , F_3 = 0.018616 .$$

### 2.2.3 SUPERHEATED STEAM.

Enthalpies h [kJ/kg] at pressures of 0.006112 bar, 0.01 bar, 0.05 bar, 0.1 bar, 0.5 bar, 0.75 bar and 1 bar can be expressed in the form:

$$h = \sum_{i=0}^{i=3} A_i t^i \quad (A2.15)$$

where t is in [ °C ].

Using polynomial regression of order 3 to fit properties of superheated steam from Rogers and Mayhew(1987) at different pressures ,the resulting constants are presented in Table A2.1.

The numerical values of the constants at the various pressures are tabulated below:

Table A2.1: REGRESSION COEFFICIENTS.

PRESSURE (bar)	$A_0$	$A_1$	$A_2$	$A_3$
0.006112	2611.61	-4.0556	$0.01367 \times 10^2$	$-0.2493 \times 10^{-1}$
0.01	2460.25	23.789	$-0.2282 \times 10^2$	$0.4013 \times 10^{-2}$
0.1	2495.92	19.308	$-0.1979 \times 10^2$	$0.6921 \times 10^{-3}$
0.5	2499.36	18.778	$-0.1140 \times 10^2$	$0.6902 \times 10^{-3}$
0.75	2500.82	18.856	$-0.1095 \times 10^2$	$0.8072 \times 10^{-3}$
1.0	2500.99	18.814	$-0.7926 \times 10^2$	$0.7430 \times 10^{-3}$

Density ( $\rho_g$ ). [Rogers and Mayhew (1987)]

$$\rho_g = \frac{130}{0.3 p(h - 1943)} \quad (A2.16)$$

$\rho_g$  [ kg/m<sup>3</sup> ] , p [bar] and h [kJ/kg] .

### 2.3.1 RECOGNITION OF A PERFECT GAS MIXTURE.

If a mixture is a perfect gas mixture, the contribution to the potential energy due to collisions (i.e interactions) between both like and unlike molecules must be negligible.

The reduced pressure  $p_{r,i}$  and the reduced temperature  $T_{r,i}$  are defined as:

$$p_{r,i} = \frac{p_i}{p_{c,i}} \quad (A2.17)$$

$$T_{r,i} = \frac{T_i}{T_{c,i}} \quad (A2.18)$$

where  $p_{c,i}$  and  $T_{c,i}$  are the critical pressure and temperature respectively.

For a mixture to be perfect, it is necessary that the reduced state of each of its constituents fall within the perfect gas region as shown on Figure 2.2. Defining the effective critical properties and reduced states of the mixture as below:

$$p_{c,m} = \sum_{i=1}^{i=I} y_i p_{c,i} \quad (A2.19)$$

$$T_{c,m} = \sum_{i=1}^{i=I} y_i T_{c,i} \quad (A2.20)$$

$$p_{r,m} = \frac{p_T}{p_{c,m}} \quad (A2.21)$$

$$T_{r,m} = \frac{T}{T_{c,m}} \quad (A2.22)$$

where  $I$  = the number of constituents in the mixture .

$y_i$  = the mole fraction of the  $i^{\text{th}}$  constituent.

$p_{r,m}$  and  $T_{r,m}$  are reduced mixture pressure and temperature respectively.

The steam-air mixture least likely to be perfect, is the one in which mass concentration of air is 30%.

Calculating its critical properties :

Molecular mass of air = 28.96 kg/kgmol.

Molecular mass of steam = 18.02 kg/kgmol.

Critical temperature of air = 149.9 K.

Critical temperature of steam = 647.1 K.

Critical pressure of air = 44.7 bar.

Critical pressure of steam = 220.5 bar.

Considering 1kg mass of the mixture(0.3kg of air and 0.7kg of steam), then:

Number of moles of air  $N_a = 0.3/28.96 = 0.0104$  Moles.

Number of moles of steam  $N_g = 0.7/18.02 = 0.0388$  Moles.

Mole fraction of air  $Y_a = 0.0104/(0.0104+0.0388) = 0.211$ .

Mole fraction of steam  $Y_g = 1-0.211=0.789$ .

From Equations A2.19 and A2.20:

$$T_{c,m} = 0.211 \times 149.9 + 0.789 \times 647.1 = 542.2 \text{ K.}$$

$$P_{c,m} = 0.211 \times 244.7 + 0.789 \times 220.5 = 183.4 \text{ bar (181.0 atm.)}$$

$$\text{Partial pressure of air } p_a = 0.211 \times 1.01325 = 0.214 \text{ bar.}$$

$$\text{Partial pressure of steam } p_g = 1.01325 - 0.214 = 0.799 \text{ bar.}$$

From Equations A2.17 and A2.18 and A2.22 the reduced states for air and steam and the mixture are:

$$\text{For air } p_{r,a} = 0.214/44.7 = 4.78 \times 10^{-3}.$$

$$T_{r,a} = (273+100)/149.9 = 2.49.$$

$$\text{For steam } p_{r,g} = 0.799/220.5 = 3.62 \times 10^{-3}.$$

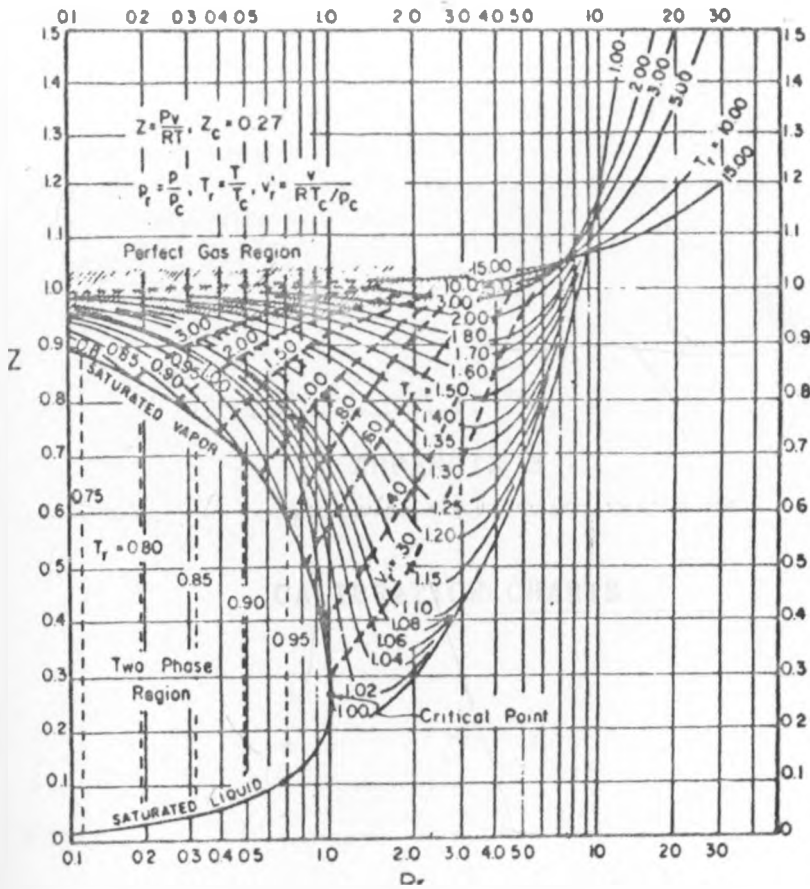
$$T_{r,g} = (100+273)/647.1 = 0.576.$$

$$\text{For the mixture } p_{r,m} = 1.01325/183.4 = 5.52 \times 10^{-3}.$$

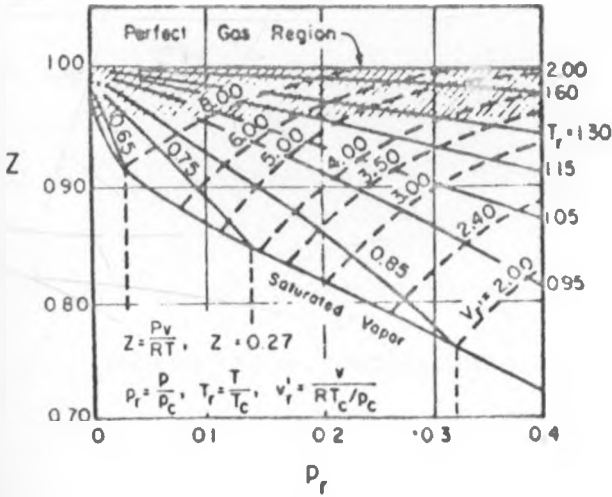
$$T_{r,m} = (100+273)/542.2 = 0.688.$$

From Figures A2.2, it is seen that all the reduced states fall within the perfect gas region hence justifying the application of perfect gas equations in this work.





a) INTERMEDIATE AND HIGH PRESSURE REGION

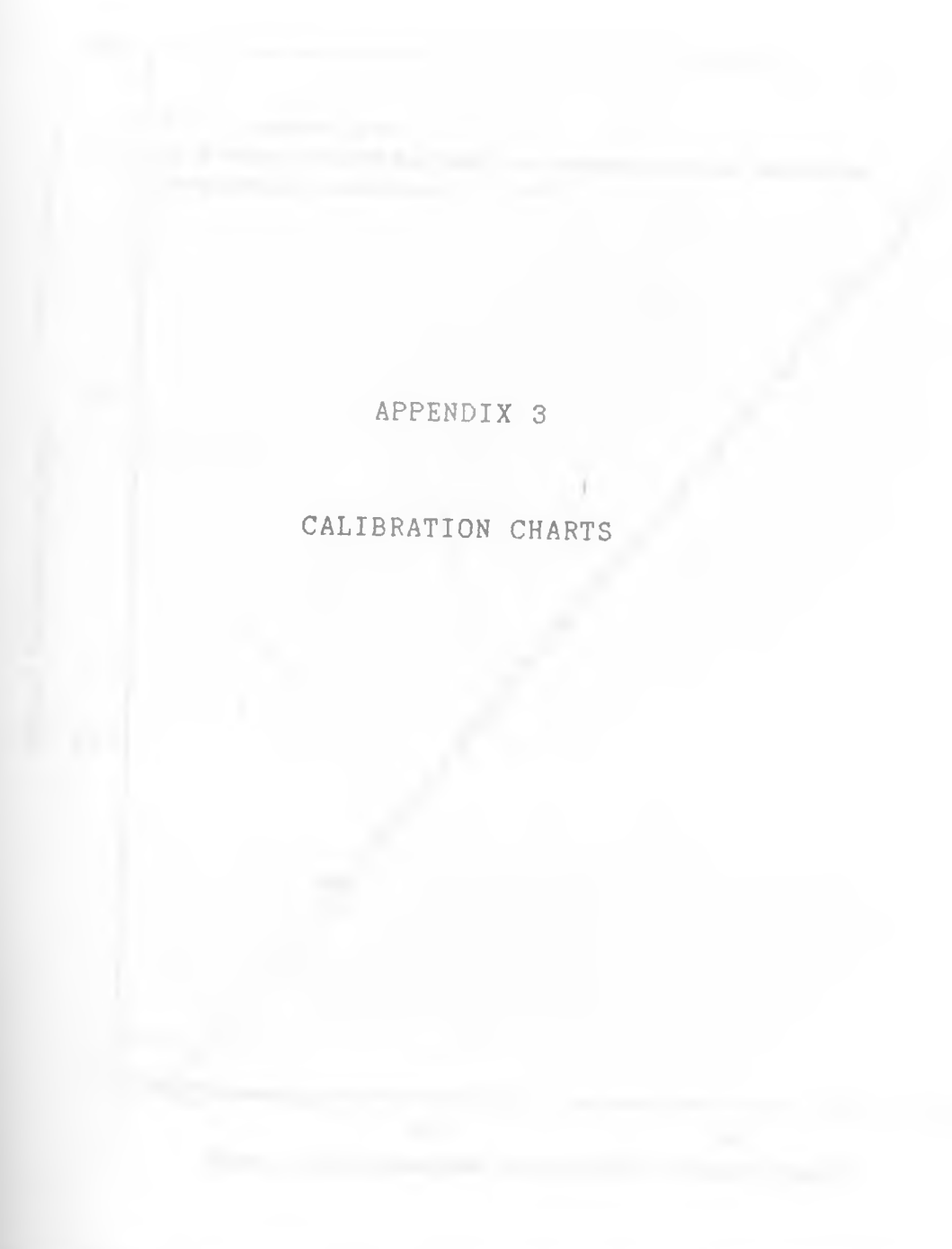


b) LOW PRESSURE REGION

FIGURE A2.1: GENERALIZED COMPRESSIBILITY CHART SONNTAG et al (1971)

APPENDIX 3

CALIBRATION CHARTS



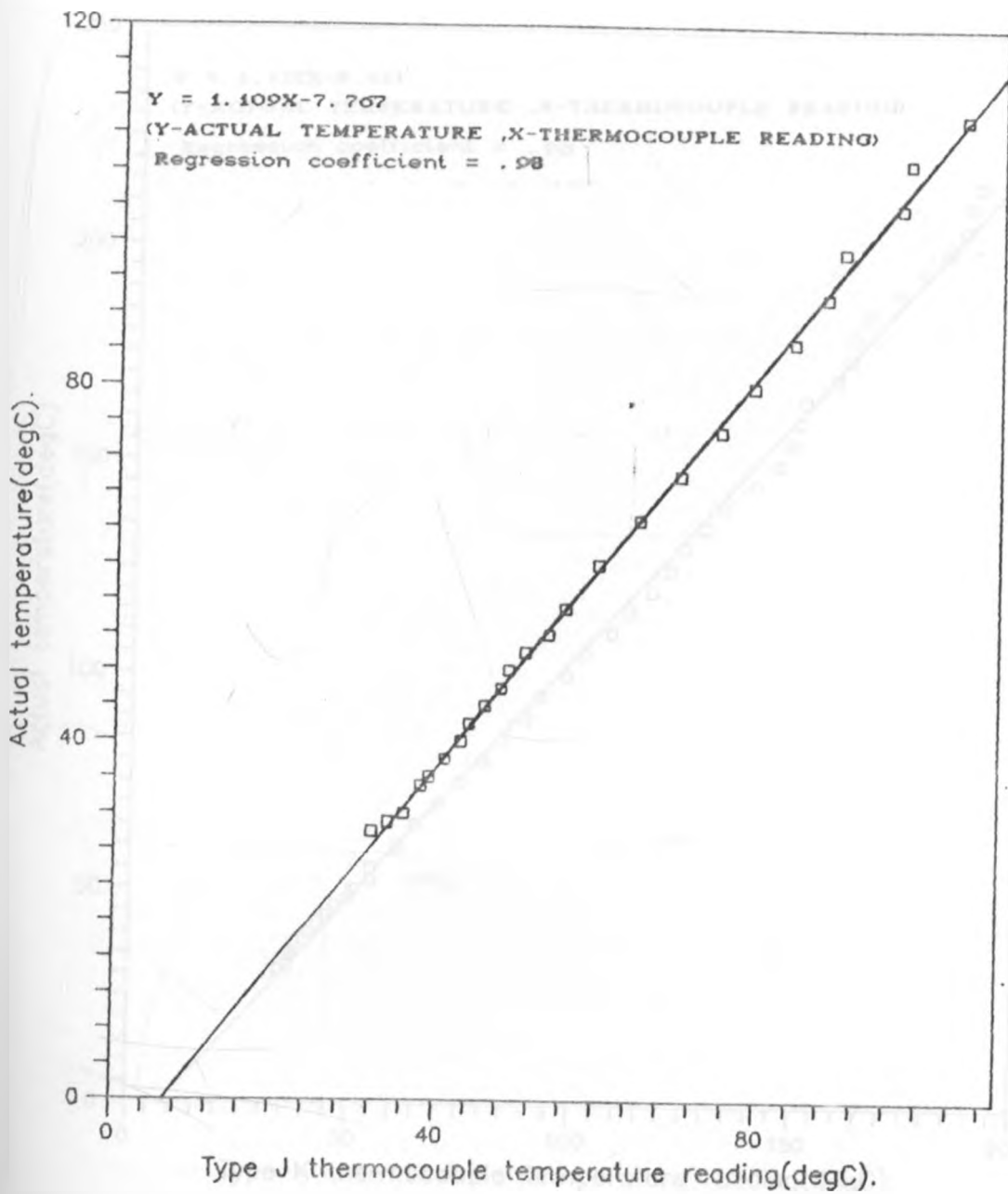


FIGURE A3.1: CALIBRATION CURVE FOR TYPE J THERMOCOUPLE

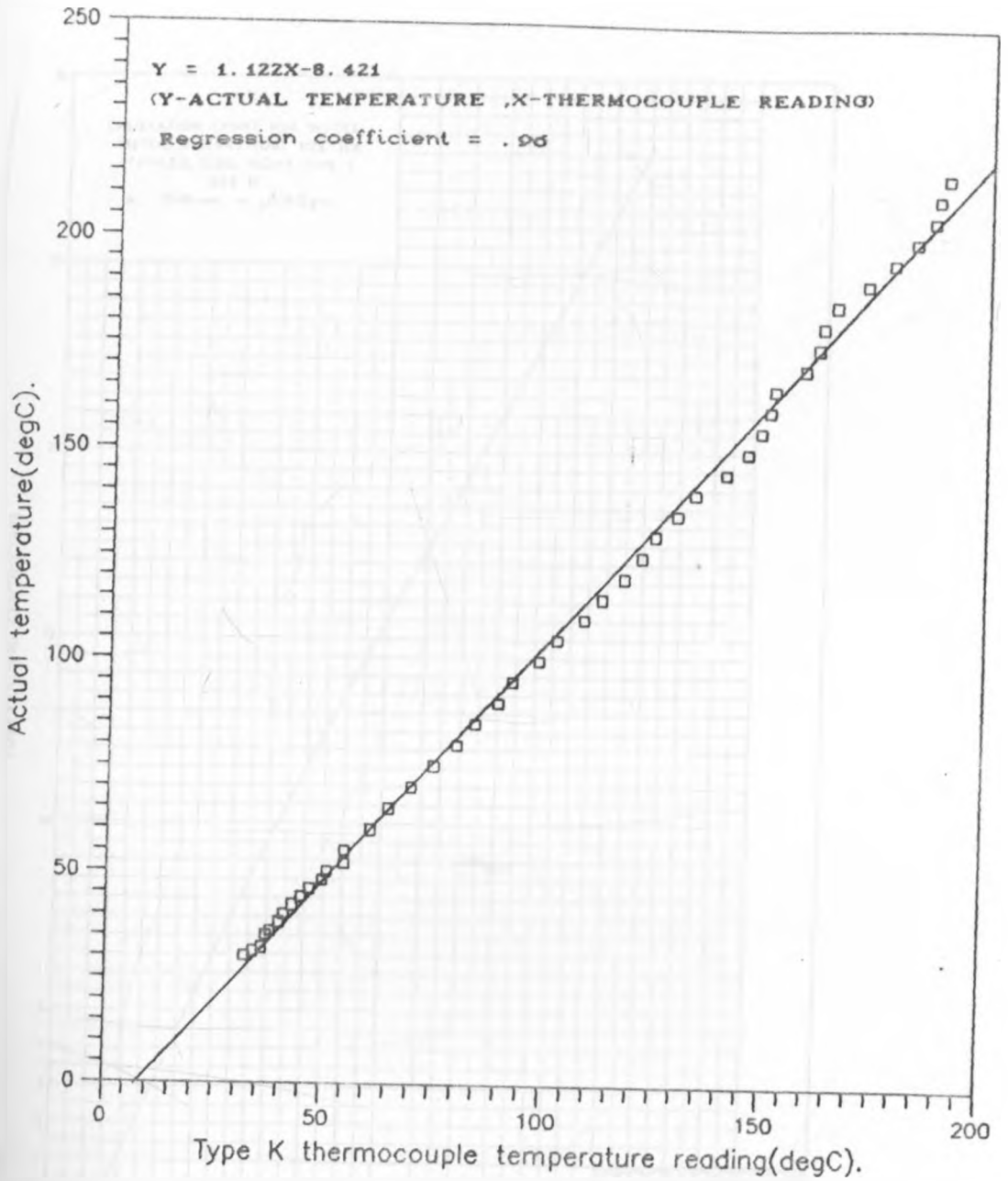


FIGURE A3.2: CALIBRATION CURVE FOR TYPE J THERMOCOUPLE

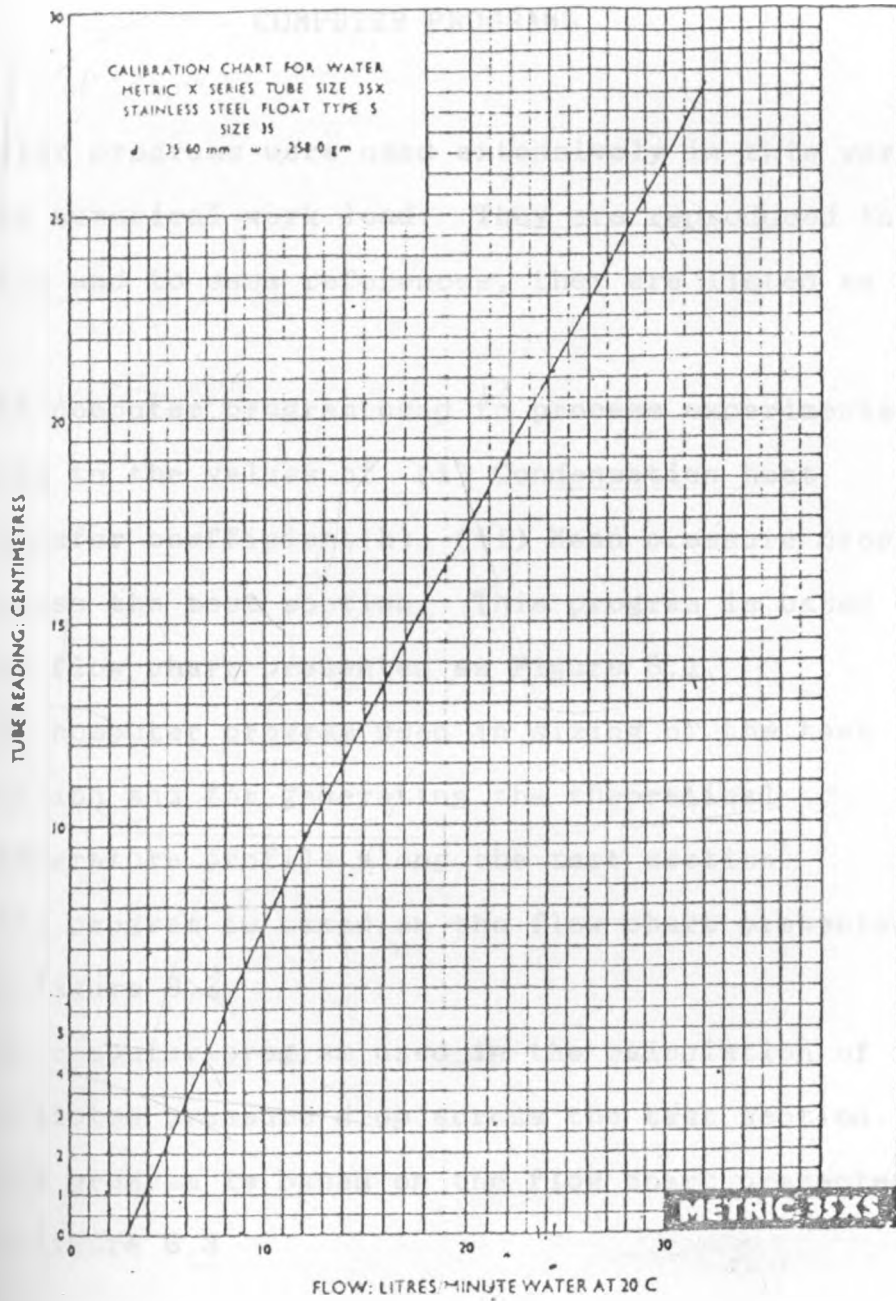


FIGURE A3.3: CALIBRATION CURVE FOR COOLING WATER ROTAMETER

## APPENDIX FOUR.

### COMPUTER PROGRAMS

Computer programs were used extensively in this work to ease the numerical work load. They are reproduced in this section and to ease references, they are listed as follows:

- 4.1- The computer program used to process experimental data to the values of (i) Condensation heat transfer coefficient(h) (ii) Mean pressure drop across the test section. This program is based on the flow chart presented as Figure 6.1.
- 4.2- The computer program used in sizing of the test section and for generating the theoretical temperature profile along the test section. This program is based on the flow chart presented as Figure 6.2.
- 4.3- The computer program used in the calculation of the predicted pressure drop across the test section. This program is based on the flow chart presented as Figure 6.3

APPENDIX 4.1

```
C WRITTEN BY ALFRED ONG'IRO
C
C PROG TO CALCULATE THE HEAT TRANSFER COEFFICIENT OF
C CONDENSATION OF PURE STEAM ,STEAM WITH VARIOUS
C CONCENTRATION OF AIR
C DIMENSION A(5,10)
WRITE(*,*) 'INPUT VALUE OF AMBIENT TEMP (T4 DEG C)'
READ(*,*) T4
2  IMAT=1
    IMAT=1
    S1=0
C TO INITIALISE THE MATRIX
DO 3 L1=1,5
DO 4 L2=1,10
A(L1,L2)=0.0
4 CONTINUE
3 CONTINUE

WRITE(*,*) 'HOW MANY SETS OF DATA N5'
READ(*,*) N5
WRITE(*,*) 'INPUT MN=3 IF VOL. FLOW RATE OF AIR IS NOT ZERO'
READ(*,*) MN
IF ( MN.EQ.3) GOTO 6
WRITE(*,*) 'INPUT NO. OF CONDENSATE MASS READINGS TAKEN N1'
READ(*,*) N1
R1=0
DO 5 I=1,N1
WRITE(*,*) 'INPUT MASS OF COND. (CM LBS)'
READ(*,*) CM
WRITE(*,*) 'INPUT TIME INTERVAL OF COLLECTION IN MINUTES(TMIN),'
WRITE(*,*) 'AND IN SECONDS (TSEC)'
READ(*,*) TMIN,TSEC
CMM=CM*0.4536/((TMIN*60)+TSEC)
R1=R1+CMM
5 CONTINUE
ACF=R1/N1
GOTO 7
6 WRITE(*,*) 'INPUT MASS FLOWRATE OF CONDENSATE (ACF KG/S)'
READ(*,*) ACF
7 WRITE(*,*) 'INPUT VALUE OF TUBE DIA(D IN ),LENGTH(RL IN ),'
WRITE(*,*) 'THICKNESS (TH IN )'
READ(*,*) D,RL,TH
WRITE(*,*) 'INPUT THERMAL CONDUCTIVITY OF TUBE (TK W/M K)'
READ(*,*) TK

DO 70 J= 1,N5
INPUT OF VARIOUS READING AT THE START OF THE EXPERIMENT
WRITE(*,*) 'INPUT VOLUME FLOW RATE OF AIR ( VAIR L/MIN )'
```

```
READ(I,I) VAIR
WRITE(I,I) 'INPUT WATER ROTAMETER READING (VROT CM )'
READ (I,I) VROT
WRITE(I,I)'INPUT COOLING WATER INLET TEMP.(TIN DEG F)'
WRITE(I,I) 'INPUT COOLING WATER OUTLET TEMP. (TOUT DEG F)'
READ(I,I) TIN ,TOUT
WRITE(I,I)'INPUT COND PRESSURE (P MM HG )'
READ(I,I) P
      S1=S1+P

C   READ(I,I) N1
C       R1=0
C   DO 10 I=1,N1
C   WRITE(I,I)'INPUT MASS OF CONDENSATE (CM LBS )'
C   READ(I,I) CM

C
C   WRITE(I,I) 'INPUT TIME INTERVAL OF COLLECTION IN MINUTES (TMIN)'
C   WRITE(I,I)'AND IN SECONDS TSEC '
C   READ(I,I) TMIN,TSEC
C       CMM =CM * 0.4536/((TMIN*60 )+TSEC)
C       R1 =R1 + CMM

C
C 10 CONTINUE
C       ACF= (R1/N1)
C   WRITE(I,I)' INPUT VALUE OF TUBE DIA (D IN), LENGTH (RL IN),'
C   WRITE(I,I) 'TUBE THICKNESS ( TH IN) '
C   READ(I,I) D ,RL ,TH
C   WRITE(I,I)'INPUT VALUE OF STEAM TEMP. AT CONDENSER INLET(TINP C)'
C   READ(I,I) TINP
C       TINPUT = (1.141 *TINP )-9.385
C       D1=D*(25.4E-03)
C       RL1=RL*(25.4E-03)
C       TH1=TH*(25.4E-03)

C   TO AVERAGE TUBE WALL TEMP. AND STEAM-AIR TEMPS.
C   WRITE(I,I)'INPUT NO. OF WALL TEMP. TAKEN N2 '
C   READ(I,I) N2
C       R2 =0
C   DO 20 J5=1,N2
C   WRITE(I,I)'INPUT WALL TEMP. (TWL DEG C )'
C   READ(I,I) TWL

C
C       TWALL= 1.124*TWL -7.791
C       R2 =R2 + TWALL

C 20 CONTINUE
C   AT2=R2/N2
C   WRITE(I,I)'INPUT NUMBER OF STEAM AIR TEMP. TAKEN N3'
C   READ(I,I)N3
C       R3=0
C   DO 30 K=1,N3
C   WRITE(I,I)'INPUT TEMP. OF STEAM AIR (TST DEG,C)'
C   READ(I,I)TST
C       TSTEAM= 1.141*TST-9.385
C       R3=R3+TSTEAM
```



```
30 CONTINUE
   AT3=(R3+TINPUT)/(N3+1)
   DTEMP1=(TOUT-TIN)*5/9
   DWTEMP=((TOUT+TIN)/2-32)*5/9
   T=DWTEMP
   CPW1=((0.162415E-09)*(T**3))+((-0.114716E-04)*(T**2))
   CPW2=((0.101299E-02)*T)+1.8559
   CPW=CPW1+CPW2
   WFR=(1.0361VR01)+2.156
   SPV1=((.206136E-09)*(T**3))+(.291365E-06)*(T**2))
   SPV2=((.12855E-04)*T)+(.998852E-01))
   SPV=SPV1+SPV2
   DENSW=(1/SPV)*(100)
   WMFR=WFR*DENSW /60
C   HEAT REMOVED BY COOLING WATER IS QTOT
   QTOT=WMFR*CPW*DTEMP1
   AREA=3.14*D1*RL1
C   TO CORRECT FOR ACTUAL TEMP. INSIDE THE TUBE
C   WRITE(*,*) 'INPUT THERMAL CONDUCTIVITY OF COPPER (TK W/MK)'
C   READ(*,*)TK
   TCCORR=(QTOT*TH1)/(TK*AREA)
C   WRITE(*,*) 'AREA = ',AREA
C   WRITE(*,*) 'THICKNESS = ',TH1
C   WRITE(*,*) 'CONDUCTIVITY = ',TK
C   WRITE(*,*) 'TOTAL HEAT TRANSFERED = ',QTOT
C   WRITE(*,*) 'CORRECTED TEMPERATURE = ',TCCORR
   DTEMP=(AT3-AT2)-TCCORR
C   TO CALCULATE MASS FLOW RATE OF AIR,VOLUME FLOW RATE OF STEAM,
C   VOLUME AND MASS CONCENTRATION OF AIR OVER TOTAL VOLUME AND MASS
C   OF MIXTURE
   VFS1=VAIR/60000
   T2=TINPUT

   DENA1=((-.118161E-07)*(T4**3))+(.107355E-04)*(T4**2))
   DENA2=((-.439621E-02)*T4)+1.28947
   DENA=DENA1+DENA2
   VS1=(121.05+(.6325*T2))
   VS2=(1.296E-03)*(T2**2)

   DENS=100/(VS1-VS2)
   WRITE(*,*) 'SPECIFIC VOLUME OF STEAM=',1/DENS,'M^3/KG'
   VFS=ACF/DENS
   VCON=(VFS1/(VFS1+VFS))*100
   FMA=VFS1*DENA
   CGN=(FMA/(FMA+ACF))*100
C
C   CALCULATE CONDENSATION HEAT TRANSFER COEFFICIENT (H W/M^2 K)
   H=QTOT/(AREA*DTEMP)
C   PRINTING RESULTS ON SCREEN OR IN A FILE
C   TO INITIALISE MATRIX MEMORY
   WRITE(*,*)IMAT
   L=IMAT
   A(L,1)=L
   A(L,2)=TINPUT
   A(L,3)=AT3
   A(L,4)=CON
   A(L,5)=VCGN
```

```
A(L,6)=AT2  
A(L,7)=WMFR /1000  
A(L,8)=TCORR  
A(L,9)=DTEMP  
A(L,10)=H  
IMAT =IMAT+1
```

```
70 CONTINUE  
PAVG=S1/N5  
WRITE(*,*) 'MEAN LOSS OF PRESSURE IN COND (mmWG) ='  
WRITE(*,75) PAVG  
75 FORMAT(38X,F6.2)  
DO 80 L5=1,10  
WRITE(*,90)(A(L4,L5),L4=1,5)  
90 FORMAT(2X,6(F10.2,1X)//)  
80 CONTINUE  
WRITE(*,*) 'MASS FLOWRATE OF CONDENSATE =',ACF,'KG/S'  
WRITE(*,*) 'IF YOU WANT ANOTHER RUN TYPE 2'  
WRITE(*,*) 'INPUT IKZ'  
READ(*,*)IKZ  
IF(IKZ.EQ.2) GO TO 2  
END
```

APPENDIX 4.2

C PROG. TO PREDICT TEMP. OF STEAM -AIR MIXTURE ALONG LENGTH OF  
C THE TEST SECTION(TUBE IN TUBE CONDENSER)

C WRITTEN BY ALFRED ONGIRO

C TO INPUT DATA FIRST

```
REAL A  
DIMENSION A(1000,1)  
WRITE(0,0)'INPUT THE FOLLOWING'  
WRITE(0,0)'MASS FLOWRATE OF STEAM FMS Kg/s '  
READ(0,0) FMS  
WRITE(0,0)'MASS CONCENTRATION OF AIR CON '  
READ(0,0) CON  
WRITE(0,0)'COOLING WATER FLOWRATE WMF Kg/s'  
READ(0,0) WMF  
WRITE(0,0)'COOLING WATER INLET TEMP TWI degC'  
READ(0,0) TWI  
WRITE(0,0)'COOLING WATER OUTLET TEMP. TWO DEG C '  
READ(0,0) TWO  
WRITE(0,0)'STEAM-AIR TEMP. AT INLET TCIN DEG.C'  
READ(0,0) TCIN  
WRITE(0,0)'STEAM-AIR TEMP. AT OUTLET TCOUT DEG.C'  
READ(0,0) TCOUT  
WRITE(0,0)'TOTAL PRESSURE IN TEST SECTION PT. BAR'  
READ(0,0) PT  
WRITE(0,0)'TUBE LENGTH TL (IN)'  
READ(0,0) TL  
WRITE(0,0)'TUBE DIAMETER DIA. (IN)'  
READ(0,0) DIA  
WRITE(0,0)'TUBE THICKNESS TH. (IN)'  
READ(0,0) TH  
WRITE(0,0)'SHELL DIAMETER SD. (IN)'  
READ(0,0) SD  
WRITE(0,0)'NO. OF AIR-STEAM TEMP. CONSIDERED N '  
READ(0,0) N
```

C  
C CALCULATE THE HEAT TRANSFERED  
C

```
DE=((SD**2)-(DIA**2))*0.5  
AREA=3.14*(DIA**2)*(0.0254**2)/4  
GO TO 700
```

800 WRITE(0,0)'DIKE '

C  
C CALCULATE INLET AND OUTLET TEMP.OF AIR-STEAM MIXTURE IN TEST  
C SECTION ASSUMING SATURATION CONITIONS  
C

GO TO 850

900 WRITE(0,0)'PIKE '

GO TO 930

950 WRITE(0,0)'LIKE '

C  
C CALCULATE THE INTERFACE TEMP.

$$DT=(TCIN-TCOUT)/(N-1)$$

```
CU=382
HP=CU/(TH*0.0254)
HDW=5000
HDS=11100
E1=((SD*SD)-(DIA*DIA))
E=E1*0.5
DE1=E*0.0254
GF=4*CFW/(3.14*DE1*DE1)
DIA1=DIA*0.0254
AREA=3.14*DIA1*DIA1/4
MIN=1
NO=1
MO=1
MINE=1
TGI=TCIN
TCI=TGI-40
TCI1=TCI+1
FNGI=FNG
TF=TWO
99  WRITE(*,*) 'TRYING A FRESH VALUE'
    WRITE(*,*) 'TGI=',TGI
    WRITE(*,*) 'TCI=',TCI
    WRITE(*,*) 'FNGI=',FNGI
    WRITE(*,*) 'TF=',TF
    JICK=1
100 WRITE(*,*) 'CONT'
    WRITE(*,*) 'TRYING NEW VALUE OF TCI'
    WRITE(*,*) 'TGI=',TGI
    WRITE(*,*) 'TCI=',TCI
    G=((FNGI*18.02)+(FNA*28.96))/AREA
    GO TO 620
630  WRITE(*,*) 'ERROR'
    PAI=PT-PGI
    FNGI=PGI*FNA/PAI
    G=((FNGI*18.02)+(FNA*28.96))/AREA
    GRAN=G*AREA
    WRITE(*,*) 'G,GRAN=',G,GRAN
    WRITE(*,*) 'WMF,CWF=',WMF,CWF
    GO TO 640
650  WRITE(*,*) 'TERR'
    SLHS1=HS7*(TGI-TCI)
    SLHS2=F*18.02*HF6
    SLHS3=(PGI-PCGI)*1E5
    SLHS=SLHS1+(SLHS2*SLHS3)
    RHS=HO*(TCI-TF)
    SLHS3=HS7*(TGI-TCI1)
    SLHS4=F*18.02*HF6
    SLHS5=(PGI-PCGI1)*1E5
    SLHS6=SLHS3+(SLHS4*SLHS5)
    RHS1=HO*(TCI1-TF)
    WRITE(*,*) 'SLHS=',SLHS
    WRITE(*,*) 'RHS=',RHS
    WRITE(*,*) 'SLHS6=',SLHS6
    WRITE(*,*) 'RHS1=',RHS1
    GO TO 660
670  WRITE(*,*) 'HERR'
    MO=MO+1
    NO=NO+1
```

```
WRITE(1,1) 'AKL1'  
JICK=JICK+1  
150 WRITE(1,1) 'CLOSE'  
RP=99.999  
QV1=HS7*(TGI-TCI)  
QV2=F*18.02*HF6  
QV3=(PGI-PCGI)*1E5  
QV4=QV1+(QV2*QV3)  
QV5=HQ*(TGI-TF)  
QT=(QV4+QV5)/2  
UDT=QT  
U=UDT/(TGI-TF)  
HT=QT/(TGI-TCI)  
BIR=(1E6)/UDT  
DELTA=RESL-RESR  
MIN1=MIN+20  
A(MIN,1)=TGI  
A(MIN+1,1)=TCI  
A(MIN+2,1)=TF  
A(MIN+3,1)=(TGI-TF)  
A(MIN+4,1)=PGI  
A(MIN+5,1)=QT  
A(MIN+6,1)=GRAN  
A(MIN+7,1)=RE  
A(MIN+8,1)=FGL  
A(MIN+9,1)=F  
A(MIN+10,1)=HS7  
A(MIN+11,1)=HT  
A(MIN+12,1)=U  
A(MIN+13,1)=UDT  
A(MIN+14,1)=BIR  
A(MIN+15,1)=RESL  
A(MIN+16,1)=RESR  
A(MIN+17,1)=DELTA  
A(MIN+18,1)=YA  
A(MIN+19,1)=YG  
A(MIN+20,1)=RP  
807 WRITE(1,1) 'TEMP OF NEXT SECTION STILL IN SUPERHEAT REGION '  
MIN=MIN+21  
809 WRITE(1,1) 'NO ROOT FOUND -ABORT '  
TGI=TGI-QT  
TCI=TGI-40  
TCI1=TCI+1  
MINE=MINE+1  
WRITE(1,1) 'MINE=', MINE  
IF (MINE.LE.N) GO TO 99  
JFK1=N*21  
WRITE(1,1) 'TO PRINT RESULTS'  
DO 500 MM=1,JFK1  
WRITE(7,600) A(MM,1)  
600 FORMAT(20X,E16.8 )  
500 CONTINUE  
GO TO 999  
620 WRITE(1,1) '0'  
IF (TGI .LT. 99) THEN  
KK=3  
KKR=5  
GO TO 710
```

```
ELSE  
  WRITE(1,1)' TO USE SUPERHEAT EQNS'  
ENDIF  
T=T6I  
KK=1  
GO TO 707  
708 WRITE(1,1)' RRR'  
  KK=KK+1  
  PGI=PRT  
  DENS=1/VVT  
  T=TCI  
  IF(TCI1.LT.99) THEN  
    GO TO 716  
  ELSE  
    GO TO 807  
  ENDIF
```

```
710 WRITE(1,1)' USING SATURATION EQN. '  
R1=T6I  
R2=T6I*T6I  
R3=R2*R1  
R4=R2*R2  
R5=R4*R1  
V1=TCI  
V2=V1*V1  
V3=V2*V1  
V4=V2*V2  
V5=V4*V1  
VS1=TCI1  
VS2=VS1**2  
VS3=VS1**3  
VS4=VS1**4  
VS5=VS1**5  
S1=TF  
S2=S1*S1  
S3=S2*S1  
S4=S2*S2  
S5=S4*S1  
AB1=(6.28606E-3)*R1  
AB2=R2*36.7147E-6  
AB3=R3*61.5688E-9  
AB4=4876.4/(R1+273)  
PSAP=17.3719+AB1-AB2+AB3-AB4  
PSA1=(EXP(PSAP))*1E-2  
PGI=PSA1
```

```
716 WRITE(1,1)' NNNNN'  
V1=TCI  
V2=TCI**2  
V3=TCI**3  
V4=TCI**4  
V5=TCI**5  
S1=TF  
S2=TF**2  
S3=TF**3  
S4=TF**4  
S5=TF**5  
R1=T6I  
R2=T6I**2  
R3=T6I**3
```

R4=T61\*4  
R5=T61\*5  
VS1=TC11  
VS2=VS1\*2  
VS3=VS1\*3  
VS4=VS1\*4  
VS5=VS1\*5

AC1=V1\*6.28606E-3  
ACC1=VS1\*6.28606E-3  
AC2=V2\*36.7147E-6  
ACC2=VS2\*36.7147E-6  
AC3=V3\*61.5688E-9  
ACC3=VS3\*61.5688E-9  
AC4=4876.4/(V1+273)  
ACC4=4876.4/(VS1+273)  
PSAP2=17.3719+AC1-AC2+AC3-AC4  
PSA2=(EXP(PSAP2))\*1E-2  
PCGI=PSA2  
PSAC2=17.3719+ACC1-ACC2+ACC3-ACC4  
PCGI1=(EXP(PSAC2))\*1E-2

715 WRITE(\*,\*, PSA='

PAI=PT-PCI  
FNGI=P6I\*FNA/PAI  
YA=F\*4/(FNGI+FNA)  
YG=1-YA  
WRITE(\*,\*) 'P6I=', P6I  
WRITE(\*,\*) 'PCGI=', PCGI  
CPA1=1003.86+(R1\*0.228945E-1)  
CPA2=(R2\*.451594E-3)-(R3\*.241506E-6)  
CPA=CPA1+CPA2  
CP61=1845.675+(4.755963\*R1)-(R2\*.1230065)  
CP62=(R3\*1.350715E-3)-(5.303748E-6\*R4)+(R5\*.417658E-9)  
CP6=CP61+CP62  
CPL1=1855.9+(V1\*1.01299)-(0.114716\*V2)  
CPL11=1855.9+(VS1\*1.01299)-(0.114716\*VS2)  
CPL2=V3\*.162415E-3  
CPL21=VS3\*.162415E-3  
CPL=CPL1+CPL2  
CPL1=CPL11+CPL21  
CPF=1855.9+(1.01299\*S1)-(0.114716\*S2)+(0.162415E-3\*S3)  
WRITE(\*,\*) 'CP =', CPA, CP6, CPL, CPF, CPL1  
HFG=2501500-(V1\*2433.5)+(V2\*1.8339)+(18.616E-3\*V3)  
VISA1=1.7161+(.49345E-2\*R1)-(0.382902E-5\*R2)+(0.278966E-8\*R3)  
VISA=VISA1\*1E-5  
VIS61=8.50377+(.032276\*R1)+(0.419613E-4\*R2)-(0.121205E-6\*R3)  
VIS6=VIS61\*1E-6  
VS=.435509E-3+(.282519E-4\*S1)+(0.344052E-7\*S2)  
VS1=1/VS  
VISF=VS1\*1E-6  
VSL1=.435509E-3+(.282519E-4\*V1)+(0.344052E-7\*V2)  
VISL=(1/VSL1)\*1E-6  
VSL11=.435509E-3+(.282519E-4\*VS1)+(0.344052E-7\*VS2)  
VISL1=(1/VSL11)\*1E-6  
WRITE(\*,\*) 'VIS=', VISA, VIS6, VISL, VISF, VSL1  
XKA=2.41319E-2+(.795942E-4\*R1)-(0.379775E-7\*R2)+(0.148707E-10\*R3)  
XKG=.016166+(0.094071E-3\*R1)-(0.24342E-6\*R2)+(0.154242E-7\*R3)  
XKF=.569034+(1.86596E-3\*S1)-(0.79983E-5\*S2)+(0.525649E-8\*S3)  
XKL=.569034+(1.96596E-3\*V1)-(0.79983E-5\*V2)+(0.525649E-8\*V3)

```
XL1=.569034+(1.86596E-3*VS1)-(79983E-5*VS2)+(.525649E-8*VS3)
WRITE(1,1)'XK=',XKA,XKG,XKL,XKF,XKL1
DENA=348.43*PA1/(R1+273)
VG1=.001+(3.97E-9*R2)
VG2=126+(.433*R1)+(441E-6*R2)-(3.9E-6*R3)
VG3=VG2/(PB1*100)
VG=VG1+VG3
DENG=1/VG
DENL1=.001+(3.97E-9*V2)
DENL=1/DENL1
DENL1=1/((.001+(3.97E-9*VS2)))
DENF1=.001+(3.97E-9*VS2)
DENF=1/DENF1
WRITE(1,1)'DEN=',DENA,DENG,DENL,DENF,DENL1
DR1=(R1+273)/273
DR2=DR1**1.8
D=.216E-4*DR2
WRITE(1,1)'D=',D
PCR=(37.5*FNA)+(224.7*FNG1)
PRED=PT/PCR
RMA=28.96
RMG=18.02
RML=18.02
RMF=18.02
WRITE(1,1)'PP2'
```

TO EVALUATE MIXTURE PROPERTIES

```
YA=FNA/(FNA+FNG1)
YG=1-YA
RM=(YA*RMA)+(YG*RMG)
CP=((YA*CPA*RMA)+(YG*CPG*RMG))/RM
W1=YA*RMA/DENA
W2=YG*RMG/DENG
DEN=RM/(W1+W2)
PIK1=(1+(XKA/XKG))**0.5
PIK2=(RMG/RMA)**.25
PIK3=(8*(1+(RMA/RMG))**.5)
PIK5=(PIK1*PIK2)**2
PIK5=PIK5/PIK3
PIK6=PIK5*(XKG*RMA)/(XKA*RMG)
XK1=(YA*XKA)/(YA+(YG*PIK5))
XK2=(YG*XKG)/(YG+(YA*PIK6))
XK=XK1+XK2
PIV1=(1+(VISA/VIS6))**.5
PIV2=PIK2
PIV3=PIK3
PIV5=((PIV1*PIV2)**2)/(PIV3**.5)
PIV6=PIV5*(VIS6*RMA)/(VISA*RMG)
VIS1=(YA*VISA)/(YA+(YG*PIV5))
VIS2=(YG*VIS6)/(YG+(YA*PIV6))
VIS=VIS1+VIS2
WRITE(1,1)'CP=',CP
WRITE(1,1)'DEN=',DEN
WRITE(1,1)'XK=',XK
WRITE(1,1)'VIS=',VIS
WRITE(1,1)'RM=',RM
```



TO EVALUATE PR,SC,RE NUMBERS

```
PRF=VISF*CPF/XKF
PR=VIS*CP/YK
PRL=VISL*CPL/XKL
PRL1=VISL1*CPL1/XKL1
SC=VIS/(DEN*D)
REF=GF*DE*.0254/VISF
GL=FNGI*18.02/AREA
REL=GL*DIA*.0254/VISL
REL=GL*DIA*.0254/VISL1
RE=G*DIA*.0254/VIS
WRITE(*,*)'PR=',PRF,PRL,PR,PRL1
WRITE(*,*)'RE=',REF,REL,RE,REL1
WRITE(*,*)'SC=',SC
WRITE(*,*)'G=',GL,G
DZ1=ALOG10(RE)
WRITE(*,*)'DZ1=',DZ1
if (DZ1.LT.1.1) GO TO 120
DY1=(-.359827)+(.332482*DZ1)
DY2=(-16.1896)+(8.0781*DZ1)-(.896849*DZ1*DZ1)
DY3=(-1.52242)+(.786781*DZ1)
DY4=(-.462039)+(.3495*DZ1)
DY5=(-10.9248)+(5.25986*DZ1)-(.530023*DZ1*DZ1)
DY6=(-.498737)+(.337669*DZ1)
DY7=(-12.9032)+(6.20868*DZ1)-(.643248*DZ1*DZ1)
WRITE(*,*)'DYI=',DY1,DY2,DY3,DY4,DY5
DJ1=10**DY1
DJ2=10**DY2
DJ3=10**DY3
DJ4=10**DY4
DJ5=10**DY5
DJ6=10**DY6
DJ7=10**DY7
WRITE(*,*)'DJI=',DJ1,DJ2,DJ3,DJ4,DJ5
PIVOT=RL/DIA
NPIV=PIVOT
NRE=RE
N6=NPIV/180
N7=NPIV/120
N8=NPIV/72
IF (N8.GT.0)THEN
```

```

ELSE
    FAJH1=DJ2
    FAJH2=DJ5
    FAJH=((((PIVOT-72)/48)*(FAJH2-FAJH1))+FAJH1

```

ENDIF

ELSE

```

    FAJH1=DJ1
    FAJH2=DJ4
    FAJH=((((PIVOT-72)/48)*(FAJH2-FAJH1))+FAJH1

```

ENDIF

```

110 WRITE(1,1) 'CHECKING'
    IF(JOR.NE.2) GOTO 120
    IF(NRE.GT.2100) THEN
        IF(NRE.GT.30000) THEN
            FAJH=DJ3

```

ELSE

```

    FAJH1=DJ5
    FAJH2=DJ7
    FAJH=((((PIVOT-120)/60)*(FAJH2-FAJH1))+FAJH1

```

ENDIF

ELSE

```

    FAJH1=DJ4
    FAJH2=DJ6
    FAJH=((((PIVOT-72)/48)*(FAJH2-FAJH1))+FAJH1

```

ENDIF

WRITE(1,1) 'FAJH=',FAJH

120 WRITE(1,1) 'NOT CHECKING FOR FAJH, FAJH =1 '

FAJH=1.1

IF(TCIN.LT.99) THEN

```

    QCI1=(FNG-FNG1)*18.02
    QCI2=(HFG+(CPF*(TCIN-T61)))
    QCI=QCI1*QCI2
    QUI=FNG1*18.02*CPF*(TCIN-T61)
    QAI=FNA*28.96*CPA*(TCIN-T61)
    QTI=QCI+QUI+QAI
    DWT=QTI/(CMF*CPF)
    TF=TWO-DWT
    PD=1

```

WRITE(1,1) 'PD=',PD

WRITE(1,1) 'QCI1,QCI2,QCI,QAI,QUI='

WRITE(1,1) QCI1,QCI2,QCI,QAI,QUI

WRITE(1,1) 'QTI,CMF,DWT,TF,TWO=',QTI,CMF,DWT,TF,TWO

WRITE(1,1) 'CPF=',CPF

ELSE

IF (T61 .LE. 99) THEN

```

    E11=T61
    E12=E11**2
    E13=E11**3
    SPS1=17.3719+(6.29606E-3*E11)-(36.7147E-6*E12)
    SPS2=(61.5688E-9*E13)-(4876.4/(E11+273))
    SPS3=SPS1+SPS2
    SPS=(EXP(SPS3))*1E-2
    FNGI=(SPS/(PT-SPS))*FNA
    G61=TCIN
    G62=TCIN**2
    G63=TCIN**3

```

TFX=2611.61-(.405561\*G61)+(0.136637\*G62)+(0.24935E-4\*G63)

XS=(FNG-FNGI)\*(TFX-417)\*18.02E3

```
XS2=(FNG-FNGI)*(99.6-TGI)*18.02*CPF
QC=XS+XS2
QA=FNA*CPA*(TCIN-TGI)*28.96
QUC=FNGI*CPG*(TCIN-TGI)*18.02
DWT=(QC+QA+QUC)/(CWF*CPF)
TF=TWO-DWT
BR=(QC+QUC+QA)
PD=2
WRITE(*,*)'QC,QUC,QA,BR=',QC,QUC,QA,BR
WRITE(*,*)'TWO,DWT,TF=',TWO,DWT,TF
WRITE(*,*)'PD=',PD
WRITE(*,*)'TFX,XS,XS2=',TFX,XS,XS2
WRITE(*,*)'FNG,FNGI,CPG,CWF,CPF,TCIN,TGI='
WRITE(*,*)FNG,FNGI,CPG,CWF,CPF,TCIN,TGI
ELSE
GO TO 807
ENDIF
ENDIF
WRITE(*,*)'PP3'
GO TO 630
650 WRITE(*,*)'P'

NLHS=SLHS
NRHS=RHS
NDIFF=NLHS-NRHS

RESL=SLHS-RHS
RESR=SLHS6-RHS1
RES=RESL*RESR
IF (LAY.EQ.6) GO TO 71
IF (TCI.GT.TCIN) GO TO 809
IF (RES.GT.0) THEN
TCI=TCI1
RESL=RESR
TCI1=TCI+1
GO TO 99
ELSE
ENDIF
30 WRITE(*,*)'TO ITERATE STILL'
IF (RES.EQ.0) THEN
IF (RESL.EQ.0) THEN
ROOT=TCI
ELSE
ROOT=TCI1
ENDIF
GO TO 101
ELSE
T1=RESL
T2=RESR
XS1=TCI1
XS2=TCI
TCI=(TCI+TCI1)/2
LAY=6
GO TO 99
ENDIF
71 WRITE(*,*)'ON'
ROD=RESL
TD=TCI
TCI=XS2
LAY=0
```

```
RES1=T1#ROD
RES2=T2#ROD
IF (RES1.LT.0) THEN
TCI1=TD
RESR=ROD
ELSE
IF (RES2.EQ.0) THEN
ROOT=TD
GO TO 101
ELSE
TCI=TD
RESL=ROD
ENDIF
ENDIF
DIFF=TCI1-TCI
RES=RESL#RESR
IF (DIFF.GE.0.05) GO TO 30
ROOT=(TCI1+TCI)/2
101 WRITE(*,*) 'ROOT FOUND'
TCI=ROOT
GO TO 150
640 WRITE(*,*) 'Q'
PAI=PT-PCI
PCA=PT-PCGI
PCAI=PT-PCGI1
WRITE(*,*) 'PCGI,PCA=',PCGI,PCA,PCGI1
WRITE(*,*) 'PCI,PAI=',PCI,PAI
YU=(PAI/PCA)
YU1=(PAI/PCAI)
IF (YU .LT. 0) GO TO 607
YUU=ALOG(YU)
YUU1=ALOG(YU1)
WRITE(*,*) 'YU=',YU
WRITE(*,*) 'YUU=',YUU
PGL=(PAI-PCA)/YUU
PGL1=(PAI-PCAI)/YUU1
GL=FNGI#18.02/AREA
REL=GL#DIA#.0254/VISL
REL1=GL#DIA#.0254/VISL
PRL=VISL#CPL/XKL
PRL1=VISL1#CPL1/XKL1
PR=VIS#CP/XK
SC=VIS/(DEN#D)
HR7=9.81#DENF/(VISF#GLH)
HR8=HR7#.3333
HC=.725#XKF#HR8
SS=PR#.3333
WRITE(*,*) 'SS=',SS
SN=1/SS
HS7=FAJH*(XK/DIA1)#SN
A4=PR/SC
A5=(A4#.6667)
WRITE(*,*) 'A5=',A5
F=(HS7#A5)/(CP#PGL#18.02#1E5)
F1=(HS7#A5)/(CP#PGL1#18.02#1E5)
WRITE(*,*) 'F=',F ,F1
REF=6F#DE#.0254/VISF
WRITE(*,*) 'GF ,REF =',6F,REF
```

```
PRF=CPF#VISF/XKF
B11=1/(REF#2)
B21=(PRF#.6667)
WRITE(8,8) 'B11=',B11,B21
HF=.023#B11#CPF#6F/B21
B3=(1/HF)+(1/HP)+(1/HDM)+(1/HDS)+(1/HC)
HO=1/B3
```

```
WRITE(8,8) 'H=',HF,HP,HC,HO
607 WRITE(8,8) 'PGL IS UNDEFINED'
    GO TO 650
700 WRITE(8,8) 'R'
```

C  
C  
C

CALCULATING TOTAL HEAT TRANSFERED IN THE TEST SECTION

```
IF(TCIN.GT.99) THEN
    FNG3=FNG/18.02
    FNG4=CON#FNG/((1-CON)#28.96)
    FNG5=FNG3+FNG4
    FNG=.97966#FNG5
    FNA=.02034#FNG5
ELSE
    FNA=CON #FNG/(28.96 *(1-CON))
    FNG=FNG/18.02
ENDIF
T#B=(T#I+T#O)/2
T#B=(TCIN+TCOUT)/2
AL1=T#B
AL2=AL1**2
AL3=AL2#AL1
AL4=AL2**2
AL5=AL1**5
BL1=T#B
BL2=BL1**2
BL3=BL1**3
BL4=BL1**4
BL5=BL1**5
CPA1=1003.86+(.0228945#BL1)+(.451594E-3#BL2)-(.241506E-6#BL3)
C3=1845.675+(4.755963#BL1)-(.1230065#BL2)
C4=(-5.303748E-6#BL4)+(1.350715E-3#BL3)+(8.417658E-9#BL5)
CPG1=C3+C4
HFG1=2501500-(2433.5#BL1)+(1.8339#BL2)-(18.616E-3#BL3)
PSA1=17.3719+(6.28606E-3#BL1)-(36.7147E-6#BL2)
PSA2=(61.5688E-9#BL3)-(4876.4/(BL1+273))
PSAP9=PSA1+PSA2
PSA=(EXP(PSAP9))#1E-2
C5=1855.9+(1.01299#AL1)
C6=(.0114716#AL2)+(.162415E-3#AL3)
CPF1=C5+C6
BR1=TCOUT
BR2=BR1**2
BR3=BR1**3
BV1=TCIN
BV2=BV1**2
BV3=BV1**3
PSAE1=17.3719+(6.28606E-3#BR1)-(36.7147E-6#BR2)
PSAI1=17.3719+(6.28606E-3#BV1)-(36.7147E-6#BV2)
PSAE2=(61.5688E-9#BR3)-(4876.4/(BR1+273))
PSAI2=(61.5688E-9#BV3)-(4876.4/(BV1+273))
```

```
PSAE=PSAE1+PSAE2
PSADI=PSAI1+PSAI2
PSAE=(EXP(PSAE) )#1E-2
PSAI=(EXP(PSADI))#1E-2
GNE=(PSAE/(PT-PSAE))#FNA
IF ( TCIN .GT. 99) GO TO 780
QUC=GNE#CP61#(TCIN-TCOUT)#18.02
QC=(FNG-GNE)#((CP61#(TCIN-TCOUT))+HF61)#18.02
QA=FNA#CPA1#(TCIN-TCOUT)#28.96
QT=QUC+QA+QC
CWF=QT/(CPF1#(TWO-TWI))
GLH=(FNG-GNE)#18.02/AREA
GO TO 781
780  WRITE(,)# 'SUPERHEATED AT ENTRY'
      ENT1=2611.61-(.405561#TCIN)
      ENT2=.0136637#TCIN#TCIN
      ENT3=.249325E-4#(TCIN#3)
      ENT=ENT1+ENT2+ENT3
      EN1=(FNG-GNE)#(ENT-417)#18.02E3
      EN2=(FNG-GNE)#(99.6-TCOUT)#CPF1
      QC=EN1+EN2
      QA=FNA#CPA1#(TCIN-TCOUT)#28.96
      QUC=GNE#CP61#(TCIN-TCOUT)#18.02
      QT=QA+QC+QUC
      CWF=QT/(CPF1#(TWO-TWI))
      GLH=(FNG-GNE)#18.02/AREA
781  WRITE(,)# 'SSSSSS'
      GO TO 800
850  WRITE(,)# 'S'
      IF (TCIN .GT. 99) GO TO 950
      T=98
      PSAT1=(FNG/(FNG+FNA))#PT
      PD1=PSAT1#1E2
      PD=ALOG(PD1)
205  WRITE(,)# 'ROTE'
      FUNC1=17.3719+(6.28606E-3#T)
      FUNC2=36.7147E-6#T#T
      FUNC3=(T#3)#61.5688E-9
      FUNC4=4876.4/(T+273)
      FUNC=FUNC1-FUNC2+FUNC3-FUNC4-(PD)

      DER1=(6.28606E-3)-(T#73.4294E-6)
      DER2=(T#2)#184.706E-9
      DER3=4876.4/((T+273)#2)
      DER=DER1+DER2+DER3
      TNEW=T-(FUNC/DER)
      FRAN=ABS((TNEW-T)#10)
      MR=FRAN
      T=TNEW
      IF (MR .GT. 5) GOTO 205
      TCIT=T
      WRITE(,)# 'TCIT=',T
      WRITE(,)# 'FRAN=',FRAN
      WRITE(,)# 'YYYYYY'
      GO TO 900
930  WRITE(,)# 'T'
      GEE=MMF#CPF1#(TWO-TWI)
      UL=0.0
```

```
UR=UL+1
DAY=0
31 WRITE(8,8)'SEARCHING FOR EXIT TEMP'
ZY1=UL
ZW1=UR
ZY2=ZY1*ZY1
ZY3=ZY2*ZY1
ZW2=ZW1*ZW1
ZW3=ZW2*ZW1
PSAL1=17.3719+(6.286061E-3*ZY1)-(36.7147E-6*ZY2)
PSAR1=17.3719+(6.286061E-3*ZW1)-(36.7147E-6*ZW2)
PSAL2=(61.5688E-9*ZY3)-(4876.4/(ZY1+273))
PSAR2=(61.5688E-9*ZW3)-(4876.4/(ZW1+273))
PSALL=PSAL1+PSAL2
PSALR=PSAR1+PSAR2
PSAL=(EXP(PSALL))*1E-2
PSAR=(EXP(PSALR))*1E-2
GNL=(PSAL/(PT-PSAL))*FNA
GNR=(PSAR/(PT-PSAR))*FNA
QUL=GNL*CP61*(TCIT-UL)
QUR=GNR*CP61*(TCIT-UR)
QCL=(FNG-GNL)*(CP61*(TCIT-UL)+HF61)*18.02
QCR=(FNG-GNR)*(CP61*(TCIT-UR)+HF61)*18.02
QAL=FNA*CPA1*(TCIT-UL)
QAR=FNA*CPA1*(TCIT-UR)
QTL=QUL+QCL+QAL
QTR=QUR+QCR+QAR
WRITE(8,8)'QEE,QTL,QTR=',QEE,QTL,QTR
UUL=(QTL-QEE)
UUR=(QTR-QEE)
UU=UUL*UUR
WRITE(8,8)'UL,UR,UUL,UUR=',UL,UR,UUL,UUR
RICK=0
IF(DAY .EQ. 6) GO TO 52
IF (RICK .GT. 100) GO TO 123
IF(UU .GT. 0) THEN
  UL=UR
  UUL=UUR
  UR=UR+1
  GO TO 31
ELSE
  ENDIF
32 WRITE(8,8)'STILL ITERATING '
IF (UU .EQ. 0) THEN
  IF (UUL .EQ. 0) THEN
    TCT=UL
  ELSE
    TCT=UR
  ENDIF
  GO TO 122
ELSE
  T1=UUL
  T2=UUR
  XS1=UR
  XS2=UL
  UL=(UR+UL)/2
  DAY=6
  GO TO 31
```

```
ENDIF
52  WRITE(*,*) 'POIT'
    FOD=UUL
    TD=UL
    UL=XS2
    DAY=0
    CRL=T1#FOD
    CRR=T2#FOD
    IF (CRL .LT. 0) THEN
        UR=TD
        UUR=FOD
    ELSE
        IF(CRR .EQ. 0) THEN
            TCT=TD
            GO TO 122
        ELSE
            UL=TD
            UUL=FOD
        ENDIF
    ENDIF
    DEV=UR-UL
    UU=UUR#UUL
    IF (DEV .GT. .05) GO TO 32
    TCT=(UR+UL)/2
123  WRITE(*,*) 'NO ROOT FOUND
122  WRITE(*,*) 'ROOT TCT=',TCT
    GO TO 950
707  WRITE(*,*) 'UUU'
    E1=T
    E2=T#T
    E3=E2#T
    P=(FNG/(FNG+FNA))#PT
    HH1=2611.61-(.405561#E1) +(.0136637#E2) -( .249325E-4#E3)
    HH2=2460.25+(2.37895#E1)-(.228235E-2#E2)+( .401267E-5#E3)
    HH3=2476.54+(2.16443#E1)-(.130415E-2#E2)+( .255383E-5#E3)
    HH4=2495.92+(1.93083#E1)-(.197971E-3#E2)+( .692052E-6#E3)
    HH5=2499.36+(1.87778#E1)-(.114E-3#E2)+( .690209E-6#E3)
    HH6=2500.82+(1.88561#E1)-(.109481E-3#E2)+( .807156E-6#E3)
    HH7=2500.99+(1.8814#E1)-(.7926E-4#E2)+( .74303E-6#E3)
    VV1=1.1912128+(.523686E-2#E1)-(.215681E-5#E2)+( .25791E-8#E3)
    VV2=1.6074+(.686646E-2#E1)-(.274589E-5#E2)+( .375218E-8#E3)
    VV3=2.4265+(.0104012#E1)-(.572655E-5#E2)+(0.97405E-8#E3)
    VV4=12.5215+(0.04715#E1)-(.494755E-5#E2)+(0.87881E-8#E3)
    VV5=25.139+(0.093067#E1)-(.0343631E-5#E2)+(0.567808E-08#E3)
    VV6=125.97+(0.46215#E1)+(0.464105E-05#E2)-(.0251482E-7#E3)
    VV7=206.096+(0.755516#E1)+(0.90844E-05#E2)-(.034467E-07#E3)
    NXYZ1=P/0.006112
    NXYZ2=P/0.01
    NXYZ3=P/0.05
    NXYZ4=P/0.1
    NXYZ5=P/0.5
    NXYZ6=P/0.75
    NXYZ7=P
    CONS1=4*(P-0.75)
    CONS2=4*(P-0.5)
    CONS3=2.5*(P-0.1)
    CONS4=(P-0.05)#20
    CONS5=(P-0.01)#25
```



```
CONS6=(F-0.006112)*257.2
AP61=17.3719+(6.28606E-3*E1)-(36.714E-6*E2)
AP62=(61.5688E-9*E3)-(4876.4/(E1+273))
AP63=AP61+AP62
AP6=(EXP(AP63))*1E-2
AV61=.001+(3.97E-9*E2)
AV62=(126+(.433*E1)+(441E-6*E2)-(3.9E-6*E3))/(AP6*100)
AV6=AV61+AV62
IF (NXY21.GT.0)THEN
  IF (NXY22.GT.0)THEN
    IF (NXY23.GT.0)THEN
      IF (NXY24.GT.0)THEN
        IF (NXY25.GT.0)THEN
          IF (NXY26.GT.0)THEN
            IF (NXY27.GT.0)THEN
              WRITE(*,*)'OUT RANGE'
            ELSE
              HH=((HH1-HH2)*CONS1)+HH2
              VV=((VV1-VV2)*CONS1)+VV2
            ENDIF
          ELSE
            HH=((HH2-HH3)*CONS2)+HH3
            VV=((VV2-VV3)*CONS2)+VV3
          ENDIF
        ELSE
            HH=((HH3-HH4)*CONS3)+HH4
            VV=((VV3-VV4)*CONS3)+VV4
          ENDIF
        ELSE
            HH=((HH4-HH5)*CONS4)+HH5
            VV=((VV4-VV5)*CONS4)+VV5
          ENDIF
        ELSE
            HH=((HH5-HH6)*CONS5)+HH6
            VV=((VV5-VV6)*CONS5)+VV6
          ENDIF
        ELSE
            HH=((HH6-HH7)*CONS6)+HH7
            VV=((VV6-VV7)*CONS6)+VV7
          ENDIF
        ELSE
            WRITE(*,*)'P IS TOO SMALL'
          ENDIF
          VVT=VV
          PRT=P
          GO TO 708
        ENDIF
      999 WRITE(*,*)'ENDING'
    END
```

## APPENDIX 4.3

```

C      PROGRAM TO EVALUATE PRESSURE DROP ACROSS THE TUBE IN THE TEST
C      SECTION . TO FIND FRICTIONAL PRESSURE LOSS BY USE OF DUCKLER'S
C      EQUATION (NO SLIP) AND ACCELERATION TERM BY ANDEEN ET AL
C      EQUATION .TOTAL PRESSURE LOSS GOT BY SUMMATION OF DIFFERENTIAL
C      PRESSURE LOSSES ACROSS EACH INTERVAL TEST SECTION IS DIVIDED
C      INTO AND THEN SUMMING THE FRICTIONAL LOSS AND ACCELERATION TERMS
      REAL A
      DIMENSION A(20,9)
      WRITE(*,*) 'STARTING '
      WRITE(*,*) 'INPUT COND FLOWRATE FMR, INLET TEMP tg, CONC OF
      WRITE(*,*) 'AIR CON, TUBE DIAMETER DIA'
      READ(*,*) FMR, tg, CON, DIA
      write(*,*) 'input number of intervals N'
      READ(*,*) N
      VMA=(CON*FMR)/((1-CON)*28.96)
      AREA=.7853981*(DIA**2)*1E-6
      M=3
      TI=TG
      FLOSS=0
      D1=0
      MK=1
      XL0=0
      XL=0
      TIO=TG
      VMD=FMR/18.02
      YA=VMA/(VMA+VMD)
DO 30 I=1,N
      IF (MK.EQ.1) GO TO 31
      WRITE(*,*) 'INPUT POSITION XL, MOLE FRACTION YA, AIRTEMP TI
      READ(*,*) XL, YA, TI
      DL=XL-XL0
      T=(TI+TIO)/2
      R1=T
      R2=T*T
      R3=R2*R1
      R4=R2*R2
      R5=R4*R1
      V1=T
      V2=V1*V1
      V3=V2*V1
      V4=V2*V2
      V5=V4*V1
      VS1=T
      VS2=VS1**2
      VS3=VS1**3
      VS4=VS1**4
      VS5=VS1**5
      S1=T
      S2=S1*S1
      S3=S2*S1
      S4=S2*S2
      S5=S4*S1
      CPA1=1000.86+(R1*0.228945E-1)
      CPA2=(R2*.451594E-3)-(R3*.241506E-6)
      CPA=CPA1+CPA2

```

```

CFG1=1845.675+(4.755967*R1)-(R2*.1230065)
CFG2=(R3*1.350715E-3)-(5.303749E-6*R4)+(R5*8.417658E-9)
CFG=CFG1+CFG2
CFL1=1855.9+(V1*1.01299)-(.0114716*V2)
CFL11=1855.9+(V1*1.01299)-(.0114716*VS2)
CFL2=V3*.162415E-3
CFL21=V3*1.162415E-3
CFL=CFL1+CFL2
CFL1=CFL11+CFL21
*
CPF=1855.9+(1.01299*S1)-(.0114716*S2)+(.162415E-3*S3)
WRITE(*,*)'CP=' ,CPA,CFG,CPL,CPF,CFL1
HFG=2501500-(V1*2433.5)+(V2*1.8339)+(18.616E-3*V3)
VISA1=1.7161+(.49345E-2*R1)-(.382902E-5*R2)+(.278966E-8*R3)
VISA=VISA1*1E-5
VISG1=8.50377+(.032276*R1)+(.419613E-4*R2)-(.121205E-6*R3)
VISG=VISG1*1E-6
VS=.435509E-3+(.282519E-4*S1)+(.344052E-7*S2)
VS1=1/VS
VISF=VS1*1E-6
VSL1=.435509E-3+(.282519E-4*V1)+(.344052E-7*V2)
VSL=(1/VSL1)*1E-6
VSL11=.435509E-3+(.282519E-4*VS1)+(.344052E-7*VS2)
VSL1=(1/VSL11)*1E-6
WRITE(*,*)'VIS=' ,VISA,VISG,VISL,VISF,VISL1
XKA=2.41319E-2+(.795942E-4*R1)-(.379775E-7*R2)+(.148707E-10*R3)
XKG=.016166+(.074071E-3*R1)-(.24342E-6*R2)+(.154242E-7*R3)
XKF=.569034+(1.86596E-3*S1)-(.79983E-5*S2)+(.525649E-8*S3)
XKL=.569034+(1.86596E-3*V1)-(.79983E-5*V2)+(.525649E-8*V3)
XKL1=.569034+(1.86596E-3*VS1)-(.79983E-5*VS2)+(.525649E-8*VS3)
WRITE(*,*)'XK=' ,XKA,XKG,XKL,XKF,XKL1

DENA=348.43*YA/(R1+273)
VG1=.001+(3.97E-9*R2)
VG2=126+(.433*R1)+(441E-6*R2)-(3.9E-6*R3)
VG3=VG2/(100*(1-YA))
VG=VG1+VG3
DENG=1/VG
DENL1=.001+(3.97E-9*V2)
DENL=1/DENL1
DENL1=1/ (.001+(3.97E-9*VS2))
DENF1=.001+(3.97E-9*S2)
DENF=1/DENF1
WRITE(*,*)'DEN=' ,DENA,DENG,DENL,DENF,DENL1
RMA=28.96
RMG=18.02
RM=(YA*RMA)+(YG*G)
CP=((YA*CPA*28.96)+(YG*CFG*18.02))/RM
W1=YA*RMA/DENA
W2=YA*RMG/DENG
DEN=RM/(W1+W2)
PIK1=(1+(XKA/XKG))*0.5
PIK2=(RMG/RMA)*.25
PIK3=(8*(1+(RMA/RMG)))*.5
PIK5=(PIK1*PIK2)*2
PIK5=PIK5/PIK3
PIK6=PIK5*(XKG*RMA)/(XKA*RMG)
XK1=(YA*XKA)/(YA+(YG*PIK5))
XK2=(YG*XKG)/(YG+(YA*PIK6))
XK=XK1+XK2
PIV1=(1+(VISA/VISG))*0.5
PIV2=PIK2
PIV3=PIK3
PIV5=((PIV1*PIV2)*2)/(PIV3*.5)
PIV6=PIV5*(VISG*RMA)/(VISA*RMG)
VIS1=(YA*VISA)/(YA+(YG*PIV5))
VIS2=(YG*VISG)/(YG+(YA*PIV6))

```

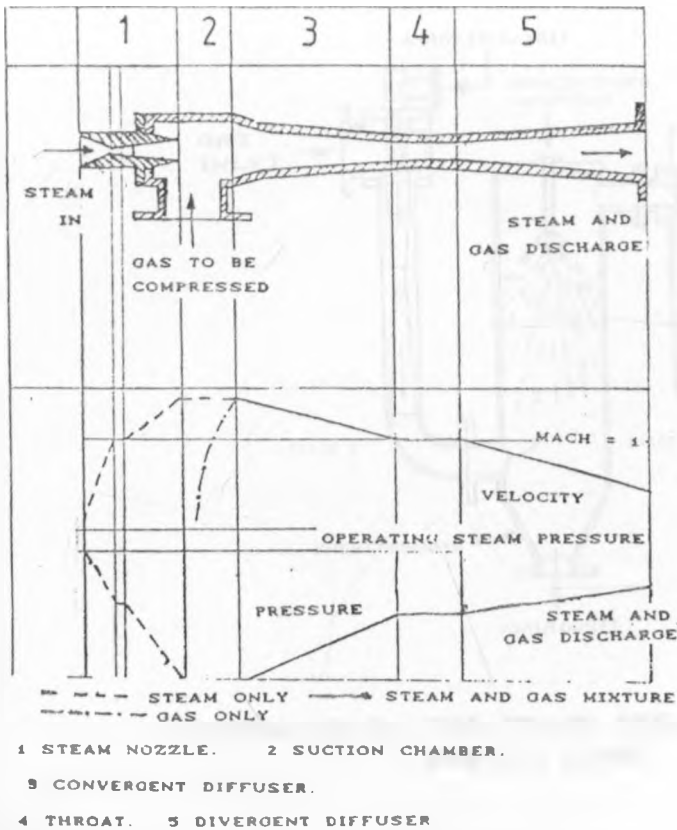
```

VIS=VIS1+VIS2
WRITE(1,1) 'CF=' ,CF
WRITE(1,1) 'DEN=' ,DEN
WRITE(1,1) 'X=' , X
  WRITE(1,1) 'VIS=' ,VIS
  WRITE(1,1) 'FM=' ,FM
  FMA=VMA*28.96
  FMG=(1-YA)*VMA*19.02/YA
  FM=FMA+FMG
  FML=FMR-FMG
  X=FM/(FM+FML)
  G=FM/AREA
  GL=FML/AREA
  QT=(FM/DEN)+(FML/DENL)
  VMI=QT/AREA
  IF (M.EQ.3) THEN
    VM1=VMI
  ELSE
    ENDIF
  VISCO=1/((X/VIS)+((1-X)/VISL))
  DENSI=1/((X/DEN)+((1-X)/DENL))
  REYN=DIA*(G+GL)/(VISCO*1E3)
  F1=4.5223*ALOG10(REYN)
  F2=F1-3.8215
  F3=REYN/F2
  F4=2*ALOG10(F3)
  F=1/(F4**2)
  FLOSSF=F*DL*DENSI*(VMI**2)/2
  FLOSSM=(FMR+FMA)*(VMI-VM1)
  DELTAP=FLOSSF+FLOSSM
  A(I,1)=YA
  A(I,2)=1-YA
  A(I,3)=TI
  A(I,4)=REYN/1E3
  A(I,5)= VMI
  A(I,6)=XL
  A(I,7)=FLOSSF
  A(I,8)=FLOSSM
  A(I,9)=DELTAP
  VM1=VMI
  FLOSS=FLOSS+DELTAP
  TIO=TI
  M=2
  XLO=XL
  MK=2
30 CONTINUE
DO 40 J=1,N
WRITE(*,*)(A(J,*),J1=1,9)
40 CONTINUE
WRITE(*,*) 'TOTAL PRESSURE LOSS (N/M**2)=' ,FLOSS
  HW=FLOSS*1E2/978
WRITE(*,*) 'TOTAL HEAD LOSS IN (CM of WATER)=' ,HW
WRITE(*,*) 'INPUT 2 FOR ANOTHER RUN'
READ(*,*) K
IF (K.EQ.2) GO TO 5
END

```

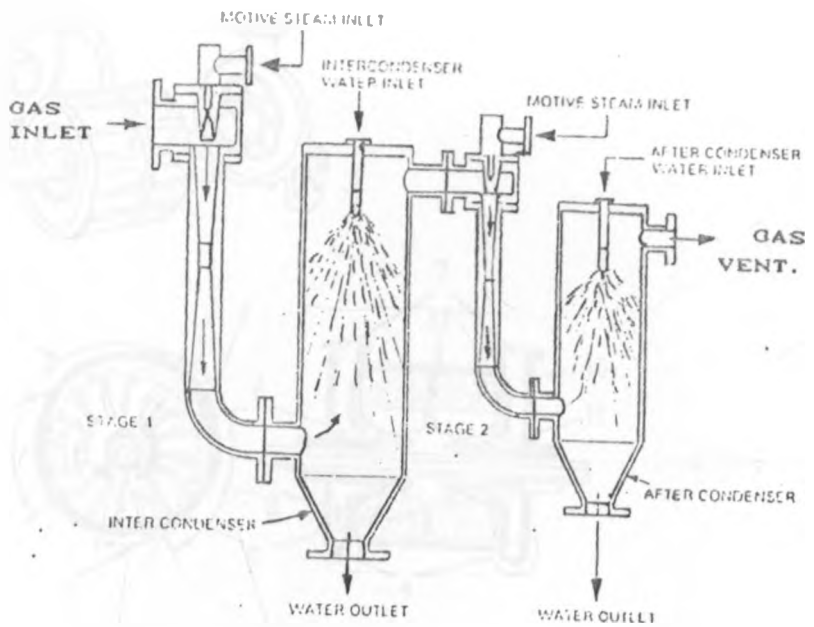
APPENDIX 5

GAS EXTRACTORS



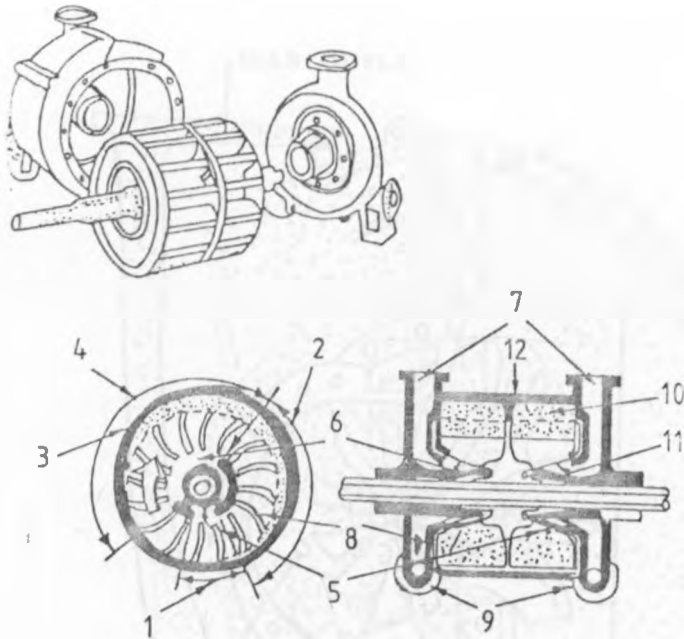
**FIGURE AS.1: STEAM JET EJECTOR BODY  
WHITE (1979)**

Diagram of a single stage steam jet ejector. A steam jet ejector operates on the venturi principle. The motive steam is expanded through the nozzle to the design suction pressure. The pressure energy of the steam is converted to velocity energy and, on leaving the nozzle at high supersonic velocities the steam passes through the suction chamber and enters the converging or entrainment section of the diffuser, where it is brought into mating contact with the suction fluid i.e. non-condensable gas and associated water vapour. An entrainment and diffusion action on the molecules of both streams occurs at the boundaries of the mating surface. Diffusion and entrainment, between the motive and suction fluids, still continues after the sonic barrier is reached but the process of compressing the two streams up to the discharge pressure commences. This action of compression is, in fact, the reconversion of the velocity energy into pressure energy and is normally sufficient to effect a discharge pressure against some predetermined back pressure.



**FIGURE A5.2: TWO STAGE STEAM JET EJECTOR SYSTEM  
WHITE (1979)**

A two stage steam jet ejector system consists of two single ejectors operating in series, with each discharging into a condenser



PARTS

- 1 IN THIS SECTOR COMPRESSED GAS ESCAPES AT DISCHARGE PORTS.
- 2 IN THIS SECTOR LIQUID MOVES INWARD - COMPRESSES GAS IN ROTOR CHAMBERS.
- 3 ROTATING LIQUID COMPRESSANT
- 4 IN THIS SECTOR ,LIQUID MOVES OUTWARD - DRAWS GAS FROM INLET PORTS INTO ROTOR CHAMBERS
- 5 DISCHARGE PORTS 6 INLET PORT 7 INLET CONNECTIONS
- 8 ROTOR
- 9 DISCHARGE CONNECTIONS 10 LIQUID 11 INLET PORT 12 BODY

FIGURE A5.3: LIQUID RING PUMP  
WHITE (1979)

OPERATING PRINCIPLES

A liquid ring pump consists of two main parts, i.e. a rotor and pump body. The rotor is housed eccentrically in the pump body. Figure A5.3 shows a diagram of in the main parts, together with a brief explanation of the operating principles.

The actual compression action is performed by a rotating band/ring of liquid. (Usually water). While power to keep the ring rotating is transmitted by the rotor, the ring tends to center itself in the pump body. As Figure A5.3 shows, water (the compressant) almost fills, then partly empties each rotor chamber during a single revolution. This sets up the piston action. Stationary cones inside the rotor blades have ported openings that separate gas inlet and discharge flows.



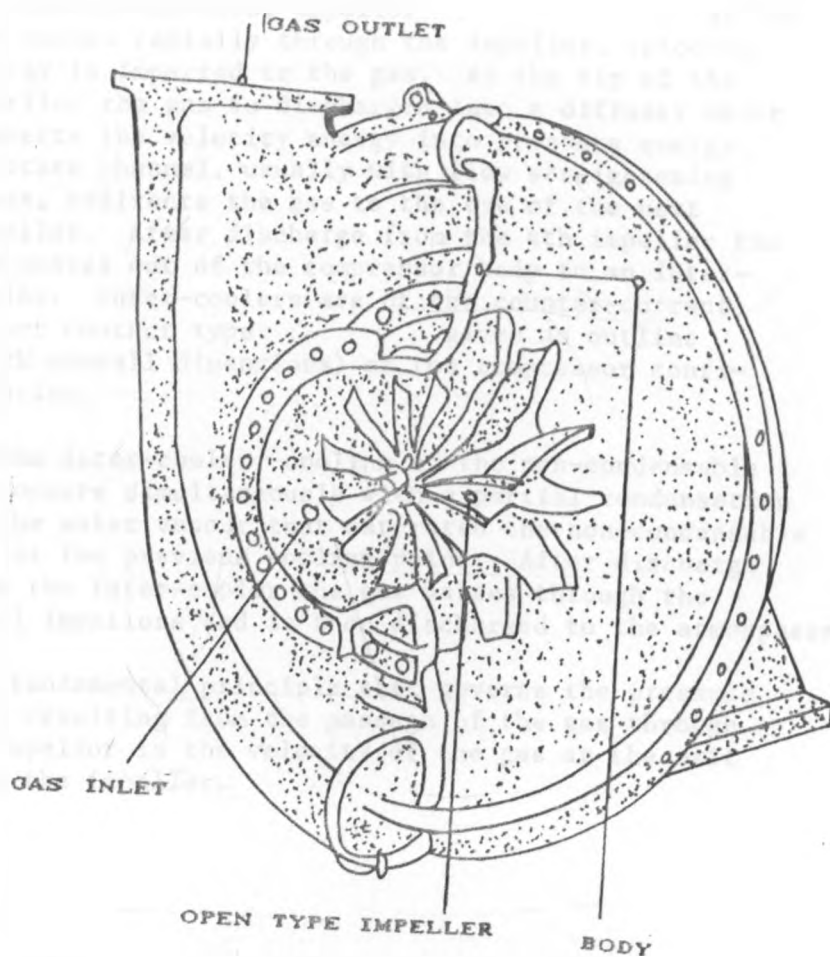


FIGURE A5. 4: RADIAL BLOWER -BODY AND IMPELLER  
WHITE (1979)

### Centrifugal Compressors

During operation of the compressor gas enters through the eye of the first impellor . As the gas passes radially through the impellor, velocity energy is imparted to the gas. At the tip of the impellor the gas is discharged into a diffuser which converts the velocity energy into pressure energy. A return channel, usually with flow straightening vanes, redirects the gas to the eye of the next impellor. After discharge from the 4th impellor the gas passes out of the compressor body to an inter-cooler. Inter-coolers are of the counter-current direct contact type. gives an outline (with overall dimensions) of the compressor configuration.

In the inter-cooler, cooling of the non-condensable gas occurs simultaneously with a partial condensation of the water vapour that saturated the non-condensable gas at the previous cooling point. After discharge from the inter-cooler the gas passes through the final impellers and is then discharged to the atmosphere.

The fundamental principle that governs the pressure rise resulting from the passage of the gas through an impellor is the velocity of the gas at the exit from the impellor.

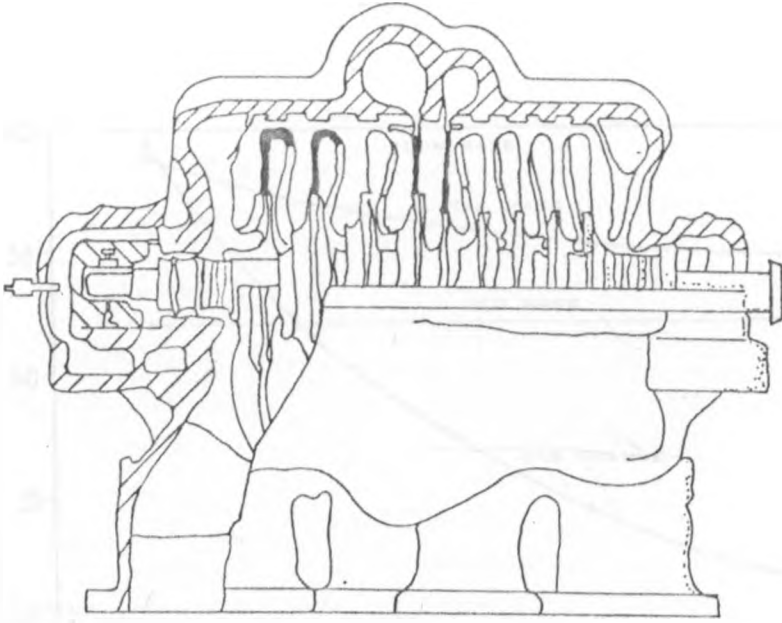


FIGURE A5.5: SINGLE BODY COMPRESSOR WITH ONE INTER-COOLER  
WHITE (1979)

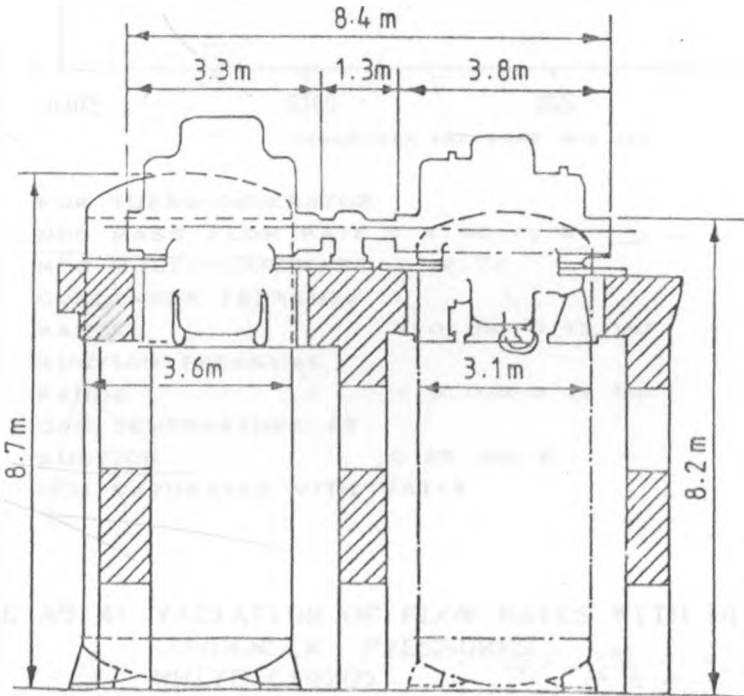
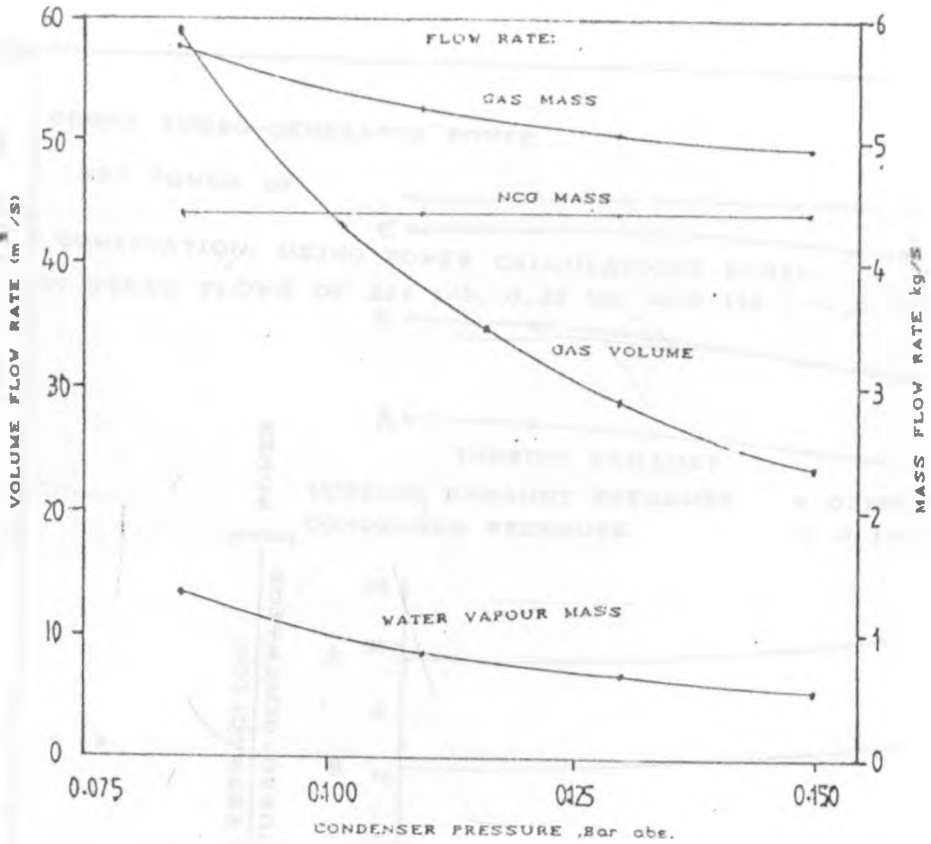


FIGURE A5.6: TWO BODY COMPRESSOR WITH TWO INTER-COOLERS  
WHITE (1979)



FOR TURBO-GENERATOR  
NCG MASS FLOW RATE = 4.40 kg/s  
NCG MOLECULAR MASS = 42.76  
CONDENSER PRESSURE RANGE = 0.085-0.15 bar  
SUCTION PRESSURE RANGE = 0.075-0.14 bar  
GAS TEMPERATURE AT SUCTION = 25 deg C  
NCG SATURATED WITH WATER

FIGURE A5.4: VARIATION OF FLOW RATES WITH DIFFERENT CONDENSER PRESSURES  
WHITE (1979)

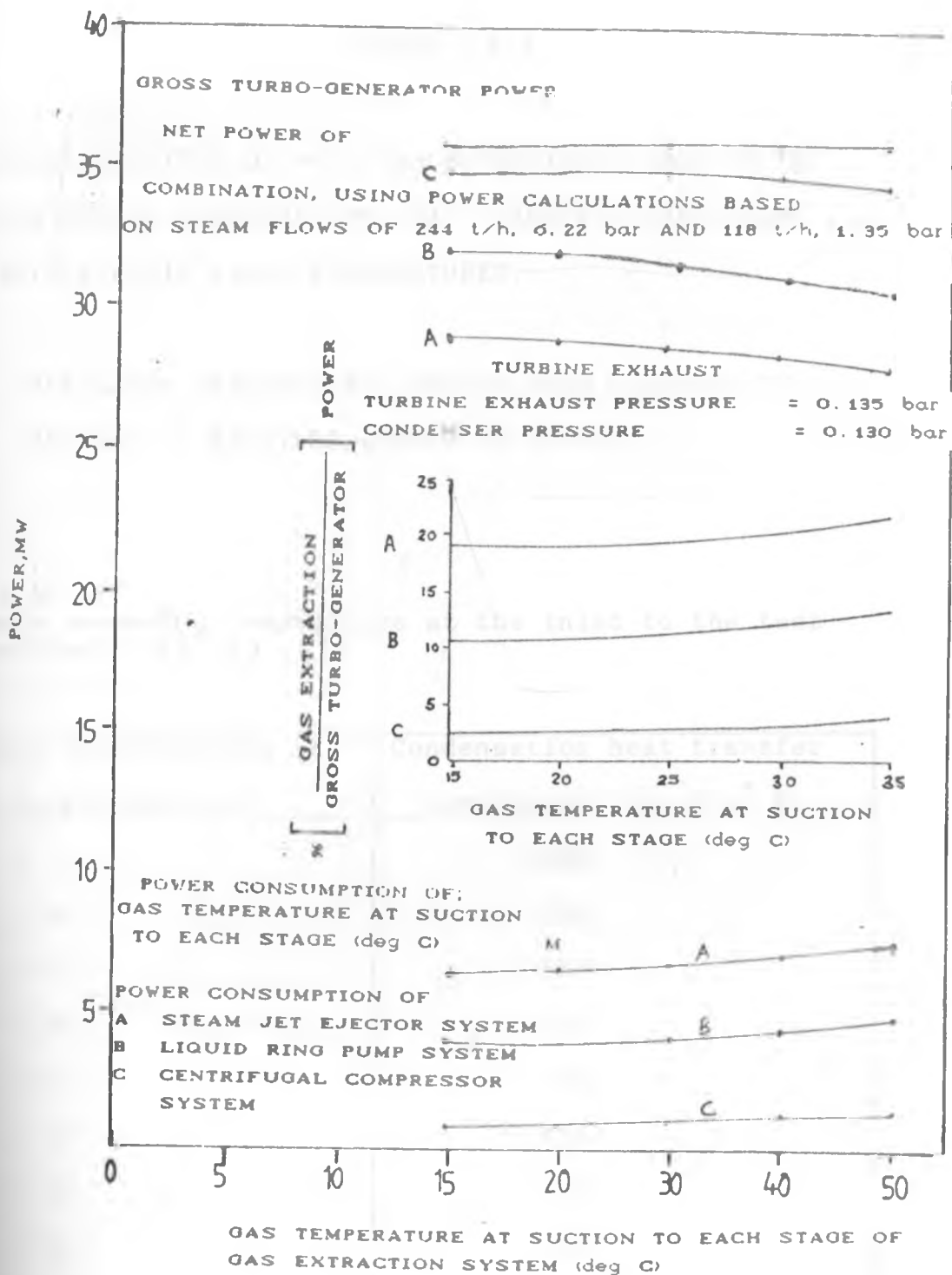


FIGURE A5.8: POWER COMPARISON OF TURBO-GENERATORS/GAS EXTRACTION SYSTEM CONSUMPTION BASED ON FIXED STEAM FLOWS WHITE (1979)

APPENDIX SIX

TABULATED READINGS OF MASS CONCENTRATION OF NCG IN THE MIXTURE VERSUS CONDENSATION HEAT TRANSFER COEFFICIENT (h), AT VARIOUS FLUID INLET TEMPERATURES.

6.1 TABULATED READINGS FOR INSIDE TUBE DIAMETER OF 25.4mm(1") AND TUBE LENGTH OF 4000mm.

Table A6.1:  
Mean steam-NCG temperature at the inlet to the test section = 141 C.

Mass concentration of NCG in the mixture.	Condensation heat transfer coefficient (h) W/m <sup>2</sup> K.
0	1666
2.01	1133
3.61	950
5.76	816
7.82	733
11.02	666
13.73	567
17.92	500
21.00	442
23.72	416
26.18	392

Table A6.2:

Mean steam- $\text{NCG}_0$  temperature at the inlet to the test section = 153 °C.

% Mass concentration of $\text{NCG}$ in the mixture.	Condensation heat transfer coefficient (h) $\text{W/m}^2 \text{K}$ .
0	1330
1.98	950
3.84	800
5.12	703
8.13	617
10.05	567
11.82	503
15.87	432
17.45	416
20.06	392
24.13	351
26.31	353

Table A6.3:

Mean steam-NCG temperature at the inlet to the test section = 164 °C.

Mass concentration of NCG in the mixture.	Condensation heat transfer coefficient (h) W/m <sup>2</sup> K.
0	1151
1.97	833
4.02	693
6.12	567
7.58	468
9.85	417
12.11	375
15.20	334
18.13	317
21.33	318
24.52	308



Table A6.4:

Mean steam-NCG temperature at the inlet to the test section = 192 C.

Mass concentration of NCG in the mixture.	Condensation heat transfer coefficient (h) W/m <sup>2</sup> K.
0	917
2.11	683
3.96	533
6.13	433
8.32	383
10.11	350
12.13	325
14.31	308
16.21	300
18.51	310
20.12	316
24.51	290

Table A6.5:

Mean steam-NCG temperature at the inlet to the test section = 200 °C.

Mass concentration of NCG in the mixture.	Condensation heat transfer coefficient (h) W/m <sup>2</sup> K.
0	850
2.99	607
3.97	451
6.22	366
8.41	319
10.02	305
14.23	266
16.08	258
18.03	253
20.32	252

6.2 TABULATED READINGS OF CONDENSATION HEAT TRANSFER COEFFICIENT v AIR MASS CONCENTRATION FOR AN INSIDE TUBE DIAMETER OF 38.1mm AND TUBE LENGTH OF 4000mm. AT VARIOUS FLUID INLET TEMPERATURES.

Table A6.6.:

Mean steam-NCG temperature at the inlet to the test section = 98 C.

% Mass concentration of NCG in the mixture.	Condensation heat transfer coefficient (h) W/m <sup>2</sup> K.
0	1212
2.11	700
3.94	481
5.72	413
9.83	363
11.02	350
12.48	318
16.22	303
20.41	287
22.11	275
24.30	262
26.05	263

Table A6.7.:

Mean steam- $\text{NCG}$  temperature at the inlet the test section =  $110^\circ\text{C}$ .

X Mass concentration of $\text{NCG}$ in the mixture.	Condensation heat transfer coefficient (h) $\text{W/m}^2\text{K}$ .
0	807
1.93	587
4.12	437
6.08	375
7.94	362
9.64	337
11.34	325
14.23	305
16.82	287
20.33	268
23.95	253
25.54	254
27.21	251

Table A6.8:  
Mean steam-NCG temperature at the inlet to the test  
section = 120 °C.

Mass concentration of NCG in the mixture.	Condensation heat transfer coefficient (h) W/m <sup>2</sup> K.
0	828
1.96	520
3.94	375
5.98	352
6.04	324
7.84	306
10.80	288
12.11	275
14.02	263
18.17	251
22.19	238
24.32	225
26.18	219

Table A6.9:  
Mean steam- $\text{NCG}$  temperature at the inlet to the test section = 157 °C.

% Mass concentration of $\text{NCG}$ in the mixture.	Condensation heat transfer coefficient (h) $\text{W/m}^2 \text{K}$ .
0	751
1.87	440
3.81	368
5.77	313
8.02	301
10.12	282
13.69	269
15.73	263
18.31	237
22.16	239
24.31	240
26.70	237

Table A6.10:

Mean steam-NCG temperature at the inlet the test section = 182 °C.

% Mass concentration of NCG in the mixture.	Condensation heat transfer coefficient (h) W/m <sup>2</sup> K.
0	500
1.99	375
3.86	325
5.81	287
8.15	275
10.11	252
12.30	239
14.01	240
16.32	237
18.01	237
20.13	241
24.14	235

Table A6.11:.

Mean steam- $\text{NCG}$  temperature at the inlet to the test section =  $210^\circ\text{C}$ .

% Mass concentration of $\text{NCG}$ in the mixture.	Condensation heat transfer coefficient ( $h$ ) $\text{W/m}^2\text{K}$ .
0	388
1.98	325
3.96	287
5.82	262
9.93	243
11.01	225
12.28	227
16.12	218
20.43	212
22.01	215



Table A6.12.:  
Mean steam-NCG temperature at the inlet to the test section = 222 °C.

Mass concentration of NCG in the mixture.	Condensation heat transfer coefficient (h) W/m <sup>2</sup> K.
0	325
1.95	307
4.21	250
6.06	226
7.92	212
9.46	203
11.43	198
14.32	197
16.78	192
20.23	195

6.3 TABULATED READINGS FOR COMPARISON OF EXPERIMENTAL CONDENSATION HEAT TRANSFER COEFFICIENT TO THOSE PREDICTED BY THE CORRELATIONS. See section 6.3 for the definitions of the variables  $H_{Ac}$ ,  $H_{Sh}$ ,  $h_{m,Ac}$  and  $h_{m,Sh}$ .

6.3.1 INSIDE TUBE DIAMETER = 25.4mm( 1" ) ,  
TUBE LENGTH 4000mm.

Table A6.13:

Mean fluid temperature at the inlet to the test section = 141 °C.  
Mean temperature difference between the fluid core and the tube wall = 20 °C.  
 $h_{m,Ac} = 1609 \text{ W/m}^2 \cdot \text{K}$  and  $h_{m,Sh} = 3941 \text{ W/m}^2 \cdot \text{K}$ .

% Mole fraction of NCG in the mixture.	$H_{Ac}$	$H_{Sh}$
0	0.725	0.295
1.26	0.704	0.287
2.28	0.590	0.241
3.67	0.507	0.207
5.01	0.456	0.186
7.16	0.414	0.169
9.01	0.352	0.144
11.96	0.311	0.127
14.19	0.275	0.112
15.47	0.259	0.105
18.08	0.244	0.099

Table A6.14:

Mean fluid temperature at the inlet to the test section = 164 °C.

Mean temperature difference between the fluid core and the tube wall = 45 °C.

$h_{m,Ac} = 1631 \text{ W/m}^2 \text{ K}$  and  $h_{m,Sh} = 3492 \text{ W/m}^2 \text{ K}$ .

% Mole fraction of NCG in the mixture.	$H_{Ac}$	$H_{Sh}$
0	0.706	0.329
1.24	0.511	0.238
2.54	0.419	0.195
3.89	0.348	0.162
4.86	0.286	0.133
6.37	0.256	0.119
7.90	0.230	0.107
10.03	0.204	0.095
12.11	0.194	0.091
14.44	0.195	0.091
16.82	0.189	0.088

Table A6.15:

Mean fluid temperature at the inlet to the test section = 192 °C.

Mean temperature difference between the fluid core and the tube wall = 68 °C.

$h_{m,Ac} = 1683 \text{ W/m}^2 \text{ K}$  and  $h_{m,Sh} = 3798 \text{ W/m}^2 \text{ K}$ .

X Mole fraction of NCG in the mixture.	$H_{Ac}$	$H_{Sh}$
0	0.545	0.240
1.32	0.406	0.179
2.50	0.317	0.140
3.91	0.257	0.113
5.35	0.228	0.100
6.54	0.208	0.092
7.91	0.193	0.085
8.41	0.183	0.081
10.76	0.178	0.079
12.38	0.184	0.081
13.55	0.190	0.086
16.81	0.172	0.076

Table A6.16:

Mean temperature of the fluid at the inlet to the test section = 200 °C.  
Mean temperature difference between the fluid core and the tube wall = 82 °C.  
 $h_{m,Ac} = 893 \text{ W/m}^2 \text{ K}$  and  $h_{m,Sh} = 1636 \text{ W/m}^2 \text{ K}$ .

% Mole fraction of CG in the mixture.	$H_{Ac}$	$H_{Sh}$
0	0.501	0.213
1.88	0.354	0.151
2.51	0.266	0.113
3.96	0.216	0.092
5.41	0.186	0.079
6.48	0.179	0.077
9.36	0.157	0.067
10.33	0.152	0.065
12.04	0.147	0.063
13.70	0.149	0.063

6.3.2 INSIDE TUBE DIAMETER = 38.1mm( 1.5" ) ,

TUBE LENGTH = 4000mm.

Table A6.17:

Mean temperature of the fluid at the inlet to the test section = 98.9 C.

Mean temperature difference between the fluid core and the tube wall = 32 C.

$h_{m,Ac} = 879 \text{ W/m}^2 \text{ K}$  and  $h_{m,Sh} = 1636 \text{ W/m}^2 \text{ K}$ .

Mole fraction of CG in the mixture.	$H_{Ac}$	$H_{Sh}$
0	1.378	0.738
1.32	0.798	0.426
2.49	0.547	0.293
3.64	0.469	0.252
6.35	0.413	0.221
7.16	0.398	0.213
8.15	0.362	0.194
10.75	0.341	0.183
13.76	0.327	0.175
15.01	0.313	0.168
16.65	0.298	0.160
18.02	0.289	0.160

Table A6.18:

Mean temperature of the fluid at the inlet to the test section = 110 °C.

Mean temperature difference between the fluid core and the tube wall = 40 °C.

$h_{m,Ac} = 893 \text{ W/m}^2 \text{ K}$ . and  $h_{m,Sh} = 1636 \text{ W/m}^2 \text{ K}$ .

% Mole fraction of NCG in the mixture.	$H_{Ac}$	$H_{Sh}$
0	1.008	0.551
1.21	0.657	0.359
2.60	0.489	0.268
3.87	0.419	0.230
5.09	0.405	0.221
6.23	0.377	0.206
7.37	0.364	0.199
9.36	0.336	0.184
11.18	0.321	0.176
13.70	0.300	0.164
16.39	0.280	0.153
17.59	0.284	0.155
18.87	0.282	0.154

Table A6.19:

Mean fluid temperature at the inlet to the test section = 120 °C.

Mean temperature difference between the fluid core and the tube wall = 51 °C.

$h_{m,Ac} = 898 \text{ W/m}^2 \text{ K}$  and  $h_{m,Sh} = 1636 \text{ W/m}^2 \text{ K}$ .

% Mole fraction of NCG in the mixture.	$H_{Ac}$	$H_{Sh}$
0	0.919	0.504
1.23	0.579	0.318
2.49	0.418	0.229
3.81	0.390	0.214
3.85	0.361	0.198
5.03	0.341	0.186
6.87	0.321	0.176
7.90	0.306	0.168
9.21	0.293	0.161
12.14	0.278	0.153
15.07	0.265	0.145
16.66	0.251	0.137
18.08	0.244	0.134



Table A6.20:

Mean temperature of the fluid at the inlet to the test section = 157 C.

Mean temperature difference between the fluid and the tube wall = 63 C.

$h_{m,Ac} = 921 \text{ W/m}^2 \text{ K}$  and  $h_{m,Sh} = 1662 \text{ W/m}^2 \text{ K}$ .

% Mole fraction of NCG in the mixture.	$H_{Ac}$	$H_{Sh}$
0	0.814	0.451
1.24	0.478	0.265
2.41	0.401	0.221
3.67	0.340	0.188
5.15	0.326	0.186
6.55	0.305	0.169
8.98	0.292	0.162
10.41	0.286	0.158
12.24	0.257	0.152
15.05	0.259	0.144
16.66	0.261	0.144
18.48	0.257	0.142

Table A6.21:

Mean temperature of the fluid at the inlet to the test section = 182 °C.

Mean temperature difference between the fluid core and the tube wall = 72 °C.

$h_{m,Ac} = 947 \text{ W/m}^2 \text{ K}$  and  $h_{m,Sh} = 1744 \text{ W/m}^2 \text{ K}$ .

% Mole fraction of NCG in the mixture.	$H_{Ac}$	$H_{Sh}$
0	0.528	0.287
1.25	0.396	0.215
2.44	0.343	0.186
3.70	0.303	0.165
5.23	0.291	0.158
6.54	0.264	0.143
8.03	0.264	0.143
9.21	0.253	0.152
10.82	0.250	0.136
12.03	0.250	0.135
15.56	0.253	0.138
16.53	0.254	0.132

Table A6.22:

Mean temperature of the fluid at the inlet to the test section = 210 °C.

Mean temperature difference between the fluid core and the tube wall = 78 °C.

$h_{m,Ac} = 971 \text{ W/m}^2 \text{ K}$  and  $h_{m,Sh} = 1876 \text{ W/m}^2 \text{ K}$ .

% Mole fraction of NCG in the mixture.	$H_{Ac}$	$H_{Sh}$
0	0.400	0.207
1.24	0.335	0.173
2.50	0.296	0.153
3.70	0.270	0.140
6.42	0.252	0.129
7.15	0.232	0.120
8.01	0.232	0.120
10.68	0.218	0.113
13.78	0.233	0.120
14.94	0.216	0.112

Table A6.23:.

Mean temperature of fluid at the inlet to the test section = 222 °C.

Mean temperature difference between the fluid core and the tube wall = 85 °C.

$h_{m,Ac} = 894 \text{ W/m}^2 \text{ K}$  and  $h_{m,Sh} = 2050 \text{ W/m}^2 \text{ K}$ .

X Mole fraction of HCG in the mixture.	$H_{Ac}$	$H_{Sh}$
0	0.327	0.159
1.21	0.302	0.148
2.68	0.251	0.121
3.96	0.226	0.110
5.08	0.213	0.103
6.11	0.201	0.098
7.43	0.188	0.091
9.42	0.201	0.098
11.15	0.193	0.094
13.63	0.196	0.095

#### 6.4 TABULATED RESULTS OF THE PREDICTED TEMPERATURE PROFILES.

The following tables are extracts of the print out from the computer program used to predict the temperature profiles along the test section . The computer program used is presented as in the Appendix 4.2. For ease of reference the meanings of the symbols used in the tables is first presented.

See section on nomenclature for any further details.

$t_g(I)$  - The temperature at steam-NCG core at any axial position (I) [ °C ].

$t_w(I)$  - The corresponding cooling water temperature [ °C ].

$Re_d(I)$ - The corresponding Reynolds number of steam-NCG core.

$Y_a(I)$  - The corresponding mole fraction of NCG in the gaseous phase.

$Y_g(I)$  - The corresponding mole fraction of steam in the gaseous phase.

$dQ(I)$  - The total amount of heat transferred to cooling water from the steam-NCG inlet(origin) up to the  $I^{th}$  axial position per unit time interval [kW].

$U \cdot \Delta t(I)$  - The corresponding product of the overall heat transfer coefficient and the mean temperature difference between the steam-NCG core and the tube wall .

These quantities are calculated from the steam-air inlet(origin) up to to the I<sup>th</sup> axial position. [ $m^2/W$ ].

$\Delta A(I)$  - The surface area from the steam-NCG inlet(origin) up to the I<sup>th</sup> axial position [ $m^2$ ].

$\Delta L(I)$  - The corresponding axial length to the I<sup>th</sup> position [m].

6.4.1 THE INSIDE TUBE DIAMETER = 25.4mm(1") ,  
TUBE LENGTH =4000mm.

Table A6.24:

Mean temperature of fluid at the inlet to the test section = 127.5 °C.

Mass concentration of NCG in the mixture = 1.742 %.

Position I	1	2	3	4	5	6	7	8	9
$t_g(I) ^\circ C$	98.3	95.6	93.0	90.3	87.6	85.0	82.3	79.6	77.0
$t_v(I) ^\circ C$	48.5	46.6	46.3	46.1	46.0	45.9	45.9	45.8	45.8
$Re_d(I) \times 10^{-3}$	19.1	6.35	3.91	2.88	2.22	1.97	1.73	1.56	1.43
$Y_o(I)$	0.05	0.13	0.21	0.29	0.36	0.42	0.48	0.53	0.58
$Y_g(I)$	0.95	0.87	0.79	0.71	0.64	0.58	0.52	0.47	0.42
dQ(I) kW	5.0	3.02	1.83	1.64	1.46	1.27	1.11	0.96	0.81
$10^7/U\Delta t \ m^2/W$	199	330	545	609	686	785	897	1046	1241
$\Delta A(I) \ m^2$	0.14	0.15	0.17	0.18	0.20	0.21	0.22	0.26	0.31
$\Delta L(I) \ m$	1.70	1.92	2.12	2.29	2.46	2.60	2.73	3.23	3.83

Table A6.25:

Mean temperature of fluid at the inlet to the test section = 141.23 °C.  
mass concentration of NCG in the mixture = 2.796 %.

Position I	1	2	3	4	5	6
$t_g(I) \text{ }^\circ\text{C}$	97.6	94.5	91.4	88.2	85.1	82.0
$t_v(I) \text{ }^\circ\text{C}$	37.4	35.9	35.6	35.4	35.3	35.2
$Re_d(I) \times 10^{-3}$	13.88	5.56	3.59	2.71	2.22	1.91
$Y_a(I)$	0.07	0.17	0.26	0.34	0.42	0.49
$Y_g(I)$	0.93	0.83	0.74	0.65	0.58	0.51
$dQ(I) \text{ kW}$	4.42	2.09	1.86	1.65	1.45	1.26
$10^7/U\Delta t \text{ m}^2/W$	226	477	538	606	688	793
$\Delta A(I) \text{ m}^2$	0.16	0.18	0.19	0.20	0.21	0.28
$\Delta L(I) \text{ m}$	2.04	2.21	2.37	2.51	2.65	3.45

Table A6.26:

Mean temperature of fluid at the inlet to the test section = 138.9 °C.  
Mass concentration of NCG in the mixture = 3.15 %.

Position I	1	2	3	4	5	6
$t_g(I) \text{ }^\circ\text{C}$	98.4	95.6	92.7	89.8	86.9	84.0
$t_v(I) \text{ }^\circ\text{C}$	48.3	45.5	45.1	44.9	44.8	44.7
$Re_d(I) \times 10^{-3}$	20.29	5.67	3.40	2.48	1.99	1.69
$Y_a(I)$	0.04	0.13	0.22	0.30	0.38	0.44
$Y_g(I)$	0.96	0.87	0.78	0.70	0.62	0.56
$dQ(I) \text{ kW}$	5.27	3.18	1.87	1.69	1.49	1.30
$10^7/U\Delta t \text{ m}^2/W$	189	314	532	591	672	769
$\Delta A(I) \text{ m}^2$	0.16	0.17	0.18	0.19	0.24	0.28
$\Delta L(I) \text{ m}$	1.96	2.13	2.29	2.41	2.97	3.49

Table A6.27:

Mean temperature of fluid at the inlet to the test section = 129.8 °C.

Mass concentration of NCG in the mixture = 4.41 %.

Position I	1	2	3	4	5	6	7	8	9
$t_g(I) \text{ } ^\circ\text{C}$	96.3	93.3	90.2	87.2	84.2	81.1	78.1	75.0	72.0
$t_v(I) \text{ } ^\circ\text{C}$	46.9	46.3	46.1	46.0	45.9	45.9	45.9	45.8	45.8
$Re_d(I) \times 10^{-3}$	10.2	5.42	3.79	2.97	2.49	2.18	1.95	1.79	1.67
$Y_a(I)$	0.11	0.21	0.29	0.37	0.44	0.50	0.56	0.61	0.66
$Y_g(I)$	0.89	0.79	0.71	0.63	0.54	0.50	0.44	0.39	0.34
$dQ(I) \text{ kW}$	3.09	1.69	1.49	1.29	1.08	0.90	0.73	0.57	0.42
$10^7/U\Delta t \text{ m}^2/W$	323	590	672	781	921	1113	1376	1759	2376
$\Delta A(I) \text{ m}^2$	0.04	0.06	0.07	0.07	0.08	0.12	0.16	0.25	0.28
$\Delta L(I) \text{ m}$	0.50	0.75	0.81	0.90	1.00	1.50	2.01	3.10	3.52



6.4.2 THE INSIDE TUBE DIAMETER = 38.1mm(1.5"),

TUBE LENGTH = 4000mm.

Table A6.28:

Mean temperature of fluid at the inlet to the test section = 135.5 °C.

Mass concentration of NCG in the mixture = 2.01 %.

Position I	1	2	3	4	5	6	7
$t_g(I) \text{ } ^\circ\text{C}$	97.6	90.8	84.1	77.3	70.6	63.8	56.9
$t_v(I) \text{ } ^\circ\text{C}$	32.3	29.3	28.9	28.7	28.4	28.4	28.3
$Re_d(I) \times 10^{-3}$	7.54	1.79	1.11	0.84	0.71	0.64	0.60
$Y_a(I)$	0.07	0.27	0.44	0.58	0.68	0.76	0.83
$Y_g(I)$	0.93	0.83	0.56	0.42	0.32	0.24	0.17
$dQ(I) \text{ kW}$	3.95	2.39	1.85	1.43	1.09	0.82	0.58
$10^7/U\Delta t \text{ m}^2/W$	253	418	541	699	914	1222	1723
$\Delta A(I) \text{ m}^2$	0.13	0.17	0.20	0.22	0.24	0.27	0.33
$\Delta L(I) \text{ m}$	1.11	1.42	1.65	1.86	2.04	2.23	2.77

Table A6.29:

Mean temperature of fluid at the inlet to the test section = 185.9 °C.

Mass concentration of NCG in the mixture = 5.32 %.

Position I	1	2	3	4	5	6
$t_g(I) \text{ }^\circ\text{C}$	96.1	89.6	83.3	76.8	70.4	64.0
$t_v(I) \text{ }^\circ\text{C}$	33.6	32.2	31.8	31.6	31.5	31.4
$Re_d(I) \times 10^{-3}$	4.32	1.63	1.08	0.85	0.73	0.66
$Y_a(I)$	0.11	0.31	0.46	0.59	0.68	0.76
$Y_g(I)$	0.89	0.69	0.54	0.41	0.32	0.24
$dQ(I) \text{ kW}$	3.28	2.23	1.74	1.34	1.03	0.76
$10^7/U\Delta t \text{ m}^2/W$	305	448	575	743	873	1309
$\Delta A(I) \text{ m}^2$	0.14	0.18	0.20	0.23	0.25	0.29
$\Delta L(I) \text{ m}$	1.23	1.48	1.70	1.92	2.09	2.42

Table A6.30:

Mean temperature of fluid at the inlet to the test section = 185.3 °C.

Mass concentration of NCG in the mixture = 5.76 %.

Position I	1	2	3	4	5	6	7
$t_g(I) \text{ }^\circ\text{C}$	97.3	94.5	91.6	88.7	85.7	82.8	80.0
$t_v(I) \text{ }^\circ\text{C}$	35.3	33.7	33.2	32.9	32.8	32.7	32.6
$Re_d(I) \times 10^{-3}$	6.74	2.99	1.98	1.51	1.24	1.07	0.75
$Y_a(I)$	0.08	0.17	0.25	0.33	0.40	0.47	0.53
$Y_g(I)$	0.92	0.83	0.75	0.67	0.60	0.53	0.47
$dQ(I) \text{ kW}$	3.77	2.68	2.39	2.13	1.91	1.70	1.52
$10^7/U\Delta t \text{ m}^2/W$	265	372	418	468	524	587	659
$\Delta A(I) \text{ m}^2$	0.07	0.18	0.19	0.20	0.21	0.22	0.26
$\Delta L(I) \text{ m}$	1.41	1.52	1.59	1.68	1.77	1.86	2.13

6.4.3 TABULATED EXPERIMENTAL STEAM-AIR CORE TEMPERATURE PROFILE.

INSIDE TUBE DIAMETER = 25.4mm AND TUBE LENGTH = 4000mm.

Table A6.31:

Mass concentration of air (%)	Axial position (m).						
	0	0.2	1.4	2.2	3.0	3.6	4
1.742	128	109	100	91	80	78	78
2.796	141	130	116	103	88	86	84
3.15	140	122	103	100	86	84	82
4.417	125	108	97	85	78	73	72

6.4.4 TABULATED EXPERIMENTAL STEAM-AIR CORE TEMPERATURE

PROFILE INSIDE TUBE DIAMETER = 38.1mm AND

TUBE LENGTH = 4000mm.

Table A6.32:

Mass concentration of air (%)	Axial position(m).								
	0	0.4	0.8	1.6	2.4	2.8	3.2	3.6	4.0
2.01	186	166	151	130	120	117	90	79	64
5.32	186	165	153	129	119	115	87	74	57
5.76	135	120	112	102	99	89	87	85	80

6.4.5 TABULATED EXPERIMENTAL STEAM-AIR CORE AND TUBE WALL TEMPERATURE PROFILES.

INSIDE TUBE DIAMETER = 25.4mm AND TUBE LENGTH = 4000mm.

a) WALL TEMPERATURE PROFILES

Table:- A6.33

Mass fraction of air (%)	Axial position (m).											
	0	0.4	08	1.2	1.6	2.0	2.4	2.8	3.2	3.6	4.0	
Super-heated Steam												
0	77	77	74	74	72	73	77	74	80	38	38	
2.94	74	75	76	78	76	76	76	76	80	70	70	
12.71	77	76	76	77	74	73	77	72	73	68	68	
19.53	75	77	77	77	74	77	77	73	72	70	70	
saturated steam												
0	42	37	30	30	28	23	19	18	17	17	17	
4.94	68	67	66	58	47	44	38	30	22	22	22	

b) STEAM-AIR CORE TEMPERATURE PROFILES.

Table:- A6.34

Mass concentration of air (%)	Axial position (m).						
	0	0.2	1.4	2.2	3.0	3.6	4.0
0	181	173	152	133	106	57	57
2.94	190	185	162	139	109	98	92
12.71	193	174	142	110	92	85	84
19.53	180	173	145	116	96	88	82
0	98	86	81	47	24	23	23
4.94	95	83	81	78	62	60	60

6.5 TABLES FOR CONDENSATION HEAT TRANSFER COEFFICIENT PROFILE  
ALONG THE TEST SECTION

6.5.1 THE INSIDE TUBE DIAMETER = 25.4mm(1"), LENGTH=4000mm.

Table:- A6.35.

The steam superheated at the inlet to the test section.  
Mass concentration of NCG in the mixture = 0%.  
The temperature rise of cooling water = 10.6 °C.

Position along the test section (m).	Local condensation heat transfer coefficient(h) W/m <sup>2</sup> K
0.5.	733
1.0.	820
1.5	995
2.0	1229
2.5	1608
3.0	2200
3.5	2787
4.0	2787

Table:- A6.36.

The steam superheated at the inlet to the test section.  
Mass concentration of NCG in the mixture = 2.94%.  
The temperature rise of cooling water = 10.5 °C.

Position along the test section (m).	Local condensation heat transfer coefficient(h) W/m <sup>2</sup> K.
0.5	637
1.0	702
1.5	829
2.0	1036
2.5	1381
3.0	1883
3.5	2588
4.0	3196

Table:- A6.37.

The steam superheated at the inlet to the test section.  
Mass concentration of NCG in the mixture = 12.71%.  
The temperature rise of cooling water = 12.4 °C.

Position along the test section (m).	Local condensation heat transfer coefficient(h) W/m <sup>2</sup> K
0.5	858
1.0	1063
1.5	1358
2.0	1881
2.5	2717
3.0	4078
3.5	5434
4.0	4891

Table:- A6.38

The steam superheated at the inlet to the test section.  
Mass concentration of NCG in the mixture = 19.53%.  
The temperature rise of cooling water = 8.3 °C.

Position along the test section (m).	Local condensation heat transfer coefficient(h) W/m <sup>2</sup> K.
0.5	735
1.0	881
1.5	1062
2.0	1428
2.5	1882
3.0	2761
3.5	4141
4.0	5178

6.5.2 THE INSIDE TUBE DIAMETER = 25.4mm(1"), LENGTH=4000mm.

Table:- A6.39.

The steam saturated at the inlet to the test section.  
 Mass concentration of NCG in the mixture = 0%.  
 The temperature rise of cooling water = 7.2 °C.

Position along the test section (m).	Local condensation heat transfer coefficient(h) W/m <sup>2</sup> K.
0.5	233
1.0	350
1.5	383
2.0	400
2.5	483
3.0	650
3.5	883
4.0	1550

Table A6.40

The steam superheated at the inlet to the test section.  
 Mass concentration of NCG in the mixture = 4.94%.  
 The temperature rise of cooling water = 6.7 °C.

Position along the test section (m).	Local condensation heat transfer coefficient(h) W/m <sup>2</sup> K
0.5	610
1.0	523
1.5	459
2.0	407
2.5	378
3.0	343
3.5	319
4.0	297



6.6 TABULATED RESULTS OF THE PREDICTED PRESSURE DROP VERSUS EXPERIMENTAL VALUES OF THE PRESSURE DROP ACROSS THE TEST SECTION [See section 6.6].

Table:- A6.41.

Inside tube diameter = 25.4 mm ( 1").  
Tube length = 4000mm.

Predicted pressure drop [mm of water]	Experimental pressure drop [mm of water]
0	0
1	0.5
2	1.5
10	11
18	22
30	30
40	43
50	47
60	55
67	64
74	68

APPENDIX 7

GRAPHS

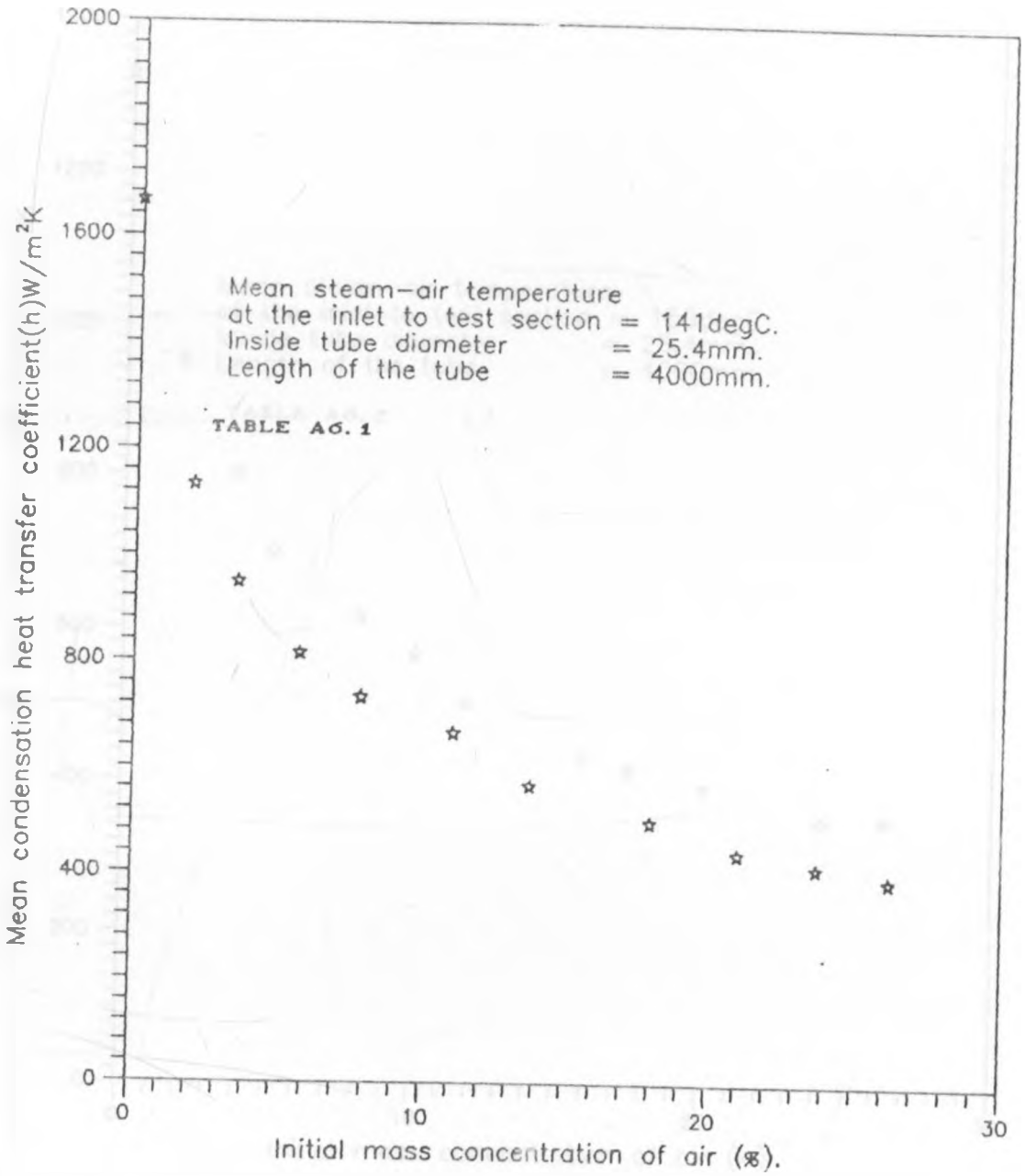


FIGURE A7.1: EXPERIMENTAL CONDENSATION HEAT TRANSFER COEFFICIENT v INITIAL AIR MASS CONCENTRATION

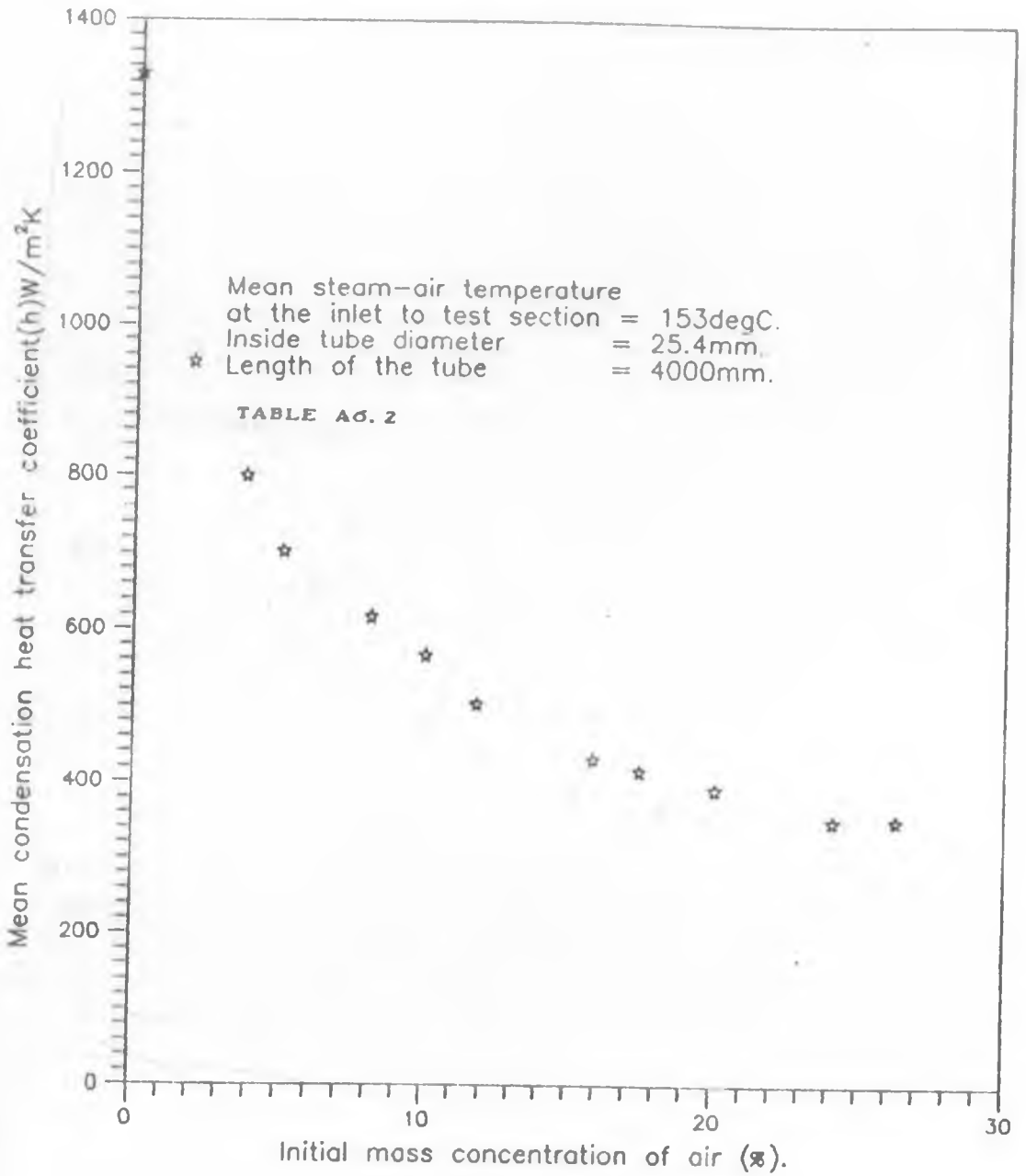


FIGURE A7.2: EXPERIMENTAL CONDENSATION HEAT TRANSFER COEFFICIENT  
v INITIAL AIR MASS CONCENTRATION

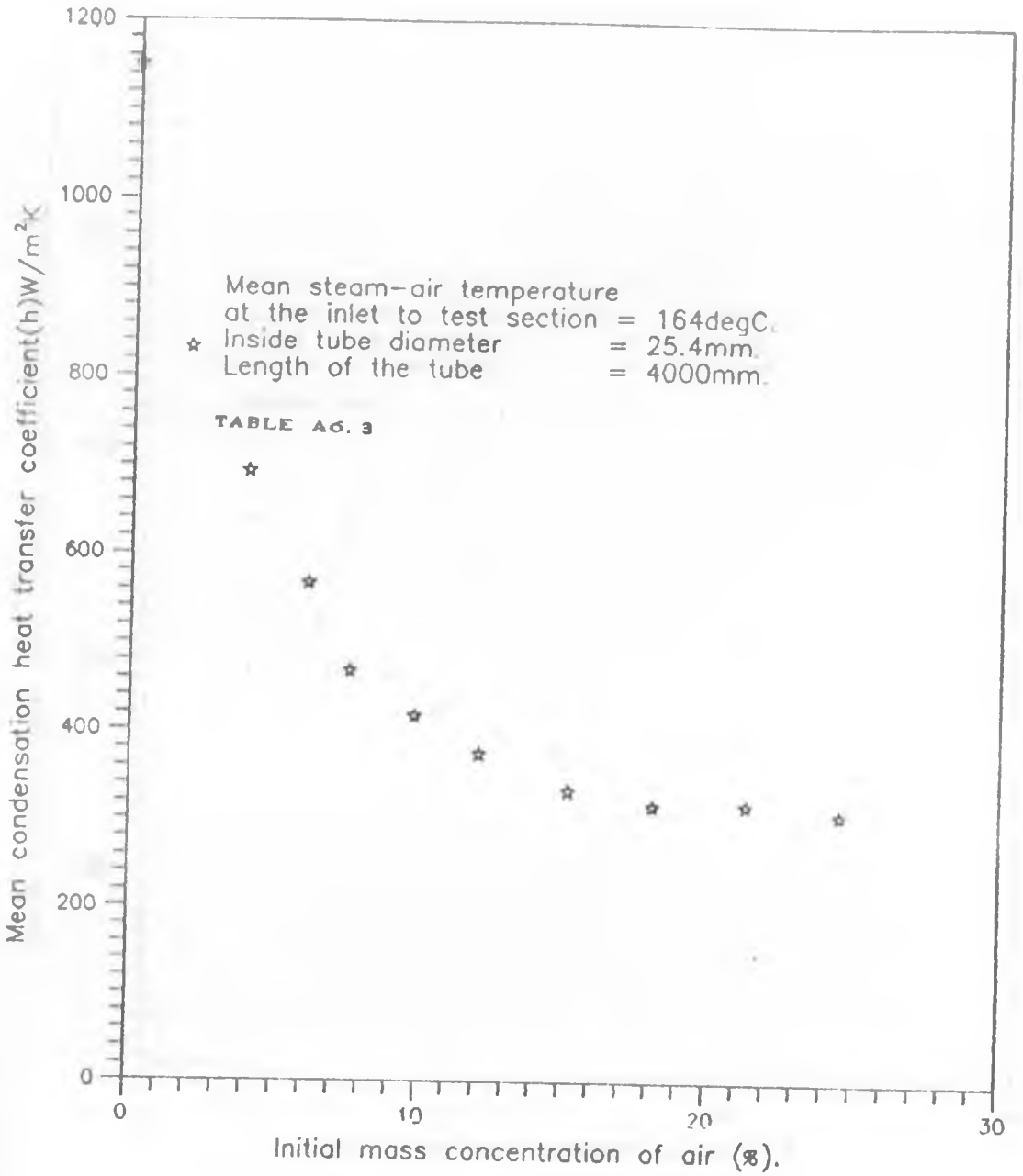


FIGURE A7.3: EXPERIMENTAL CONDENSATION HEAT TRANSFER COEFFICIENT  $\nu$  INITIAL AIR MASS CONCENTRATION

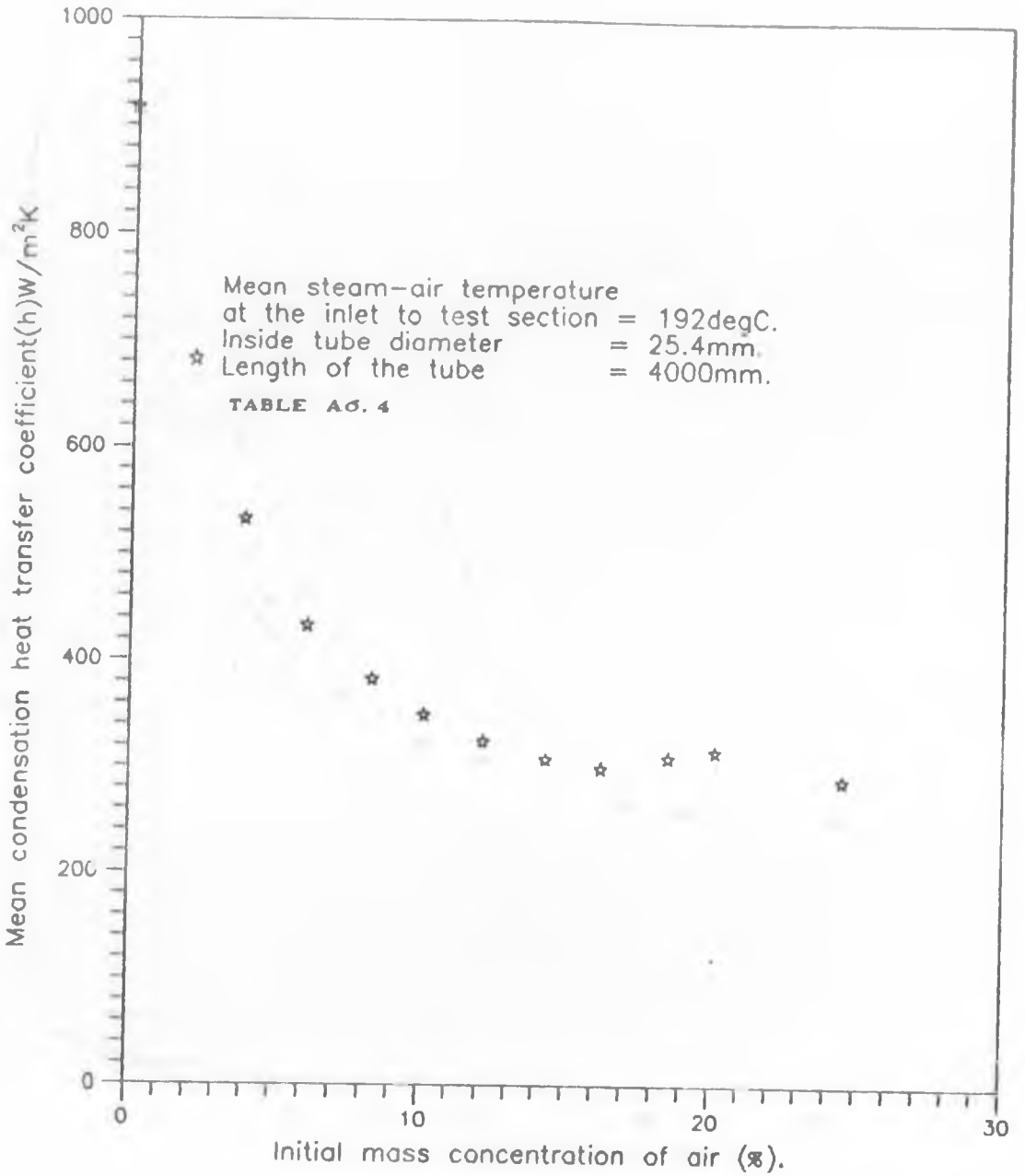


FIGURE A7.4: EXPERIMENTAL CONDENSATION HEAT TRANSFER COEFFICIENT  
v INITIAL AIR MASS CONCENTRATION

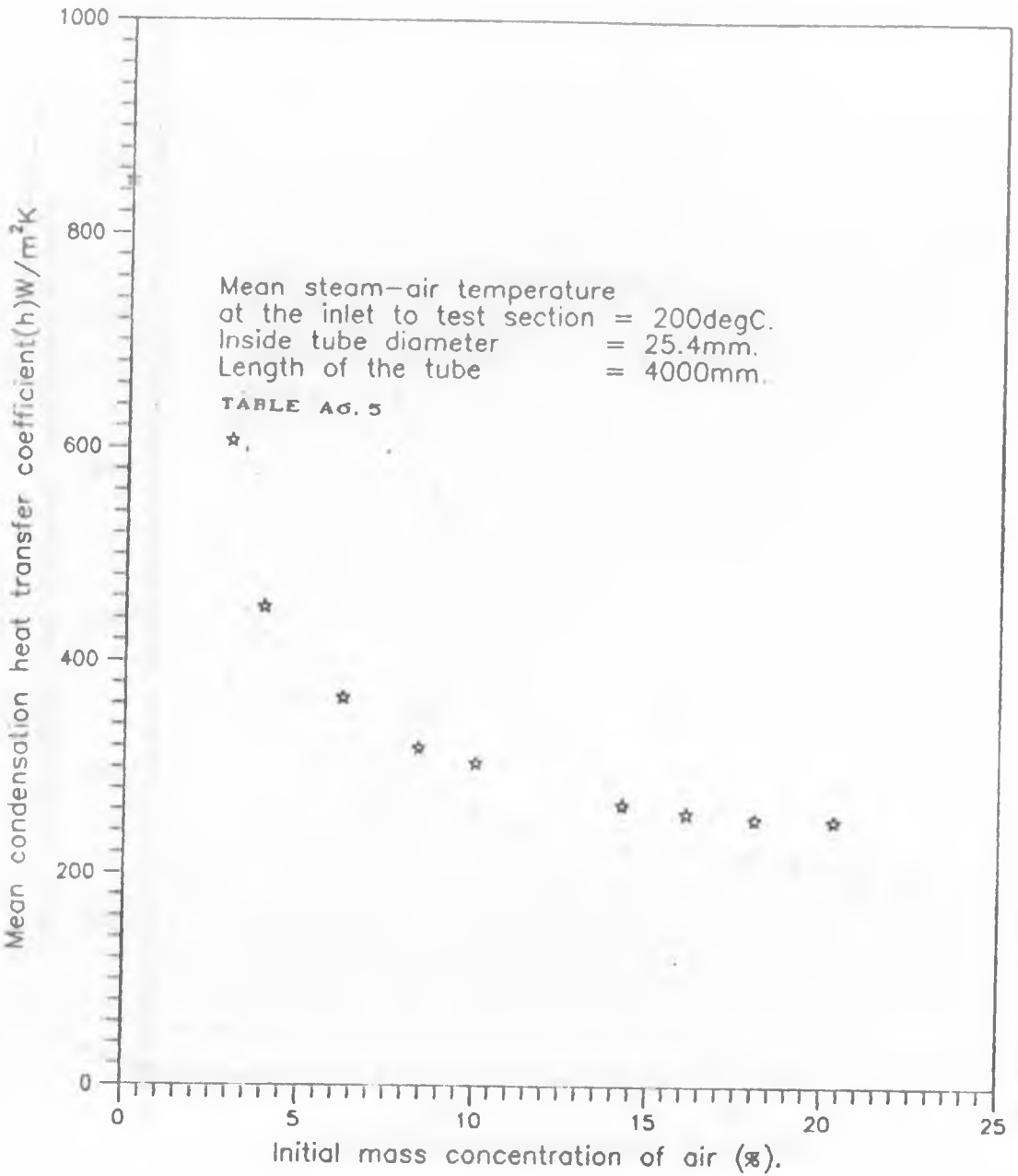


FIGURE A7.5: EXPERIMENTAL CONDENSATION HEAT TRANSFER COEFFICIENT v INITIAL AIR MASS CONCENTRATION

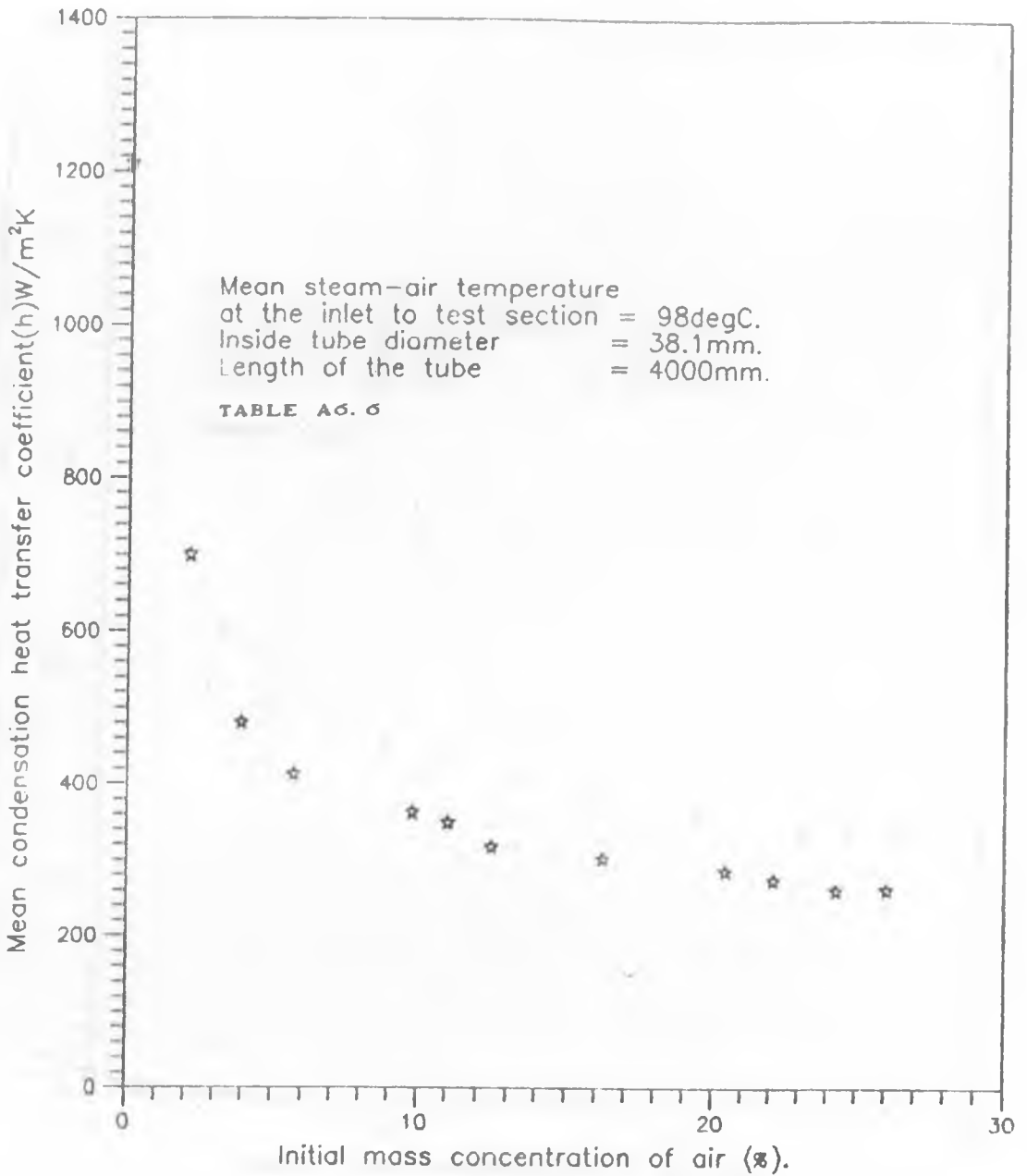


FIGURE A7.6: EXPERIMENTAL CONDENSATION HEAT TRANSFER COEFFICIENT v INITIAL AIR MASS CONCENTRATION



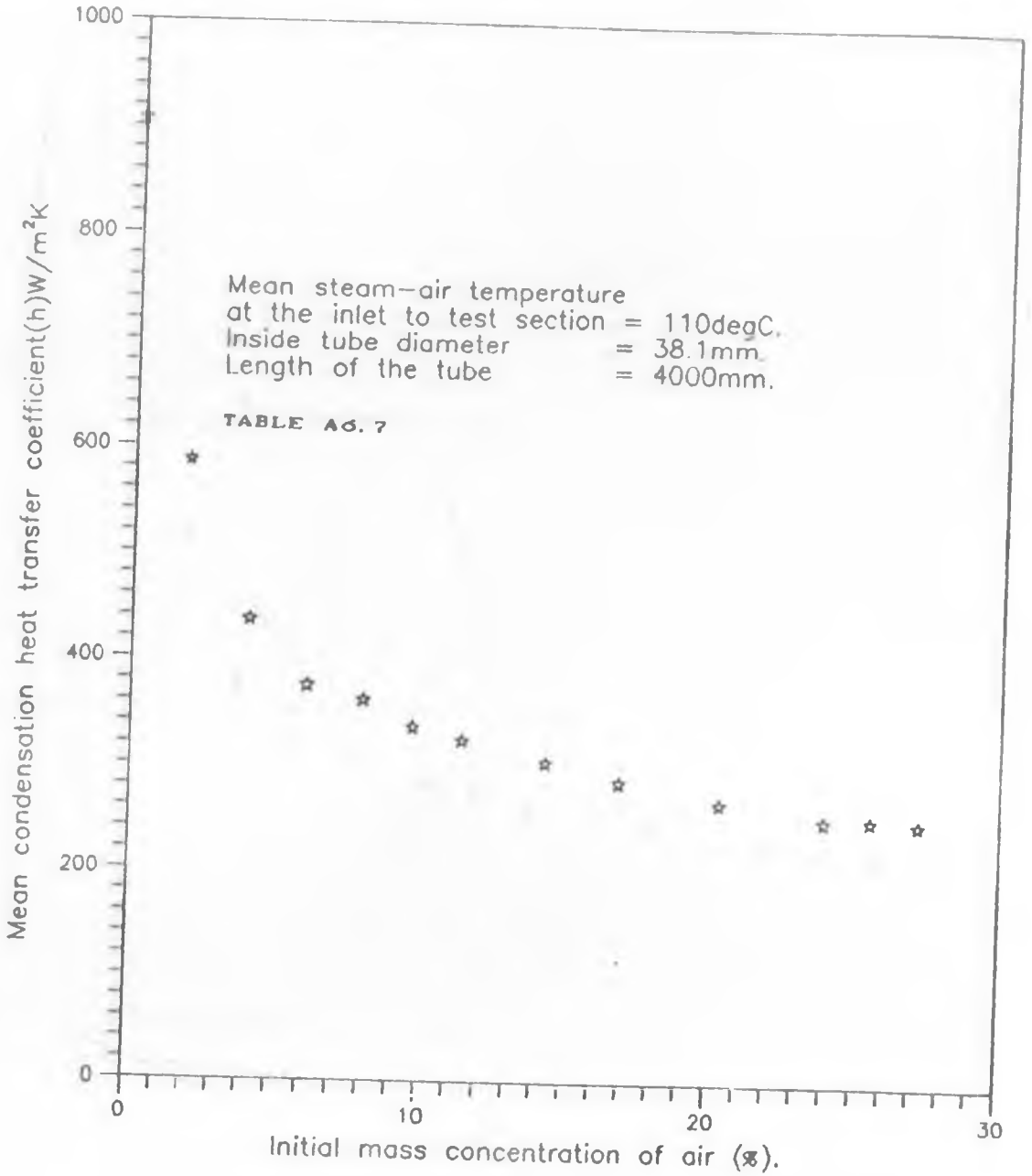


FIGURE A7.7: EXPERIMENTAL CONDENSATION HEAT TRANSFER COEFFICIENT  
v INITIAL AIR MASS CONCENTRATION

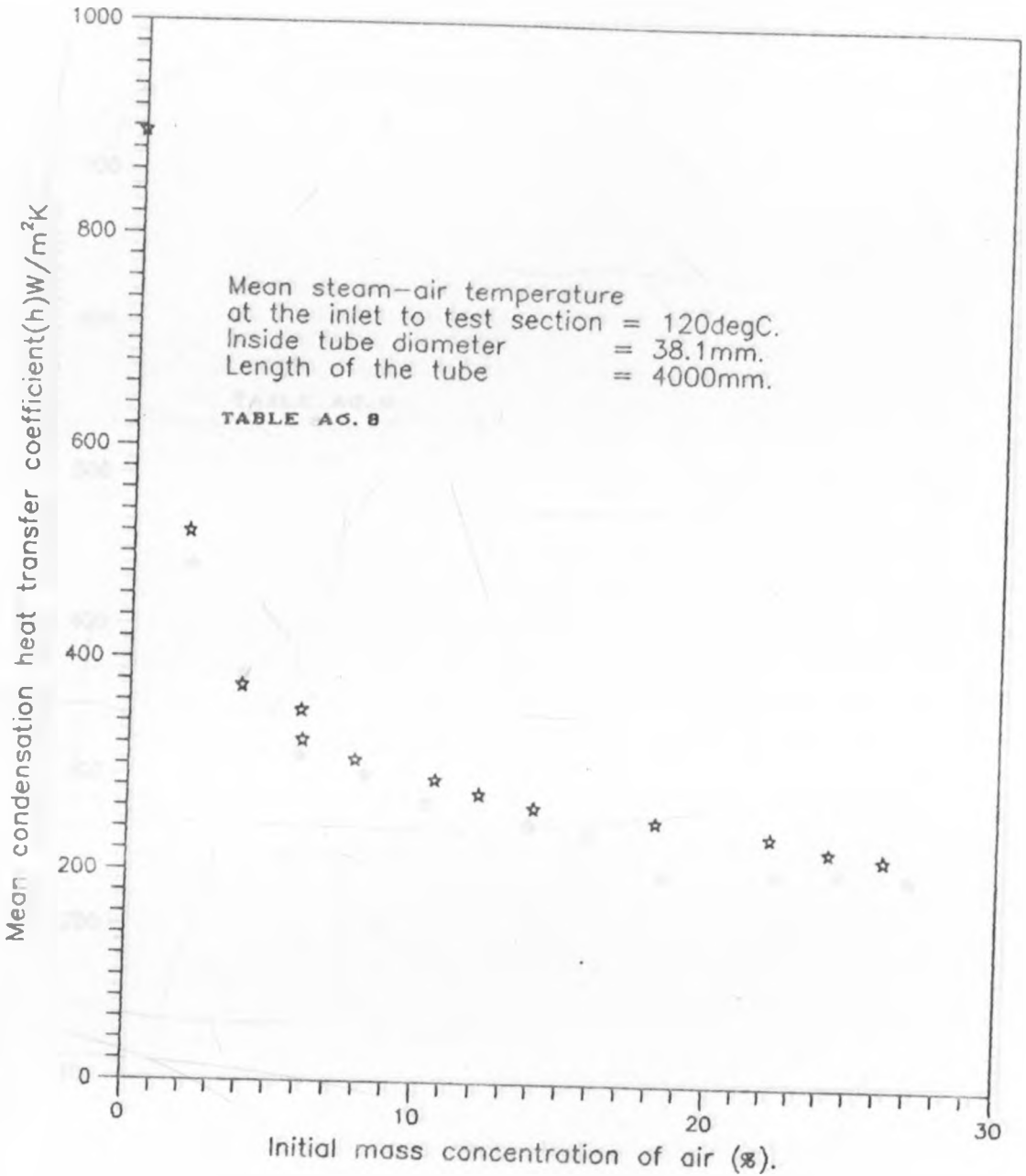


FIGURE A7.8: EXPERIMENTAL CONDENSATION HEAT TRANSFER COEFFICIENT v INITIAL AIR MASS CONCENTRATION

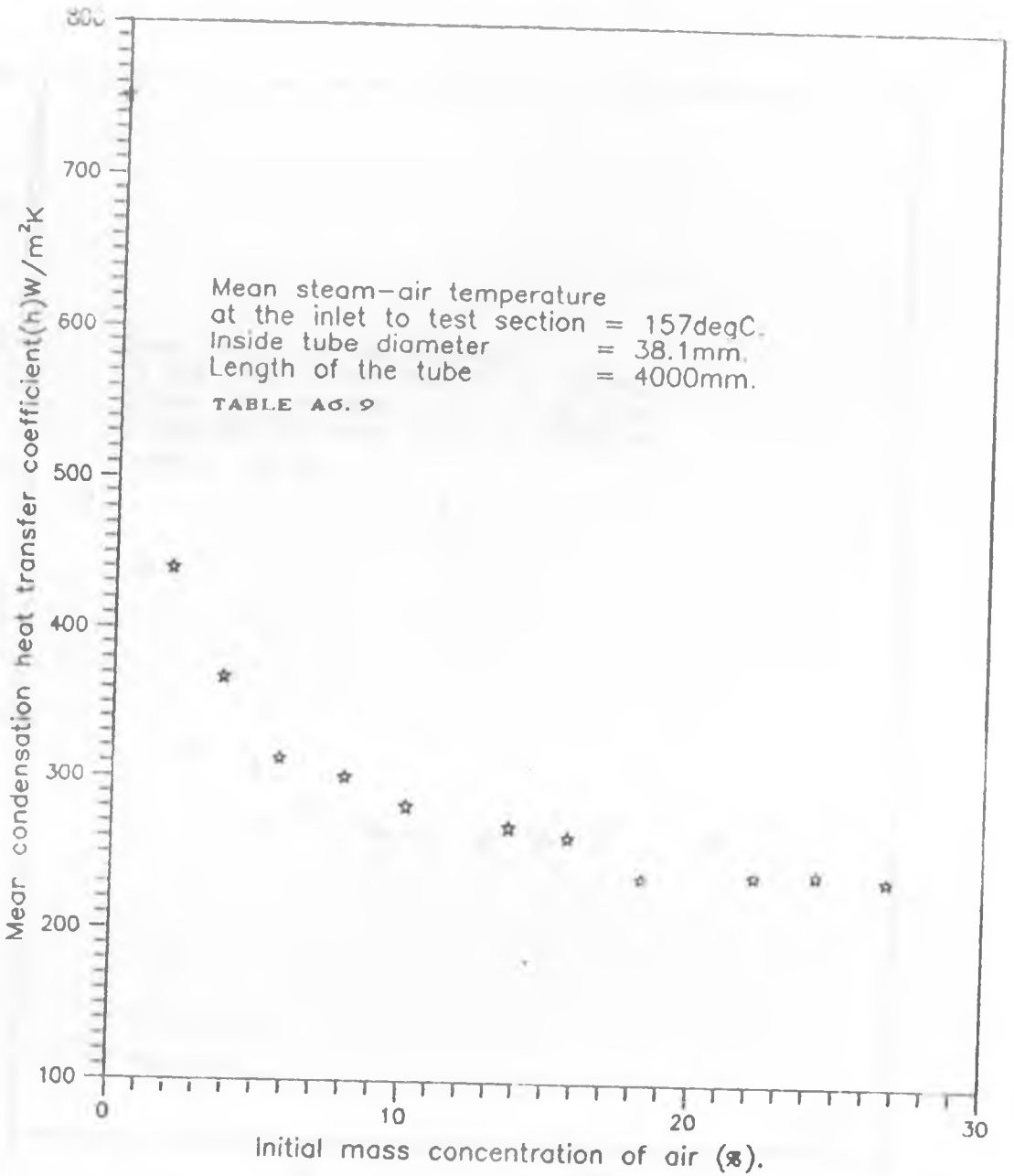


FIGURE A7.9: EXPERIMENTAL CONDENSATION HEAT TRANSFER COEFFICIENT v INITIAL AIR MASS CONCENTRATION

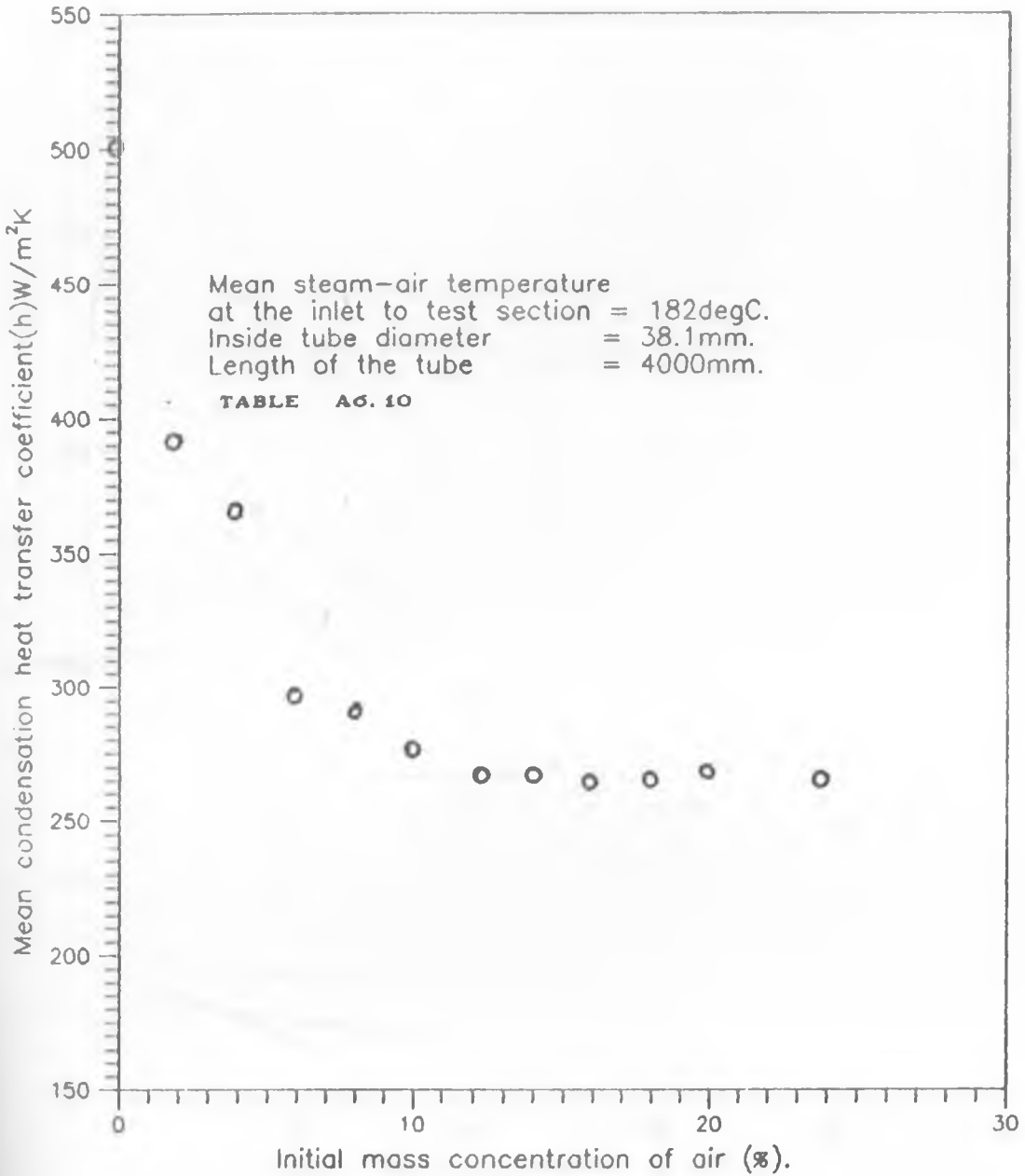


FIGURE A7.10: EXPERIMENTAL CONDENSATION HEAT TRANSFER COEFFICIENT v INITIAL AIR MASS CONCENTRATION

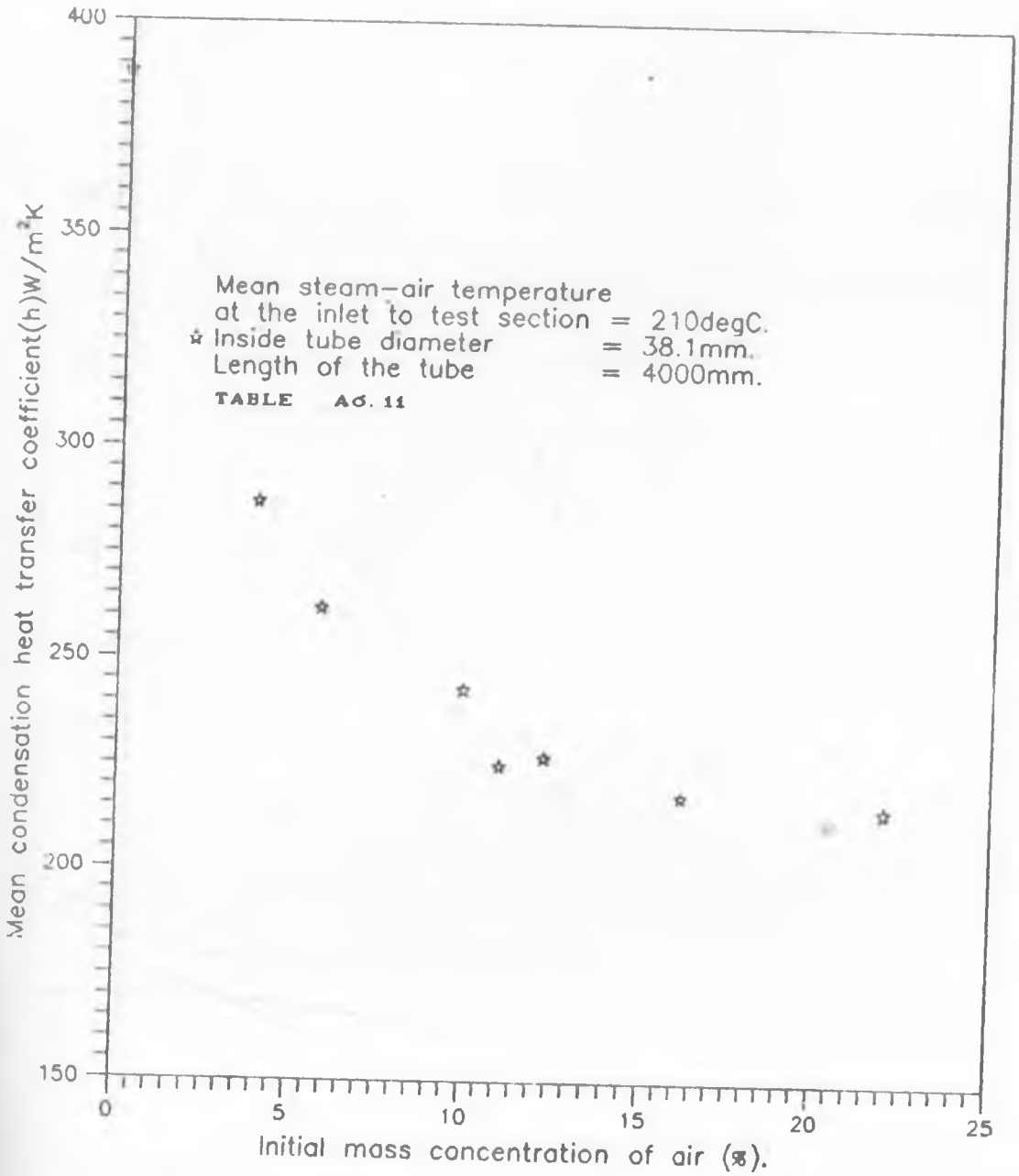


FIGURE A7.11: EXPERIMENTAL CONDENSATION HEAT TRANSFER COEFFICIENT v INITIAL AIR MASS CONCENTRATION

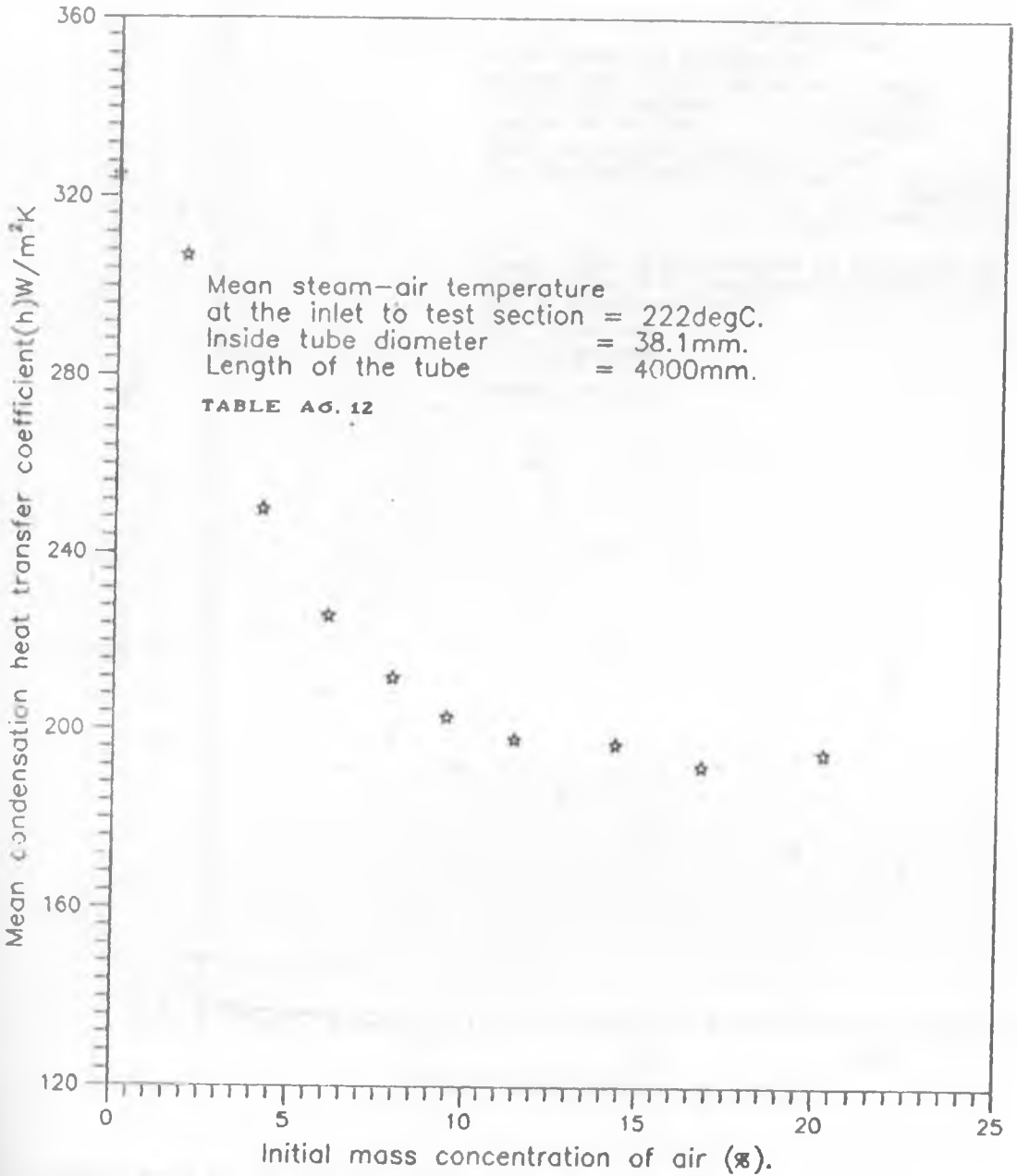


FIGURE A7.12: EXPERIMENTAL CONDENSATION HEAT TRANSFER COEFFICIENT  $\nu$  INITIAL AIR MASS CONCENTRATION

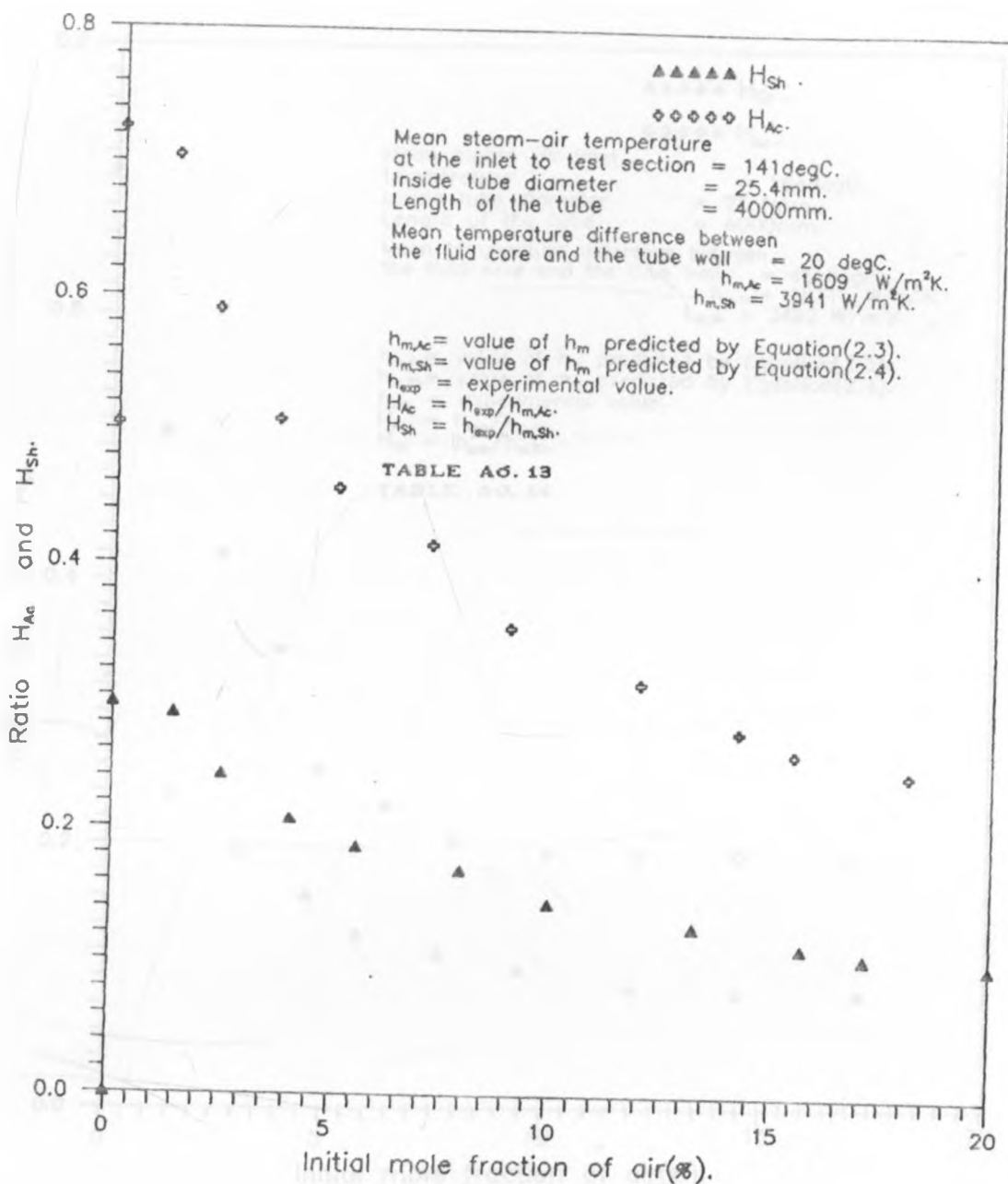


FIGURE A7.13: RATIOS OF EXPERIMENTAL TO PREDICTED CONDENSATION HEAT TRANSFER COEFFICIENT  $\nu$  INITIAL MOLE FRACTION OF AIR IN THE MIXTURE

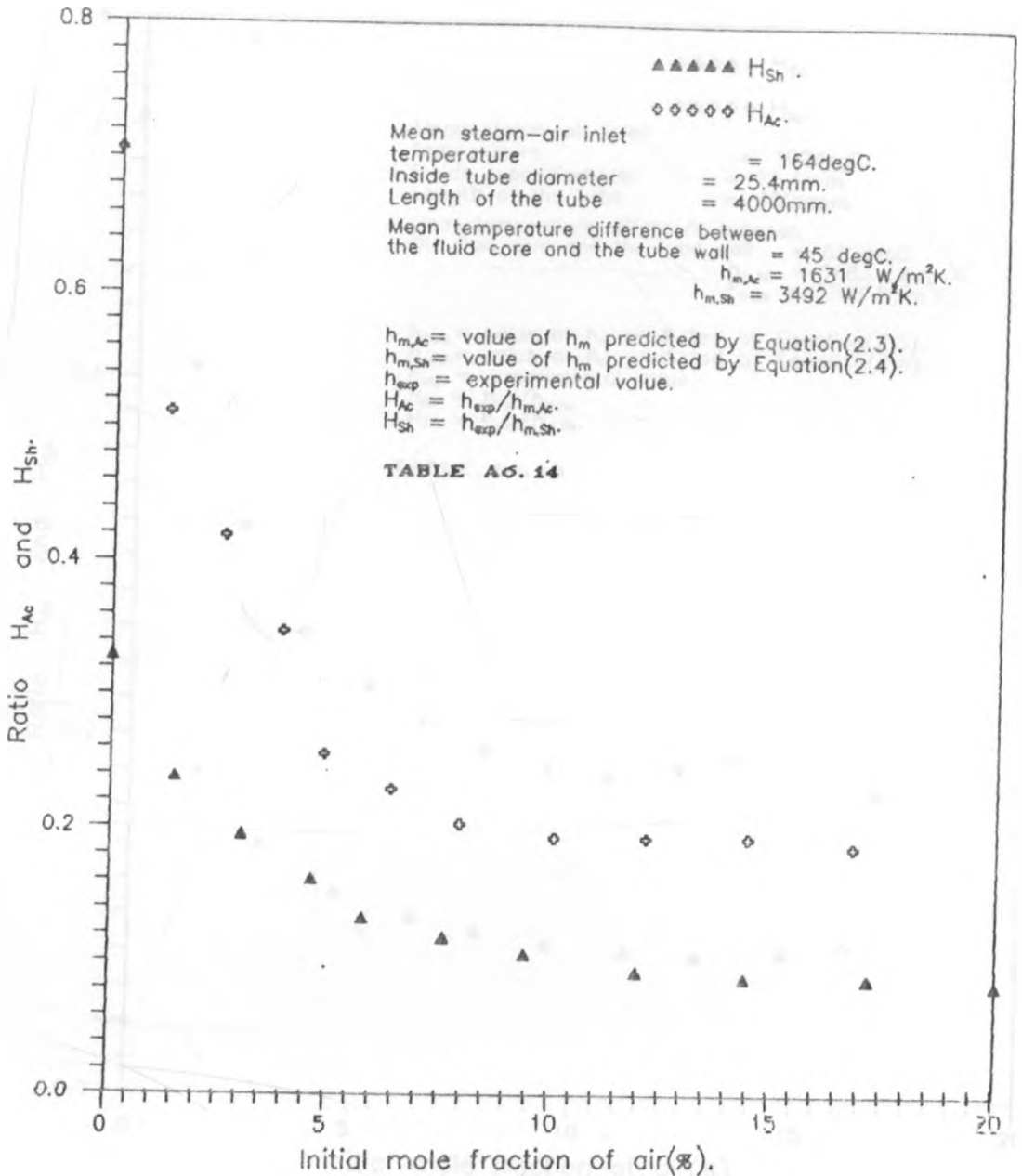


FIGURE A7.14: RATIOS OF EXPERIMENTAL TO PREDICTED CONDENSATION HEAT TRANSFER COEFFICIENT  $\nu$  INITIAL MOLE FRACTION OF AIR IN THE MIXTURE



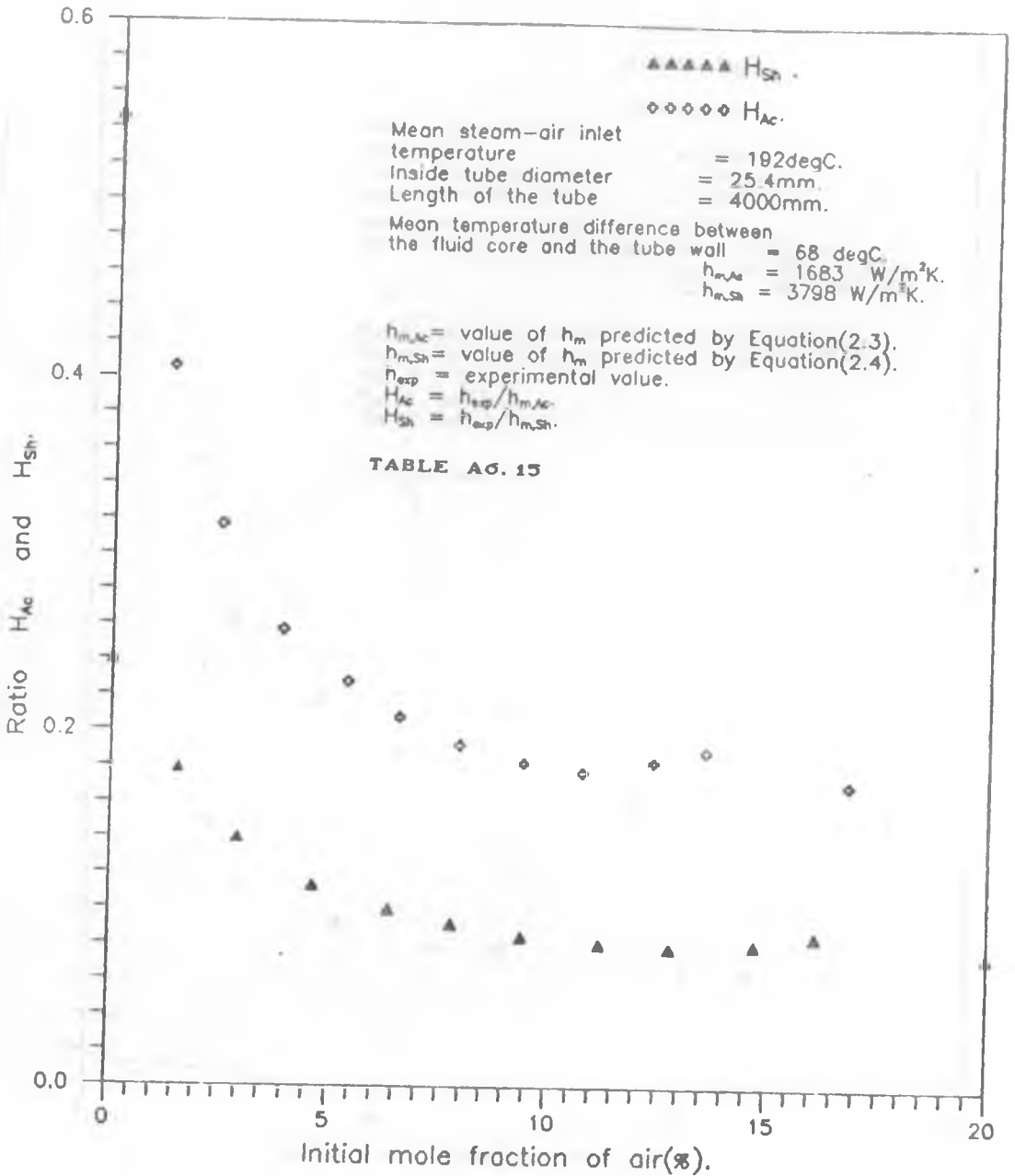


FIGURE A7.15: RATIOS OF EXPERIMENTAL TO PREDICTED CONDENSATION HEAT TRANSFER COEFFICIENT v INITIAL MOLE FRACTION OF AIR IN THE MIXTURE

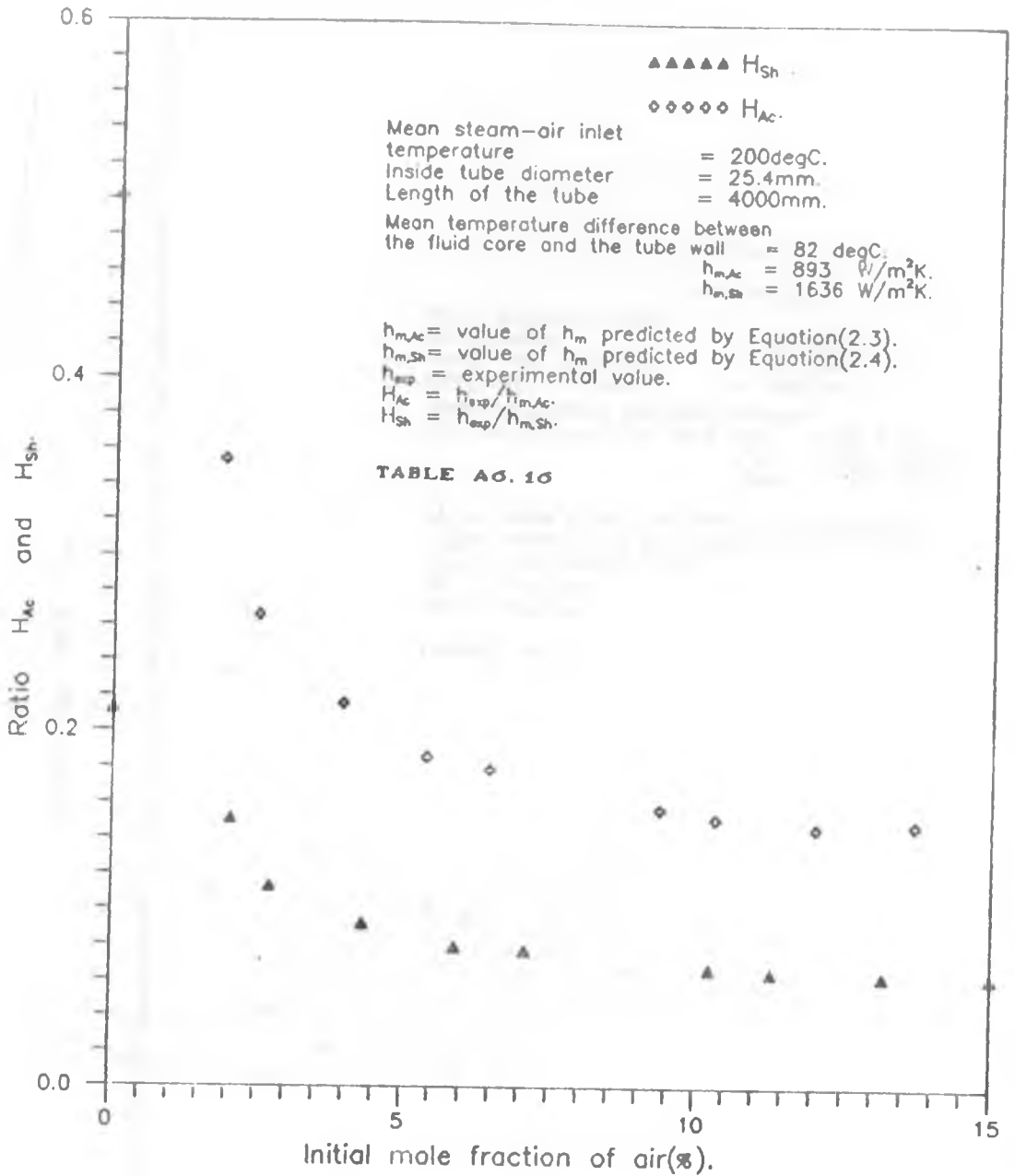


FIGURE A7.16: RATIOS OF EXPERIMENTAL TO PREDICTED CONDENSATION HEAT TRANSFER COEFFICIENT  $\nu$  INITIAL MOLE FRACTION OF AIR IN THE MIXTURE

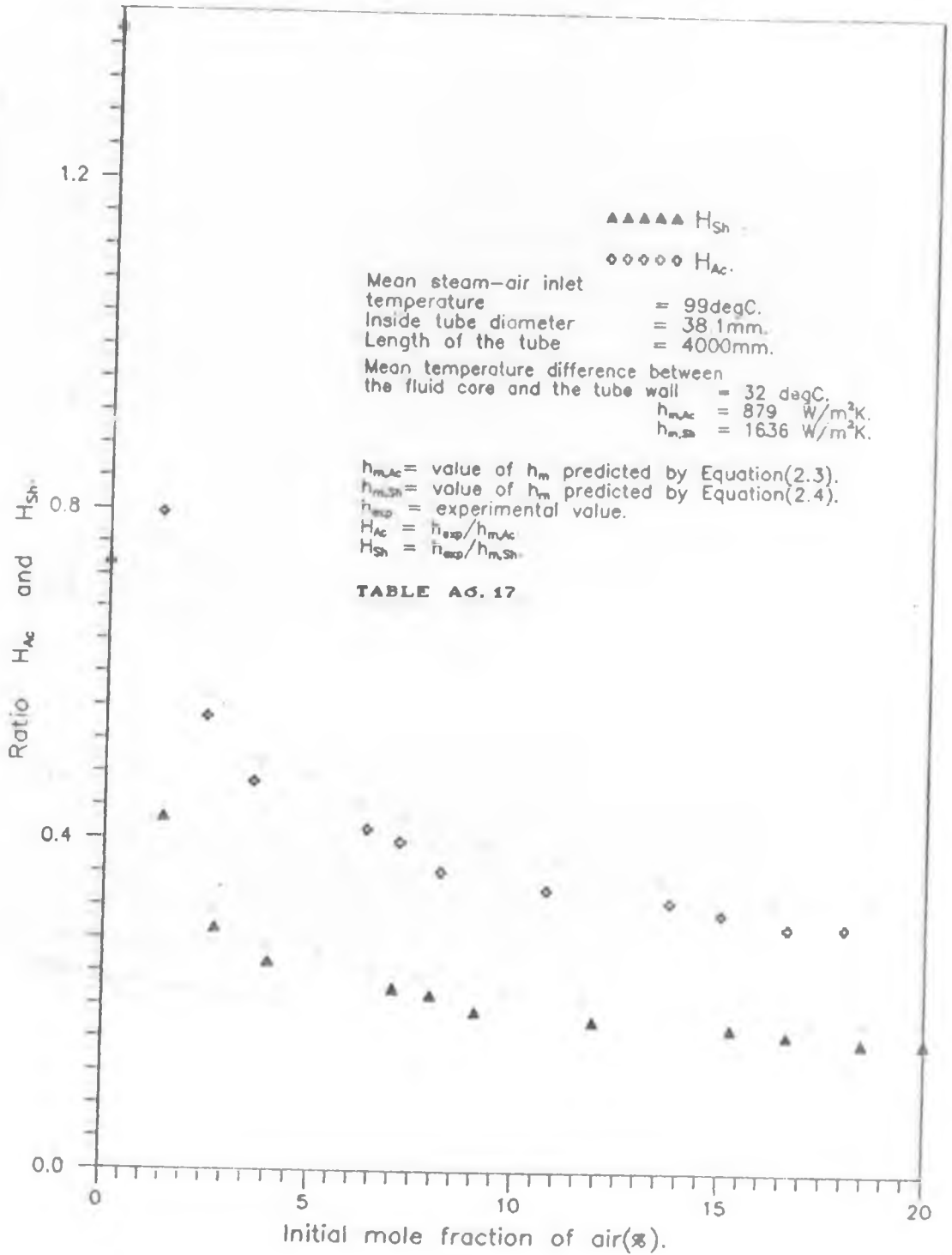


FIGURE A7.17: RATIOS OF EXPERIMENTAL TO PREDICTED CONDENSATION HEAT TRANSFER COEFFICIENT  $\nu$  INITIAL MOLE FRACTION OF AIR IN THE MIXTURE

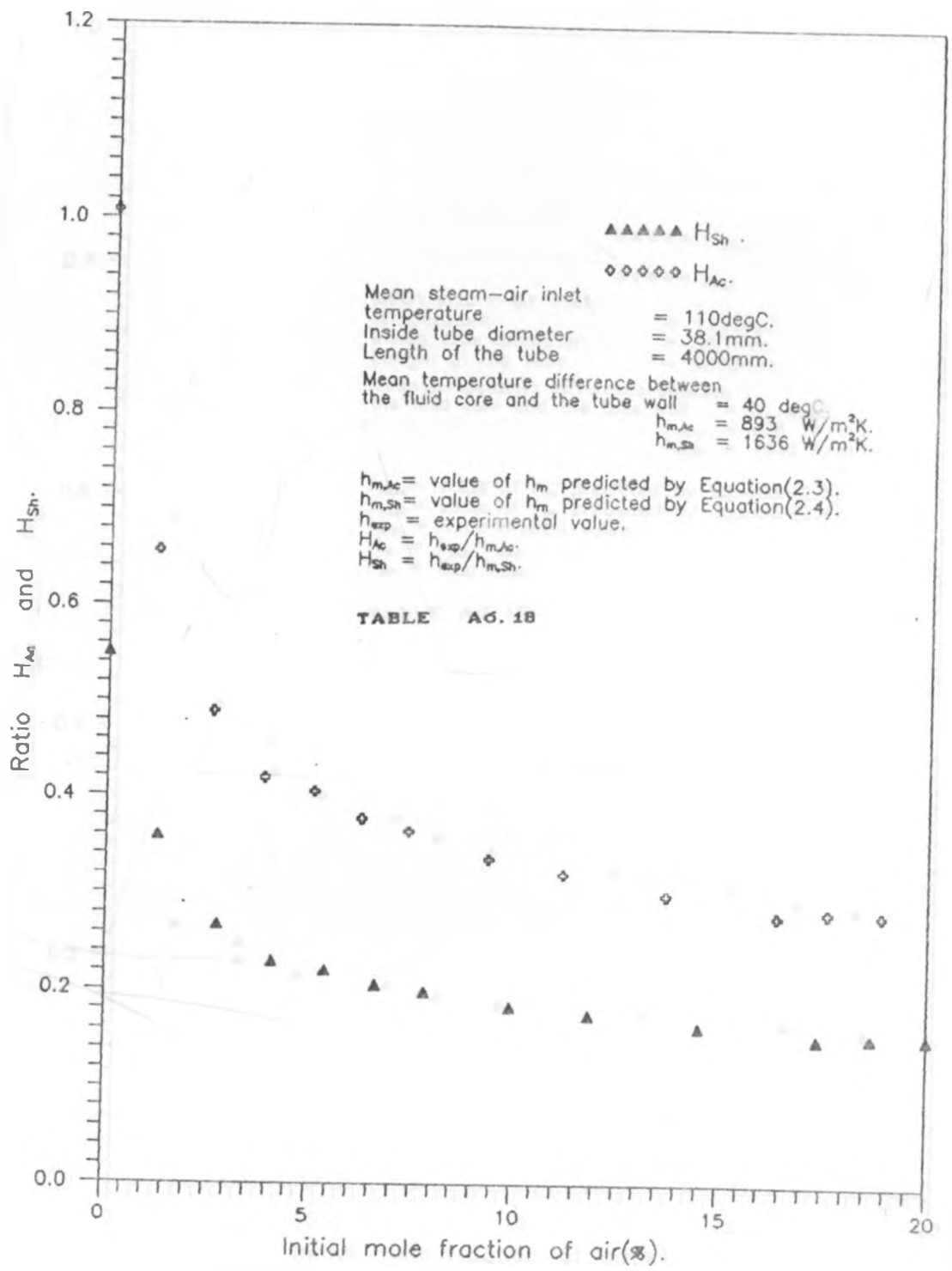


FIGURE A7.18: RATIOS OF EXPERIMENTAL TO PREDICTED CONDENSATION HEAT TRANSFER COEFFICIENT v INITIAL MOLE FRACTION OF AIR IN THE MIXTURE

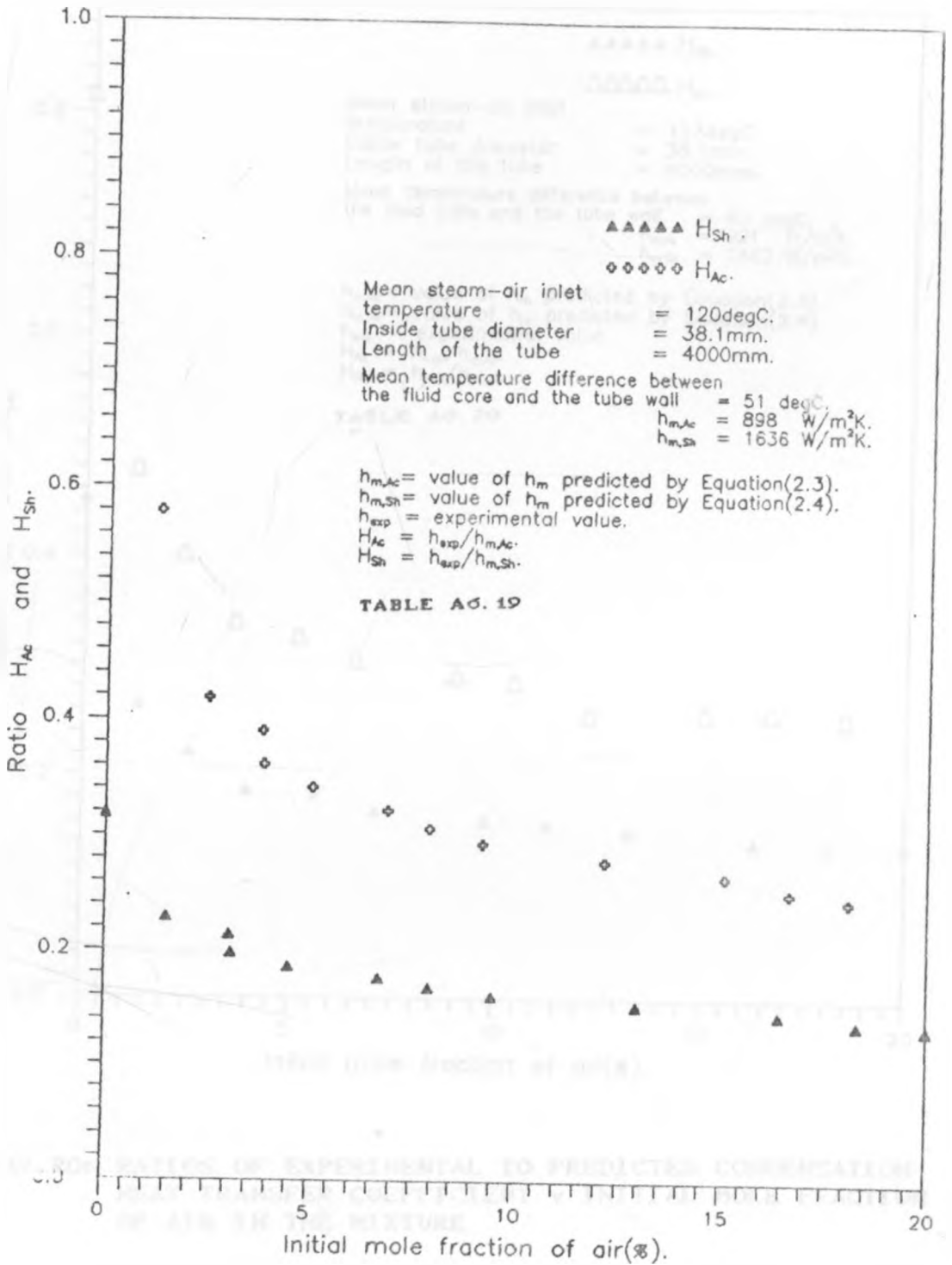


FIGURE A7.19: RATIOS OF EXPERIMENTAL TO PREDICTED CONDENSATION HEAT TRANSFER COEFFICIENT  $\nu$  INITIAL MOLE FRACTION OF AIR IN THE MIXTURE

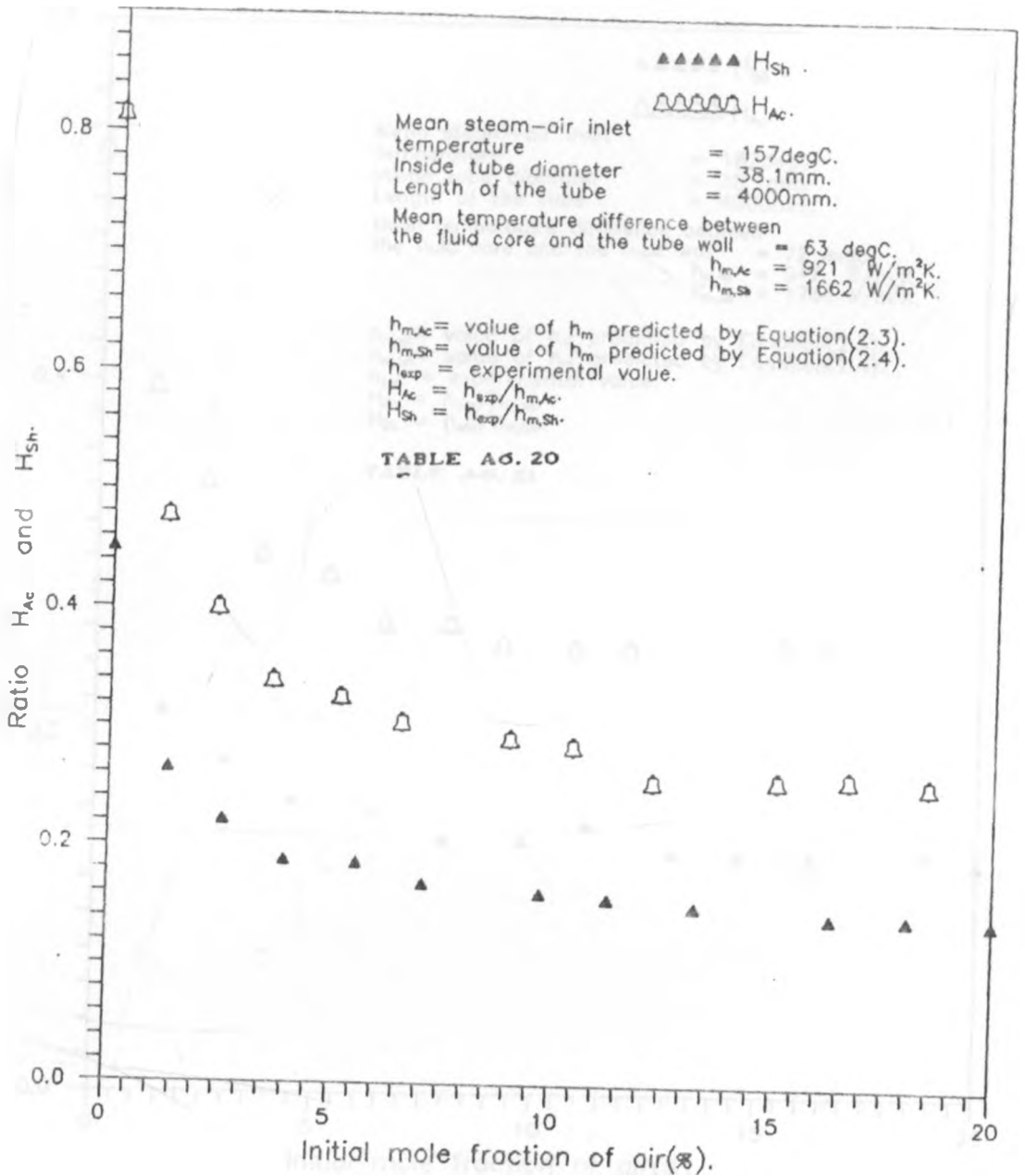


FIGURE A7.20: RATIOS OF EXPERIMENTAL TO PREDICTED CONDENSATION HEAT TRANSFER COEFFICIENT  $\nu$  INITIAL MOLE FRACTION OF AIR IN THE MIXTURE

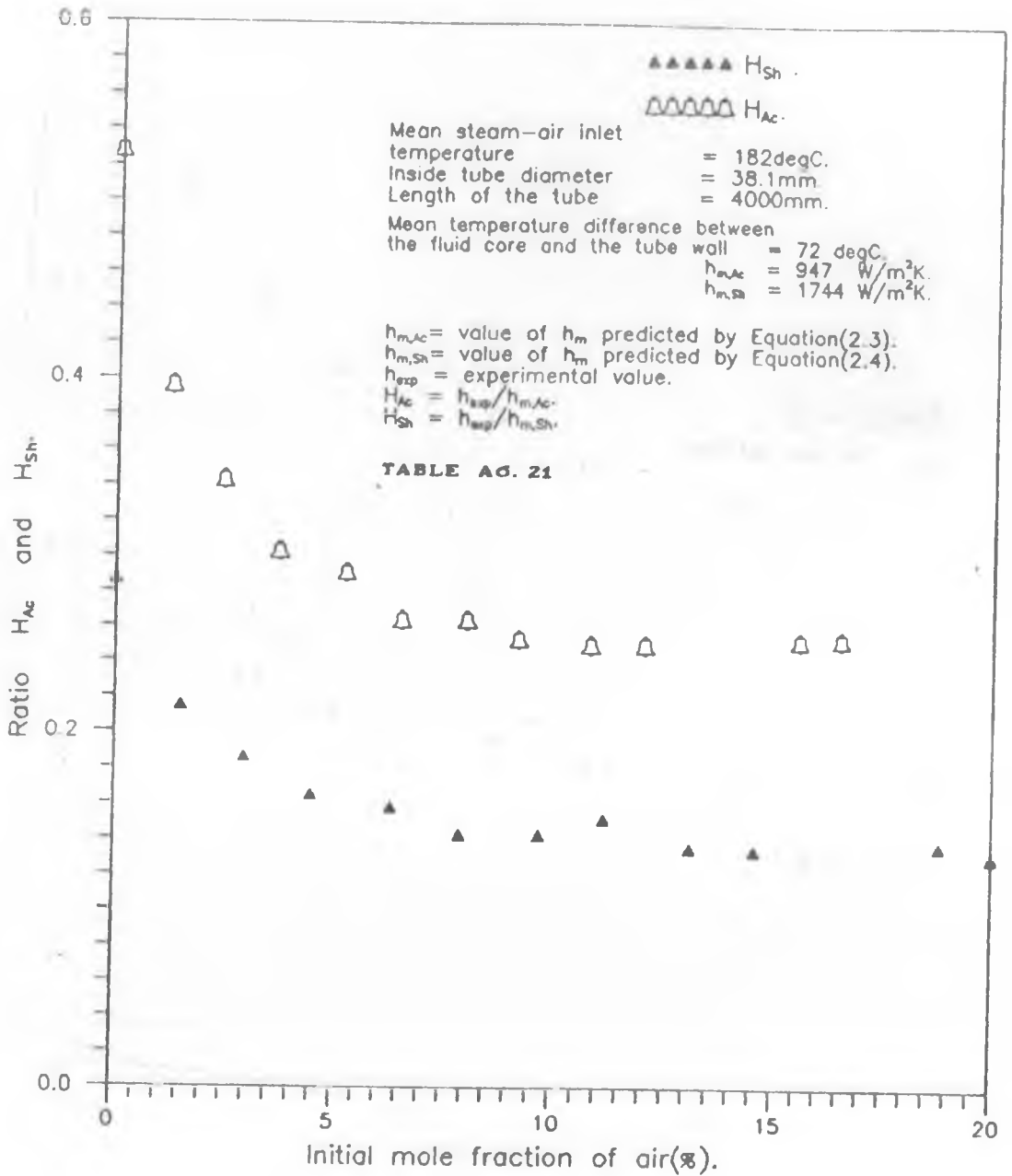


FIGURE A7.21: RATIOS OF EXPERIMENTAL TO PREDICTED CONDENSATION HEAT TRANSFER COEFFICIENT  $\nu$  INITIAL MOLE FRACTION OF AIR IN THE MIXTURE

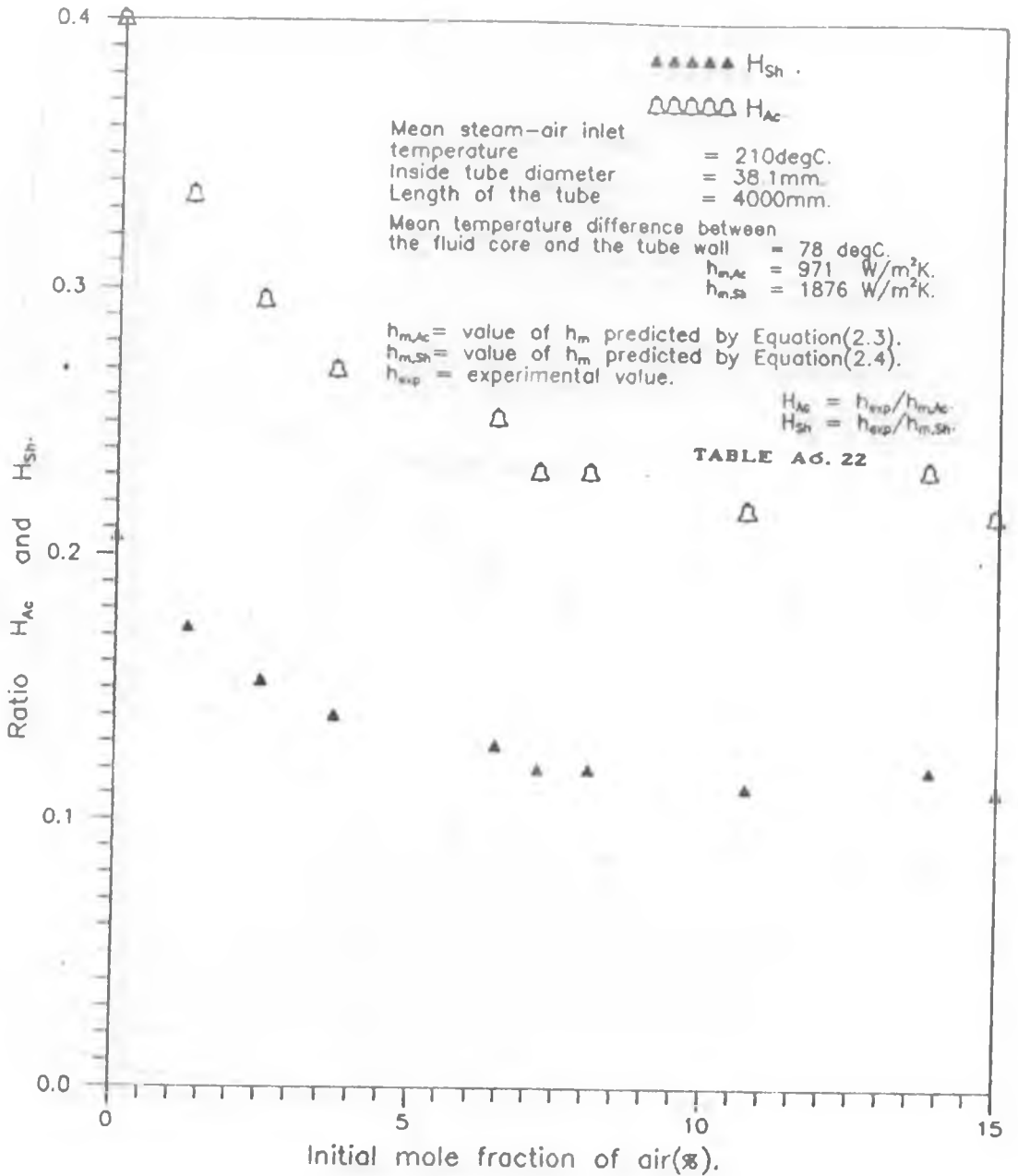


FIGURE A7.22: RATIOS OF EXPERIMENTAL TO PREDICTED CONDENSATION HEAT TRANSFER COEFFICIENT v INITIAL MOLE FRACTION OF AIR IN THE MIXTURE



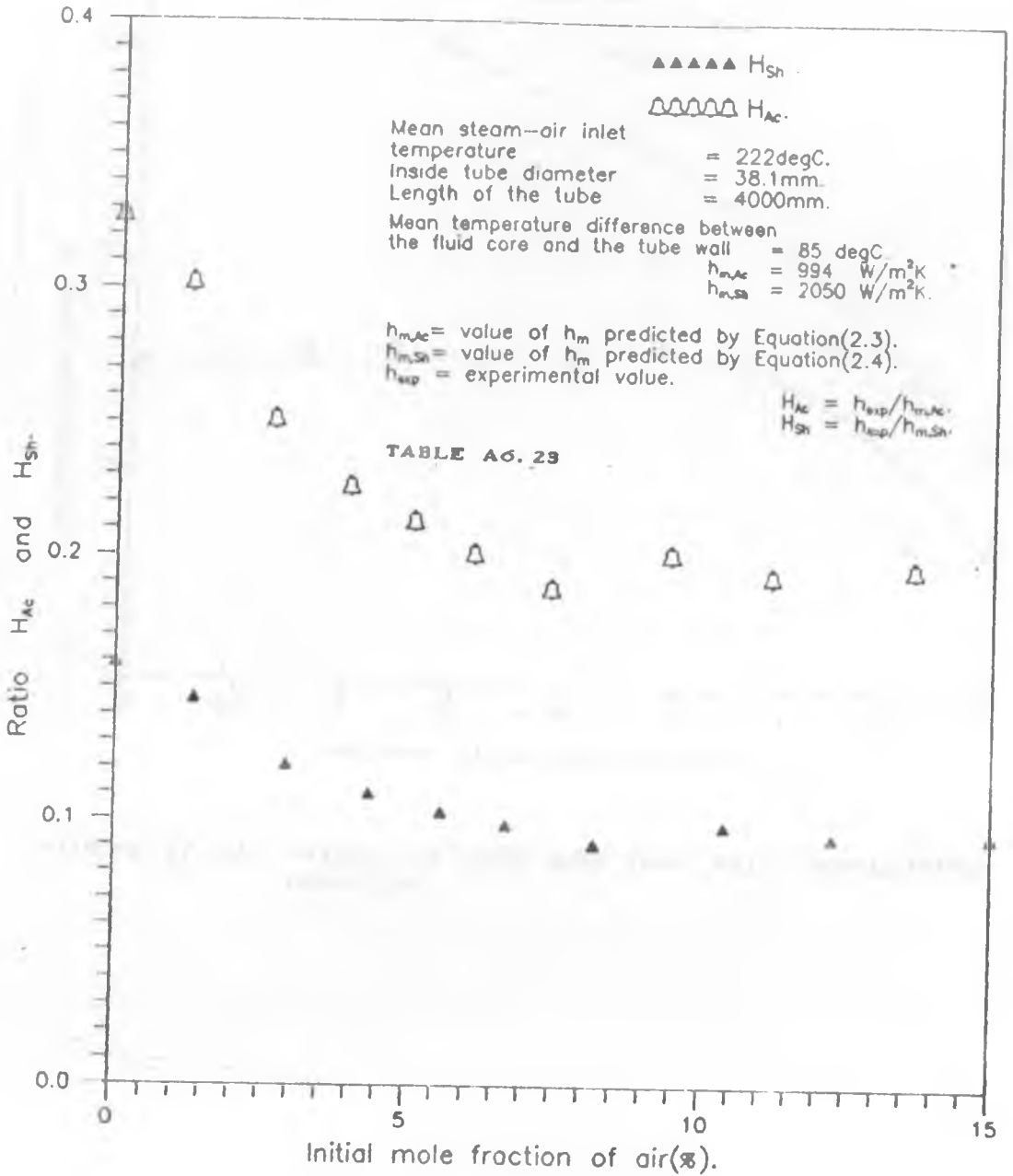


FIGURE A7.23: RATIOS OF EXPERIMENTAL TO PREDICTED CONDENSATION HEAT TRANSFER COEFFICIENT  $\nu$  INITIAL MOLE FRACTION OF AIR IN THE MIXTURE

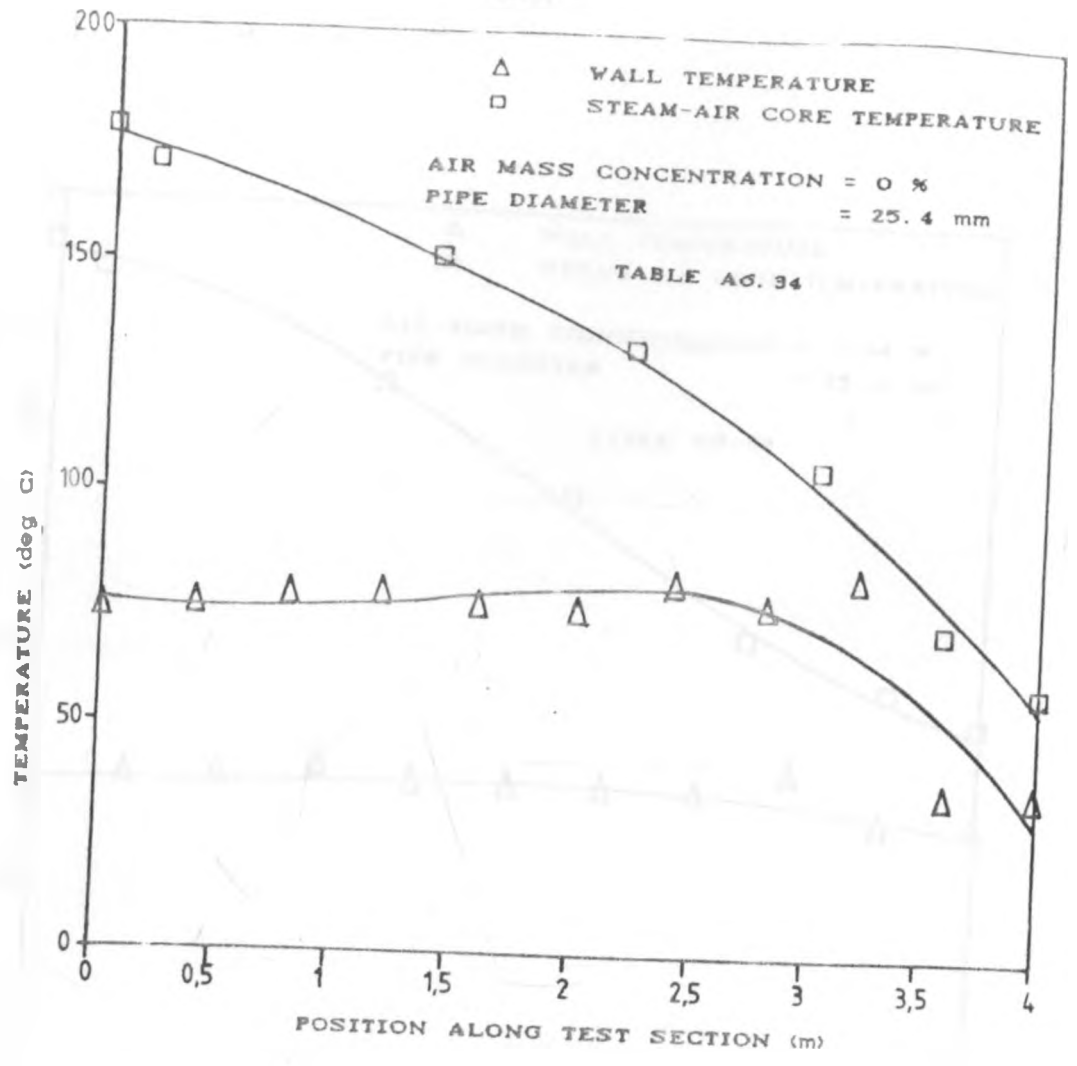


FIGURE A7.24: STEAM-AIR CORE AND TUBE WALL TEMPERATURE PROFILES

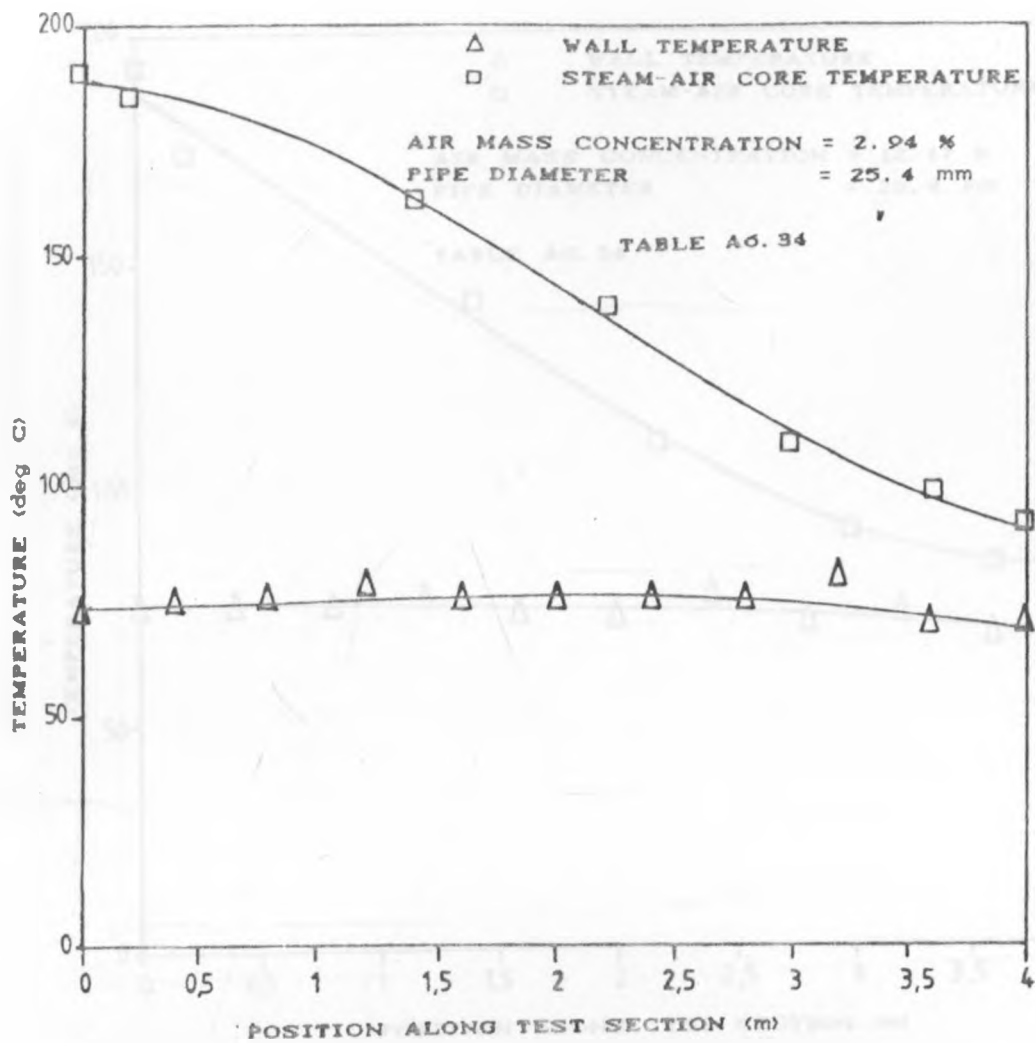


FIGURE A7.25: STEAM-AIR CORE AND TUBE WALL TEMPERATURE PROFILES

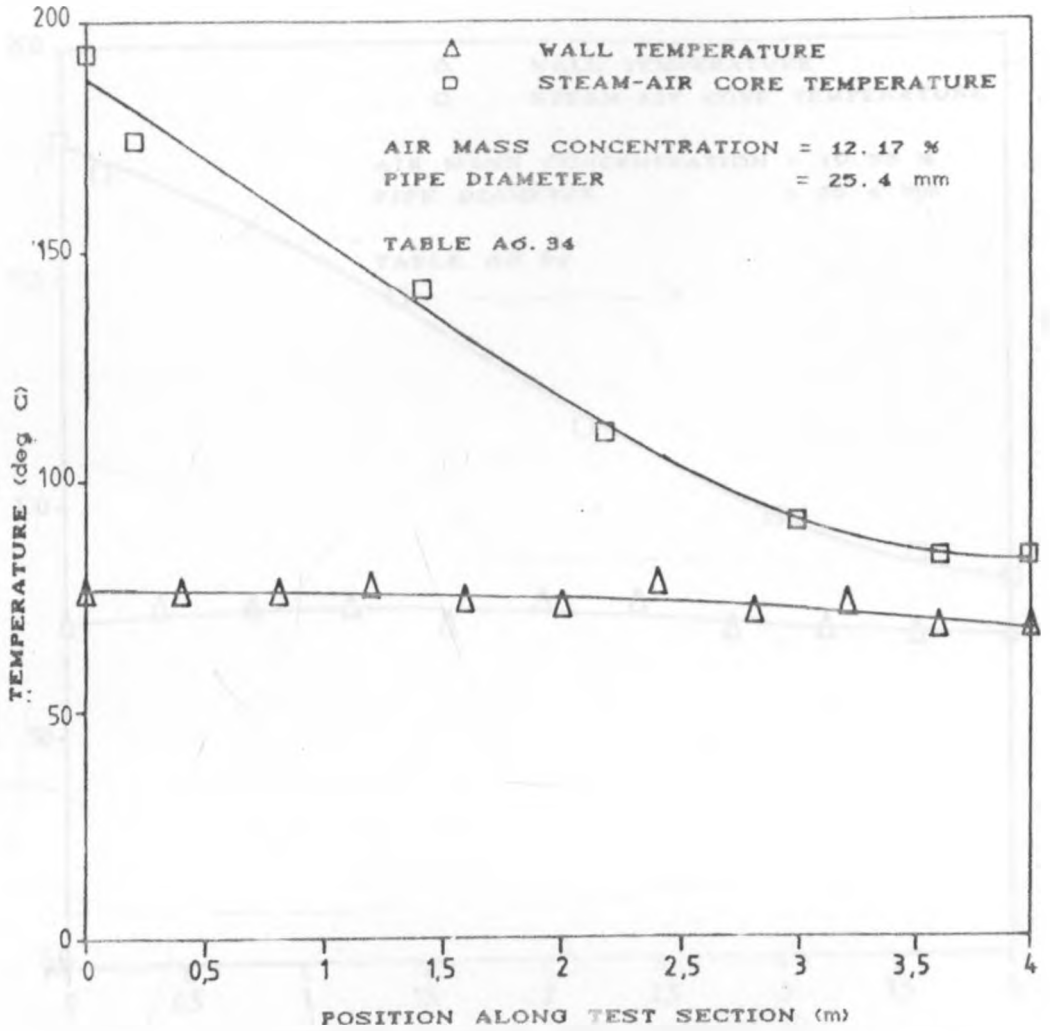


FIGURE A7.26: STEAM-AIR CORE AND TUBE WALL TEMPERATURE PROFILES

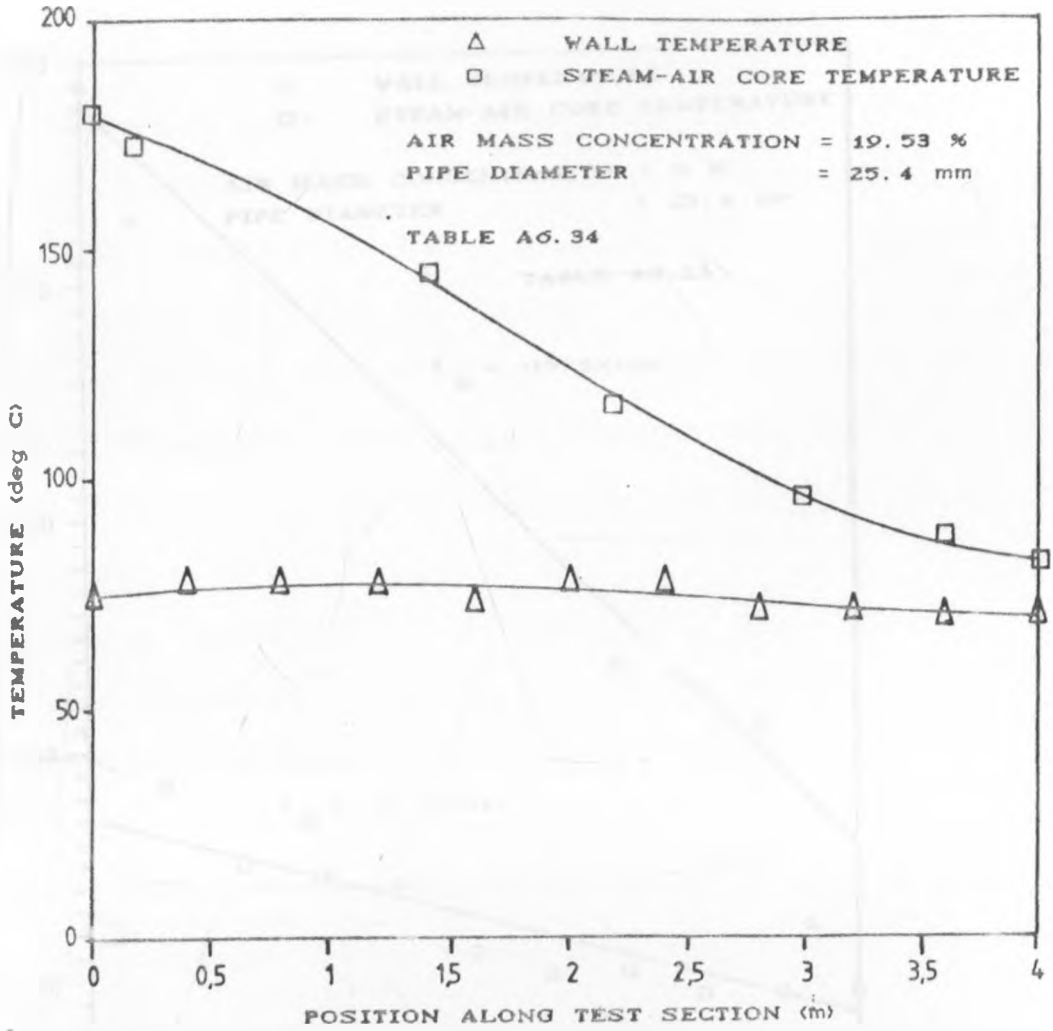


FIGURE A7.27: STEAM-AIR CORE AND TUBE WALL TEMPERATURE PROFILES

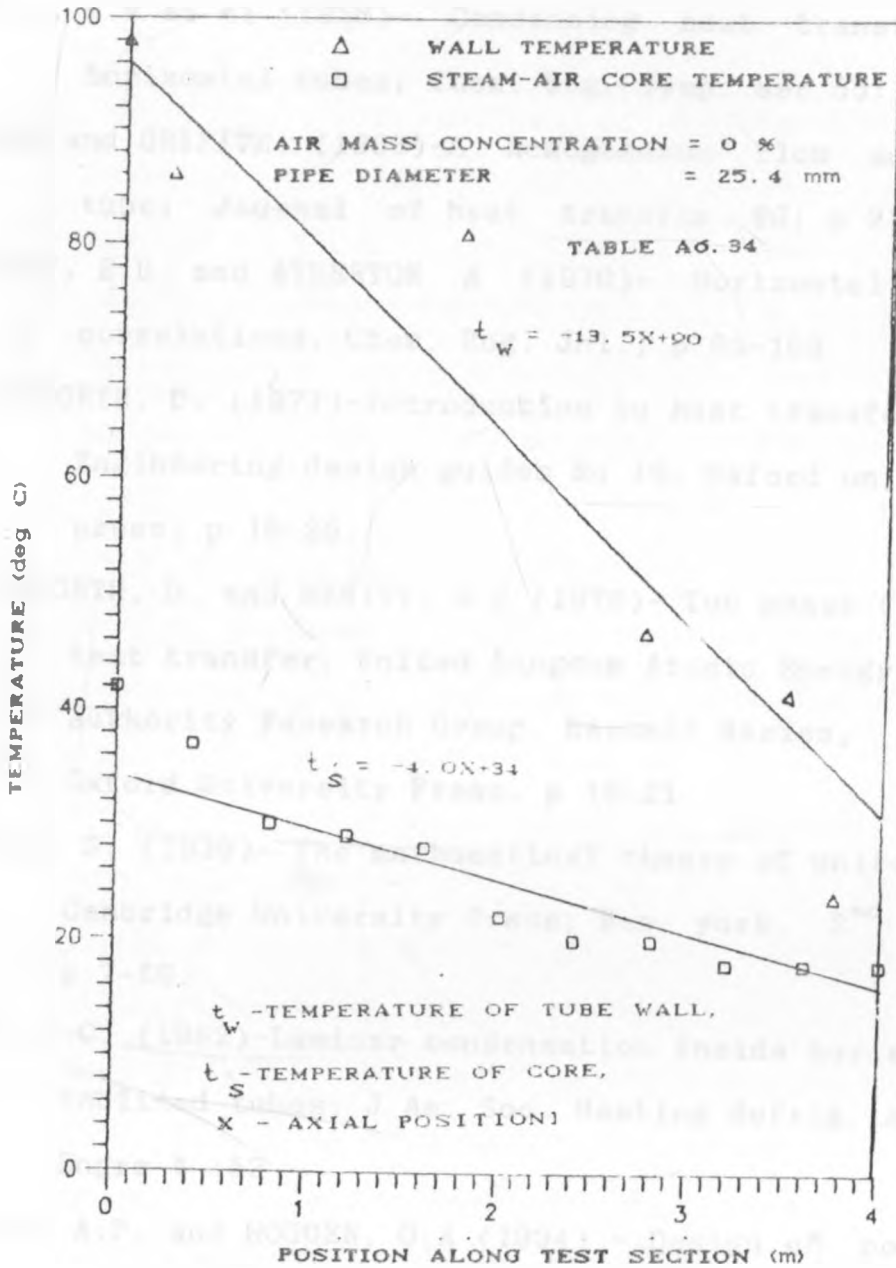


FIGURE A7.28: STEAM-AIR CORE AND TUBE WALL TEMPERATURE PROFILES

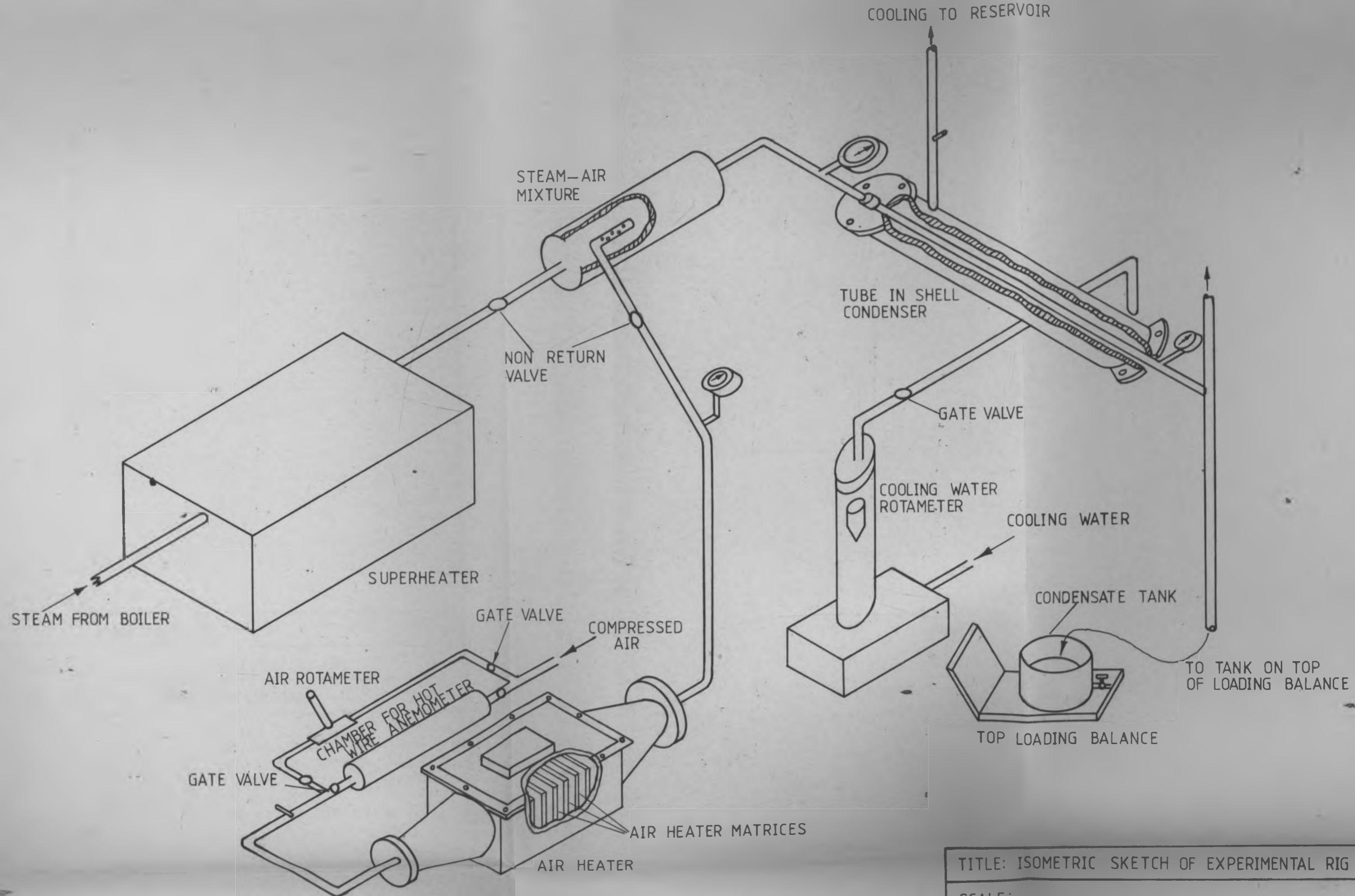
REFERENCES.

- AKERS , W.W et al (1958)- Condensing heat transfer within horizontal tubes; Chem. Eng. Symp. ser 55:171
- ANDEEN and GRIFITH (1968)-A homogeneous flow model in a tube; Journal of heat transfer 90; p 211-22.
- ANTHONY, E.D. and ATHERTON A (1970)- Horizontal flow correlations, Chem. Eng. Jnl.; p 95-103
- BUTTERWORTH, D. (1977)-Introduction to heat transfer; Engineering design guides No 18; Oxford university press; p 16-25.
- BUTTERWORTH, D. and HEWITT, G.F (1979)- Two phase flow and heat transfer, United Kingdom Atomic Energy Authority Research Group, Harwell Series, Oxford University Press, p 18-21.
- CHAPMAN, S. (1939)- The mathematical theory of uniform gases; Cambridge University Press; New york. 2<sup>nd</sup> Edition; p 7-50.
- CHATO, J.C. (1962)-Laminar condensation inside horizontal and inclined tubes; J Am. Soc. Heating Refrig. Air Cond., Engrs 4 :52
- COLBURN, A.P. and HOUGEN, O.A (1934) - Design of cooler condensers for mixtures of vapours with non condensable gases; Ind. and Eng. Chem.; Vol. 26; p 1178-1182.
- DUCKLER, A.E. (1964)-Pressure and hold up in two-phase flow; Am. Inst. Chem. Eng. J 10 (1); p 38
- HAMPSON, H. (1951)- Pro. of Gen Disc. of Heat Trans; I .M. E (London) and ASME. p 58-84.

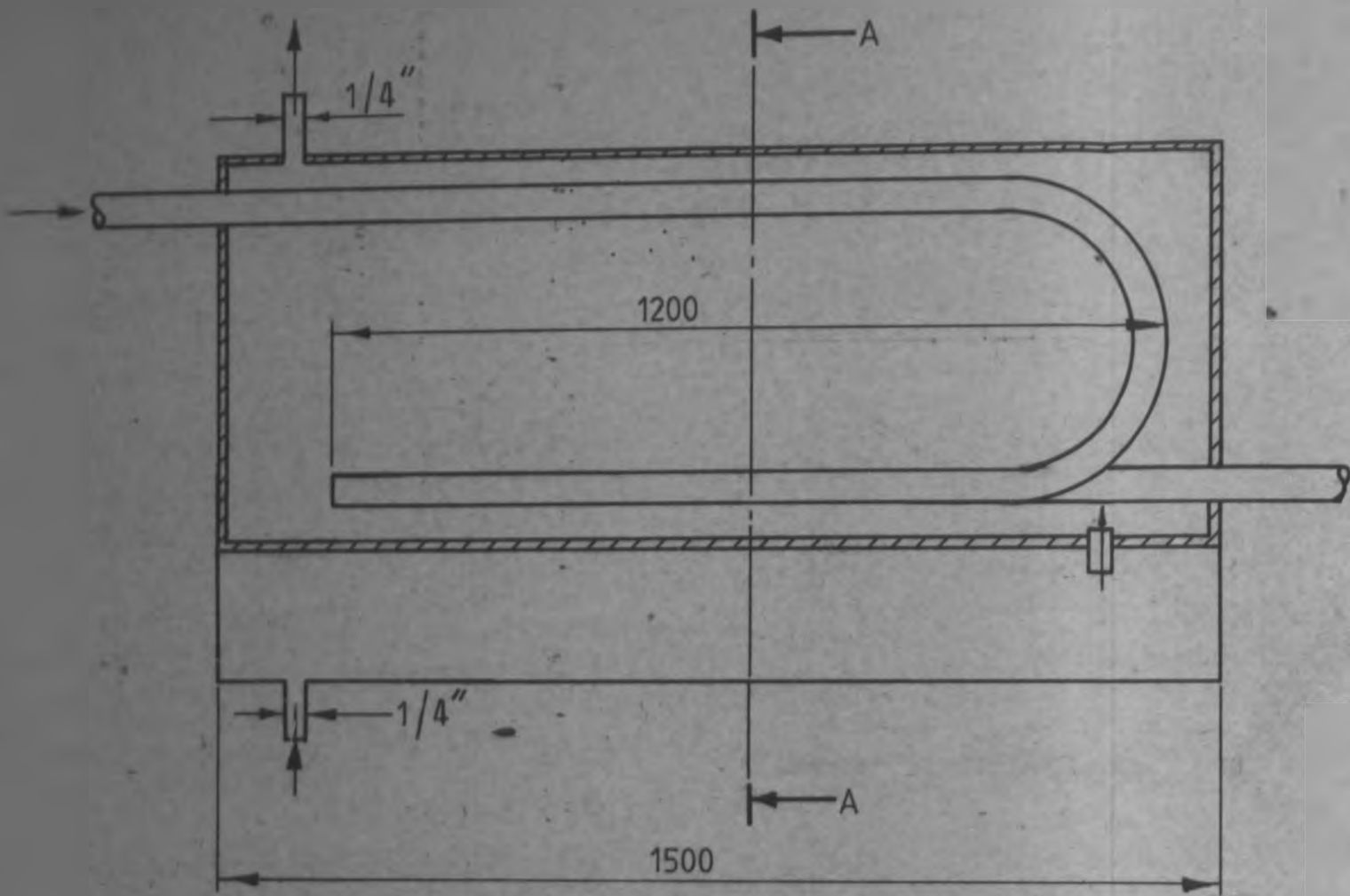
- HENDERSON, C. L. and MARCHELLO, J.M (1969)- Film condensation in presence of a non condensable gas; J. Trans. ASME; p 447-450.
- HOLMAN, J.P. (1985)- Experimental methods for Engineers; International student edition ;McGraw Hill book co.
- KENYA POWER and LIGHTING Co. (1986)- The environmental view point Olkaria Geothermal Project Kenya.
- KERN, D. Q. (1950)- Process heat transfer; International student edition; McGraw-Hill; New york; p 339-351.
- KHALIFA, H.E. and MICHAELLIDES, E (1978)-The effect of non-condensable gases on the performance of geothermal steam power systems;Brown University Report No CATMEC/28.
- MEISENBURG, S. J et al (1936)- Trans. Am. I. Chem. Engrs; vol. 32; p 100.
- MINKOWYCZ, W. J. and SPARROW, E. M. (1966)- Condensation heat transfer in the presence of NCG., Interfacial resistance, superheating, variable properties and diffusion; Int. J. Heat Mass Transfer, Vol. 9; p 1125-1144.
- MINKOWYCZ, W. J. and SPARROW, E. M. (1969)- Effects of superheated vapour and NCG on laminar film condensation; A .I .Ch. E; p 473-477
- NUSSELT, W. (1916)- The surface condensation of water vapour (in German); Z. ver. Dt. Ing. 60; p 541-646; p 575-596.
- OTHMER, D. F. (1929)- The condensation of steam; Ind. Eng. Chem. 21; p 577-583.

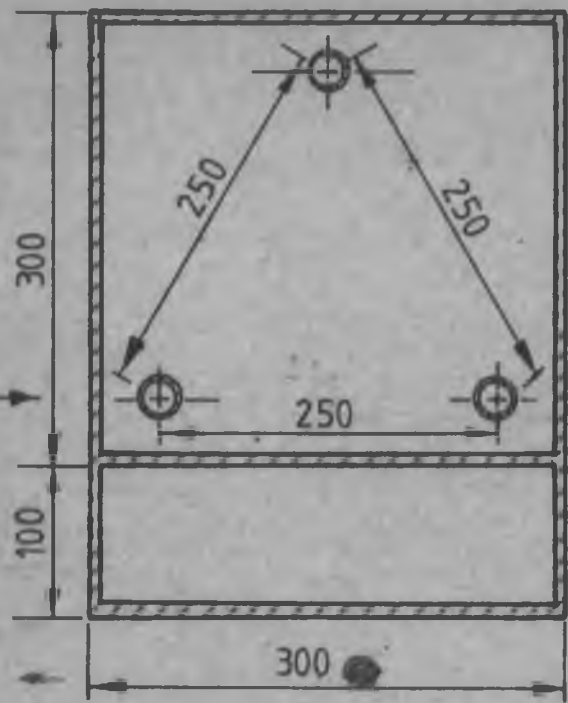


- ÖZİŞİK, M. N. (1985)- Heat transfer, a basic approach;  
International student Edition; McGraw-Hill, New York  
p 385-390, p 506-513.
- PERRY, R. H. and CHILTON, C.H (1973)- Chemical Engineers  
handbook, International student Edition,  
McGraw-Hill Chemical Engineering series, New York.  
p 5.40-5.44.
- ROGERS, G. F. C. and MAYHEW, Y. R (1984) -Thermodynamic and  
transport properties of fluids; 3<sup>rd</sup> Edition;  
Basil Blackwell.
- SHAH, M.M. (1979)- A general correlation for heat transfer  
during film condensation inside pipes; Int. J. Heat  
Mass Transfer; Vol.23; p 547-555.
- SIEDDER, E. N. and TATE, G. E (1936)- Ind. Eng. Chem; 28; 1149.
- SPARROW, E.M. and LIN, S.H (1964)- Condensation heat transfer  
in the presence of a non-condensable gas; J. Heat  
Transfer C86; p 430-436.
- SONNTAG, R.E et al (1972)- Introduction to thermodynamics:  
Classical and statistical; Wiley.
- TOPPING, J. (1962)- Errors of observation and their treatment;  
UNWIN Brothers limited; Working and London; p 1-40
- VARGAFTIK , N. B. (1975)- Tables on the thermophysical  
properties of liquids and Gases, second Edition;  
John Wiley and Sons Inc.; p 654-665.
- WASSILJEWA, A. (1904)- Physik 2.5 : 737.
- WHITE, M. C. (1979)- Gas exhausters; New Zealand Electricity,  
A division of the Ministry of Energy.



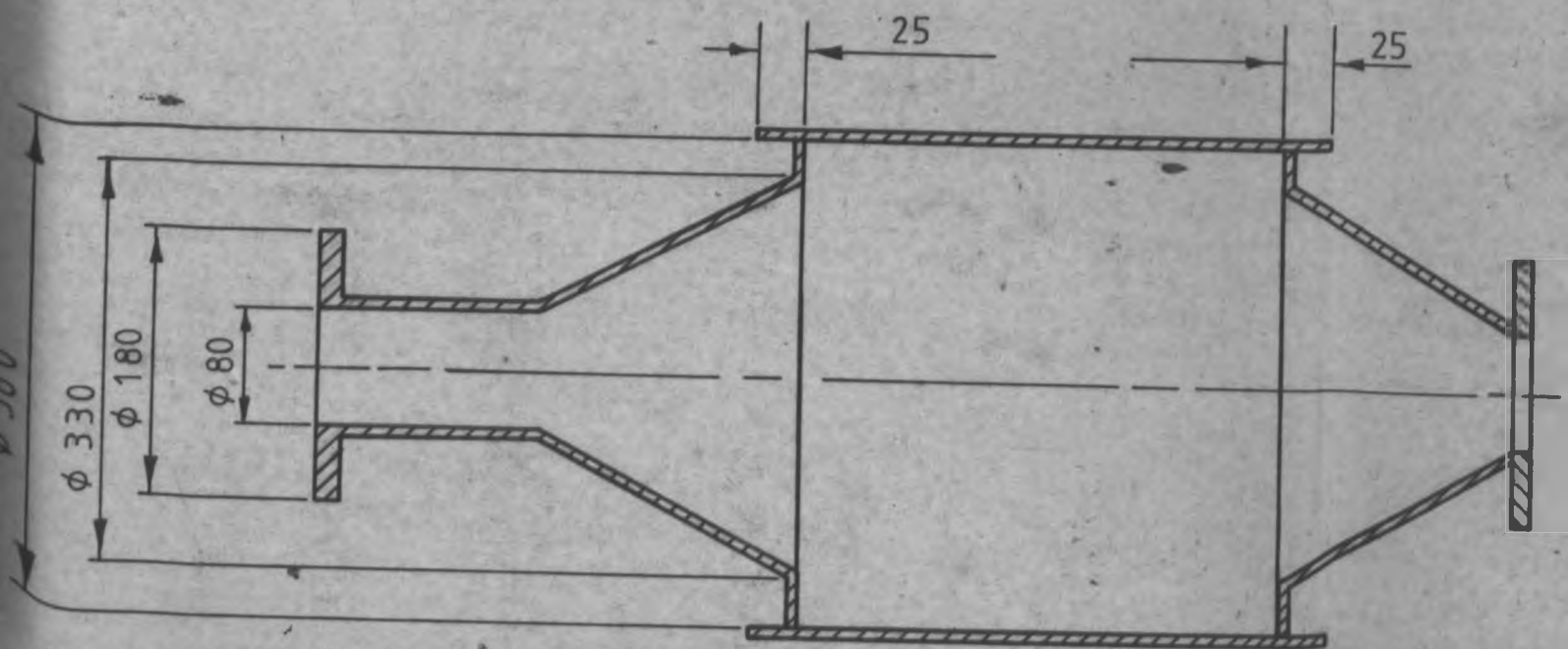
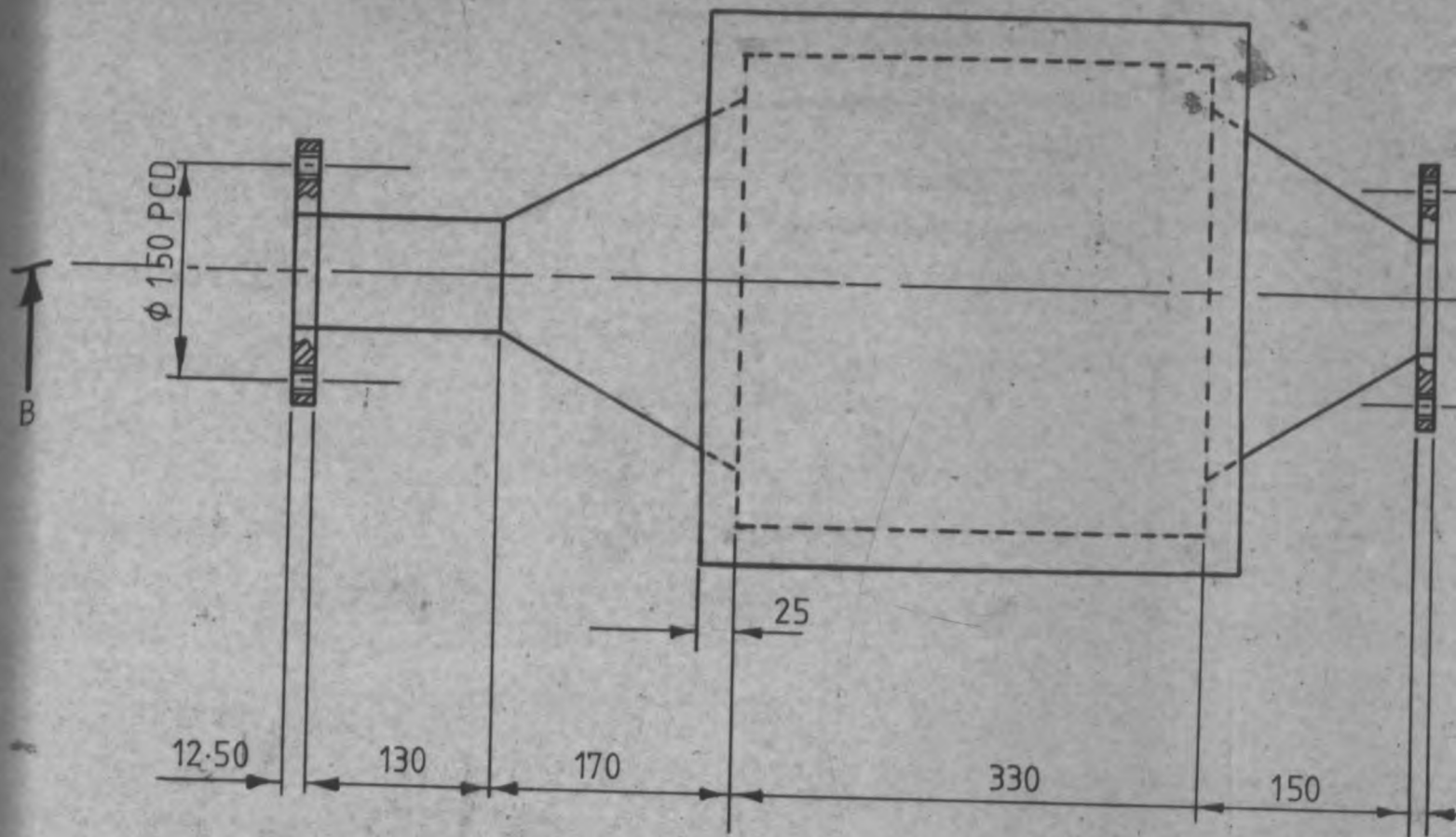
TITLE: ISOMETRIC SKETCH OF EXPERIMENTAL RIG LAB	
SCALE:	
MATERIAL:	TOLERANCE:





SECTION A-A

TITLE: SUPER STEAM HEATER	
SCALE:	DIMENSIONS IN MM.
MATERIAL: BLACK MILD STEEL COPPER TUBE	
TOLERANCE:	DRAWING N <sup>o</sup> . 2
DESIGNED BY: ONGÍRO A.	DRAWN BY: ONGÍRO A.
CHECKED BY: KANYUA J.F.	DATE: 25-09-90

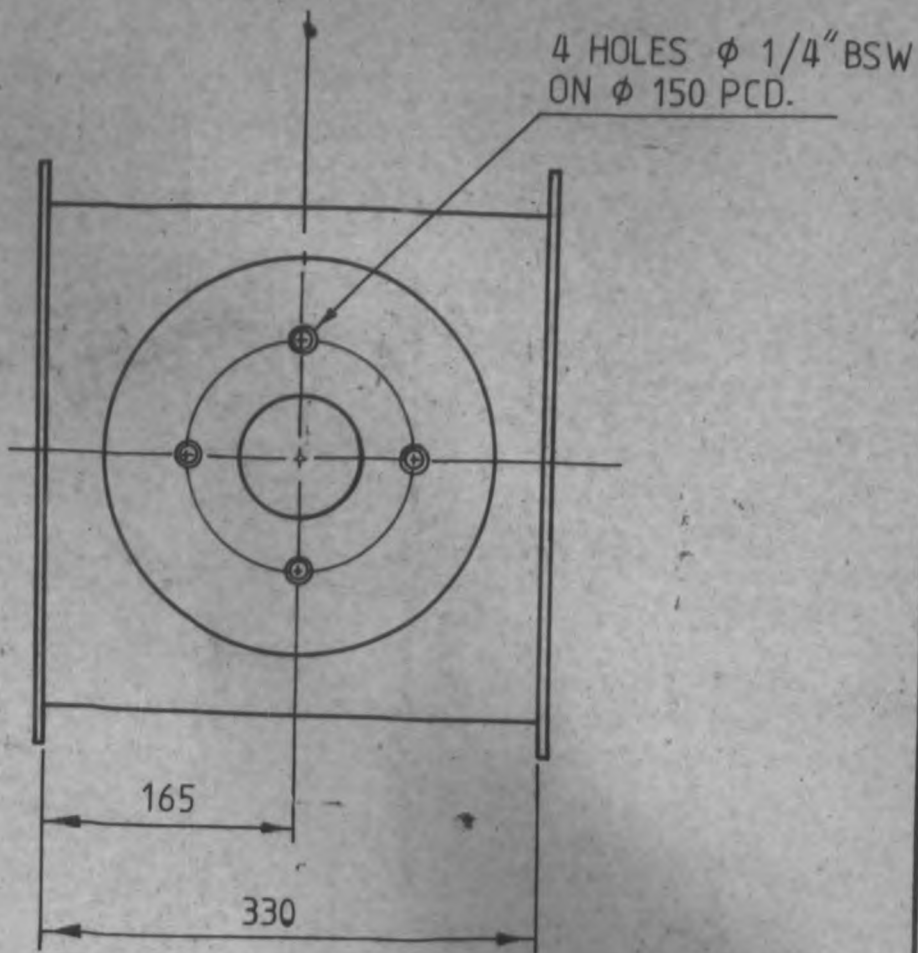


SECTION B-B



$\phi$  150 PCD

B



12.50

TITLE: AIR HEATER	
SCALE: 1 : 10	DRAWING N <sup>o</sup> . 3
MATERIAL: 1/8" BLACK MILD STEEL SHEET	
TOLERANCE: $\pm$ 0.50	DIMENSIONS IN MM.
DESIGNED BY: ONGIRO. A.	DRAWN BY: ONGIRO A.
CHECKED BY: KANYUA J.F.	DATE: 25-09-90

φ 1" B.S.W.

30 HOLES φ 3 MM AT 10  
CIRCUMFERENTIAL POSITIONS  
3 HOLES AT 120° TO EACH OTHER  
IN SPACE AT EVERY  
POSITION FIRST POSITION  
IN LINE WITH NOZZLE  
OUTLET.

A

A

φ 12.50

φ 50

50

1300

150

20

13

25

φ 1" B.S.W.

φ 12.70

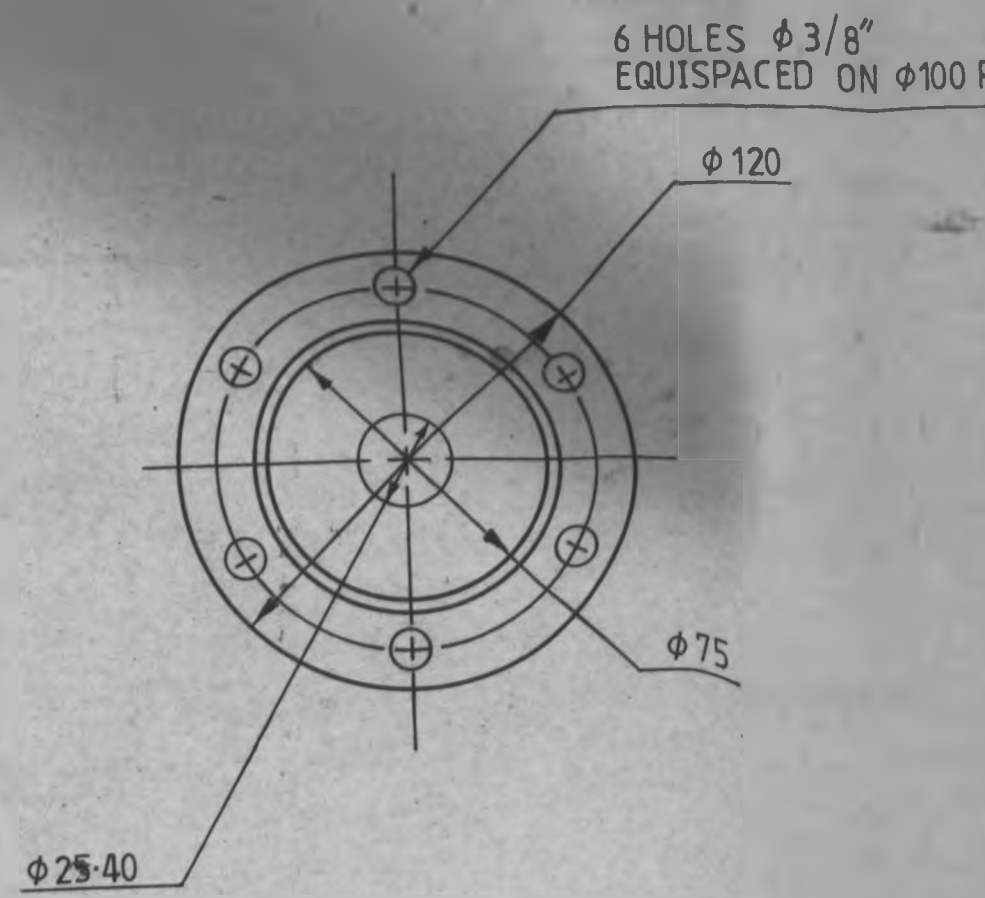
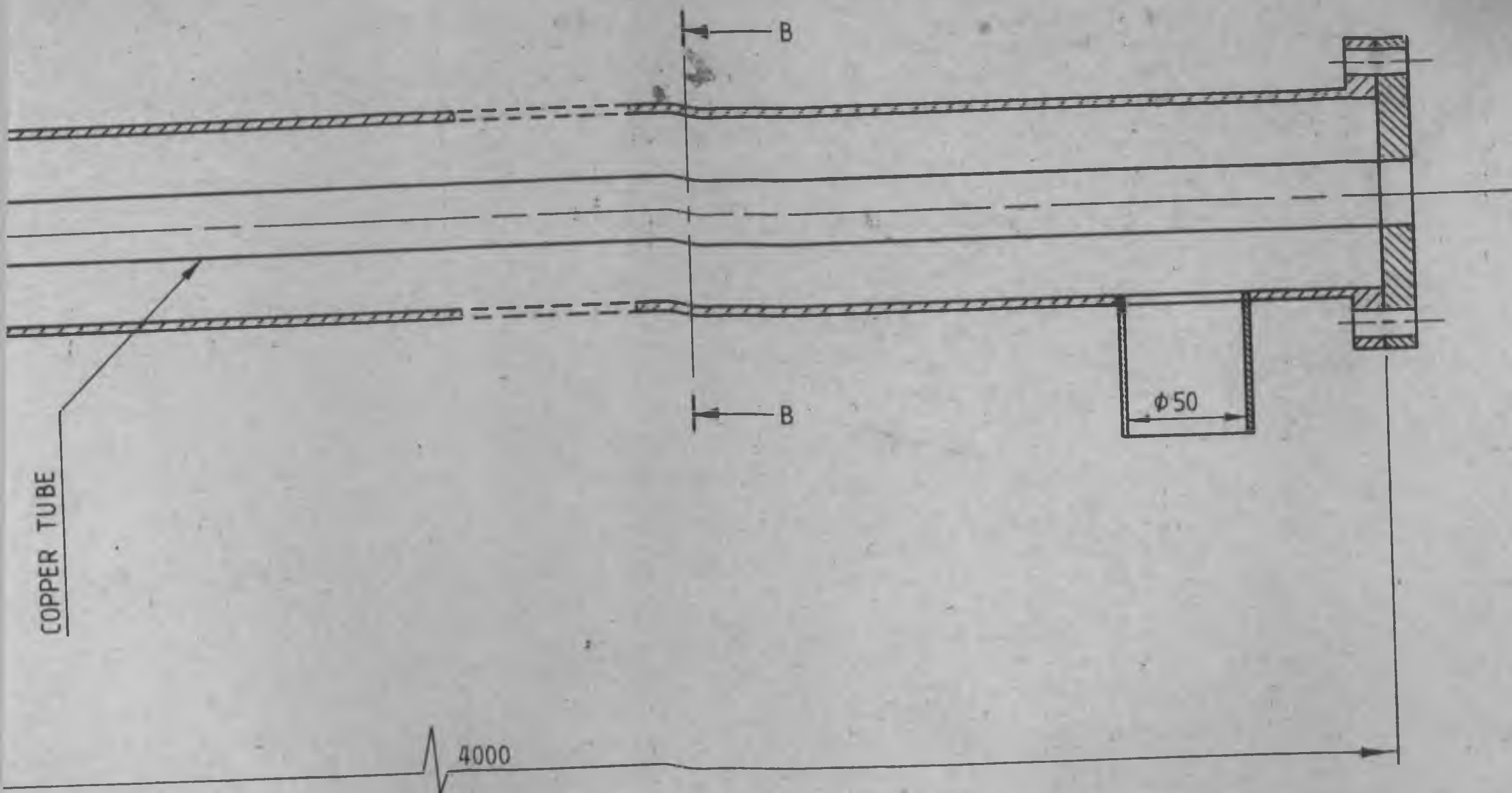
φ 3

SECTION A-A

70

φ 50

TITLE: AIR STEAM MIXTURE	DIMENSIONS IN MM.
SCALE: NOT TO SCALE	
MATERIAL:	
DRAWN BY ONGIRO A.	



SECTION B-B

TITLE: TEST SECTION	
SCALE: 1:2	DIMENSIONS IN MM.
MATERIAL: GALVANIZED STEEL PIPE AND COPPER TUBE.	
TOLERANCE:	DRAWING No. 5
DESIGNED BY: ONGIRO A..	DRAWN BY: ONGIRO A.
CHECKED BY: KANYUA J.F.	DATE 25-09-90